Demographic Processes and Behaviour of Snapping Turtles (*Chelydra serpentina*) in the Context of Past Catastrophes and Ongoing Threats

by

Matthew G. Keevil

Thesis submitted in partial fulfillment of the requirements for the degree of

Doctor of Philosophy in Boreal Ecology

Faculty of Graduate Studies

Laurentian University

Sudbury, Ontario, Canada

THESIS DEFENCE COMMITTEE/COMITÉ DE SOUTENANCE DE THÈSE
Laurentian Université/Université Laurentienne
Office of Graduate Studies/Bureau des études supérieures

Title of Thesis
Titre de la thèse Demographic Processes and Behaviour of Snapping Turtles (Chelydra serpentina) in the Context of Past Catastrophes and Ongoing Threats

Name of Candidate
Nom du candidat Keevil, Matthew G.

Degree

Diplôme Doctor of Philosophy

Program
Programme Boreal Ecology

Date of Defence
Date de la soutenance April 14, 2023

APPROVED/APPROUVÉ

Thesis Examiners/Examinateurs de thèse:

Dr. Jackie Litzgus
(Supervisor/Directeur(trice) de thèse)

Dr. David Lesbarrères
(Committee member/Membre du comité)

Dr. Ron Brooks
(Committee member/Membre du comité)

Dr. Doug Armstrong

Dr. Brian Halstead
(External Examiner/Examinateur externe)

Dr. Tom Johnston
(Internal Examiner/Examinateur interne)

Approved for the Office of Graduate Studies

Approuvé pour le Bureau des études supérieures
Tammy Eger, PhD
Vice-President Research (Office of Graduate Studies)
Vice-rectrice à la recherche (Bureau des études supérieures)
Laurentian University / Université Laurentienne

ACCESSIBILITY CLAUSE AND PERMISSION TO USE

Abstract

Lifetime patterns of somatic growth, reproduction, and survival comprise life history, which links individual traits to the vital rates that determine the properties of populations, such as generation time, potential rate of increase, and responses to environmental perturbation. Individual life-history traits, such as survival, age at first reproduction, reproductive frequency, and the size and number of offspring covary along a limited number of dimensions forming the pace-of-life continuum because they are tightly linked by trade-offs and constraints. Furthermore, variation in life history also covaries with morphological, physiological, and behavioural traits.

This dissertation focuses on interconnectedness of life-history traits with social behaviour, population dynamics, and conservation. The Algonquin long-term field study of Snapping Turtles (*Chelydra serpentina*) provides a unique opportunity to analyze these relationships in a long-lived organism with a slow life history by building upon a productive foundation of previous research. Turtles' slow life history, low and variable juvenile recruitment, and reliance on high adult survivorship makes them vulnerable to anthropogenic threats resulting in turtles being disproportionately imperilled.

In Chapter 1, I analyzed the patterns of abundance and survival during and after a population catastrophe and revealed individuals transitioning between sites in a connected population but no recovery over 23 years. Because of their cryptic behaviour, the mating system of Snapping Turtles was poorly known, so in Chapter 2 I quantify sexual size dimorphism and frequency of wounds to infer patterns of intraspecific aggression consistent with a mating system mediated by male combat. The third chapter focused on the somatic growth component of life-history by refining growth modelling by developing a model of seasonal variation in growth rates. In Chapter 4, I examine the demography of Snapping Turtles dispersing across roads by testing hypotheses based on the mating system revealed in Chapter 2 using a demographic model parameterized with survivorship estimated in Chapter 1 and the growth modeling approach developed in Chapter 3. I show that juveniles are overrepresented on roads and face higher mortality risk and that the lost reproductive value of juveniles killed on roads contributes substantially to the overall burden of road mortality in this long-lived species.

Key words:

Population ecology, life history, Bayes, Bayesian, von Bertalnffy; somatic growth; sexual size dimorphism, mating system; male combat; ; sexual coercion; capture mark recapture; Jolly Seber; survivorship; temporary emigration; multi-state mark-recapture model; multinomial m-array; parameter-expanded data augmentation; road ecology; Lefkovitch matrix; stage-structured model; reproductive value

Dedication

For my mother, who taught me how to find salamanders and catch frogs, and who would have been proud of this achievement.

Acknowledgements

I am deeply grateful to Amanda Bennett for her scientific insight, editorial advice, turtle wrangling skill, love, support, commiseration, and patience.

I have received wonderful, encouraging, and stimulating mentorship, for which I will always be thankful. Thank you, Jackie. I am grateful to Ron Brooks for all his insights, humour, and his infectious appreciation for Snapping Turtles and their life history and for giving me the awesome opportunity and responsibility of free reign over more than four decades of data. David Lesbarrères has been an invaluable source of advice and critical feedback as well as a lovely place to housesit for a semester. Doug Armstrong introduced me to the world of Bayesian analysis and has been generous with his books, code, and knowledge of wildlife conservation, and with opportunities to collaborate.

The Algonquin turtle life-history projects are the result of dedication by supervisors, students, field assistants, and volunteers whose individual contributions over decades have become too numerous to list. During my time on the project, I have been extremely grateful for the friendship and intellectual and moral support of fellow graduate researchers on the turtle project, Patrick Moldowan and Julia Riley. We also relied on the hard work, dedication, and camaraderie of amazing undergraduate (at the time) field technicians: Hannah McCurdy-Adams, Shawna Sanders, Taylor Wynia, Steven Kell, and my coauthor Brittainy Hewitt, as well as volunteers Jason Flatt and Michelle Anagnostou. We all relied constantly on the amazing staff at the Algonquin Wildlife Research Station. I am very appreciative of the company, and frequent help in the lab and the field, of fellow researchers at the Station. Thanks especially to Hugo Kitching, who showed me the turtle project ropes and what life at the Algonquin WRS is all about.

I am indebted to my coauthors for their insightful critiques, helpful suggestions, and for supplying the right turn of phrase when words failed me. I am very grateful to Lenore Fahrig and the Geomatics and Landscape Ecology Lab at Carleton University who generously devoted an entire lab meeting, and a humbling assembly of expertise, to providing helpful advice and critiques to help me revise and find a home for my final chapter.

My analysis of the demographics of road killed juvenile Snapping Turtles depended on hours of dissection work by coauthor and undergraduate thesis student Natasha Noble. That analysis was made possible by Hannah McCurdy-Adams, Kelsey Moxley, Jeff Hathaway, S.T.A.R.T. project technicians, Scales Nature Park, Patrick Moldowan, Paul Gelok, Rory Eckinswiller, Kari Gunson, Dave Seburn, Julia Riley, and James Baxter-Gilbert who donated specimens that they generously collected and allocated freezer space to.

Aspects of this work were supported by Natural Sciences and Engineering Research Council (NSERC) Discovery Grants to Dr. Jacqueline Litzgus, David Lesbarrères,, and Ronald J. Brooks the Ontario Ministry of Natural Resources and Forestry (MNRF) (SARSF #57-14-LU2 held by Sean Boyle, myself, and Jacqueline Litzgus and David Lesbarrères; SARFFO #14-15-LU held by Sean Boyle and David Lesbarrères), Ontario Ministry of Environment and Climate Change (MOECC) (GLGCF #3-729 held by Sean Boyle and David Lesbarrères). In-kind contributions were provided by the Algonquin WRS, Friends of Presqu'ile Provincial Park, Laurentian University, the University of Guelph, and Algonquin Provincial Park through the assistance of Paul Gelok, Jennifer Hoare, Brad Steinberg, Alison Lake, Rory Eckinswiller, and David LeGros.

Table of Contents

Table of tables

Table of Figures

General Introduction

Through my dissertation, I set out to explore the interconnectedness of life history traits with social behaviour, population dynamics, and conservation. The Algonquin long-term field study of Snapping Turtles (*Chelydra serpentina*), which began in 1972, provides a unique opportunity to analyze these relationships in a long-lived organism with a slow life history by building upon a productive foundation of previous research. My objectives are to analyze a historic catastrophe and subsequent population dynamics, fill in knowledge gaps about mating system and somatic growth, and synthesize those insights into testable hypotheses and a demographic model that can be applied to the ongoing threat of road mortality.

Life-history traits are interconnected

Life history, which is the timing and pattern of growth, reproduction, and survival (Stearns, 1992), encompasses both individual traits as well as determining the properties of populations. Fundamental aspects of populations, such as generation time, potential rate of increase, and the response to perturbation, are determined by vital rates (rates of survival, reproduction and dispersal), which emerge from life history. Individual life-history traits, such as survival, age at first reproduction, reproductive frequency, and the size and number of offspring, are not independent; instead they are linked by trade-offs and constraints (Hutchings, 2021; Rivalan et al., 2005; Roff, 2002; Stearns, 1992; Williams, 1966). Because life-history traits are linked, much of the life-history variation among organisms can be accounted for along a small number of dimensions comprising the pace of life continuum from fast to slow life histories (Congdon et al., 2022; Gaillard et al., 1989; Jones et al., 2008). Furthermore, variation in life history also covaries with morphological, physiological, and behavioural traits at multiple scales, resulting in trait

associations referred to as pace-of-life syndromes (Byer et al., 2019; Ricklefs and Wikelski, 2002; Wolf et al., 2007). Therefore, the constraints and trade-offs inherent in life-history traits produce strong interconnections among elements of population and behavioural ecology, which then interact with environmental change and impact conservation and management.

Population response to perturbations

Life-history traits influence the response of populations to perturbations in abundance caused by environmental variation including anthropogenic events. Populations at the fast end of the slow–fast continuum are most vulnerable perturbations in reproductive success, whereas those with slow life histories are most sensitive to changes in adult survivorship (Congdon et al., 2022; Jonsson and Ebenman, 2001). Density-dependent compensation is an increase in population growth rate when densities are low, and stronger compensation implies a more rapid recovery from perturbations. Organisms with fast life histories are more vulnerable to environmental stochasticity, which tends to affect earlier life stages, resulting in more frequent fluctuations in abundance (Bjørkvoll et al., 2012; Gaillard et al., 2005; Jonsson and Ebenman, 2001; Sæther et al., 2005). By contrast, populations with slower life histories are less variable in abundance but are slower to recover from perturbations (Hutchings and Reynolds, 2004; Neubauer et al., 2013; Roff, 2002), at least when viewed by absolute time scales. However, length of generation time (i.e., slower life history) is associated with stronger density-dependent compensation at the generation time scale across multiple vertebrate groups (Bjørkvoll et al., 2012; Sæther et al., 2005; Vélez-Espino and Koops, 2012).

Population catastrophes—abrupt declines approaching or exceeding 50% of abundance (Gerber and Hilborn, 2001; Ward et al., 2007)—are particularly severe perturbations in abundance. Catastrophes may be the most important influence on the probability of persistence in wild

populations (Mangel and Tier, 1994; Menges, 1990). The risk that catastrophes pose to population persistence is expected to depend on their frequency relative to generation time (Frankham and Brook, 2004; O'Grady et al., 2008). Thus, for long-lived species, catastrophes that are spaced far apart in time could still have important effects on abundance and persistence. Unfortunately, published reports of catastrophes often fail to quantify long-term consequences (Fey et al., 2015).

Because of the slow life history of chelonians, and because constraints on vital rates limit the potential to increase survival or fecundity, turtles have a limited capacity to recover after declines (Brooks et al. 1991, Congdon et al. 1993, 1994, Cunnington and Brooks 1996, Heppell 1998, Enneson and Litzgus 2008). Nonetheless, density-dependent compensatory responses in abundance or vital rates have been reported for several chelonian species (Bjorndal et al., 2000; Fordham et al., 2009; Spencer et al., 2006; Stubbs et al., 1985). Unlike chronic anthropogenic impacts, such as hunting, road mortality, or introduced predators (Colteaux and Johnson, 2017; Drost et al., 2021; Piczak et al., 2019), catastrophes have a limited duration and so can present an opportunity to study population responses without confounding by persistent threats.

Somatic growth rate as a component of life history

Growth interacts dynamically with other evolved aspects of life history such as size and age at maturity, survival, and fecundity (Armstrong et al., 2018; Day and Rowe, 2002; Shine and Iverson, 1995). Building population models requires quantifying life-history traits, which in turn depend on fitting accurate growth models (Bjorndal et al., 2019; Bulté and Blouin-Demers, 2009; Hatch et al., 2019). This link between growth and population vital rates means that somatic growth models are critical for parameterizing many applied population demographic models such as integral projection models (Rose et al., 2019) and allometric models (Hatch et al., 2019).

Across three freshwater turtle species, Congdon et al. (2018) found that juvenile growth rate had more influence on individual life-history trait variation—age and size at maturity and subsequent reproductive output—than other parameters such as hatching size or adult growth rate. However, in chelonians, growth continues for some period after maturity (Congdon et al., 2012) and variation in post-maturity growth may still have substantial effects on individual reproductive value when both fertility and survival are correlated with body size (Armstrong et al., 2018).

Growth is also a component of extrinsic (environmental variation) and intrinsic (density-dependent) population regulation (Lorenzen, 2016). Among chelonians, density-dependent growth (i.e., compensatory growth) has been observed among Green Turtles (*Chelonia midas*) in habitats with fluctuating density (Bjorndal et al., 2019, 2000). Density dependence has also been proposed as an explanation for the slower growth and smaller body size evidenced in historic Wood Turtle (*Glyptemys insculpta*) collections relative to recent samples from depleted populations (Jones et al., 2019). Stubbs et al. (1985) reported increased juvenile growth rates within a population of Hermann's Tortoise (*Testudo hermannii*) following a catastrophic fire, although this did not result in the recovery of the sexually mature population in a subsequent study (Hailey 2000).

Dispersal and density dependence

Dispersal mechanisms can be an important component of population dynamics that can promote population or metapopulation persistence and regulation. Models of dispersal evolution relate dispersal to density dependence by examining how local density affects dispersal, for example by making dispersal conditional on local density, (Dytham, 2009; Poethke et al., 2003; Sæther et al., 1999). Implicit in most of these models is the reciprocal effect – the effect of dispersal on local population density within a metapopulation (Poethke et al., 2003). Dispersal may be conditional

on density in several ways: positive density-dependent emigration (the tendency of individuals to leave crowded patches), negative density-dependent emigration (the tendency of individuals to disperse more readily from low density populations, as predicted by the social fence hypothesis), positive density-dependent immigration (immigrants are attracted to patches of high density, as in conspecific attraction), and negative density dependent immigration (the tendency of individuals to settle in empty or low density patches) (Lande et al., 1998; Matthysen, 2005). Positive density dependent dispersal (dispersal from high- to low-density patches) will tend to have a stabilizing effect by promoting increased patch occupancy and higher population sizes averaged across a metapopulation (Poethke et al., 2003; Ruxton and Rohani, 1999; Sæther et al., 1999).

Even when dispersal is not conditional on density, density dependence is implicit in the most often cited ultimate reasons for dispersal (Bowler and Benton, 2005; Cadet et al., 2003; Parvinen et al., 2003). In order for density dependence to drive the evolution of dispersal, patches must occasionally approach or exceed carrying capacity so that individuals are likely to experience an increase in fitness by emigrating to other, potentially less dense, patches (Cadet et al., 2003; Parvinen et al., 2003). Local resource competition (LRC) is a form of kin competition—competition against relatives that incurs a higher inclusive fitness cost than equivalent competition against unrelated individuals—and is an important driver of dispersal evolution (Hamilton and May, 1977; Li and Kokko, 2019). Resource competition implies density effects, and LRC can only drive dispersal if per capita population growth rates are negatively affected by local density (Bach et al., 2006; Brom et al., 2016; Cadet et al., 2003). The idea that environmental and demographic stochasticity (including periodic catastrophic local extinction events) promote dispersal is pervasive and well supported in the theoretical literature (Dytham, 2009; Sæther et al., 1999). These effects also presume density dependence because the fitness

advantage of dispersal to low density destination patches relative to phylopatry when source patches are saturated (Cadet et al., 2003).

Sex-biased dispersal

Simulation models have shown that inbreeding avoidance tends to promote sex-biased dispersal by causing unbiased (with respect to sex) dispersal to be an unstable equilibrium but that inbreeding avoidance alone does not intrinsically determine which sex will be more dispersive (Gandon, 1999; Perrin and Mazalov, 2000, 1999). Models show that the sex that experiences the most intense local competition is the more dispersive sex (Leturque and Rousset, 2004; Perrin and Mazalov, 2000). In the scenarios modelled by Perrin and Mazalov (2000) males experienced much higher kin competition for mates (local mate competition, LMC) than females did for local resources such as breeding territories (LRC), resulting in male-biased dispersal. Gros et al. (2009) and (2016) showed that a difference in the magnitude of among-patch variance in reproductive success between males and females was sufficient to induce sex-biased dispersal, and that this effect was strongest under polygynous/monandrous mating systems. However, high male mate competition did not always select for male biased dispersal if dispersal costs are sufficiently high or there is little variance among patches. Empirically, high male mate competition is associated with male-biased dispersal in mammals and birds (Dobson, 1982; Greenwood, 1980; Mabry et al., 2013) and sex-biased dispersal in the few non-avian reptiles studied to date is frequently male biased (Trochet et al., 2016).

Populations differ in their sensitivity to mortality among different demographic classes depending on mating system and life-history strategies (Cunnington and Brooks, 1996; Jonsson and Ebenman, 2001; Lindström, 1998). Therefore, the demographic impact of disperser mortality depends both on population attributes and on the demographic distribution of dispersers

(Rytwinski and Fahrig, 2012). Roads are frequent cause of mortality for dispersing juveniles in a variety of taxa (Bonnet et al., 1999; Kim et al., 2019; Massemin et al., 1998; Storm et al., 1976). This mortality burden is expected to have a higher effect on populations when dispersal rates are high and includes females. Therefore, the disperser sex ratio is a critical component determining the impact of dispersal mortality caused by roads. However, Snapping Turtle juveniles cannot be sexed reliably based on external sex characters and predictions of dispersal sex-bias depend on adequate knowledge of the mating system, which is poorly known for Snapping Turtles.

Sexual size dimorphism, conspecific injuries, and mating system

Turtles exhibit a wide range of sexual-size dimorphism (SSD), from extremely female biased to moderately male-biased SSD, with female bias being more frequent (Agha et al., 2018; Berry and Shine, 1980; Ceballos et al., 2013). Snapping Turtles have male-biased SSD (Ceballos et al., 2013), which is strongly associated with mating systems with high male mate competition mediated by male combat in many taxa, including squamates, crocodilians, and chelonians (Berry and Shine, 1980; Cox et al., 2007; Shine, 1978). However, male biased SSD might also be explained by sexual selection based on female preference for larger male body size, which has been demonstrated in Desert Tortoises (Niblick et al., 1994), or based coercive mating, which has been suggested for Snapping Turtles and other bottom-walking species (Berry and Shine, 1980). Ecological niche divergence is another potential explanation (Shine, 1989).

Additional evidence can potentially be gleaned from patterns of wounding caused by interspecific aggression. Revealed patterns of aggressive interactions allow inference about the current adaptive value of aggression (Tinbergen, 1963), which can be applied to test hypothesized mating strategies. This strategy has been applied to other taxa with cryptic behaviour such as marine mammals (Orbach et al., 2015; Scott et al., 2005), salamanders (Camp, 1996; Fauth and

Resetarits, 1999), fossil taxa such as tyrannosaurids (Brown et al., 2022), and other chelonians (Moldowan et al., 2020).

Approach and objectives

Building upon the Algonquin long-term field study of Snapping Turtles, the four chapters of my dissertation explore multifaceted connections among life-history traits, behaviour, and population dynamics. I analyzed the population response following a historic catastrophe, explored the behavioural context and life-history constraints that limited recovery, and synthesized these elements into a demographic model to analyze an ongoing threat.

In Chapter 1, I analyze the patterns of abundance and survival in Snapping Turtles during and after a population catastrophe and revealed individuals transitioning between sites in a connected population but no recovery over 23 years in this long-lived animal with a slow life history. Because of their cryptic behaviour, the mating system of Snapping Turtles was poorly known, so in Chapter 2 I quantify sexual size dimorphism and frequency of wounds to infer patterns of intraspecific aggression consistent with a mating system mediated by male combat. In Chapter 3, I develop a model of seasonal variation in somatic growth rates, a component of life history, and apply it to two turtle species, Snapping Turtles and Painted Turtles. Finally, in Chapter 4, I examine the demography of Snapping Turtles dispersing across roads by testing hypotheses based on the mating system revealed in Chapter 2 using a demographic model parameterized with survivorship estimated in Chapter 1 and the growth modeling approach developed in Chapter 3. I show that juveniles are overrepresented on roads and face higher mortality risk and that the lost reproductive value of juveniles killed on roads contributes substantially to the overall burden of road mortality in this long-lived species.

References

Agha, M., Ennen, J.R., Nowakowski, A.J., Lovich, J.E., Sweat, S.C., Todd, B.D., 2018. Macroecological patterns of sexual size dimorphism in turtles of the world. J. Evol. Biol. 31, 336–345. https://doi.org/10.1111/jeb.13223

Armstrong, D.P., Keevil, M.G., Rollinson, N., Brooks, R.J., 2018. Subtle individual variation in indeterminate growth leads to major variation in survival and lifetime reproductive output in a long-lived reptile. Funct. Ecol. 32, 752–761. https://doi.org/10.1111/1365-2435.13014

Bach, L.A., Thomsen, R., Pertoldi, C., Loeschcke, V., 2006. Kin competition and the evolution of dispersal in an individual-based model. Ecol. Modell. 192, 658–666. https://doi.org/10.1016/J.ECOLMODEL.2005.07.026

Berry, J.F., Shine, R., 1980. Sexual size dimorphism and sexual selection in turtles (Order Testudines). Oecologia 44, 185–191. https://doi.org/http://dx.doi.org/10.1007/BF00572678

Bjørkvoll, E., Grøtan, V., Aanes, S., Sæther, B.-E., Engen, S., Aanes, R., 2012. Stochastic population dynamics and life-history variation in marine fish species. Am. Nat. 180, 372–387. https://doi.org/10.1086/666983

Bjorndal, K.A., Bolten, A.B., Chaloupka, M.Y., 2019. Green Turtle somatic growth dynamics: Distributional regression reveals effects of differential emigration. Mar. Ecol. Prog. Ser. 616, 185–195. https://doi.org/10.3354/meps12946

Bjorndal, K.A., Bolten, A.B., Chaloupka, M.Y., 2000. Green Turtle somatic growth model: evidence for density dependence. Ecol. Appl. 10, 269–282. https://doi.org/10.2307/2641001

Bonnet, X., Naulleau, G., Shine, R., 1999. The dangers of leaving home: Dispersal and mortality in snakes. Biol. Conserv. 89, 39–50. https://doi.org/10.1016/S0006-3207(98)00140-2

Bowler, D.E., Benton, T.G., 2005. Causes and consequences of animal dispersal strategies: Relating individual behaviour to spatial dynamics. Biol. Rev. 80, 205–225. https://doi.org/10.1017/S1464793104006645

Brom, T., Massot, M., Legendre, S., Laloi, D., 2016. Kin competition drives the evolution of sex-biased dispersal under monandry and polyandry, not under monogamy. Anim. Behav. 113, 157–166. https://doi.org/10.1016/j.anbehav.2016.01.003

Brooks, R.J., Brown, G.P., Galbraith, D.A., 1991. Effects of a sudden increase in natural mortality of adults on a population of the Common Snapping Turtle (*Chelydra serpentina*). Can. J. Zool. 69, 1314–1320. https://doi.org/10.1139/z91-185

Brown, C.M., Currie, P.J., Therrien, F., 2022. Intraspecific facial bite marks in tyrannosaurids provide insight into sexual maturity and evolution of bird-like intersexual display. Paleobiology 48, 12–43. https://doi.org/10.1017/pab.2021.29

Bulté, G., Blouin-Demers, G., 2009. Does sexual bimaturation affect the cost of growth and the operational sex ratio in an extremely size-dimorphic reptile? Ecoscience 16, 175–182. https://doi.org/10.2980/16-2-3243

Byer, N.W., Reid, B.N., Peery, M., 2019. Implications of slow pace-of-life for nesting behavior in an armored ectotherm. Behav. Ecol. Sociobiol. 73, 47. https://doi.org/10.1007/s00265-019-2658-z

Cadet, C., Ferrière, R., Metz, J.A.J., Baalen, M. van, 2003. The evolution of dispersal under demographic stochasticity. Am. Nat. 162, 427–441.

Camp, C.D., 1996. Bite scar patterns in the black-bellied salamander, *Desmognathus quadramaculatus*. J. Herpetol. 30, 543–546. https://doi.org/10.2307/1565701

Ceballos, C.P., Adams, D.C., Iverson, J.B., Valenzuela, N., 2013. Phylogenetic patterns of sexual size dimorphism in turtles and their implications for Rensch's rule. Evol. Biol. 40, 194–208. https://doi.org/10.1007/s11692-012-9199-y

Colteaux, B.C., Johnson, D.M., 2017. Commercial harvest and export of Snapping Turtles (*Chelydra serpentina*) in the United States: Trends and the efficacy of size limits at reducing harvest. J. Nat. Conserv. 35, 13–19. https://doi.org/10.1016/j.jnc.2016.11.003

Congdon, J.D., Buhlmann, K.A., Gibbons, J.W., 2022. Comparing life histories of the shortest-lived turtle known (Chicken Turtles, *Deirochelys reticularia*) with long-lived Blanding's Turtles (*Emydoidea blandingii*). Chelonian Conserv. Biol. 21, 28–36. https://doi.org/10.2744/CCB-1521.1

Congdon, J.D., Dunham, A.E., van Loben Sels, R.C., 1994. Demographics of Common Snapping Turtles (*Chelydra serpentina*): Implications for conservation and management of long-lived organisms. Am. Zool. 34, 397–408.

Congdon, J.D., Dunham, A.E., Van Loben Sels, R.C., 1993. Delayed sexual maturity and demographics of Blanding's Turtles (*Emydoidea blandingii*): Implications for conservation and management of long-lived organisms. Conserv. Biol. 7, 826–833.

Congdon, J.D., Gibbons, J.W., Brooks, R.J., Rollinson, N., Tsaliagos, R.N., 2012. Indeterminate growth in long-lived freshwater turtles as a component of individual fitness. Evol. Ecol. 27, 445–459. https://doi.org/10.1007/s10682-012-9595-x

Congdon, J.D., Nagle, R.D., Kinney, O.M., 2018. Front-loading life histories: The enduring influence of juvenile growth on age, size, and reproduction of primiparous female freshwater turtles. Evol. Ecol. Res. 19, 353–364.

Cox, R.M., Butler, M.A., John-Alder, H.B., 2007. The evolution of sexual size dimorphism in reptiles, in: Fairbairn, D.J., Blanckenhorn, W.U., Székely, T. (Eds.), Sex, Size and Gender

Roles: Evolutionary Studies of Sexual Size Dimorphism. Oxford University Press, Oxford, United Kingdom, pp. 38–49. https://doi.org/10.1093/acprof:oso/9780199208784.001.0001

Cunnington, D.C., Brooks, R.J., 1996. Bet-hedging theory and eigenelasticity: a comparison of the life histories of Loggerhead Sea Turtles (*Caretta caretta*) and Snapping Turtles (*Chelydra serpentina*). Can. J. Zool. 74, 291–296. https://doi.org/10.1139/z96-036

Day, T., Rowe, L., 2002. Developmental thresholds and the evolution of reaction norms for age and size at life-history transitions. Am. Nat. 159, 338–350. https://doi.org/10.1086/338989

Dobson, F.S., 1982. Competition for mates and predominant juvenile male dispersal in mammals. Anim. Behav. 30, 1183–1192. https://doi.org/doi:10.1016/S0003-3472(82)80209-1

Drost, C.A., Lovich, J.E., Rosen, P.C., Malone, M., Garber, S.D., 2021. Non-native Pond Sliders cause long-term decline of native Sonora Mud Turtles: A 33-year before-after study in an undisturbed natural environment. Aquat. Invasions 16, 542–570. https://doi.org/10.3391/ai.2021.16.3.10

Dytham, C., 2009. Evolved dispersal strategies at range margins. Proc. R. Soc. B Biol. Sci. 276, 1407–1413. https://doi.org/10.1098/rspb.2008.1535 ER

Fauth, J.E., Resetarits, W.J., 1999. Biting in the salamander *Siren intermedia intermedia*: Courtship component or agonistic behavior? J. Herpetol. 33, 493–496. https://doi.org/10.2307/1565651

Fey, S.B., Siepielski, A.M., Nusslé, S., Cervantes-Yoshida, K., Hwan, J.L., Huber, E.R., Fey, M.J., Catenazzi, A., Carlson, S.M., 2015. Recent shifts in the occurrence, cause, and magnitude of animal mass mortality events. Proc. Natl. Acad. Sci. 112, 1083–1088. https://doi.org/10.1073/pnas.1414894112

Fordham, D.A., Georges, A., Brook, B.W., 2009. Experimental evidence for density-dependent responses to mortality of Snake-necked Turtles. Oecologia 159, 271–281. https://doi.org/10.1007/s00442-008-1217-5

Frankham, R., Brook, B.W., 2004. The importance of time scale in conservation biology and ecology. Ann. Zool. Fennici 41, 459–463.

Gaillard, J.-M., Pontier, D., Allainé, D., Lebreton, J., Trouvilliez, J., Clobert, J., 1989. An analysis of demographic tactics in birds and mammals. Oikos 56, 59–76. https://doi.org/10.2307/3566088

Gaillard, J.-M., Yoccoz, N.G., Lebreton, J., Bonenfant, C., Devillard, S., Loison, A., Pontier, D., Allaine, D., 2005. Generation time: A reliable metric to measure life-history variation among mammalian populations. Am. Nat. 166, 119–123. https://doi.org/10.1086/430330

Gandon, S., 1999. Kin competition, the cost of inbreeding and the evolution of dispersal. J. Theor. Biol. 200, 345–364. https://doi.org/10.1006/jtbi.1999.0994

Gerber, L.R., Hilborn, R., 2001. Catastrophic events and recovery from low densities in populations of otariids: implications for risk of extinction. Mamm. Rev. 31, 131–150. https://doi.org/10.1046/j.1365-2907.2001.00081.x

Greenwood, P.J., 1980. Mating systems, philopatry and dispersal in birds and mammals. Anim. Behav. 28, 1140–1162. https://doi.org/10.1016/S0003-3472(80)80103-5

Gros, A., Poethke, H.J., Hovestadt, T., 2009. Sex-specific spatio-temporal variability in reproductive success promotes the evolution of sex-biased dispersal. Theor. Popul. Biol. 76, 13–18. https://doi.org/10.1016/j.tpb.2009.03.002

Hamilton, W.D., May, R.M., 1977. Dispersal in stable habitats. Nature 269, 578–581.

Hatch, J.M., Haas, H.L., Richards, P.M., Rose, K.A., 2019. Life-history constraints on maximum population growth for Loggerhead Turtles in the northwest Atlantic. Ecol. Evol. 9, 9442–9452. https://doi.org/10.1002/ece3.5398

Heppell, S.S., 1998. Application of life-history theory and population model analysis to turtle conservation. Copeia 1998, 367–375. https://doi.org/10.2307/1447430

Hutchings, J.A., 2021. A Primer of Life Histories : Ecology, Evolution, and Application. Oxford University Press, New York. https://doi.org/10.1093/oso/9780198839873.001.0001

Hutchings, J.A., Reynolds, J.D., 2004. Marine fish population collapses: Consequences for recovery and extinction risk. Bioscience 54, 297–309. https://doi.org/10.1641/0006-3568(2004)054[0297:MFPCCF]2.0.CO;2

Jones, M.T., Willey, L.L., Riichmond, A.M., Sievert, P.R., 2019. Reassessment of Agassiz's Wood Turtle collections reveals significant change in body size and growth rates. Herpetol. Conserv. Biol. 14, 41–50.

Jones, O.R., Gaillard, J.M., Tuljapurkar, S., Alho, J.S., Armitage, K.B., Becker, P.H., Bize, P., Brommer, J., Charmantier, A., Charpentier, M., Clutton-Brock, T., Dobson, F.S., Festa-Bianchet, M., Gustafsson, L., Jensen, H., Jones, C.G., Lillandt, B.G., McCleery, R., Merilä, J., Neuhaus, P., Nicoll, M.A.C., Norris, K., Oli, M.K., Pemberton, J., Pietiäinen, H., Ringsby, T.H., Roulin, A., Saether, B.E., Setchell, J.M., Sheldon, B.C., Thompson, P.M., Weimerskirch, H., Jean Wickings, E., Coulson, T., 2008. Senescence rates are determined by ranking on the fast–slow life-history continuum. Ecol. Lett. 11, 664–673. https://doi.org/10.1111/J.1461-0248.2008.01187.X

Jonsson, A., Ebenman, B., 2001. Are certain life histories particularly prone to local extinction? J. Theor. Biol. 209, 455–463. https://doi.org/10.1006/jtbi.2001.2280

Kim, K., Serret, H., Clauzel, C., Andersen, D., Jang, Y., 2019. Spatio-temporal characteristics and predictions of the endangered Leopard Cat *Prionailirus bengalensis euptilura* road-kills in the Republic of Korea. Glob. Ecol. Conserv. 19, e00673. https://doi.org/10.1016/j.gecco.2019.e00673

Lande, R., Engen, S., Sæther, B.-E., 1998. Extinction times in finite metapopulation models with stochastic local dynamics. Oikos 83, 383–389. https://doi.org/10.2307/3546853

Leturque, H., Rousset, F., 2004. Intersexual competition as an explanation for sex-ratio and dispersal biases in polygynous species. Evolution. 58, 2398–2408. https://doi.org/10.1554/04-186

Li, X.Y., Kokko, H., 2019. Intersexual resource competition and the evolution of sex-biased dispersal. Front. Ecol. Evol. 7, 111. https://doi.org/10.3389/FEVO.2019.00111/BIBTEX

Lindström, J., 1998. Harvesting and sex differences in demography. Wildlife Biol. 4, 213–221. https://doi.org/10.2981/wlb.1998.024

Lorenzen, K., 2016. Toward a new paradigm for growth modeling in fisheries stock assessments: Embracing plasticity and its consequences. Fish. Res. 180, 4–22. https://doi.org/10.1016/j.fishres.2016.01.006

Mabry, K.E., Shelley, E.L., Davis, K.E., Blumstein, D.T., Van Vuren, D.H., 2013. Social mating system and sex-biased dispersal in mammals and birds: a phylogenetic analysis. PLoS One 8, e57980. https://doi.org/10.1371/journal.pone.0057980

Mangel, M., Tier, C., 1994. Four facts every conservation biologists should know about persistence. Ecology 75, 607–614. https://doi.org/10.2307/1941719

Massemin, S., Maho, Y. Le, Handrich, Y., 1998. Seasonal pattern in age, sex and body condition of barn owls *Tyto alba* killed on motorways. Ibis. 140, 70–75. https://doi.org/10.1111/j.1474-919X.1998.tb04543.x

Matthysen, E., 2005. Density-dependent dispersal in birds and mammals. Ecography 28, 403–416.

Menges, E.S., 1990. Population viability analysis for an endangered plant. Conserv. Biol. 4, 52–62. https://doi.org/10.1111/j.1523-1739.1990.tb00267.x

Moldowan, P.D., Brooks, R.J., Litzgus, J.D., 2020. Demographics of injuries indicate sexual coercion in a population of Painted Turtles (*Chrysemys picta*). Can. J. Zool. cjz-2019-0238. https://doi.org/10.1139/cjz-2019-0238

Neubauer, P., Jensen, O.P., Hutchings, J.A., Baum, J.K., 2013. Resilience and recovery of overexploited marine populations. Science 340, 347–349. https://doi.org/10.1126/science.1230441

Niblick, H.A., Rostal, D.C., Classen, T., 1994. Role of male-male interactions and female choice in the mating system of the Desert Tortoise, *Gopherus agassizii*. Herpetol. Monogr. 8, 124–132. https://doi.org/10.2307/1467076

O'Grady, J.J., Reed, D.H., Brook, B.W., Frankham, R., 2008. Extinction risk scales better to generations than to years. Anim. Conserv. 11, 442–451. https://doi.org/10.1111/j.1469-1795.2008.00201.x

Orbach, D.N., Packard, J.M., Piwetz, S., Würsig, B., 2015. Sex-specific variation in conspecific-acquired marking prevalence among dusky dolphins (*Lagenorhynchus obscurus*). Can. J. Zool. 93, 383–390. https://doi.org/10.1139/cjz-2014-0302

Parvinen, K., Dieckmann, U., Gyllenberg, M., Metz, J.A.J., 2003. Evolution of dispersal in metapopulations with local density dependence and demographic stochasticity. J. Evol. Biol. 16, 143–153. https://doi.org/10.1046/j.1420-9101.2003.00478.x

Perrin, N., Mazalov, V., 2000. Local competition, inbreeding, and the evolution of sex-biased dispersal. Am. Nat. 155, 116–127. https://doi.org/10.1086/303296

Perrin, N., Mazalov, V., 1999. Dispersal and inbreeding avoidance. Am. Nat. 154, 282–292. https://doi.org/10.1086/303236

Piczak, M.L., Markle, C.E., Chow-Fraser, P., 2019. Decades of road mortality cause severe decline in a Common Snapping Turtle (*Chelydra serpentina*) population from an urbanized wetland. Chelonian Conserv. Biol. 18, 231–240. https://doi.org/10.2744/CCB-1345.1

Poethke, H.J., Hovestadt, T., Mitesser, O., 2003. Local extinction and the evolution of dispersal rates: Causes and correlations . Am. Nat. 161, 631–640. https://doi.org/10.1086/368224

Ricklefs, R.E., Wikelski, M., 2002. The physiology/life-history nexus. Trends Ecol. Evol. 17, 462–468. https://doi.org/10.1016/S0169-5347(02)02578-8

Rivalan, P., Prévot-Julliard, A.C., Choquet, R., Pradel, R., Jacquemin, B., Girondot, M., 2005. Trade-off between current reproductive effort and delay to next reproduction in the Leatherback Sea Turtle. Oecologia 145, 564–574. https://doi.org/10.1007/S00442-005-0159-4

Roff, D.A., 2002. Life History Evolution. Sinauer, Sunderland, MA.

Rose, J.P., Ersan, J.S.M., Wylie, G.D., Casazza, M.L., Halstead, B.J., 2019. Demographic factors affecting population growth in Giant Gartersnakes. J. Wildl. Manage. 83, 1540–1551. https://doi.org/10.1002/jwmg.21728

Ruxton, G.D., Rohani, P., 1999. Fitness-dependent dispersal in metapopulations and its consequences for persistence and synchrony. J. Anim. Ecol. 68, 530–539. https://doi.org/10.1046/j.1365-2656.1999.00300.x

Rytwinski, T., Fahrig, L., 2012. Do species life history traits explain population responses to roads? A meta-analysis. Biol. Conserv. 147, 87–98. https://doi.org/10.1016/j.biocon.2011.11.023

Sæther, B.-E., Engen, S., Lande, R., 1999. Finite metapopulation models with density-dependent migration and stochastic local dynamics. Proc. R. Soc. B Biol. Sci. 266, 113–118.

Sæther, B.-E., Lande, R., Engen, S., Weimerskirch, H., Lillegard, M., Altwegg, R., Becker, P.H., Bregnballe, T., Brommer, J.E., McCleery, R.H., Merila, J., Nyholm, E., Rendell, W., Robertson, R.R., Tryjanowski, P., Visser, M.E., 2005. Generation time and temporal scaling of bird population dynamics. Nature 436, 99–102. https://doi.org/10.1038/nature03666

Scott, E.M., Mann, J., Watson-Capps, J.J., Sargeant, B.L., Connor, R.C., 2005. Aggression in bottlenose dolphins: Evidence for sexual coercion, male-male competition, and female tolerance through analysis of tooth-rake marks and behaviour. Behaviour 142, 21–44. https://doi.org/10.1163/1568539053627712

Shine, R., 1989. Ecological causes for the evolution of sexual dimorphism: A review of the evidence. Q. Rev. Biol. 64, 419–461. https://doi.org/10.1086/416458

Shine, R., 1978. Sexual size dimorphism and male combat in snakes. Oecologia 33, 269–277. https://doi.org/10.1007/BF00348113

Shine, R., Iverson, J.B., 1995. Patterns of survival, growth and maturation in turtles. Oikos 72, 343–348. https://doi.org/10.2307/3546119

Spencer, R.-J., Janzen, F.J., Thompson, M.B., 2006. Counterintuitive density-dependent growth in a long-lived vertebrate after removal of nest predators. Ecology 87, 3109–3118. https://doi.org/10.1890/0012-9658(2006)87[3109:CDGIAL]2.0.CO;2

Stearns, S.C., 1992. The Evolution of Life Histories. Oxford University Press.

Storm, G.L., Andrews, R.D., Phillips, R.L., Bishop, R.A., Siniff, D.B., Tester, J.R., 1976. Morphology, reproduction, dispersal, and morality of midwestern red fox populations. Wildl. Monogr. 49, 3–82.

Stubbs, D., Swingland, I.R., Hailey, A., Pulford, E., 1985. The ecology of the Mediterranean Tortoise *Testudo hermanni* in Northern Greece: the effects of a catastrophe on population structure and density. Biol. Conserv. 31, 125–152. https://doi.org/10.1016/0006-3207(85)90045-X

Tinbergen, N., 1963. On aims and methods of ethology. Z. Tierpsychol. 20, 410–433. https://doi.org/10.1111/j.1439-0310.1963.tb01161.x

Trochet, A., Courtois, E.A., Stevens, V.M., Baguette, M., Chaine, A., Schmeller, D.S., Clobert, J., Wiens, J.J., 2016. Evolution of sex-biased dispersal. Q. Rev. Biol. 91, 297–320. https://doi.org/10.1086/688097

Vélez-Espino, L.A., Koops, M.A., 2012. Capacity for increase, compensatory reserves, and catastrophes as determinants of minimum viable population in freshwater fishes. Ecol. Modell. 247, 319–326. https://doi.org/10.1016/j.ecolmodel.2012.09.022

Ward, E.J., Hilborn, R., Towell, R.G., Gerber, L., 2007. A state–space mixture approach for estimating catastrophic events in time series data. Can. J. Fish. Aquat. Sci. 64, 899–910. https://doi.org/10.1139/f07-060

Williams, G.C., 1966. Natural selection, the costs of reproduction, and a refinement of Lack's Principle. Am. Nat. 100, 687–690. https://doi.org/10.1086/282461

Wolf, M., Van Doorn, G.S., Leimar, O., Weissing, F.J., 2007. Life-history trade-offs favour the evolution of animal personalities. Nat. 2007 4477144 447, 581–584. https://doi.org/10.1038/nature05835

Chapter 1

Post-catastrophe patterns of abundance and survival reveal no evidence of population recovery in a long-lived animal

Published as:

Keevil, M.G., Brooks, R.J., Litzgus, J.D., 2018. Post-catastrophe patterns of abundance and survival reveal no evidence of population recovery in a long-lived animal. Ecosphere 9, e02396. https://doi.org/10.1002/ecs2.2396

Abstract.

Population catastrophes are widespread, unpredictable phenomena occurring in natural populations that have important, yet frequently underappreciated, consequences for persistence. As human impacts on ecosystems increase globally, the frequency of catastrophes is likely to rise as increasingly fragmented and depleted populations become more vulnerable. Species with slow life histories are expected to recover slowly from catastrophes because of their longer generation times, and assessing their population recovery requires data spanning long periods. We report results from a long-term mark-recapture study of Snapping Turtles (*Chelydra serpentina*) in Algonquin Provincial Park, Ontario, that experienced a major mortality event from winter predation by River Otters. We estimated abundance and survival of nesting females before, during, and 23 years following the catastrophe. We built multi-state mark-recapture models incorporating movement between sites, temporary emigration, and observation effects. We found that during the 3-year mortality event, abundance of nesting females declined by 39% overall, and by 49% at our focal nesting area. Apparent survivorship of nesting females during these three years fell from 0.94 before the mortality event to 0.76 at the focal site and 0.86 at adjacent nest sites. Survivorship over the following 23-year period averaged 0.972 and 0.940 at the two sampling areas. Despite high post-catastrophe survivorship and connectivity with other populations, the population failed to recover, displaying consistently reduced abundances across 23 post-catastrophe years. We discuss the relationship between life-history attributes and the causes and consequences of local catastrophes and their conservation implications.

Introduction

The current global extinction crisis has resulted in an estimated one-thousand-fold increase in extinction above the baseline rate (Pimm et al., 2014). A recent assessment of vertebrate populations based on the Living Planet Index (Collen et al., 2009) estimates that average declines in abundance since 1970 have reached 52% (World Wildlife Fund, 2014). The greatest single contributing factor to these observed declines is direct exploitation (World Wildlife Fund, 2014). Another emerging global threat is climate change (World Wildlife Fund, 2014), which is increasing environmental variability, including the potential for increases in the frequency of extreme weather related events such as wildfires, droughts, and floods (IPCC, 2014). Both classes of threats can produce catastrophes, resulting in sudden and severe declines in abundance of affected populations (Fey et al., 2015). A catastrophe may be defined as a short-term decline of over 50% of a population, and the probability of catastrophes in vertebrate populations is estimated to be 14% per generation (Gerber and Hilborn, 2001; Reed et al., 2003; Ward et al., 2007). Natural and anthropogenic population catastrophes can have a disproportionately large impact on population persistence and in many cases may be the dominant process causing extinctions (Menges 1990, Mangel and Tier 1994; but see Finkelstein et al. 2010). The risk that catastrophes pose to population persistence is expected to depend on their frequency relative to generation time (Frankham and Brook, 2004; O'Grady et al., 2008). Thus, for long-lived species, catastrophes that are spaced far apart in time could still have important effects on abundance and persistence. Unfortunately, published reports of catastrophes often fail to quantify long-term consequences (Fey et al., 2015).

Life-history traits have important consequences for population responses to potentially catastrophic events. Populations with faster life histories are more vulnerable to perturbations in

reproductive success, whereas those with slow life histories are most sensitive to adult survivorship (Jonsson and Ebenman, 2001) and thus take longer to recover from depletion (Hutchings and Reynolds, 2004; Neubauer et al., 2013; Roff, 2002). Conversely, length of generation time is positively correlated with per-generation strength of density-dependent compensation in some groups such as birds (Sæther et al., 2005), marine fishes (Bjørkvoll et al., 2012), and freshwater fishes (Vélez-Espino and Koops, 2012). Species with fast life histories also tend to be more sensitive to environmental stochasticity, which disproportionately impacts younger age classes, and show more variation in population growth rate (Bjørkvoll et al., 2012; Gaillard et al., 2005; Jonsson and Ebenman, 2001; Sæther et al., 2005). Effective density-dependent compensation increases population growth rate following declines, eventually allowing for recovery from perturbations.

Among vertebrates, turtles are disproportionately imperilled (Böhm et al., 2013; Gibbons et al., 2000). Turtles typify the slow end of the life-history spectrum, exhibiting iteroparity, high adult survivorship, and low and variable juvenile recruitment. Populations of organisms with slow life history strategies are vulnerable to even small decreases in adult survivorship, with as little as a 2–3% reduction in survivorship resulting in severe population decline (Congdon et al. 1993, 1994, Cunnington and Brooks 1996, Enneson and Litzgus 2008). As with other long-lived organisms, much concern in chelonian conservation has been focused on anthropogenic increases in chronic mortality caused by threats such as road mortality (Steen et al., 2006), fishing gear entanglement (Midwood et al., 2015; Steen et al., 2014), hunting and collecting (Colteaux and Johnson, 2017; Garber and Burger, 1995; Nickerson and Pitt, 2012), boat strikes (Bennett and Litzgus, 2014; Bulté et al., 2010), and introduced or subsidized predators (Fordham et al., 2007). In addition to chronic threats, acute catastrophes have been observed in populations of multiple

chelonian species in different ecological contexts. Catastrophic local declines have been caused by droughts (*Gopherus agassizii* (Longshore et al., 2003), *Chrysemys picta* (Christiansen and Bickham, 1989)), fire (*Testudo hermanii* (Hailey and Willemsen, 2000; Stubbs et al., 1985)), pathogens (*Terrapene carolina* (Johnson et al., 2008), *Myuchelys georgesi* (Spencer et al., 2018)), road mortality (Aresco, 2005), and hunting (Nickerson and Pitt, 2012). In some cases the causes are mysterious (Catrysse et al., 2015; Sheppard, 2014). Many ecologists and conservationists believe that turtles are likely to have only a weak ability to compensate for perturbations and that recovery of turtle populations after declines will be extremely slow, if they occur at all (Brooks et al. 1991, Congdon et al. 1993, 1994, Cunnington and Brooks 1996, Heppell 1998, Enneson and Litzgus 2008). However, some authors have suggested that some turtle populations show a more robust compensatory response (Bjorndal et al., 2000; Fordham et al., 2009; Spencer et al., 2006; Stubbs et al., 1985). For long-lived species, a better understanding of the long-term risks associated with short-term perturbations is needed to inform management decisions.

Snapping Turtles (*Chelydra serpentina*) are near the northern limit of their distribution in Algonquin Park, Ontario, Canada where a population in Lake Sasajewun has been the subject of a long-term life-history study since 1972. Snapping Turtles in this population have very slow life histories with late age at maturity (16–19 years for females), low and variable recruitment, and high adult survival (Armstrong and Brooks, 2013; Brooks et al., 1991; Cunnington and Brooks, 1996; Galbraith et al., 1989). During the winters of 1986–1989, the study population experienced predation by River Otters (*Lontra canadensis*) that amounted to an acute catastrophe in which approximately 50% of the adult population was killed (Brooks et al., 1991). Given the slow life-history of turtles, and the climatic constraints experienced by northern populations, Brooks, et al.

(1991) predicted a very slow and limited recovery. Here we present updated abundance and survival for this population to evaluate the recovery 23 years after the catastrophe and in light of a second putative mortality event resulting from the blowout of the dam on the study lake. Abundance and survival of nesting females were analyzed using multistate models that allowed for survival and detection to vary with time and between sites, and accounted for movement between sites and temporary emigration. We assess evidence for density dependent compensation in nesting female survivorship by comparing survival before and after the catastrophe using Bayesian variable selection and examining the trend in abundance. We also estimate recent abundance of adults in the study lake and compare it to previously-reported pre- and post-catastrophe estimates.

Methods

Study site and sampling methods

The long-term Snapping Turtle life-history project began in 1972 at the Algonquin Wildlife Research Station (WRS) in Algonquin Provincial Park, Ontario, Canada. Because of the combination of high latitude and cold regional climate, the study site is near the northern climatic limit of the distribution of Snapping Turtles (Bobyn and Brooks, 1994). Annual capture-mark-recapture (CMR) sampling with baited hoop traps, opportunistic capturing from canoe, and nest site monitoring occurs at the WRS population within the North Madawaska River drainage basin and at several alternate sites near the Highway 60 corridor within 10 km of the WRS. Lake Sasajewun, a 43.5 ha impoundment of the North Madawaska River, has received the majority of the trapping effort although surrounding water bodies have also been surveyed. Turtles are marked by notching the marginal scutes (Cagle, 1939) and adults are tagged by wiring aluminum tags into holes drilled through the marginal scutes (Loncke and Obbard, 1977). Further details of

the study site and field methods are described elsewhere (Galbraith et al., 1988; Keevil et al., 2017; Obbard and Brooks, 1981).

Defining Populations for Analyses

We performed two separate mark-recapture analyses. First, we analyzed survivorship and abundance of females sampled during 34 years of nesting surveys at sites within the North Madawaska River basin (NMB; Figure 1.1). Second, we estimated recent abundance of the adult male and female residents of Lake Sasajewun sampled by trapping and canoe captures to assess recovery of both sexes using data that are independent of nest site selection.

The analysis of survival and abundance of nesting females was performed for the period from 1980 to 2013. Females were considered to have entered the population upon their first capture at a nesting site within the NMB and only subsequent recaptures during nest site monitoring were included. Recaptures by aquatic sampling were excluded from this portion of the analysis as they would be biased towards the subset of females whose summer home ranges are in Lake Sasajewun. The embankment of the Sasajewun dam at the southeast end of the lake is the most intensively monitored and most important nest site for turtles residing within the lake and in water bodies upstream. Between the dam and the mouth of the river at Lake of Two Rivers are five other known nesting areas (Figure 1.1). In addition, we also included nesting sites around Mew Lake, which is 200 m away from the North Madawaska River and is connected by a short tributary (700 m). The greatest straight-line distance between any two nesting sites is 2.3 km (Figure 1.1).

Abundance of adult females at monitored nesting sites might not track abundance of adults in aquatic habitat. To assess this possibility we estimated the recent adult population size at Lake

Sasajewun, our focal aquatic sampling site, and assessed similarity to historical abundance estimates before and during the 1986–89 mortality event reported by Brooks et al. (1991). Adult turtles (females with straight-line carapace lengths (SCL) > 24 cm; males SCL > 30 cm) captured by baited hoop trap or by canoe in Lake Sasajewun from 2009 to 2013 were included in survival and abundance estimates of the lake population. During this period, data on secondary (within-season) captures were available. Juveniles and sub-adult turtles were excluded from the analysis because of their substantially lower recapture rate (*unpubl. data*). The criterion for minimum female size reflects the known threshold for maturity in our study area (Armstrong and Brooks, 2013) whereas that for males is based on our observation that smaller males are less likely to be recaptured within the same water body and less likely to show sex-specific behaviors such as eversion of the penis and wounding from conspecific aggression (Keevil et al. 2017).

Mark-recapture analysis I: Nesting females (1980−2013)

To estimate abundance and survival of nesting females, we developed CMR models that treated nesting on the Sasajewun dam as a state and nesting on the other sampled sites within the NMR basin ("alternate sites") as a second state to allow for possible differences in survival and detection among sites. Population analysis of nesting females was therefore done in a multistate framework (Brownie et al., 1993). Development of models proceeded in four steps: 1) Goodness-of-fit (GOF) testing for standard, initial multistate models was performed in Programs MARK and U-CARE; 2) Incorporating observation effects and temporary emigration to create candidate base models using the multistate m-array parameterization (Burnham et al., 1987; Lebreton et al., 2009) implemented in Program JAGS (Plummer, 2003) to account for lack of fit. Fit was then reassessed using posterior predictive checks. 3) After selecting a base model, further model selection was done for recapture and survivorship parameters using Gibbs Variable Selection

(GVS) (Dellaportas et al., 2000; O'Hara and Sillanpää, 2009) to assess support for hypotheses of survival differences between periods (before, during, and after mortality events) and states (dam and alternate sites) and to select an appropriate structure with which to assess abundance; 4) Abundance was assessed using a state-space model with parameter-expanded data augmentation implemented in WinBUGS (Lunn et al. 2000; Royle and Dorazio 2012). Each of these steps is described in the following sections, and further details are given in Appendix S1.

Initial model construction and GOF. The CMR data of nesting females were analysed using multistate models with nesting on the Sasajewun dam as one state and nesting at pooled alternate sites as another state to allow for transitions and differential survival and detection probability between sites (Brownie et al., 1993). We included *period* as a categorical time effect on survival and movement to reflect *a priori* hypotheses about the effects of the otter predation event (before, during = *otter*, after = *after*) and the temporary failure of the Sasajewun dam during the spring of 1998 (*blowout*) (Table A.1). Program U-CARE (Choquet et al., 2005) was used to test GOF of the fully parameterized multistate model (Pradel et al., 2003). GOF of a reduced parameter model was tested using the parametric bootstrap GOF procedure implemented in MARK (White et al., 2006; White and Burnham, 1999).

Construction of candidate general models. Three candidate general models were implemented in Program JAGS (Plummer, 2003) and assessed for adequate fit to the data before further model selection: constrained Conditional Arnason–Schwarz (CAS), CAS modified for temporary emigration (TE), and CAS with immediate observation effects (OE). Because of sparseness of the data, and informed by a preliminary exploration in MARK that indicated that many parameters were not identifiable in models with fixed time effects on survival and transitions, we started with a constrained, reduced-parameter model:

$$S_{site*period+E(t)}\, p_{site*t}\, \psi^{S-}_{E(t)}$$

which has fixed effects of *period*, *site*, and their interaction as well as random year effects ($E(t)$) on survivorship, S; fixed period and site effects on recapture probability p; and random time effects on state transitions ψ. Treating year as a random effect requires far fewer parameters than fixed time effects while avoiding the potentially unrealistic constraint of identical parameters across multiple years. Using random effects leverages the large number of sampled occasions to estimate time variation and to share data across years despite relatively low numbers of observations per occasion. We treated year as a fixed effect on p because our initial data exploration indicated multi-year trends and because *a priori* knowledge of long-term fluctuations in recapture effort suggested that separate parameters for each year would be more appropriate.

We chose the m-array parameterization for model selection and GOF analysis because it was better-suited than state-space models for posterior predictive checking and comparing among candidate models (Kéry and Schaub, 2012). See Appendix S1 for details of multistate m-array model construction.

Temporary emigration. We modified the CAS framework to account for temporary emigration (TE) by adding unobservable states (Figure 1.2) (Fujiwara and Caswell, 2002; Kendall and Nichols, 2002; Schaub et al., 2004). We used two unobservable states: C1 for individuals that became temporarily unavailable for capture from the Sasajewun dam (A), and C2 for individuals temporarily unavailable from the alternate sites (B). Under this model, individuals could not transition between C1 and C2, B and C1, or A and C2. Survival in C1 was the same for A, and C2 survival was the same as B. Because our dataset is relatively sparse, we modelled transition

probabilities involving unobservable states as time-invariant fixed effects. See Appendix S1 for multistate m-array model modifications for TE.

Observation effects. Observation effects (OE) occur when the probability of detection varies depending on whether an individual was observed on a previous occasion, and are often called behavioral response or trap dependence (Otis et al., 1978; Pradel, 1993), although such effects can result from observer behavior rather than behavioral responses of animals (Kéry and Schaub, 2012; Papadatou et al., 2012; Schaub et al., 2005). Observation effects can be modeled using a separate, individually indexed recapture matrix (Kéry and Schaub, 2012; Pradel and Sanz-Aguilar, 2012) or multiple states can be used to model immediate observation effects in the state-space framework (Gimenez et al., 2003; Pradel and Sanz-Aguilar, 2012; Schaub et al., 2009). Instead, we devised another method that was more straight-forward to implement in the multistate m-array formulation (see Appendix S1 for details).

Comparing candidate general models. We assessed the fit of our three candidate general models, CAS, TE, and OE, using posterior predictive checks (Gelman et al., 2004). We compared model discrepancy, calculated as the Freeman-Tukey statistic, between the observed data and data simulated using the model (Brooks et al., 2000; Kéry and Schaub, 2012). Fit statistics were computed within the JAGS model code and assessed visually using scatterplots and Bayesian p-values (Gelman et al., 2004). DIC (deviance information criterion; Spiegelhalter et al. 2002) was computed in JAGS and used to compare TE and OE models.

Variable selection. We used a generalized linear model (GLM) parameterization for *S* and *p* to examine effects of individual parameters and for variable selection. The general model for survivorship is

$$\text{logit}(S) = \beta_0 + \beta_1 + \beta_2 + \beta_3 + \beta_4 + \beta_5 + \beta_6 + \beta_7 + \epsilon_t$$

where β_0 = intercept, $\beta_{1\ldots3}$ are the effects for three of the four levels of *period* (the first level is the intercept), β_4 is the effect of site, and $\beta_{5\ldots7}$ are the interactions of *site* and *period*, and ϵ_t is the random time effect. To induce a minimally informative prior for mean survivorship on the probability scale, we used a $\mu_i = 0$ for the mean and an inverse gamma hyperprior (King et al., 2010) for the variance, $\sigma_i^2 \sim \Gamma^{-1}(4,5)$, as β_i priors. This produces an approximately flat prior for sums of three parameters (Figure A.1). We used the same prior for each parameter in our general model of recapture probability *p*:

$$\text{logit}(p) = \beta_{site} + \beta_{\text{T}(1)} + \ldots + \beta_{\text{T}(T)} + \beta_{\text{site*T}(1)} + \ldots + \beta_{\text{site*T}(T)}$$

or

$$\text{logit}(p_{site,t}) = \beta_{site} + \beta_{\text{T}(t)} + \beta_{\text{site*T}(t)}$$

where β_{site} are the fixed site effects, $\beta_{\text{T}(t)}$ are the fixed effects of occasion *t*, and $\beta_{\text{site}*\text{T}(t)}$ are the interactions of *site* and occasion *t*.

We used GVS (Dellaportas et al., 2000) to assess support for the inclusion of parameters affecting *S* and *p*. To assess effects of *site*, *occasion*, and their interaction on recapture probability, the 33 occasion parameters were assigned a single inclusion parameter, as were the 33 interaction parameters, with the result that these variables were selected (or not) as single blocks. We only considered nested sub-models so that models with an interaction always included both *occasion* and *site* main effects. This resulted in five possible sub-models which were (adapting the notation of Lebreton et al. 1992): *p*(.), *p*(*t*), *p*(*site*), *p*(*site*+*t*), and *p*(*site***t*).

In order to apply GVS to survivorship parameters, we used dam = 1, alternate sites = 0 dummy coding in the design matrix of the survivorship GLM so that the interaction *site* * $period_i$ without one or both of the corresponding main effects parameters implies a model in which the effect of $period_i$ applies only to the dam nesting females. We view such non-nested candidate models as meaningful hypotheses in which survival changed at the Sasajewun dam but not at the alternate sites which were farther from the observed mortality. Further details about our implementation of GVS are available in Appendix S1.

Estimation of abundance of nesting females using data augmentation. In the CAS family of models, individuals are excluded from the likelihood before first capture and therefore abundance cannot be directly estimated. To estimate abundance, we modified our preferred model, TE, identified using the procedure described above (and see Results), to implement it in a state-space formulation with parameter-expanded data augmentation (Figure 1.2). This model was implemented in Program WinBUGS (Lunn et al., 2000) through the R package R2WinBUGS (R Development Core Team, 2020; Sturtz et al., 2005). While not a focus of our analysis, a consequence of the abundance model with TE is that it produces an estimate of the number of females that are unavailable during nesting which has bearing on reproductive frequency, an important but difficult-to-estimate life history parameter. State-space CMR models separate the observation (captured in A, captured in B, not captured) and population processes (entry, survival, and site transitions) (Gimenez et al., 2007; Royle and Dorazio, 2012), and are convenient to implement in WinBUGS. In the multi-state formulation described in Royle and Dorazio (2012), the removal entry probability, $\gamma_{t,s}$, is the probability that an individual M_i in the pre-entry state will be recruited into an alive state *s* (in our case, one of two nesting areas: A = dam and B = alternate) on occasion *t*. This parameter is required to implement data augmentation

but does not have direct biological meaning (Kéry and Schaub, 2012; Royle and Dorazio, 2012). A dummy occasion was added before the first occasion (so that indexing differs between m-array and state-space models, see Table A.1) and thus $\gamma_{1,s}$ becomes the proportions of individuals present on the first real occasion at each site and the multi-state model becomes conditional on individuals being present rather than conditional on initial capture, allowing abundance and time-dependent recruitment of adults at nesting sites to be estimated (Kéry and Schaub, 2012). Details of our implementation of the data-augmented state-space model are provided in the Appendix S1.

To quantify the effect of the single dam blowout event in early spring 1998, we estimated the number of nesting female turtles that died during that 1997/98 interval by subtracting the number expected to die in a typical post-catastrophe interval (mean survivorship during 1989/90−2012/13, subscript pc) from the estimated number of actual deaths:

$$deaths = \sum_{i=1}^{M} \mathrm{I}(z_{i,19} \neq 6 \,\mathrm{AND}\, z_{i,20} = 6) - \mathrm{Bin}\left(\left(N_{97}^{A} + N_{97}^{C1}\right), \left(1 - \bar{S}_{\mathrm{pc}}^{A}\right)\right) - \mathrm{Bin}\left(\left(N_{97}^{B} + N_{97}^{C2}\right), \left(1 - \bar{S}_{\mathrm{pc}}^{B}\right)\right)$$

where z_{ij} is the latent state matrix that contains information on the known or estimated state of each individual *i* on each occasion *j* (see Appendix S1 for details).

Mark-recapture analysis II: Abundance of males and females (2009−2013)

We performed a simple robust design analysis to estimate mean adult male and female abundance in Lake Sasajewun using trap and canoe captures over five years (primary occasions). We consolidated trapping and canoe surveys within each year into 1 to 3 secondary occasions (Table 1.1) and counted the number secondary occasions in which each individual was captured in each year. We analyzed these data using a state-space formulation with data augmentation similar to that described above for abundance of nesting females. We assumed that the number of observed encounters of each individual in each occasion was a binomial random variable with the total equal to the number of secondary occasions, and probability as the product of recapture probability $p_{i,t}$ and the latent state $z_{i,t}$ (Royle and Dorazio, 2012). Because of the small sample of individuals and occasions, and our limited objectives for this analysis (mean abundance), we did not use formal model selection to rank a large number of models, and instead chose a reasonable reduced-parameter fixed effects model ($\varphi_{sex}p_{sex+t}\gamma_{t*sex}$) that assumed apparent survival φ varied only by sex, recapture probability varied by primary occasion with a constant additive effect of sex on the logit scale, and removal entry probability varied by time and sex. This analysis was carried out in Program WinBUGS (v.1.4) (Lunn et al. 2000) through the R2WinBUGS package in Program R (Sturtz, Ligges and Gelman 2005; R Development Core Team, 2012).

Results

Mark-recapture analysis I: Nesting females (1980−2013)

Between 1980 and 2013, 140 individual female Snapping Turtles were observed at the North Madawaska Basin (NMB) nesting sites. Fifty-eight females were observed nesting across sites on the first occasion but only 22 were confirmed on the last occasion. Seven turtles were observed on both the first and last occasions, and another two females were known to be alive but not observed on one of those occasions. One female that nested in 2013 had been recorded nesting in 1972, which was the first year the population was studied. Three others observed in 2013 were first observed nesting in 1973. All four had already been nesting for some years, based on size at initial capture (Armstrong and Brooks, 2014).

Model selection. A multistate model with temporary emigration (TE) emerged as our preferred model (see Appendix S1 for detailed results of GOF analysis and initial model selection). Apparent survival beta parameters, posterior means, and 95% CRI of the general model are compared with those of the observation effects (OE) model (see Appendix S1 for OE model results) and the TE preferred model in Figure 1.3. TE model averaged apparent survival, state transition, and recapture probabilities are shown in Figure 1.4. Marginal posterior probabilities of each parameter were averaged across models for survivorship parameters and recapture sub-models to assess their relative support (Table 1.2 and Table 1.3). Support for an effect of otter predation on apparent survival was very high, with 99.8% posterior probability of effects of *otter* or *otter*site* (Table 1.2). Likewise, pooling main and interaction effects, there were >90% posterior probabilities for a change in survival during the post-otter low abundance period (*after*) and for the *blowout* effect. Only *after* had higher support for the interaction term alone than for

the main effects or main effects and interaction, which indicates that the *after* effect primarily affected individuals nesting on the dam. There was little support for excluding any of the *period* effects (Table 1.2). Out of a model space of 635, no single combination of survival and recapture parameters achieved >10% posterior probability following GVS, indicating that no single model received unambiguous support and therefore we selected the highest probability combination of main and *site* interaction effects for each *period* resulting in the following model used to estimate abundance:

$$\text{logit}\left(S_{i,t}\right) = \beta_0 + \beta_{\text{otter}} + \beta_{\text{otter}*\text{site}} + \beta_{\text{after}*\text{site}} + \beta_{\text{blowout}} + \varepsilon_t$$

A time-dependent model of recapture probabilities ($p(t)$, 72% posterior probability) was highly supported while a model with additive *site* effects was the second most supported ($p(site+t)$, 23% posterior probability) (Table 1.3).

Survivorship, transition, and recapture probability. Apparent survival, taking into account model uncertainty, varied across *site* and *period* (Figure 1.4; Figure 1.5). Mean apparent survivorship estimates of the abundance model over the four periods (*before, otter, after, blowout*) are shown with credible intervals in Figure 1.5. Survival at the alternate sites was mostly constant across years except for the otter predation and dam blowout events (Figure 1.4). The impact of the otter mortality event was more severe for dam-nesting turtles. After the mortality event, apparent survivorship of dam-nesting females was higher than at the alternate sites and higher than during the *before* period.

Mean annual probability of a female switching nest sites from the dam to an alternate site was 0.062 (95% CRI 0.041, 0.084) with variance 0.3 (0.0, 0.8) whereas switching from an alternate site to the dam was 0.081 (0.043, 0.12) with variance 0.6 (0.0, 1.4) (Figure 1.4; Figure 1.5). The

estimate of constant transition probability from the dam to an unobservable state (psiAC1) was 0.024 (0.002, 0.066) and that from alternate (psiBC2) sites was 0.13 (0.08, 0.18). Females returned to the alternate sites from an unobserved state (psiC2B) with probability 0.42 (0.29, 0.56). The probability of returning to the dam from an unobserved state was 0.49 (0.030, 0.96), which is essentially the same mean and CRI as the U[0,1] prior, strongly suggesting that this parameter was not identifiable (Figure A.4; Gimenez et al., 2009).

Estimated recapture probability varied with occasion but was essentially the same between sites when differences in temporary emigration were accounted for (Figure 1.4;), reflecting the high averaged posterior probability obtained for the *p(t)* sub-model (Table 1.3). Recapture probabilities declined after about 2000, reached the lowest point in 2009, and increased after that, matching our expectations based on trends in sampling effort. In general, estimated recapture probability was high, with a median of 0.86 across years and sites.

Patterns of abundance of nesting females. Total median abundance estimates in the NMB varied from 57 to 69 females (mean = 65.1) between 1980 and 1986 and then dropped rapidly to 41 during the subsequent three winters of high mortality (Figure 1.6). Mean total abundance was 41.6 over the five years following the catastrophe between 1989 and 1993, and 40.4 over the most recent five years (2009–2013). The decline was more severe for the subset of turtles nesting on the dam whose abundance decreased from a mean estimate of 34.7 (0.4 unobservable) in 1986 to 17.9 in 1989 (0.3 unobservable) and then 16.0 (0.01 unobservable) the following year. Mean abundance over the most recent five years is estimated at 18.8 (0.44 unobservable). Abundance in 2013, the last occasion, was 18.8 (0.18 unobservable) and 20.3 (3.3 unobservable) for the dam and alternate sites, respectively. A graphical comparison of parameter estimates between the state-space abundance model and the conditional multinomial m-array showed estimates were

very similar (Figure 1.5) with slightly higher precision of apparent survivorship in the state-space model, likely because it did not include model uncertainty. Over all occasions included in this analysis (excluding the first when no estimate is available), the proportion of individuals estimated to be temporarily unobservable during a nesting season was 0.016 (95% CRI = 0.00, 0.050) for dam nesting females and 0.19 (0.15, 0.24) at alternate sites. The relative abundance of the temporarily unavailable fraction of the nesting populations averaged 1.6% (95% CRI, 0 – 5.0%) at the dam and 19% (95% CRI, 15 – 24%) at the alternate sites across all occasions.

The estimated number of individuals recruited (individuals newly maturing and nesting in situ or new immigrants) annually is shown in Figure 1.7. A median of 57 individual nesting females was estimated to be present at the NMB on the first occasion and a further 82 entered the population from 1981 to 2013. Annual recruitment (entry of new adults) was higher over the first seven intervals (median = 5) than over the remaining 26 intervals (median = 2). The median estimated number of individuals killed during the blowout was 8, (mean 7.5, 95% CRI = 3, 12). One individual, an adult female, was found dead in 1998 on the occasion following the blowout.

Mark-recapture analysis II: Abundance of males and females (2009–2013)

Estimates of adult male and female abundance using a simple robust model of trapping and canoe observations in Lake Sasajewun from 2009 to 2013 are shown in Figure 1.8. The mean abundance over all five occasions was 12.5 for females and 9.5 males, respectively. Apparent survivorship was substantially lower at 0.84 than survivorship estimated from nest site surveys and likely indicates lower fidelity or higher transience or temporary emigration. Mean recapture probabilities were 0.40 (range 0.32, 0.61) for males and 0.31 (range 0.24, 0.51) for females over the five occasions.

Discussion

Our analyses show that despite a return to pre-catastrophe survivorship, abundances of Snapping Turtles 23 years after a major decline (i.e., long enough for offspring born after the catastrophe to begin to be recruited) are essentially the same as they were in the years immediately after the catastrophe. Such a limited population response is consistent with constraints posed by the life history traits of Snapping Turtles. There has been limited evidence of population recovery.

Abundance and survival of nesting females. Our analysis of the nesting female population produced similar estimates of declining abundance as those reported in the earlier analysis by Brooks et al. (1991). Three winters of elevated predation during which survivorship fell from 0.94 to 0.76 (dam) and 0.86 (alternate sites) was enough to reduce the population by approximately 39% (Figure 1.6). The abundance trend was nearly flat over the subsequent 23 years indicating that recovery has been very slow to non-existent. There was some evidence that the early spring flood followed by failure of the Sasajewun dam in 1998 resulted in further excess mortality, also contributing to lack of recovery. Furthermore, annual recruitment (entry of new adults) to the nesting population was essentially flat over most of the study (Figure 1.7), and was balanced by mortality except during the catastrophes.

A density-dependent response in survival would be expected to have a substantial positive impact on population recovery. There was some evidence for an increase in survivorship of adult females nesting at the dam after the catastrophe, but not for females nesting at the alternate sites who may be subjected to road mortality as some of the alternate sites are adjacent to a two-lane highway. It is also possible that predation by otters began, but was undetected, prior to the three

intervals of high mortality that we observed. This would lower the relative survival during the pre-catastrophe period and could contribute to the pattern we observed. Another possibility, conditional on survival heterogeneity among individual adults, is that turtles surviving the mortality event have higher survivorship in general and made up a higher proportion of the post-mortality event population. Adult survival heterogeneity based on size has been detected in our population (Armstrong et al., 2018) but no size bias was detected for predated turtles (Brooks et al., 1991). The lack of recovery suggests that any possible density-dependent compensatory responses of other life-history traits, such as immigration, juvenile growth, and fecundity, have not affected abundance at the observed time scale. Further, direct assessment of these vital rates may reveal weak density-dependent effects that are not yet detectable from abundance series, even at the present time scale (Brook and Bradshaw, 2006; Lebreton, 2009); future work will examine responses in these vital rates.

Temporary emigration and inferences about reproductive frequency. Annual temporary emigration was much lower for females nesting at the dam (2.4%) compared to those at the alternate sites (12%). The difference in temporary emigration can be interpreted as differences in two processes, biological and observational. It is possible that observers were more likely to detect individuals that they had seen on the previous occasion because of increased vigilance at a particular sub-site and time-of-day on the subsequent occasion. This may have been a factor at the alternate sites, which were scattered and heterogeneous, but not at the dam. This difference could appear as a difference in temporary emigration between sites. The biological process is temporary emigration to nest at other sites. Transitions away from the dam are usually downstream to the alternate sites and so are already accounted for by the observed state transitions in our analysis. In contrast, temporary transitions from alternate sites to nest at

downstream sites take individuals outside of the NMR watershed which delineates the study area (i.e., to an unobservable state).

The lower influence of observer effects and transitions to unmonitored nesting areas by females at the Sasajewun dam means that temporary emigration from the dam is likely to be a reasonable estimate of the upper boundary of the annual frequency of skipped reproductive events. The relative abundance of the temporarily unavailable fraction of the dam nesting population was low across all occasions (Figure 1.6). This is a maximum estimate because the proportion of temporary emigration that is due to nesting at unmonitored upstream sites is unknown, so true frequency of skipped reproduction is likely to be somewhat lower. Our estimated reproductive frequency is higher than previously estimated in Michigan (85%, Congdon et al. 1994). The high reproductive frequency we observed is notable given the cool climate and low productivity of this habitat (Galbraith et al., 1988). Among iteroparous taxa, reproductive frequency is one of the most difficult life-history traits to estimate (Gibbons, 1982; Moll and Iverson, 2008); analyses of mark-recapture data using models that include temporary emigration has potential to allow inferences of this important parameter.

Abundance of males and females. Our recent (2009–13) abundance estimates (males = 9.5, females = 12.5; Figure 1.8) of adults in Lake Sasajewun are similar to those reported by Brooks et al. (1991) for the years at the end of the catastrophe caused by otter predation (1988–89; males and females combined = 20.5, minimum alive = 16). This concordance indicates that the lack of recovery is not limited to females at particular nest sites, but applies to the population as a whole.

Conservation and management implications. An important feature of our study population is high connectivity with adjacent habitats. The slow recovery is notable because our study area is

open to immigration from an abundance of surrounding patches and does not only rely on *in situ* recruitment. Our observations confirm that individuals do occasionally emigrate from, and immigrate to, distant sites. For example, one female that was recruited to an alternate site in 2013 had previously only been observed nesting 9.3 km away by water. However, the frequency of immigration events to nesting areas and to Lake Sasajewun has apparently not sufficiently increased relative to mortality and emigration to compensate for decreased abundance during a catastrophe. This suggests that movement between patches is not sensitive to density and so contributes little to any compensatory response following a catastrophe. In contrast, managers often assume that localized depletion will be compensated for by *ex situ* recruitment from less exploited patches (e.g. Cain 2010). Such an assumption, made without provisions for follow-up empirical validation, is an explicit feature of the management of some exploited turtle populations (Cain, 2010).

More generally, our results demonstrate an absence of effective recovery indicating an absence of a substantial contribution of density-dependent compensation to this point. This is consistent with other analyses of turtle life history which emphasize the limited ability of many populations to compensate for chronic or catastrophic mortality (Brooks et al., 1991; Congdon et al., 1994, 1993; Cunnington and Brooks, 1996; Heppell, 1998). Our study provided a unique opportunity to empirically test these principles over a long time series following a perturbation. The lack of recovery at management-relevant time scales, and the manifest risk of further, unanticipated catastrophes, strongly supports prioritizing protection of existing populations rather than relying on recovery after declines have already occurred.

For conservation biologists, it is important to consider both human-centric and generation time scales when evaluating factors impacting population persistence. Intrinsic population processes

such as population growth rate and density dependence are best understood on the scale of generation time (Sæther et al., 2005) but many extrinsic processes, such as frequency of catastrophes, aspects of community dynamics, and management actions and policy, scale more or less independently. Anthropogenic and environmental impacts on long-term viability must be related back to the scale of population processes to be understood in that context. In a meta-analysis of extinction risk and temporal scaling, O'Grady et al. (2008) found that generation time was the appropriate frame of reference despite the lack of direct connection to extrinsic processes. Using estimated age at first reproduction (*AFR*) of 17 years (Galbraith et al., 1989) and adult survivorship (*S*) in typical (non-catastrophe) periods as 0.942 to 0.976 (this study), we can calculate a crude estimate of generation time for our population as $AFR + (1 - S)^{-1}$ = 34.2 to 58.7 years, indicating that perhaps we should not expect to see signs of population recovery for at least 59 years post-catastrophe.

Slow life histories entail not only vulnerabilities to certain demographic perturbations but also robustness in the face of many kinds of environmental stochasticity (Jonsson and Ebenman, 2001). We suggest that definitions of catastrophes should incorporate differences in relative sensitivity of different life-history parameters among taxa. In a study of catastrophes in pinniped populations (Gerber and Hilborn, 2001), most natural catastrophes were characterized by nearly complete reproductive failure or very high pup mortality, and resulted in abrupt population declines. In contrast, the life-history of turtles is typified by low and variable reproductive success and their strategy of constant, high adult survivorship insulates the population from routine environmental stochasticity which primarily affects the youngest age classes (Congdon et al., 1994; Cunnington and Brooks, 1996; Jonsson and Ebenman, 2001). In some years, reproductive success in turtle populations may be essentially nil (Bobyn and Brooks, 1994) and

although chronic reproductive failure has obvious consequences, even drastic short-term fluctuations in reproductive success are unlikely to impact abundance severely enough to warrant naming them a catastrophe. Taking into account the elasticity of different life-history stages (Cunnington and Brooks 1996, Enneson and Litzgus 2008), catastrophes in turtles and other organisms with similar life histories can be characterized solely by abrupt increases in adult and older juvenile mortality. The extended lack of recovery that we have observed suggests that perturbations to adult survivorship of long-lived species will be potentially catastrophic even when short-term mortality is substantially lower than the commonly used 50% threshold used to evaluate catastrophic events.

Predator-induced catastrophes. It is startling to consider that the dominant environmental influence on the study population over 41 years of monitoring is the predilections of one or at most a few individual River Otters. This dramatically underscores both the importance and unpredictability of catastrophes. Population dynamics of cyclic species such as small mammals and clupeid fishes are often mediated by predation, but we suggest that it is not productive to lump catastrophes, which are defined partly by their unpredictability, in with these regular phenomena. Excluding such cyclic predator-prey dynamics, population catastrophes due to predation by native predators are rare compared to other causes such as extreme environmental events, starvation, and disease (Young, 1994). Predator-mediated catastrophes have been reported in some circumstances, usually commensurate with one or more other abiotic factors (Young, 1994). Another instance of mass mortality of turtles (*Emys orbicularia*) resulting from otter (*Lutra lutra*) predation was attributed to reduced availability of prey fish (Lanszki et al., 2006). Human-subsidized native predators have also been implicated in acute mortality events that may affect chelonians (Fincham and Lambrechts, 2014).

Because syntopic predators are a constant, predictable, feature of populations on which they prey, it is surprising that these predators can occasionally induce sudden, unpredictable catastrophes. One potential explanation is that individual specialisation to depredate adult Snapping Turtles may be a rare realization of a heterogeneous suite of potential foraging personalities. Individual specialisation in foraging strategy is widespread in many animals and many predators will adopt strategies that are unique amongst a sample of their conspecifics (Araújo et al., 2011; Wolf and Weissing, 2012). Snapping Turtles themselves exhibit individual specialisation in habitat selection during the active season and hibernation (Brown and Brooks, 1994; Paterson et al., 2012) and heterogeneity of overwintering sites may have protected a proportion of the population that used refugia inaccessible to otters (Brooks et al., 1991).

Conclusions

Although natural catastrophes are unpredictable in their timing, evidence is accumulating that they do happen and represent a real threat, and this risk must be appreciated by population ecologists and conservation planners (Lande, 1993; Mangel and Tier, 1994; Reed et al., 2003). Increasing rates of habitat fragmentation, direct exploitation, and increasing climate variability mean that in many ecosystems, the frequency of both natural and anthropogenic catastrophes may also be expected to increase. Organisms with slow life histories are somewhat insulated from typical environmental variation but may be extremely vulnerable to any catastrophes that result in substantial adult female mortality. Following such a catastrophe, our study population of Snapping Turtles has been unable to substantially recover, despite a return to high survivorship and continued connectivity with neighbouring populations. The lack of recovery suggests that density-dependent compensation is limited. This aligns with the prediction of Brooks et al. (1991) who suggested that intrinsic environmental constraints on vital rates would impose limits

on Snapping Turtle populations to compensate for declines. Our analyses at two spatial scales – basin level nest surveys and local aquatic habitat surveys – demonstrate population impacts persisting over more than two decades. We strongly support a risk-averse, precautionary approach to conservation and management of long-lived animals given their limited ability to compensate for declines and the unpredictable continuing risk that catastrophes pose to depleted populations.

References

Araújo, M.S., Bolnick, D.I., Layman, C.A., 2011. The ecological causes of individual specialisation. Ecol. Lett. 14, 948–958. https://doi.org/10.1111/j.1461-0248.2011.01662.x

Aresco, M.J., 2005. Mitigation measures to reduce highway mortality of turtles and other herpetofauna at a north Florida lake. J. Wildl. Manage. 69, 549–560. https://doi.org/10.2193/0022-541X(2005)069[0549:MMTRHM]2.0.CO;2

Armstrong, D.P., Brooks, R.J., 2014. Estimating ages of turtles from growth data. Chelonian Conserv. Biol. 13, 9–15. https://doi.org/http://dx.doi.org/10.2744/CCB-1055.1

Armstrong, D.P., Brooks, R.J., 2013. Application of hierarchical biphasic growth models to long-term data for Snapping Turtles. Ecol. Modell. 250, 119–125. https://doi.org/10.1016/j.ecolmodel.2012.10.022

Armstrong, D.P., Keevil, M.G., Rollinson, N., Brooks, R.J., 2018. Subtle individual variation in indeterminate growth leads to major variation in survival and lifetime reproductive output in a long-lived reptile. Funct. Ecol. 32, 752–761. https://doi.org/10.1111/1365-2435.13014

Bennett, A.M., Litzgus, J.D., 2014. Injury rates of freshwater turtles on a recreational waterway in Ontario, Canada. J. Herpetol. 48, 262–266. https://doi.org/10.1670/12-161

Bjørkvoll, E., Grøtan, V., Aanes, S., Sæther, B.-E., Engen, S., Aanes, R., 2012. Stochastic population dynamics and life-history variation in marine fish species. Am. Nat. 180, 372–387. https://doi.org/10.1086/666983

Bjorndal, K.A., Bolten, A.B., Chaloupka, M.Y., 2000. Green Turtle somatic growth model: evidence for density dependence. Ecol. Appl. 10, 269–282. https://doi.org/10.2307/2641001

Bobyn, M.L., Brooks, R.J., 1994. Incubation conditions as potential factors limiting the northern distribution of Snapping Turtles, *Chelydra serpentina*. Can. J. Zool. 72, 28–37. https://doi.org/http://dx.doi.org/10.1139/z94-005

Böhm, M., Collen, B., Baillie, J.E.M., Bowles, P., Chanson, J., Cox, N., Hammerson, G., et al. 2013. The conservation status of the world's reptiles. Biol. Conserv. 157, 372–385. https://doi.org/10.1016/j.biocon.2012.07.015

Brook, B.W., Bradshaw, C.J.A., 2006. Strength of evidence for density dependence in abundance time series of 1198 species. Ecology 87, 1445–1451. https://doi.org/10.1890/0012-9658(2006)87[1445:SOEFDD]2.0.CO;2

Brooks, R.J., Brown, G.P., Galbraith, D.A., 1991. Effects of a sudden increase in natural mortality of adults on a population of the Common Snapping Turtle (*Chelydra serpentina*). Can. J. Zool. 69, 1314–1320. https://doi.org/10.1139/z91-185

Brooks, S.P., Catchpole, E.A., Morgan, B.J.T., Barry, S.C., 2000. On the Bayesian Analysis of Ring-Recovery Data. Biometrics 56, 951–956. https://doi.org/10.1111/j.0006-341X.2000.00951.x

Brown, G.P., Brooks, R.J., 1994. Characteristics of and fidelity to hibernacula in a northern population of Snapping Turtles, *Chelydra serpentina*. Copeia 1994, 222. https://doi.org/10.2307/1446689

Brownie, C., Hines, J.E., Nichols, J.D., Pollock, K.H., Hestbeck, J.B., 1993. Capture-recapture studies for multiple strata including non-Markovian transitions. Biometrics 49, 1173. https://doi.org/10.2307/2532259

Bulté, G., Carrière, M.-A., Blouin-Demers, G., 2010. Impact of recreational power boating on two populations of Northern Map Turtles (*Graptemys geographica*). Aquat. Conserv. Mar. Freshw. Ecosyst. 20, 31–38. https://doi.org/10.1002/aqc.1063

Burnham, K.P., Anderson, D.R., White, G.C., Brownie, C., Pollock, K.H., 1987. Design and analysis methods for fish survival experiments based on release-recapture. Am. Fish. Soc. Monogr. 5, 1–437.

Cagle, F.R., 1939. A system of marking turtles for future identification. Copeia 1939, 170–183. https://doi.org/http://dx.doi.org/10.2307/1436818

Cain, P.W., 2010. The Cost Of Soup: An Assessment of The Commercial Harvest of Snapping Turtles (*Chelydra serpentina*) in Maryland. (Master's Thesis). Townsend University, Townsend, Maryland.

Catrysse, J., Slavik, E., Choquette, J., Leifso, A.E., Davy, C.M., 2015. Mass mortality of Northern Map Turtles (*Graptemys geographica*). Can. F. Nat. 129, 80–83.

Choquet, R., Reboulet, A.M., Lebreton, J.-D., Gimenez, O., Pradel, R., 2005. U-Care 2.2 User's Manual.

Christiansen, J.L., Bickham, J.W., 1989. Possible historic effects of pond drying and winterkill on the behavior of *Kinosternon flavescens* and *Chrysemys picta*. J. Herpetol. 23, 91–94. https://doi.org/10.2307/1564327

Collen, B., Loh, J., Whitmee, S., McRae, L., Amin, R., Baillie, J.E.M., 2009. Monitoring change in vertebrate abundance: the Living Planet Index. Conserv. Biol. 23, 317–327. https://doi.org/10.1111/j.1523-1739.2008.01117.x

Colteaux, B.C., Johnson, D.M., 2017. Commercial harvest and export of Snapping Turtles (*Chelydra serpentina*) in the United States: trends and the efficacy of size limits at reducing harvest. J. Nat. Conserv. 35, 13–19. https://doi.org/10.1016/j.jnc.2016.11.003

Congdon, J.D., Dunham, A.E., van Loben Sels, R.C., 1994. Demographics of Common Snapping Turtles (*Chelydra serpentina*): Implications for conservation and management of long-lived organisms. Am. Zool. 34, 397–408.

Congdon, J.D., Dunham, A.E., Van Loben Sels, R.C., 1993. Delayed sexual maturity and demographics of Blanding's Turtles (*Emydoidea blandingii*): Implications for conservation and management of long-lived organisms. Conserv. Biol. 7, 826–833.

Cunnington, D.C., Brooks, R.J., 1996. Bet-hedging theory and eigenelasticity: A comparison of the life histories of Loggerhead Sea Turtles (*Caretta caretta*) and Snapping Turtles (*Chelydra serpentina*). Can. J. Zool. 74, 291–296. https://doi.org/10.1139/z96-036

Dellaportas, P., Forster, J., Ntzoufras, I., 2000. Bayesian variable selection using the Gibbs sampler., in: Dey, D., Ghosh, S., Mallick, B. (Eds.), Generalized Linear Models: A Bayesian Perspective, Vol. 5. CRC Press, New York, USA, pp. 273–286.

Fey, S.B., Siepielski, A.M., Nusslé, S., Cervantes-Yoshida, K., Hwan, J.L., Huber, E.R., Fey, M.J., Catenazzi, A., Carlson, S.M., 2015. Recent shifts in the occurrence, cause, and

magnitude of animal mass mortality events. Proc. Natl. Acad. Sci. 112, 1083–1088. https://doi.org/10.1073/pnas.1414894112

Fincham, J.E., Lambrechts, N., 2014. How many tortoises do a pair of Pied Crows *Corvus alba* need to kill to feed their Chicks? Ornithol. Obs. 5, 135–138.

Finkelstein, M.E., Wolf, S., Goldman, M., Doak, D.F., Sievert, P.R., Balogh, G., Hasegawa, H., 2010. The anatomy of a (potential) disaster: Volcanoes, behavior, and population viability of the Short-tailed Albatross (*Phoebastria albatrus*). Biol. Conserv. 143, 321–331. https://doi.org/10.1016/j.biocon.2009.10.013

Fordham, D.A., Georges, A., Brook, B.W., 2009. Experimental evidence for density-dependent responses to mortality of Snake-Necked Turtles. Oecologia 159, 271–281. https://doi.org/10.1007/s00442-008-1217-5

Fordham, D.A., Georges, A., Brook, B.W., 2007. Demographic response of Snake-Necked Turtles correlates with indigenous harvest and feral pig predation in tropical northern Australia. J. Anim. Ecol. 76, 1231–1243. https://doi.org/10.1111/j.1365-2656.2007.01298.x

Frankham, R., Brook, B.W., 2004. The importance of time scale in conservation biology and ecology. Ann. Zool. Fennici 41, 459–463.

Fujiwara, M., Caswell, H., 2002. A general approach to temporary emigration in mark-recapture analysis. Ecology 83, 3266. https://doi.org/10.2307/3072077

Gaillard, J.-M., Yoccoz, N.G., Lebreton, J., Bonenfant, C., Devillard, S., Loison, A., Pontier, D., Allaine, D., 2005. Generation time: A reliable metric to measure life-history variation among mammalian populations. Am. Nat. 166, 119–123. https://doi.org/10.1086/430330

Galbraith, D.A., Bishop, C.A., Brooks, R.J., Simser, W.L., Lampman, K.P., 1988. Factors affecting the density of populations of Common Snapping Turtles (*Chelydra serpentina serpentina*). Can. J. Zool. 66, 1233–1240. https://doi.org/http://dx.doi.org/10.1139/z88-178

Galbraith, D.A., Brooks, R.J., Obbard, M.E., 1989. The influence of growth rate on age and body size at maturity in female Snapping Turtles (*Chelydra serpentina*). Copeia 1989, 896–904. https://doi.org/10.2307/1445975

Garber, S.D., Burger, J., 1995. A 20-yr study documenting the relationship between turtle decline and human recreation. Ecol. Appl. 5, 1151–1162. https://doi.org/10.2307/2269362

Gelman, A., Carlin, J.P., Stern, H.S., Runin, D.B., 2004. Bayesian Data Analysis. CRC/Chapman & Hall, Boca Raton, F.L.

Gerber, L.R., Hilborn, R., 2001. Catastrophic events and recovery from low densities in populations of otariids: implications for risk of extinction. Mamm. Rev. 31, 131–150. https://doi.org/10.1046/j.1365-2907.2001.00081.x

Gibbons, J.W., 1982. Reproductive patterns in freshwater turtles. Herpetologica 38, 222–227.

Gibbons, J.W., Scott, D.E., Ryan, T.J., Buhlmann, K.A., Tuberville, T.D., Metts, B.S., Greene, J.L., Mills, T., Leiden, Y., Poppy, S., Winne, C.T., 2000. The global decline of reptiles, déjà vu amphibians. Bioscience 50, 653–666.

Gimenez, O., Choquet, R., Lebreton, J.-D., 2003. Parameter redundancy in multistate capture-recapture models. Biometrical J. 45, 704–722.

Gimenez, O., Morgan, B.J.T., Brooks, S.P., 2009. Weak identifiability in models for mark-recapture-recovery data, in: Thomson, D.L., Cooch, E.G., Conroy, M.J. (Eds.), Modeling Demographic Processes in Marked Populations. Springer, New York, pp. 1055–1067.

Gimenez, O., Rossi, V., Choquet, R., Dehais, C., Doris, B., Varella, H., Vila, J.-P., Pradel, R., 2007. State-space modelling of data on marked individuals. Ecol. Modell. 206, 431–438. https://doi.org/10.1016/j.ecolmodel.2007.03.040

Hailey, A., Willemsen, R.E., 2000. Population density and adult sex ratio of the tortoise *Testudo hermanni* in Greece: Evidence for intrinsic population regulation. J. Zool. 251, 325–338. https://doi.org/10.1111/j.1469-7998.2000.tb01083.x

Heppell, S.S., 1998. Application of life-history theory and population model analysis to turtle conservation. Copeia 1998, 367–375. https://doi.org/10.2307/1447430

Hutchings, J.A., Reynolds, J.D., 2004. Marine fish population collapses: Consequences for recovery and extinction risk. Bioscience 54, 297–309. https://doi.org/10.1641/0006-3568(2004)054[0297:MFPCCF]2.0.CO;2

IPCC, 2014. Climate Change 2014: Synthesis Report. Contribution of Working Groups I, II and III to the Fifth Assessment Report of the Intergovernmental Panel on Climate Change. IPCC, Geneva, Switzerland.

Johnson, A.J., Pessier, A.P., Wellehan, J.F.X., Childress, A., Norton, T.M., Stedman, N.L., Bloom, D.C., Belzer, W., Titus, V.R., Wagner, R., Brooks, J.W., Spratt, J., Jacobson, E.R., 2008. *Ranavirus* infection of free-ranging and captive box turtles and tortoises in the United States. J. Wildl. Dis. 44, 851–863.

Jonsson, A., Ebenman, B., 2001. Are certain life histories particularly prone to local extinction? J. Theor. Biol. 209, 455–463. https://doi.org/10.1006/jtbi.2001.2280

Keevil, M.G., Hewitt, B.S., Brooks, R.J., Litzgus, J.D., 2017. Patterns of intraspecific aggression inferred from injuries in an aquatic turtle with male-biased size dimorphism. Can. J. Zool. 95, 393–403. https://doi.org/10.1139/cjz-2016-0182

Kendall, W.L., Nichols, J.D., 2002. Estimating state-transition probabilities for unobservable states using capture-recapture/resighting data. Ecology 83, 3276. https://doi.org/10.2307/3072078

Kéry, M., Schaub, M., 2012. Bayesian Population Analysis Using WinBUGS: A Hierarchical Perspective. Academic Press, Waltham, Massachussets, USA.

King, R., Morgan, B.J.T., Gimenez, O., Brooks, S.P., 2010. Bayesian Analysis for Population Ecology. CRC Press, Boca Raton, FL.

Lande, R., 1993. Risks of population extinction from demographic and environmental stochasticity and random catastrophes. Am. Nat. 142, 911–927. https://doi.org/10.1086/285580

Lanszki, J., Molnár, M., Molnár, T., 2006. Factors affecting the predation of Otter (*Lutra lutra*) on European Pond Turtle (*Emys orbicularis*). J. Zool. 270, 219–226. https://doi.org/10.1111/j.1469-7998.2006.00132.x

Lebreton, J.-D., 2009. Assessing density dependence: where are we left?, in: Thomson, D.L., Cooch, E.G., Conroy, M.J. (Eds.), Modeling Demographic Processes in Marked Populations. Springer, New York, New York, pp. 19–42.

Lebreton, J.-D., Burnham, K.P., Clobert, J., Anderson, D.R., 1992. Modeling survival and testing biological hypotheses using marked animals: A unified approach with case studies. Ecol. Monogr. 62, 67–118. https://doi.org/10.2307/2937171

Lebreton, J.-D., Nichols, J.D., Barker, R.J., Pradel, R., Spendelow, J.A., 2009. Chapter 3 Modeling Individual Animal Histories with Multistate Capture–Recapture Models, in: Caswell, H. (Ed.), Advances in Ecological Research. Elsevier, San Diego, pp. 87–173. https://doi.org/10.1016/S0065-2504(09)00403-6

Loncke, D.J., Obbard, M.E., 1977. Tag success, dimensions, clutch size and nesting site fidelity for the Snapping Turtle, *Chelydra serpentina* (Reptilia, Testudines, Chelydridae) in Algonquin Park, Ontario, Canada. J. Herpetol. 11, 243–244. https://doi.org/http://dx.doi.org/10.2307/1563158

Longshore, K.M., Jaeger, J.R., Sappington, J.M., 2003. Desert Tortoise (*Gopherus agassizii*) survival at two eastern Mojave Desert sites: Death by short-term drought? J. Herpetol. 37, 169–177. https://doi.org/10.1670/0022-1511(2003)037[0169:DTGASA]2.0.CO;2

Lunn, D.J., Thomas, A., Best, N., Spiegelhalter, D.J., 2000. WinBUGS – a Bayesian modelling framework: concepts, structure, and extensibility. Stat. Comput. 10, 325–337.

Mangel, M., Tier, C., 1994. Four facts every conservation biologists should know about persistence. Ecology 75, 607–614. https://doi.org/10.2307/1941719

Menges, E.S., 1990. Population viability analysis for an endangered plant. Conserv. Biol. 4, 52–62. https://doi.org/10.1111/j.1523-1739.1990.tb00267.x

Midwood, J.D., Cairns, N.A., Stoot, L.J., Cooke, S.J., Blouin-Demers, G., 2015. Bycatch mortality can cause extirpation in four freshwater turtle species. Aquat. Conserv. Mar. Freshw. Ecosyst. 25, 71–80. https://doi.org/10.1002/aqc.2475

Moll, D., Iverson, J.B., 2008. Geographic Variation in Life-History Traits, in: Brooks, R.J., Steyermark, A.C., Finkler, M.S. (Eds.), The Biology of the Snapping Turtle. Johns Hopkins Univ Press, pp. 181–192.

Neubauer, P., Jensen, O.P., Hutchings, J.A., Baum, J.K., 2013. Resilience and recovery of overexploited marine populations. Science 340, 347–349. https://doi.org/10.1126/science.1230441

Nickerson, M.A., Pitt, A.L., 2012. Historical turtle population decline and community changes in an Ozark river. Bull. Florida Museum Nat. Hist. 51, 257–267.

O'Grady, J.J., Reed, D.H., Brook, B.W., Frankham, R., 2008. Extinction risk scales better to generations than to years. Anim. Conserv. 11, 442–451. https://doi.org/10.1111/j.1469-1795.2008.00201.x

O'Hara, R.B., Sillanpää, M.J., 2009. A review of Bayesian selection methods: What, how, and which? Bayesian Anal. 4, 85–118.

Obbard, M.E., Brooks, R.J., 1981. A radio-telemetry and mark-recapture study of activity in the Common Snapping Turtle, *Chelydra serpentina*. Copeia 1981, 630–637. https://doi.org/http://dx.doi.org/10.2307/1444568

Otis, D.L., Burnham, K.P., White, G.C., Anderson, D.R., 1978. Statistical inference from capture data on closed animal populations. Wildl. Monogr. 1–135.

Papadatou, E., Pradel, R., Schaub, M., Dolch, D., Geiger, H., Ibañez, C., Kerth, G., Popa-Lisseanu, A., Schorcht, W., Teubner, J., Gimenez, O., 2012. Comparing survival among species with imperfect detection using multilevel analysis of mark-recapture data: a case study on bats. Ecography 35, 153–161. https://doi.org/10.1111/j.1600-0587.2011.07084.x

Paterson, J.E., Steinberg, B.D., Litzgus, J.D., 2012. Generally specialized or especially general? Habitat selection by Snapping Turtles (*Chelydra serpentina*) in central Ontario. Can. J. Zool. 90, 139–149. https://doi.org/10.1139/z11-118

Pimm, S.L., Jenkins, C.N., Abell, R., Brooks, T.M., Gittleman, J.L., Joppa, L.N., Raven, P.H., Roberts, C.M., Sexton, J.O., 2014. The biodiversity of species and their rates of extinction, distribution, and protection. Science 344, 1246752. https://doi.org/10.1126/science.1246752

Plummer, M., 2003. JAGS: a program for analysis of Bayesian graphical models using Gibbs sampling, in: Hornik, K., Leisch, F., Zeileis, A. (Eds.), Proceedings of the 3rd International Workshop on Distributed Statistical Computing (DSC 2003), Vienna, Austria, March 20–22, 2003. Austrian Association for Statistical Computing (AASC) and the R Foundation for Statistical Computing, Vienna, Austria, pp. 1–10.

Pradel, R., 1993. Flexibility in survival analysis from recapture data: Handling trap-dependence, in: Lebreton, J.D., North, P.M. (Eds.), Marked Individuals in the Study of Bird Population. Birkhaeuser Verlag, Basel, Switzerland, pp. 29–37.

Pradel, R., Sanz-Aguilar, A., 2012. Modeling trap-awareness and related phenomena in capture-recapture studies. PLoS One 7, e32666. https://doi.org/10.1371/journal.pone.0032666

Pradel, R., Wintrebert, C.M.A., Gimenez, O., 2003. A Proposal for a Goodness-of-Fit Test to the Arnason-Schwarz Multisite Capture-Recapture Model. Biometrics 59, 43–53. https://doi.org/10.1111/1541-0420.00006

R Development Core Team, 2020. R: A language and environment for statistical computing.

Reed, D.H., O'Grady, J.J., Ballou, J.D., Frankham, R., 2003. The frequency and severity of catastrophic die-offs in vertebrates. Anim. Conserv. 6, 109–114. https://doi.org/10.1017/S1367943003147

Roff, D.A., 2002. Life History Evolution. Sinauer, Sunderland, MA.

Royle, J.A., Dorazio, R.M., 2012. Parameter-expanded data augmentation for Bayesian analysis of capture–recapture models. J. Ornithol. 152, 521–537. https://doi.org/10.1007/s10336-010-0619-4

Sæther, B.-E., Lande, R., Engen, S., Weimerskirch, H., Lillegard, M., Altwegg, R., Becker, P.H., Bregnballe, T., Brommer, J.E., McCleery, R.H., Merila, J., Nyholm, E., Rendell, W., Robertson, R.R., Tryjanowski, P., Visser, M.E., 2005. Generation time and temporal scaling of bird population dynamics. Nature 436, 99–102. https://doi.org/10.1038/nature03666

Schaub, M., Gimenez, O., Schmidt, B.R., Pradel, R., 2004. Estimating survival and temporary emigration in the multistate capture–recapture framework. Ecology 85, 2107–2113. https://doi.org/10.1890/03-3110

Schaub, M., Kania, W., Koppen, U., 2005. Variation of primary production during winter induces synchrony in survival rates in migratory White Storks *Ciconia ciconia*. J. Anim. Ecol. 74, 656–666. https://doi.org/10.1111/j.1365-2656.2005.00961.x

Schaub, M., Zink, R., Beissmann, H., Sarrazin, F., Arlettaz, R., 2009. When to end releases in reintroduction programmes: Demographic rates and population viability analysis of Bearded Vultures in the Alps. J. Appl. Ecol. 46, 92–100. https://doi.org/10.1111/j.1365-2664.2008.01585.x ER

Sheppard, A.C., 2014. *Emydoidea blandingii* (Blanding's Turtle) mass mortality. Herpetol. Rev. 45, 312–313.

Spencer, R.-J., Janzen, F.J., Thompson, M.B., 2006. Counterintuitive density-dependent growth in a long-lived vertebrate after removal of nest predators. Ecology 87, 3109–3118. https://doi.org/10.1890/0012-9658(2006)87[3109:CDGIAL]2.0.CO;2

Spencer, R.-J., Van Dyke, J., Petrov, K., Ferronato, B., McDougall, F., Austin, M., Keitel, C., Georges, A., 2018. Profiling a possible rapid extinction event in a long-lived species. Biol. Conserv. 221, 190–197. https://doi.org/10.1016/J.BIOCON.2018.03.009

Spiegelhalter, D.J., Best, N.G., Carlin, B.P., Van Der Linde, A., 2002. Bayesian measures of model complexity and fit. J. R. Stat. Soc. Ser. B – Stat. Methodol. 64, 583–639. https://doi.org/http://dx.doi.org/10.1111/1467-9868.00353

Steen, D.A., Aresco, M.J., Beilke, S.G., Compton, B.W., Condon, E.P., Dodd Jr., C.K., Forrester, H., Gibbons, J.W., Greene, J.L., Johnson, G., Langen, T.A., Oldham, M.J., Oxier, D.N., Saumure, R.A., Schueler, F.W., Sleeman, J.M., Smith, L.L., Tucker, J.K., Gibbs, J.P., 2006. Relative vulnerability of female turtles to road mortality. Anim. Conserv. 9, 269–273. https://doi.org/10.1111/j.1469-1795.2006.00032.x

Steen, D.A., Hopkins, B.C., Van Dyke, J.U., Hopkins, W.A., 2014. Prevalence of ingested fish hooks in freshwater turtles from five rivers in the southeastern United States. PLoS One 9, e91368. https://doi.org/10.1371/journal.pone.0091368

Stubbs, D., Swingland, I.R., Hailey, A., Pulford, E., 1985. The ecology of the Mediterranean Tortoise *Testudo hermanni* in Northern Greece: the effects of a catastrophe on population structure and density. Biol. Conserv. 31, 125–152. https://doi.org/10.1016/0006-3207(85)90045-X

Sturtz, S., Ligges, U., Gelman, A., 2005. R2WinBUGS: a package for running WinBUGS. J. Stat. Softw. 12, 1–16.

Vélez-Espino, L.A., Koops, M.A., 2012. Capacity for increase, compensatory reserves, and catastrophes as determinants of minimum viable population in freshwater fishes. Ecol. Modell. 247, 319–326. https://doi.org/10.1016/j.ecolmodel.2012.09.022

Ward, E.J., Hilborn, R., Towell, R.G., Gerber, L., 2007. A state–space mixture approach for estimating catastrophic events in time series data. Can. J. Fish. Aquat. Sci. 64, 899–910. https://doi.org/10.1139/f07-060

White, G.C., Burnham, K.P., 1999. Program MARK: Survival estimation from populations of marked animals. Bird Study 46, S120–S139.

White, G.C., Kendall, W.L., Barker, R.J., 2006. Multistate survival models and their extensions in Program MARK. J. Wildl. Manage. 70, 1521–1529. https://doi.org/10.2193/0022-541X(2006)70[1521:MSMATE]2.0.CO;2

Wolf, M., Weissing, F.J., 2012. Animal personalities: consequences for ecology and evolution. Trends Ecol. Evol. 27, 452–461. https://doi.org/10.1016/j.tree.2012.05.001

World Wildlife Fund, 2014. Living Planet Report 2014: Species and Spaces, People and Places. World Wildlife Fund, Gland, Switzerland.

Young, T.P., 1994. Natural die-offs of large mammals: Implications for vonservation. Conserv. Biol. 8, 410–418. https://doi.org/10.1046/j.1523-1739.1994.08020410.x

Tables

Table 1.1. Timing and duration, trap days, and number of captures of Snapping Turtles (*Chelydra serpentina*) for secondary (within a season) sampling occasions using baited hoop traps and dip nets in Lake Sasajewun, Algonquin Park, Ontario. Juveniles and subadults (females straight-line carapace length (SCL) < 24 cm, males SCL < 30 cm), which were not used in our analyses, are excluded from counts.

Survey period		Trap days	Captures	
Start	End		Male	Female
1-May-09	1-Jun-09	0	4	5
1-Jul-09	1-Oct-09	113	5	4
1-Jun-10	1-Jul-10	0	3	3
1-Jul-10	15-Sep-10	32	2	2
1-May-11	25-May-11	0	3	5
26-May-11	1-Jul-11	45	9	8
1-May-12	1-Jul-12	0	5	7
1-Jul-12	15-Sep-12	276	13	14
14-Apr-13	21-May-13	2.5	3	3
21-May-13	1-Jul-13	72.5	3	4
1-Jul-13	15-Sep-13	61	4	3

Table 1.2. Results of Gibbs Variable Selection (GVS) for main effects and site interactions of apparent survival parameters of nesting female Snapping Turtles in Algonquin Park over 33 occasions with two observable states (dam and alternate nesting sites) and two unobservable states to account for temporary emigration. Models with only an interaction effect ("ixn only") have a period effect for dam nesting females but not alternate site females.

Effect	Probabilities of main effect and interaction with site						
	marg. main	marg. ixn	both	either	main only	ixn only	neither
otter	0.82	0.68	0.50	1.00	0.32	0.18	0.00
after	0.23	0.91	0.21	0.93	0.03	0.70	0.07
blowout	0.76	0.51	0.31	0.96	0.45	0.20	0.04
site	0.25	NA	NA	NA	NA	NA	NA

Table 1.3. Support for recapture probability sub-model structure assessed using marginal posterior probabilities from Gibbs Variable Selection (GVS) within a multistate model of nesting female Snapping Turtles in Algonquin Park over 33 occasions with two observable states (dam and alternate nesting sites) and temporary emigration

Model	marg. probability
p(.)	0.00
p(t)	0.72
p(site)	0.00
p(t + site)	0.23
p(t*site)	0.05

Figures

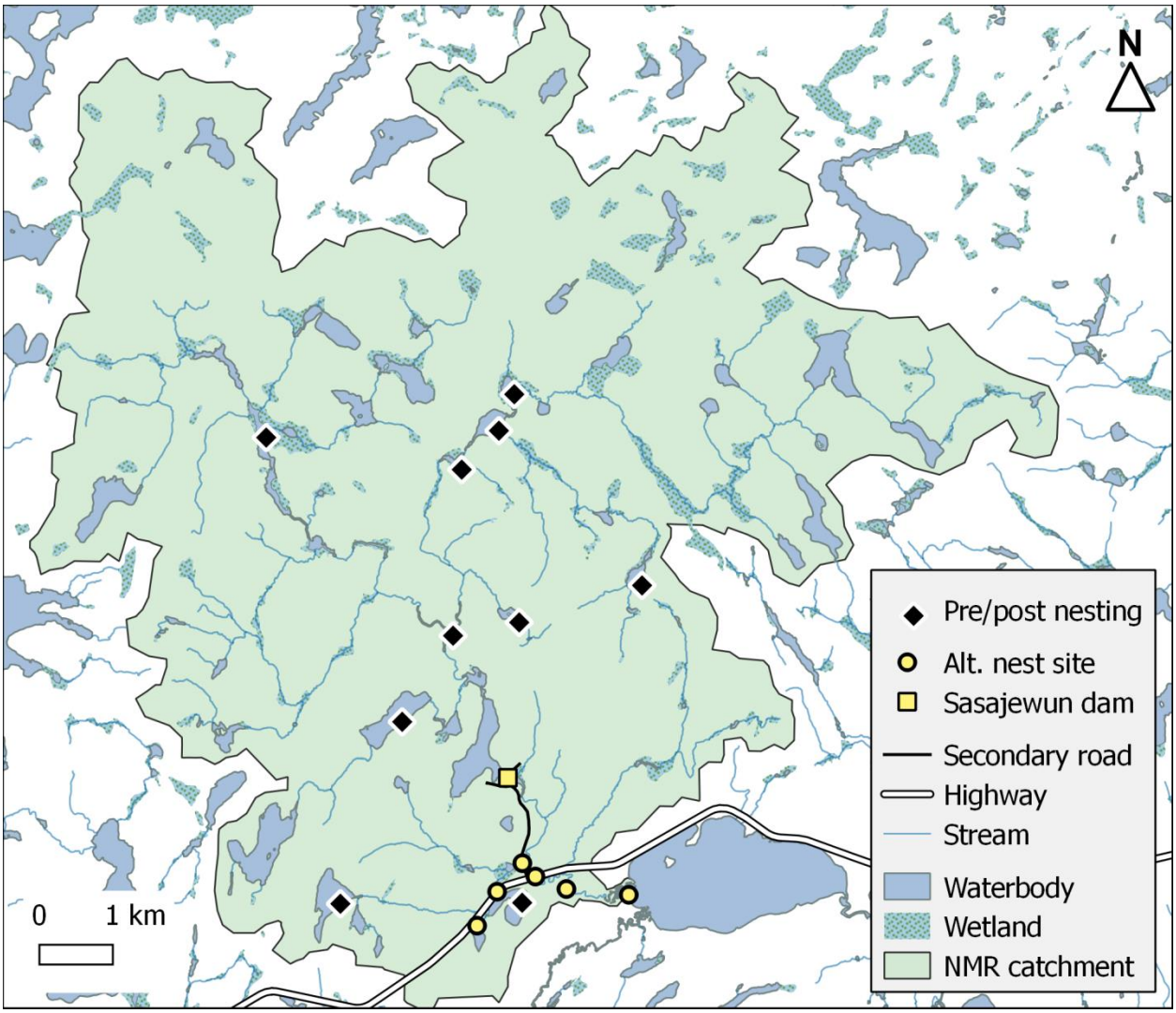

Figure 1.1. The North Madawaska River basin in Algonquin Park, Ontario. The Sasajewun dam Snapping Turtle nesting site (open square) and alternate nesting sites (open circles) are indicated, as well as selected distant observations of dam-nesting females outside of nesting season (black diamonds) (Obbard and Brooks, 1980; previously unpublished data).

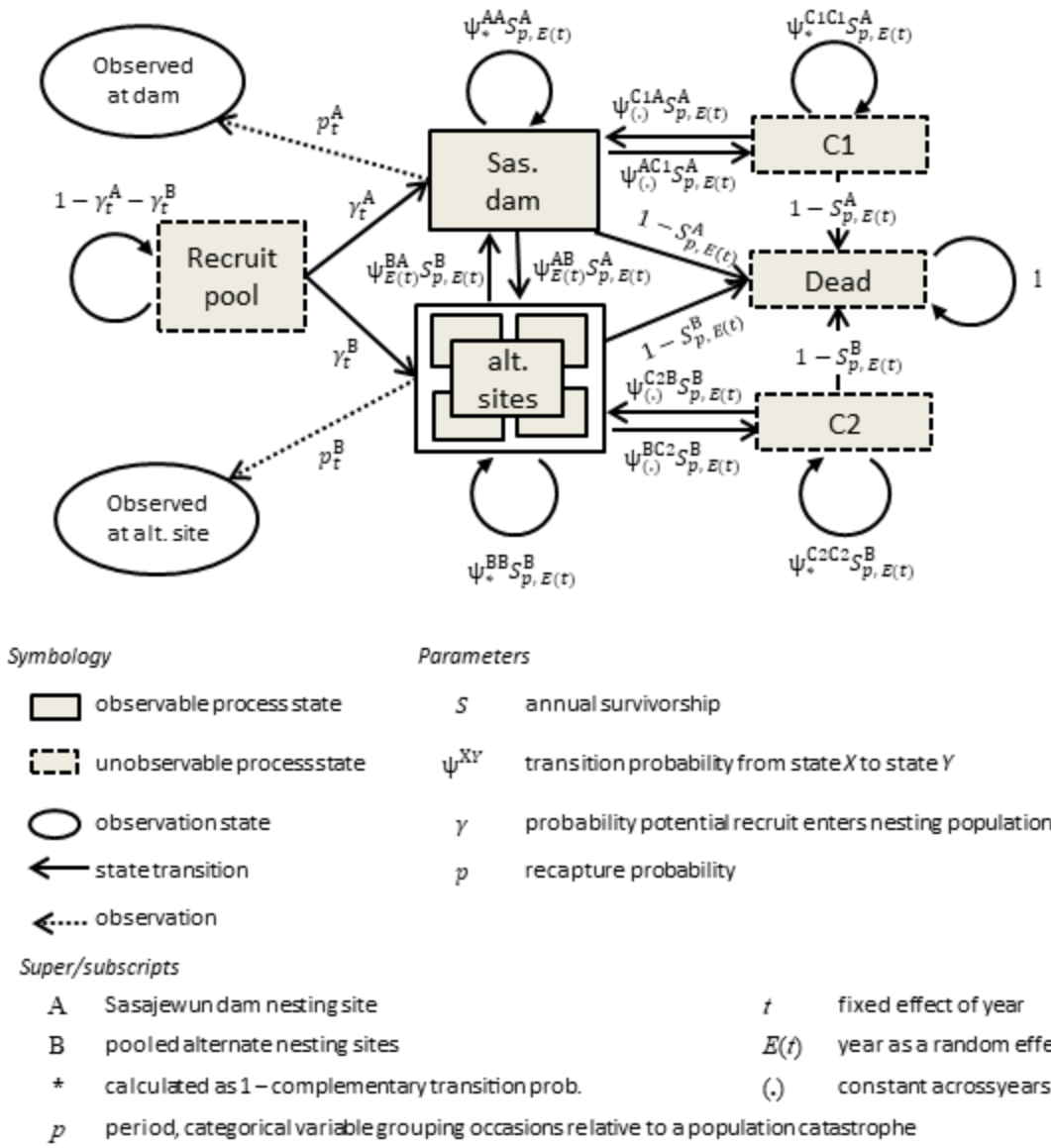

Figure 1.2. Structure of the general multistate mark-recapture model with temporary emigration for nesting female Snapping Turtles in Algonquin Park. The recruit pool and associated transitions occur in the state-space model of abundance but not in the multinomial m-array parameterization used for model selection.

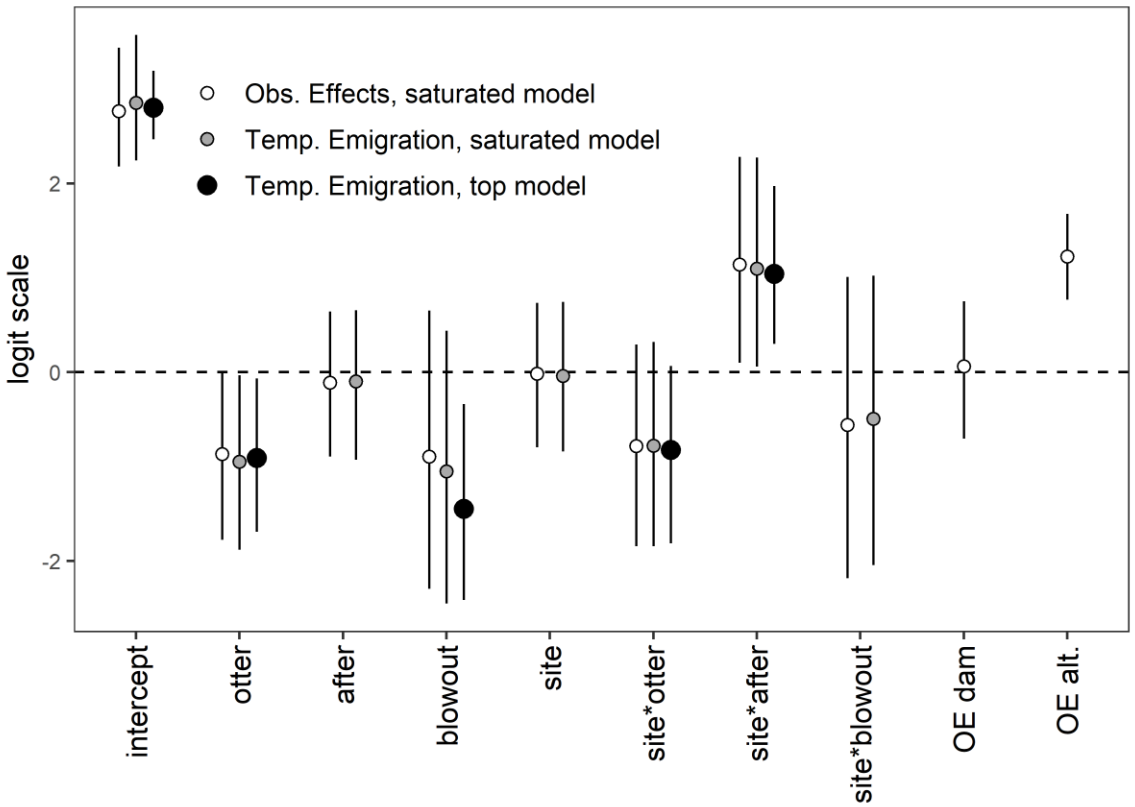

Figure 1.3. Relative strength and uncertainty (means and 95% CRIs) of period and site effects on survival, and observation effects on detection, compared among three multistate models of nesting female Snapping Turtles. Positive effects are associated with increases in survival or in recapture probability. Models shown are the temporary emigration (TE) and observation effects (OE) models before Gibbs Variable Selection (GVS) and the top TE model after GVS. The first eight parameters are effects of four periods (the first is the intercept), site (dam or alternate), and interactions on apparent survival. Because of the design matrix coding, site interactions without corresponding main effects apply to the dam, but not to alternate sites. The final two parameters are the immediate observation effect on recapture probability of dam (*OE dam*) and alternate site (*OE alt.*) nesters. There was good agreement on survivorship parameters between the TE and OE models. Within the OE model, there was a "trap-happy" response at the alternate sites but not at the dam site.

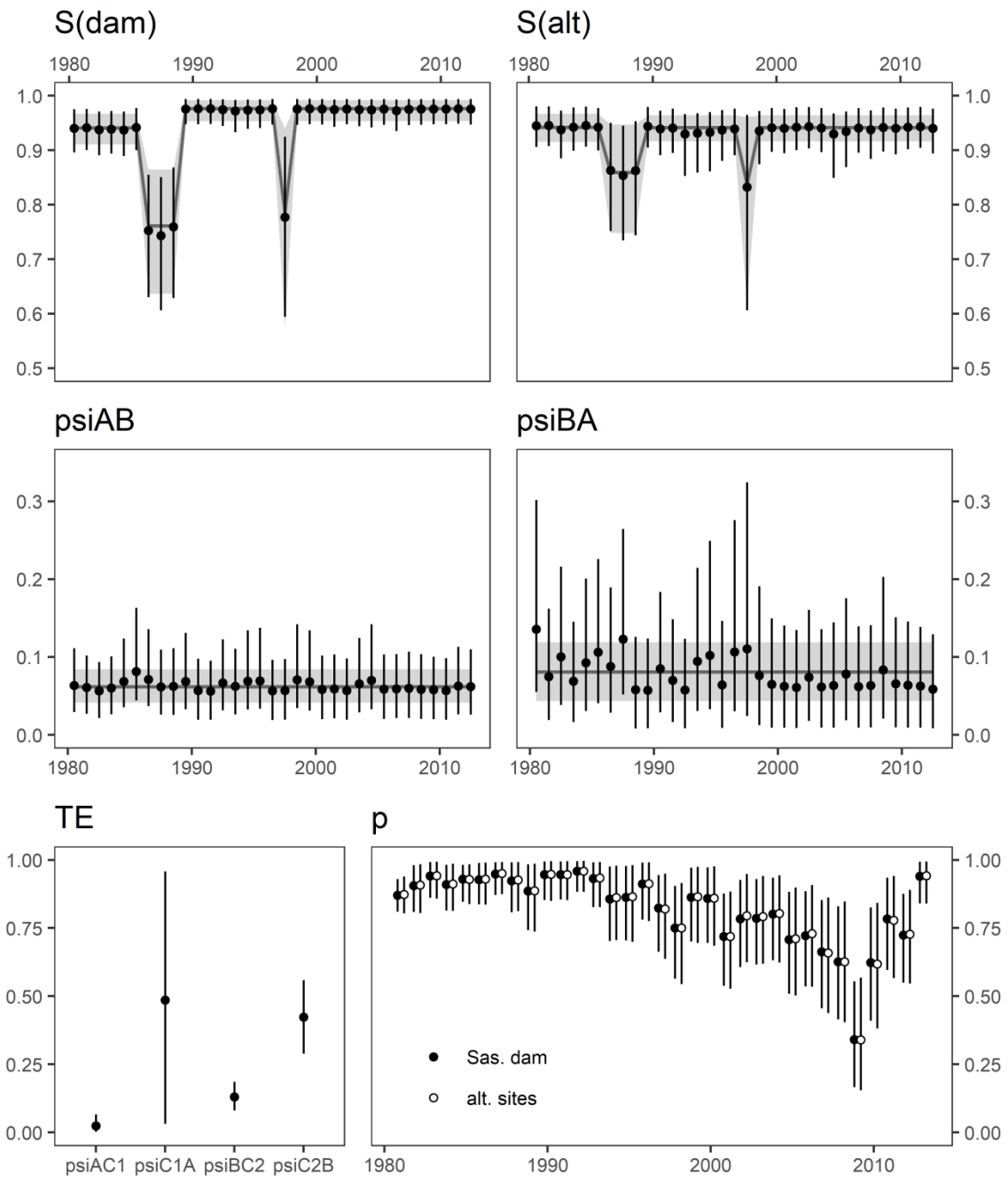

Figure 1.4. Model-averaged estimates of survival, transition, and recapture parameters from multistate mark-recapture models of nesting female Snapping Turtles in Algonquin Park. Models were averaged using Gibbs Variable Selection on apparent survival (*S*) and recapture (*p*) effects.

Hyperparameter means are shown by solid lines with shaded 95% CRIs. *S(dam)* and *S(alt)* show estimates of survival for females nesting at dam and alternate sites, respectively. *psiAB* is transition from dam to alternate sites, while *psiBA* is the reverse. TE shows constant (no time variation) transition probabilities to (*psiAC1*, *psiBC2*) and from (*psiC1A*, *psiC2B*) unobservable states (i.e., temporary emigration). Parameter *psiC1A* was not identifiable (Appendix S1: Fig. S4).

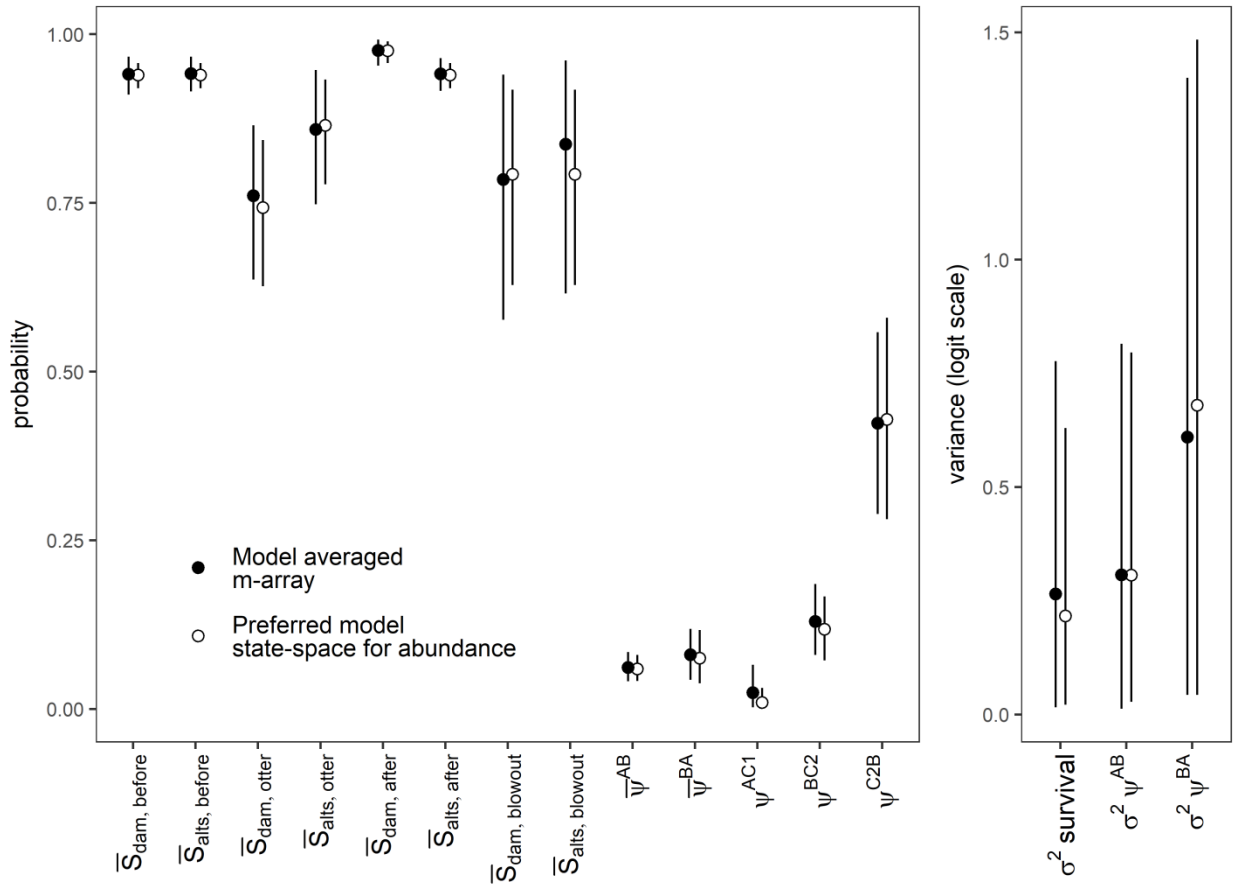

Figure 1.5. Comparison of nesting female Snapping Turtle survival and transition parameters (means with 95% CRIs) among models, sites (dam, alternate sites), and periods. Models shown are the multinomial m-array with model averaging using Gibbs Variable Selection (GVS) and a state-space model constructed using the most supported parameter structure from GVS. Subscript

before denotes mean annual survival from 1980 to 1986, before the otter predation event; *otter* denotes three years (1986-1989) of elevated mortality from predation by otters; *after* is mean post-catastrophe survivorship from 1989 to 2013. During the 1997-1998 interval (*blowout*), the Sasajewun dam failed. Mean apparent survivorship estimates of the abundance model over the four periods (*before, otter, after, blowout*) at the dam were 0.941, 0.761, 0.976, 0.785, and at alternate sites were 0.942, 0.860, 0.942, and 0.837, respectively. Parameters ψ^{YZ} are annual transition probabilities from Y to Z where superscript A is the Sasajewun dam, C1 is its corresponding unobservable state, B is the alternate sites, and C2 is the corresponding unobservable state. Transitions involving unobservable states were modeled without time variation, while other transitions and survival were random effects means with corresponding variances $\sigma^2\psi^{AB}$, $\sigma^2\psi^{BA}$, and σ^2 *survival*.

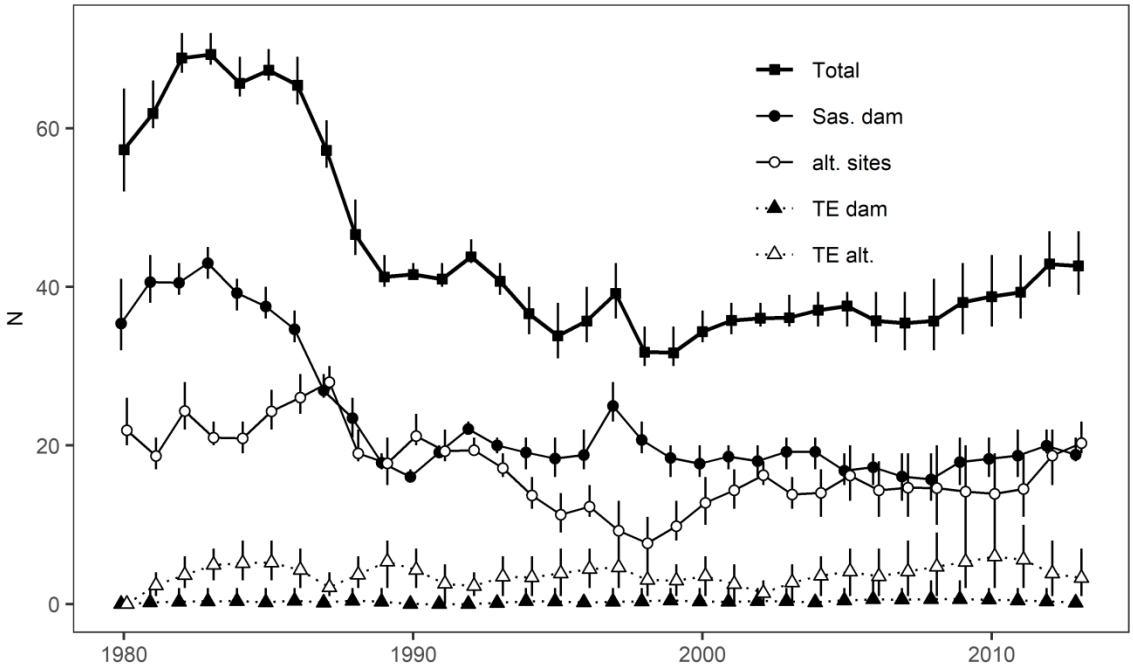

Figure 1.6. Abundance estimates for female Snapping Turtles nesting at monitored sites in Algonquin Park from 1980 to 2013. States are: available for detection at the Sasejewun dam (Sas. dam) or the alternate sites (alt. sites), or temporarily unavailable from either of those sites (TE dam, TE alt., respectively). Filled squares indicate total abundance across all four states. Error bars are 95% CRIs.

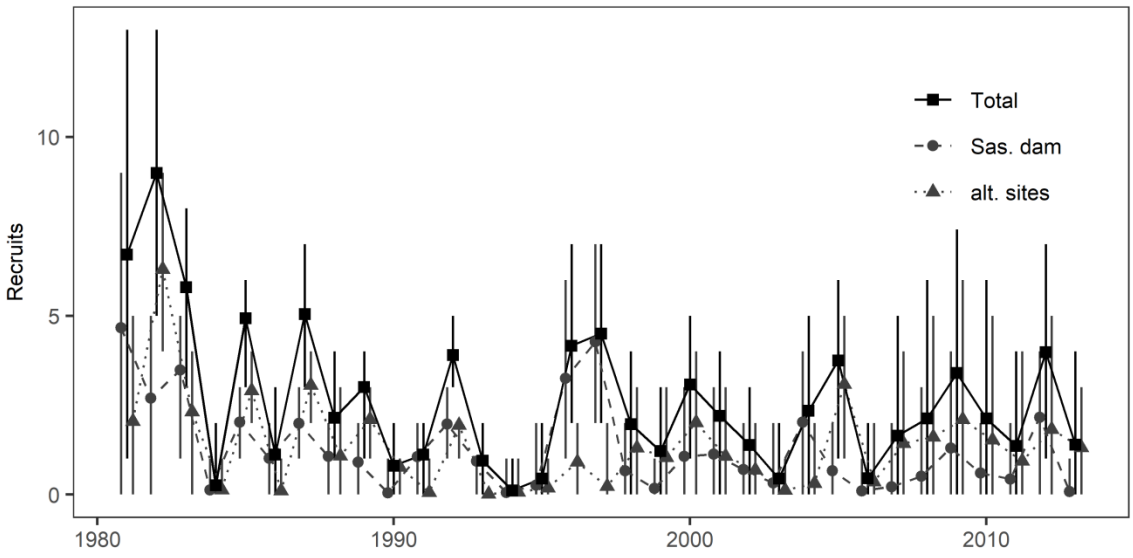

Figure 1.7. Estimated recruitment (medians and 95% CRIs) of new nesting female Snapping Turtles to two nesting areas, the Sasajewun dam and alternate sites, in Algonquin Park from 1981 to 2013. We attribute the relatively high recruitment estimates over the first three intervals to returning temporary emigrants.

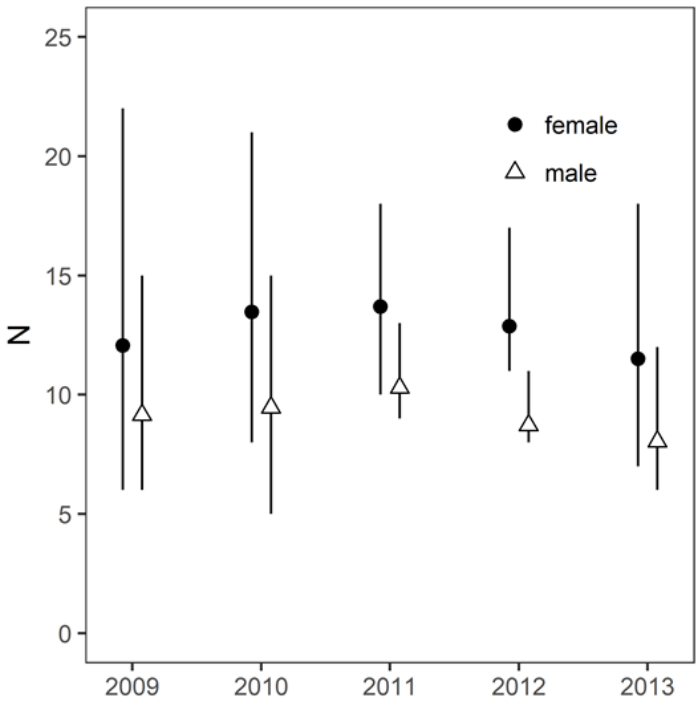

Figure 1.8. Abundance estimates and 95% CRIs of Lake Sasajewun resident adult Snapping Turtles (females >24cm SCL, males >30cm SCL) estimated using a robust design model of trap captures and canoe observations

Chapter 2

The adaptive value of intraspecific aggression, inferred from injuries, in an aquatic turtle with male-biased size dimorphism

Published as:

Keevil, M. G., Hewitt, B. S., Brooks, R. J., & Litzgus, J. D. (2017). Patterns of intraspecific aggression inferred from injuries in an aquatic turtle with male-biased size dimorphism. *Canadian Journal of Zoology*, *95*(6), 393–403. https://doi.org/10.1139/cjz-2016-0182

Abstract

Patterns of sexual size dimorphism (SSD) in turtles are correlated with ecological mode, and it has been hypothesized that mating systems are also shaped by ecological mode. Male combat and coercive mating are competing explanations for male-biased SSD, but are difficult to assess empirically in aquatic species with cryptic behaviour. We quantified SSD and compiled observations of putative combat wounds collected from over 500 captures of Snapping Turtles (*Chelydra serpentina*) in Algonquin Provincial Park, Ontario, to test hypotheses of mate competition and coercion. We found that both sex and body size were important predictors of risk of wounding, consistent with the hypothesis that male-male sexual competition is the primary driver of intraspecific aggression. Low wounding rates among females suggests that resource competition and coercive mating are not important causes of injuries. The risk of wounding increased monotonically with body size in adult males but not in adult females, and small males were less likely to be injured, suggesting that they employ a risk-averse strategy by avoiding direct competition for mates. There was no evidence of asymptotic or decreasing wounding probability in the largest males, which is consistent with the hypothesis that large males compete most intensively to monopolize mates.

Introduction

Sexual size dimorphism (SSD) is widespread among animals and derives from differential equilibria of selection on body size in males and females resulting from sexual selection, fecundity selection, and intersexual niche partitioning and is mediated by ecological, genetic, and other constraints (Andersson, 1994; Blanckenhorn, 2005; Fairbairn et al., 2007; Shine, 1989). Four categories of selection pressures have been suggested to act specifically on male body size: male combat, female choice, male dispersal, and sexual coercion (Darwin, 1871; Ghiselin, 1974).

Of these, male combat and sexual coercion are both mediated by aggression and are predicted to consistently select for larger male body size (Andersson, 1994; Berry and Shine, 1980; Clutton-Brock and Parker, 1995; Darwin, 1871; Dawkins and Krebs, 1979; Ghiselin, 1974; Krüger et al., 2014). Examining patterns of aggressive interactions can allow inferences about the current adaptive value (Tinbergen, 1963) of aggression and whether such patterns are consistent with the hypothesized role of aggression in the evolution of SSD in a lineage. If large male body size primarily functions to increase success in contests between males, then signs of aggression should be most evident in males when SSD is male-biased. Conversely, if the function of male-biased dimorphism is coercive mating, then females are expected to receive proportionately higher levels of aggression than males. As a corollary, levels of aggression experienced by both males and females are likely to be lower in species that have not evolved male-biased SSD. In this paper we investigate the current adaptive value of aggression in an aquatic species with cryptic behaviour by comparing the distribution of wounds across sexes and body sizes to predictions based on contrasting hypotheses of the role of aggression and SSD.

Turtles, one of the major extant tetrapod lineages, exhibit a large range of sexual size dimorphism (SSD). The similarity of reproductive mode among turtles—oviparity and a nearly universal lack of post-oviposition parental care—makes chelonians an attractive group in which to study the role of sexual selection, fecundity selection, and intraspecific niche divergence in the evolution of SSD with fewer of the confounding influences that obscure general mechanisms behind patterns of dimorphism in other taxa (Cox et al., 2007; Lindenfors et al., 2007). Consequently, there has been considerable interest in comparative investigations of patterns of SSD in turtles (Berry and Shine, 1980; Ceballos et al., 2013; Halámková et al., 2013; Lindeman, 2008; Stephens and Wiens, 2009). However, broad, cross-taxa surveys have limited ability to

select among mechanistic hypotheses when behavioural data are missing or of low quality, as is unfortunately the case for turtles (Cox et al., 2007; Halámková et al., 2013). Put another way, investigation of the evolution of SSD in a lineage can be hampered by a lack of information regarding its current adaptive function.

In their seminal paper, Berry and Shine (1980) documented strong correlations between ecological mode (terrestrial, semi-aquatic, bottom-walking, and aquatic swimming) with mating systems and the direction of SSD across a broad sampling of chelonian taxa. Recent analysis supports the correlation between ecology and SSD (Ceballos et al., 2013). Multiple explanations have been advanced to explain the relationships between mating systems, ecology, and SSD in turtles, but testing of these hypotheses has been hampered because the mating systems of most aquatic taxa, even for otherwise well-studied species, remain poorly known. Berry and Shine (1980) concluded that the predominance of male-biased SSD among terrestrial species was caused by male-male combat, a view that continues to be supported by more recent analyses (Halámková et al., 2013). In contrast, sexual coercion is a hypothesized driver of evolution of male-biased SSD in semi-aquatic and bottom-walking species, such as Snapping Turtles (*Chelydra serpentina*), because females are less able to avoid persistent males (Berry and Shine, 1980). In contrast, the predominance of female-biased SSD among aquatic swimming turtles is attributed to the high mobility of females which precludes coercion and instead favours male dispersal, courtship, and female choice (Berry and Shine, 1980). Other proposed contributing factors are differences in aquatic and terrestrial predation risk and energetics (Lindeman, 2008). Additional hypotheses such as intersexual niche divergence in emydids (Lindeman, 2008; Stephens and Wiens, 2009) and sex differences in selection for timing of maturity (Gibbons and

Lovich, 1990; Lovich et al., 2014) are applicable but do not explain the observed correlation with ecological mode.

More data on behaviour and mating systems in turtles have accumulated since Berry and Shine (1980) first tried to explain the relationships among dimorphism, mating system, and ecology, but studies continue to be biased against more aquatic turtles and especially bottom-walkers as they are the most difficult to observe in the wild. Most systematic and detailed behavioural observations of interactions between turtles have been done in captivity (Kramer and Burghardt, 1998; Liu et al., 2008; Poschadel et al., 2006; Thomas, 2002), focus on species whose interactions occur mostly on land (Boglioli et al., 2003; Kaufmann, 1992), or focus on the subset of social behaviours that occur above the water surface (Bury and Wolfheim 1973; Lindeman 1999; but see Kramer and Fritz 1989; Rovero et al. 1999; Schofield et al. 2007). However, for difficult-to-observe animals such as salamanders (Fauth and Resetarits, 1999; Staub, 1993), caecilians (Teodecki et al., 1998), and cetaceans (e.g. Scott et al. 2005; Orbach et al. 2015), the presence of wounds or scars has been used to make inferences about the frequency of male combat and coercive mating. Therefore, given the difficulty of direct behavioural observations of cryptic, aquatic species, we tested hypotheses about the role of intraspecific interactions in driving male-biased SSD in Snapping Turtles by analyzing the demographic distribution of wounds putatively arising from fights. We compared these data to predictions from hypotheses about the effects of body size and sex on the frequency of aggressive interactions among individuals. In addition to analyzing demographic patterns of wounding, we also quantified SSD within our sample to test a premise of our hypotheses (that Snapping Turtles show male-biased SSD) and to place our study system in the context of variation in SSD across chelonian taxa.

Hypotheses for sex effects on wounding probability

Mate competition among males is often more intense than among females because of higher variance in reproductive success and lower parental investment by males (Bateman 1948; Wade 1979; Collet et al. 2014; but see Schulte-Hostedde et al. 2004; Snyder and Gowaty 2007; Williams and DeWoody 2009). Snapping Turtles have male-biased SSD (Gibbons and Lovich 1990) which suggests an important role of male-male combat in determining reproductive success (Andersson, 1994). However, there has been criticism of the assumption that evolution of SSD is driven by sexual selection (Candolin and Tukiainen, 2015; Shine, 1989). Recent analyses have cast doubt on even some classic examples of intra-sexual arms races in male body size, such as the correlation between SSD and polygyny, by presenting evidence that ecological divergence or selection for coercive mating, rather than high levels of polygyny, caused SSD in pinnipeds (González-Suárez and Cassini, 2014; Krüger et al., 2014). In their analysis of SSD and mating systems across chelonian taxa, Berry and Shine (1980) scored Snapping Turtles as bottom-walkers with a mating system featuring male-biased SSD and forcible copulation, but not male-male combat. In contrast, higher wounding rates among male Snapping Turtles have been postulated to result from male-male combat (Kiviat, 1980), thus, the cause of male-biased SSD in Snapping Turtles has yet to be resolved. If the coercion hypothesis is correct, then we expect females to have higher or similar wounding rates relative to males (e.g., Figure 2.1A or B) and much higher rates than juveniles. If the male-male combat hypothesis is correct, we expect that males will have higher wounding rates than either females or juveniles (Figure 2.1C through F).

Hypotheses for size effects on wounding probability

The high cost of fighting favours adaptations for prospective combatants to obtain and update information on competitors' abilities and to avoid or discontinue fighting against potential

opponents that have superior fighting ability (Maynard Smith and Price 1973; Enquist and Leimar 1987, 1990). Therefore it is often adaptive for competitors to employ sequential assessment during agonistic encounters (Enquist and Leimar, 1987). Aggressive encounters between turtles of many species often proceed by escalation of stereotyped signals (Bury and Wolfheim, 1973; Kaufmann, 1992; Rovero et al., 1999; Schofield et al., 2007). Anecdotal observations that suggest stereotyped signalling during aggressive encounters between Snapping Turtles have been reported (Merrill, 2014) but not studied systematically. In the context of male mate competition, we expect that smaller males will avoid physical conflict with larger males that they perceive to have high relative fighting ability. Given this expectation, we predict different relationships between wound frequency and body size depending on the mating system and male strategies in our population:

- After maturity, fighting and wounding increase gradually with size (Figure 2.1C). Larger males are able to monopolize access to females to some degree. Smaller males cannot defeat dominant males and receive little benefit from winning against similarly-sized males and so adopt a more risk-averse strategy.
- Fighting is rare among small males and increases steeply among the largest males (Figure 2.1D). Only the largest males can use combat to compete for mates effectively and thus monopolize females, resulting in high levels of polygyny and variance in male fitness.
- Wounds are equally likely to appear on any male larger than size at maturity (Figure 2.1E). Males begin to fight after maturity and form a dominance hierarchy. Confrontations escalate to combat only between similarly-sized individuals. Mates are not monopolized so all males participate in competing for dominance.

- Similar to above, but very large males are rare so the largest males rarely encounter each other, therefore they fight less frequently and receive fewer wounds (Figure 2.1F).

Materials and methods

Study site

Turtles were captured at several sites within the Western Highlands of Algonquin Provincial Park, Ontario, Canada as part of a long-term life-history project. This project is based out of the Wildlife Research Station (WRS) where it has been conducted since 1972 (R. J. Brooks, University of Guelph). Focal sites were sampled annually and include nesting areas, wetlands, streams, and lakes on the WRS property (45.6ºN, 78.5ºW) and other lakes within or adjacent to the Lake of Two Rivers catchment, as well as wetlands in the Arowhon study area (45.6ºN, 78.7ºW; approximately 15 km from WRS). In addition to focal sites, Snapping Turtles from intermittently sampled sites within 30 km of the WRS were also included in the present analysis.

Field data collection

All work involving animals was carried out under an approved Laurentian University Animal Care protocols (AUP #s 2008-12-02 and 2013-03-01) and was authorized by permits from the Ontario Ministry of Natural Resources and Forestry. Turtles were captured during nesting surveys, by baited hoop trap, and from canoe or while wading using hand or dip net, transported to a field laboratory at the WRS for measuring and marking, and returned to their site of capture within 24 h. Turtles were individually marked by notching the marginal scutes (Cagle, 1939) and adults received an aluminum tag affixed to the rear margin of the carapace (Loncke and

Obbard, 1977). Tree calipers (50 cm maximum, ± 0.1 cm) were used to measure straight-line carapace length (SCL). When SCL was less than 20 cm, Vernier calipers (25 cm maximum, ± 0.01 cm) were used to measure SCL. We weighed turtles using 1 kg, 5 kg, or 20 kg Pesola® spring scales, depending on individual size. Sex of adults was determined using the ratio of pre-cloacal tail length/length of the posterior lobe of the plastron, measured using calipers; ratios greater than 1.0 indicated adult males (de Solla et al., 1998). We confirmed sex by attempting to induce penile eversion by rocking, which is effective for adults and older juveniles (de Solla et al., 2001; Dustman, 2013). We could not confidently determine sex in some subadults and most juveniles under 20 cm SCL, for whom we recorded sex as 'unknown'. Other morphometrics (carapace width, plastron length, shell height) were recorded along with drawings and verbal descriptions of injuries, deformities, and behavioural observations. Beginning in 2010, the dorsal and ventral side of each individual was photographed; photographs of injuries and other physical abnormalities supplemented verbal descriptions.

Sexual size dimorphism

We quantified SSD in our sample using median SCL for each individual. Because penile eversion can potentially indicate sex of individuals before maturity (Dustman, 2013), we analyzed SSD using only those males with a median ratio of pre-cloacal tail length/length of the posterior lobe > 1. This ratio is a secondary sex character that develops around sexual maturity (de Solla et al., 1998; Mosimann and Bider, 1960). We included females only on or after the year of their first nesting observation. These criteria ensured that only mature individuals of each sex were included in our assessment of SSD. We tested for sex differences in SCL and mass using a Mann-Whitney-Wilcoxon test. We quantified SSD by calculating the sexual

dimorphism index (SDI) of Lovich and Gibbons (1992) using mean and maximum sizes of males and females (Ceballos et al. 2013; Lovich et al. 2014).

Data selection and scoring

We used photos and descriptions to score observations as 'wounded' or 'not wounded'. Only observations from 2009 to 2013 were included in the present analysis because descriptive notes over that period were more detailed and consistently recorded because of high observer continuity, and photos were available for most observations during this period. We used only the first capture of the year for each individual and excluded individuals for which SCL < 10 cm. We regarded multiple, fresh injuries sustained to the soft tissue of the head, neck, or tail regions as putative combat wounds ('wounds' hereafter). Superficial wounds of this nature are typical after observed aggressive interactions (MGK, pers. obs.). Diet, habitat selection, and home range size are similar for males and females (Brown and Brooks, 1993; Obbard and Brooks, 1981) and so we make the assumption that differences in injury rates result from differences in intraspecific interactions rather than systematic differences in exposure to other hazards. We excluded old, healed (dark colored) scars and bone injuries (missing digits, truncated rostrum, truncated tail, and scrapes, dents, and gouges to the shell).

Our observations of wounds on turtles that were captured in successive years suggests that combat wounds remain apparent for about one year (Figure 2.3) although severe wounds may remain light-coloured for longer, and minor wounds likely heal more quickly. We compared photos to ensure that the same wounds were not counted twice in successive captures. If wounds last longer than one year, then observations occurring in successive years are less likely to detect wounds than observations preceded by longer intervals during which persistent wounds could conceivably accumulate without being observed. We assessed this possibility using a test of

independence of *wound* from *interval* conditional on *sex* using the log linear model function `loglm()` in the MASS package (Venables and Ripley, 2001). For this test we scored factor *interval* using two levels: one year, or, two or more years. We excluded observations of individuals of unknown sex.

We considered the possibility that wounds were caused by fights that occurred when two or more individuals were confined within the same trap. Multiple captures per trap were uncommon in our study, likely owing to the low density of the population. In cases when a wounded turtle was captured in the same trap as another turtle, we examined photos to assess whether the injuries were fresh. Using the criterion of fresh wounds on individuals captured in a trap with one or more other turtles, we counted how many of the wound observations might be attributable to trap-cohabitation injuries.

Data analyses

We constructed binomial generalized linear models with number of occasions that wounds were observed (*wounds*) vs. number of captures for each individual (*obs*) as the response variable, with *sex* and scaled SCL (*size*) as independent variables, and we used a logistic link function. Scaled SCL is a sex-dependent measure that quantifies size of an individual relative to other members of the same sex. We used this parameterization of *size* to reduce the confounding of size and sex that is intrinsic to populations having SSD. Scaled SCL was implemented by dividing SCL by the population mean maximum body size (the mean asymptote of a von Bertalanffy growth model) which was previously estimated for our population as 30.19 cm (females) and 38.19 cm (males) (Armstrong and Brooks, 2013). Therefore *size* is the proportion

of expected sex-specific maximum size achieved by an individual at the time of observation. We used median SCL for those individuals that were observed more than once during the study period. Within-individual SCL varied for individuals with more than one capture due to growth and measurement error. Within-individual measured size variation was minor over the sampling period. The greatest absolute deviation of each observed SCL from each individual's median SCL was 1.5 cm, but 95% of observations deviated by less than 0.5 cm.

We included second order polynomial $size^2$ and $size^2 \times sex$ terms to test hypotheses featuring declining wound frequency at the largest body sizes (Figure 2.1). To test for a threshold/plateau relationship between *size* and *wounds*, we modified the logit link function to include asymptote parameters *asym*[1] and *asym*[2]×*sex*. Including the intercept *a*, the saturated model is therefore:

```
logit.p[i]=a + B[1]*sex[i] + B[2]*size[i] + B[3]*sex[i]*size[i] +
B[4]*size[i]^2 + B[5]*sex[i]*size[i]^2
```

with link function:

```
p[i]=(asym[1] + asym[2]*sex[i]) / (1 + exp(logit.p[i]))
```

where *wounds* is binomially distributed with probability *p*[i] sampled over *obs*[i] observations per individual:

```
wounds[i]~dbin(p[i],obs[i])
```

Models that did not include *asym* parameters had the numerator of the link function set to 1 which is the standard logit link function.

We used a Bayesian approach to fit models because it provided a straightforward way to incorporate juveniles for whom *sex* is a missing variable. In those cases, we assigned a *Bin*(0.5)

prior on *sex*, which implies a 1:1 sex ratio, and *size* was calculated in each Markov-chain Monte Carlo (MCMC) iteration to accommodate the sex-specific denominator (expected maximum SCL). The intercept and beta parameters were given uninformative $N(\mu,\sigma^2) = N(0, 100)$ priors. Asymptote parameters were constrained so that their sum was between 0 and 1 using the multinomial logit function:

```
asym[j]=exp(logit.a[j])/(1+exp(logit.a[1])+exp(logit.a[2]))
```

where *logit.a*[j] has prior distribution $N(0, 100)$. When only *logit.a*[1] was present in a model we used a logit function of *logit.a*[1] alone. Models were fitted using MCMC implemented in Program JAGS (Plummer, 2013) run through the R package R2jags (R Development Core Team, 2020; Su and Yajima, 2014). Please see Appendix A2.1 for R and JAGS code. Models were run with three chains until convergence was achieved ($\hat{R} < 1.1$ (Brooks and Gelman, 1998)) using the `autojags()` function of R2jags followed by a further 10,000 iterations of each chain.

We took an information theoretic approach to compare models of the effects of sex and body size (SCL) on the probability of observing combat wounds. We used the deviance information criterion (DIC), a Bayesian analog to Akaike's AIC (Spiegelhalter et al., 2002). We used treatment contrasts for the categorical variable *sex* with males dummy-coded as 1 and females as 0. Because of this, models with interaction effects *sex*× *size* or *sex*× $size^2$ without corresponding main effects are interpretable as fitting a *size* effect on males but not females. Because the corresponding hypotheses are biologically reasonable we included such non-hierarchical models in our candidate set. Therefore, given five beta parameters (excluding the intercept), there are $2^5 = 32$ possible parameter combinations. We replicated these across three combinations of asymptote parameters: 1, *asym*[1], and *asym*[1] + *asym*[2]×*sex* for a total of $3 \times 32 = 96$ potential

models. From this set we excluded the four models having an *asym*[*j*] parameter without any *size* effects; therefore, our model set had 92 candidates. Models were analyzed five times each to assess MCMC variability in DIC estimates and the median score was used in model selection. We also did separate runs with *Bin*(0.3) and *Bin*(0.7) priors on *sex* to assess sensitivity to the assumption of equal sex ratio among unsexed juveniles.

We assessed goodness-of-fit of our saturated model using a posterior predictive check (Gelman et al., 2004). To obtain a discrepancy statistic we calculated the sum of squared Pearson residuals across observations during each MCMC iteration for our observed data and for replicate data simulated from the estimated parameters (Kéry, 2010). We then calculated the Bayesian *P*-value as the frequency that observed discrepancies exceeded expected discrepancies, and made a scatterplot of observed and expected discrepancies to perform a visual check (Gelman et al., 2004).

Results

Sexual size dimorphism

We confirmed that our population had significantly male-biased SSD. The distribution of body sizes of males was left-skewed with a greater range than that of females, which it completely overlapped (Figure 2.2). Among mature individuals, males were significantly larger on average than females (Table 2.1). Median mass of males was 1.8 times greater than median female mass. Maximum size for males was 41.5 cm SCL, 18.1 kg and for females was 33.3 cm SCL, 8.8 kg. Our calculated index of SSD (Lovich and Gibbons, 1992) was -0.12 using mean SCLs (31.9 cm males, 28.6 cm females), -0.24 using maximum SCLs, and -1.06 for maximum body mass. The

SSD index calculated from means of our population ranked 14th of 139 species summarized by Ceballos et al. (2013) and the SSD index calculated for maximum sizes ranked 10th out of 140 species, indicating that Snapping Turtles in Algonquin Park have a relatively high degree of male-biased SSD. In addition, our data suggest that the sex that achieves the larger size (males) initially matures at a smaller size than females, contrary to the framework proposed by Lovich et al. (2014) to explain SSD.

Demographic distribution of wounds and model selection

We scored 510 observations of 297 Snapping Turtles for presence of wounds (Table 2.2). Putative combat wounds were observed in both males and females (Figure 2.3). However, despite the number of observations being heavily female-biased, there were nearly three times more wounds observed on males. None of the juveniles were observed with wounds. Although wounds tended to be qualitatively more severe in males, one female was found with quite severe wounds similar to the more serious instances observed in males (Figure 2.3). We were able to exclude the possibility that wounds were inflicted by another turtle while in a trap in all cases except for two observations, both males. There was no significant effect of the length of the interval (one year or more than one year) preceding observations on the probability of wounding (Pearson $\chi^2 = 1.57$, df = 2, $P = 0.46$).

We fit 92 binomial models of potential combat wounds using *sex* and *size* as explanatory variables. Our posterior predictive check of the most saturated model indicated that it fit the data well with a Bayesian *P*-value of 0.45. Differences among replicate DIC scores were less than 0.71 in 95% of instances. Although each of the seven parameters occurs in at least one of the top models (ΔDIC < 2, (Spiegelhalter et al., 2002)), the form of the relationship between wounding probability, sex, and size was highly consistent across supported models (Figure 2.4). All well-

supported models featured very low wounding probability at small sizes, a monotonically increasing probability of wounding with size in males, and little or no effect of size on female wounding probability which was always low. The most supported model was $a+B_5 size^2 * sex$ (model 16; Table 2.3, Figure 2.4 and Figure 2.5) which had the lowest DIC score in every run of the candidate set, including when priors for individuals with unknown *sex* were set to *Bin*(0.3) and *Bin*(0.7). Twelve other models also received considerable support (ΔDIC < 2; Table 2.3, Figure 2.4; Spiegelhalter et al. 2002). The null (intercept only) model was the least supported (ΔDIC = 33.7). Models with only sex effects (model 1, ΔDIC = 9.4) or only size effects (model 2, ΔDIC = 33.5) received negligible support.

Discussion

Within the context of the correlations among ecological mode, mating system, and the direction of SSD, we found that both sex and body size were important predictors of risk of wounding, consistent with the hypothesis that male-male sexual competition is the primary driver of intraspecific aggression in Snapping Turtles. We recognize that natural selection can also play a role in the evolution of SSD; however, we did not set out to test these alternative explanations because although they have been explored in chelonians by other researchers (Berry and Shine, 1980; Ceballos et al., 2013; Halámková et al., 2013; Lindeman, 2008; Stephens and Wiens, 2009), they do not correlate with ecological mode, which was the scope of our interest. The frequency of putative combat wounds was very low in females and zero in juveniles. Our model-fitting and selection results indicate that there was minimal support for any effect of size or maturity on female wounding rates (Table 2.3, Figure 2.4 and Figure 2.5). Wounds were present at much higher frequency in males and there was strong support for an effect of size,

with the probability of wounding increasing with carapace length (Figure 2.4). There was no support for an asymptotic effect with size, or for a lower wounding probability at very large sizes.

Size distribution of wounds in males

There was no evidence for either a plateau effect in wounding probability with increasing size (Figure 2.1E and Figure 2.4) or a decline in wounding at large sizes (Figure 2.1F and Figure 2.4). Our results suggest that rates of wounding in males are not substantially increased until well after the size at which sexual maturity is attained (Figure 2.5). The size distribution of wounding that we observed in Snapping Turtles is different than that reported in emydid turtles by Davis (2009), who found that in captivity it was often the most subordinate, smaller males in a dominance hierarchy that were targeted for aggression and received wounds. Our results also differ from those of Scott et al. (2005), who found that juvenile male bottlenosed dolphins (*Tursiops* sp.) had a higher frequency of tooth rake marks than older males.

The distribution of wounding probability with carapace length under the most supported model is shown in Figure 2.5. Although turtles are often thought to grow indeterminately, much of the variation in size after maturity is not due to differences in age (Congdon et al., 2012). Older males in our population may go decades without showing appreciable growth (unpubl. data). Therefore, the relationship between wounding probability and size (Figure 2.5) is not entirely equivalent to the relationship with age. Figure 2.6 shows the relationship between size and wound frequency projected onto the relationship between size and age using the von Bertalanffy growth model estimated for males in our population (Armstrong and Brooks 2013). The expected wounding frequency over a typical male's lifetime changes, assuming there is no age

effect independent of size. We were unable to test for age effects directly as age estimates of large individuals have low precision (Armstrong and Brooks, 2014; Congdon et al., 2012).

Our results are intermediate between the predictions shown in Figures 1C and 1D, which is consistent with the hypothesis that at larger sizes, males are increasingly able to monopolize access to females whereas small males are more likely to avoid physical confrontation. This differs from the pattern revealed by Kauffman's (1992) detailed behavioural observations of wild Wood Turtles (*Glyptemys insculpta*), which are semi-terrestrial with male-biased SSD and, like Snapping Turtles, do not maintain exclusive territories. Unlike Snapping Turtles, aggressive interactions in Wood Turtles rarely resulted in visible injuries and were not limited to the largest males (Kaufmann, 1992). All male Wood Turtles participated in a linear dominance hierarchy and many opportunities for direct competition for mates occurred when the long duration of copulation provided opportunities for males to displace one another (Kaufmann, 1992). The greater degree of SSD, high frequency of wounds, and apparent conflict avoidance by smaller males that we observed suggests more intense mate competition in Snapping Turtles than in Wood Turtles.

If the male-biased SSD (Table 2.1, Figure 2.2) and inter-male aggression that we have demonstrated reflect an adaptive strategy, then there must be a mechanism for dominant males to monopolize mating opportunities. The potential for polygyny, and hence variance in male fitness and strength of mate competition, depends in large part on the existence of opportunities for males to control access to females, which is often dependent on the spatial and temporal clumping of potential mates (Emlen and Oring, 1977). Male-biased SSD in reptiles is associated with territory defense polygyny in which dominated male territories are large and overlap multiple female home ranges (Cox et al., 2003). Telemetry studies on our focal population

showed that during most of the active season, males do not maintain large home ranges (males and females have similar-sized home ranges) and males do not defend exclusive territories (Galbraith et al., 1987; Obbard and Brooks, 1981). However, female nesting migrations suggest a possible mechanism by which male aggression could mediate fitness by giving dominant males an advantage over competitors vying for access to females (Brown and Brooks, 1993). In the pre-nesting period, some male Snapping Turtles move into bottlenecks, e.g., sites such as streams along nesting migration routes that multiple females pass through on their way to limited nesting sites, and even at the nesting sites themselves (Brown and Brooks, 1993). Aggressively maintaining a monopoly on migration bottlenecks may be a way for males to use dominance to increase their reproductive success. Consistent with the migration bottleneck hypothesis, the frequency of observed mating attempts and male combat is highest during the period prior to nesting (Brown and Brooks, 1993). In addition to exploiting migration corridors, communal overwintering or mating aggregations occur in northern populations of other turtle species (Litzgus et al., 1999; Newton and Herman, 2009; Rasmussen and Litzgus, 2010) and such aggregations could conceivably provide circumstances for males to monopolize females. However, despite the severe winters experienced by Snapping Turtles in Algonquin Park, hibernacula may be less limited as individuals show only moderate fidelity to hibernacula and may hibernate alone or in aggregations (Brown and Brooks, 1994; Paterson et al., 2012).

Other circumstances that allow dominant males of other species to restrict access to mates are unlikely to apply to Snapping Turtles. In other large-bodied reptiles, such as viperid snakes in which females reproduce biennially and may have lower survivorship (e.g., *Vipera berus*, *Crotalus atrox*), male-biased operational sex ratios can also lead to increased mate competition, allowing some males to monopolize mating opportunities (Clark et al., 2014; Madsen et al.,

1993). Prolonged courtship and mate guarding further increase opportunities for male combat to influence fitness (Kaufmann, 1992; Madsen et al., 1993). In our study population, copulation is comparatively brief (5 min to 1 hour, Legler, 1955), female survival is high, adult sex ratios are approximately even, and reproduction is usually annual (Brooks et al., 1991; Galbraith and Brooks, 1987).

Wounds on females and implications for coercive mating

The probability of females being wounded was low, but not zero (Table 2.2, Figure 2.3). There are several possible causes of wounds on females and juveniles, including competition for resources and coercive mating attempts by males. Female turtles of several species engage in agonistic encounters in the wild (Bury and Wolfheim, 1973; Kaufmann, 1992; Rovero et al., 1999; Schofield et al., 2007) and juvenile Snapping Turtles in competition for food will fight and form linear dominance hierarchies in captivity (Froese and Burghardt, 1974). Therefore, the relatively low number of females with putative combat wounds could be due to fights over resources rather than coercive attacks by males. In other vertebrate species in which aggressive coercion by males is common, such as in bottlenose dolphins, the frequency of visible injuries to females can be high (Scott et al., 2005). Although some authors suggest forced copulation in turtles is unlikely (Gibbons and Lovich, 1990; Liu et al., 2013), seemingly coercive mating tactics have been frequently observed in numerous chelonian species and can result in injuries to females (Berry and Shine, 1980; Hailey, 1990; Miller, 2003; Moldowan et al., 2020) and a lack of forcible copulation need not imply a lack of sexual coercion (Han and Jablonski, 2010; Rowe, 1992). Multiple paternity exists in our Snapping Turtle population (Galbraith et al., 1993) and there is little support for general fitness benefits to polyandry for females in other reptiles (Uller and Olsson, 2008). Therefore, it may seem surprising that we did not observe more wounds on

females given the large size and formidable armament of male Snapping Turtles. This result is perhaps less surprising when female decisions are considered in the context of other types of conflict.

Following Clutton-Brock and Parker (1995), we suggest that females' responses to males' attempts at forcible copulation may be predicted using the same framework as that used to predict adaptive strategies of males faced with male aggressors (Maynard Smith and Price 1973; Enquist and Leimar 1987, 1990). Snapping Turtles exemplify the bet-hedging life history strategy in which adult female survival is exceptionally high and lifetime reproductive effort is spread out over many years with relatively little invested in any one bout (Cunnington and Brooks, 1996). The cost that an individual (defender) is expected to tolerate before giving up is expected to depend on the relative fighting ability of the aggressor and the value of the contested resource to the defender relative to the 'value of the future' (Maynard Smith and Price 1973; Enquist and Leimar 1987, 1990). The life-history strategy of female turtles implies that at any given moment the current value of the contested resource (paternity of one or a few clutches) is quite low compared to expected future reproductive output. Because the relative fighting ability of males is high, so is the potential cost to females of continuing to fight (the 'cost of coercion') (Clutton-Brock and Parker, 1995). Therefore, we surmise that female Snapping Turtles are not willing to incur high costs, such as risk of injury, in attempting to avoid sexual coercion by males and may therefore choose 'convenience polyandry' (Rowe, 1992). Similarly, Wright et al. (2013) and Lee and Hays (2004) suggested that polyandry in Green Turtles (*Chelonia mydas*) is a result of females avoiding the costs of refusing persistent or coercive males.

While our results do not support sexual coercion as an important current adaptive function of large male size, we wish to acknowledge two broad caveats. The first is that the current utility of

a trait does not necessarily reflect its past adaptive function (Gould and Vrba, 1982), what Blanckenhorn (2005) paraphrased as the ghost of SSD evolution past. Secondly, hypotheses of SSD are typically not mutually exclusive (Blanckenhorn, 2005) so we do not preclude the occurrence of sexual coercion in Snapping Turtles, nor that it may have some effect on SSD despite our inference that male-male aggression is much more frequent.

Conclusion

Investigation into the evolution of SSD can be hampered by a lack of information on current mating systems. We used wounding and size data from a long-term Snapping Turtle study to infer the mating system of an otherwise cryptic organism. The distribution of putative combat wounds by sex and size in Snapping Turtles is most consistent with a mating system characterized by moderate polygyny with mate competition mediated by male-male combat. Fights among males can result in serious injuries and it is likely that large males are able to achieve some degree of monopolization over access to females while smaller males avoid fights. Some females appear to have wounds from conspecific attacks but we do not know if these result from resource competition or sexual coercion, thus sexual coercion may occur but is not an important source of injury in females. Our study demonstrates the use of long-term data for elucidating the evolutionary processes contributing to SSD in a long-lived and difficult-to-observe species.

References

Andersson, M., 1994. Sexual selection. Princeton University Press, Princeton, New Jersey.

Armstrong, D.P., Brooks, R.J., 2014. Estimating ages of turtles from growth data. Chelonian Conserv. Biol. 13, 9–15. https://doi.org/http://dx.doi.org/10.2744/CCB-1055.1

Armstrong, D.P., Brooks, R.J., 2013. Application of hierarchical biphasic growth models to long-term data for Snapping Turtles. Ecol. Modell. 250, 119–125. https://doi.org/10.1016/j.ecolmodel.2012.10.022

Bateman, A.J., 1948. Intra-sexual selection in *Drosophila*. Heredity (Edinb). 2, 349–368. https://doi.org/10.1038/hdy.1948.21

Berry, J.F., Shine, R., 1980. Sexual size dimorphism and sexual selection in turtles (Order Testudines). Oecologia 44, 185–191. https://doi.org/http://dx.doi.org/10.1007/BF00572678

Blanckenhorn, W.U., 2005. Behavioral causes and consequences of sexual size dimorphism. Ethology 111, 977–1016. https://doi.org/10.1111/j.1439-0310.2005.01147.x

Boglioli, M.D., Guyer, C., Michener, W.K., 2003. Mating opportunities of female Gopher Tortoises, *Gopherus polyphemus*, in relation to spatial isolation of females and their burrows. Copeia 2003, 846–850. https://doi.org/http://dx.doi.org/10.1643/h202-009.1

Brooks, R.J., Brown, G.P., Galbraith, D.A., 1991. Effects of a sudden increase in natural mortality of adults on a population of the Common Snapping Turtle (*Chelydra serpentina*). Can. J. Zool. 69, 1314–1320. https://doi.org/10.1139/z91-185

Brooks, S.P., Gelman, A., 1998. General methods for monitoring convergence of iterative simulations. J. Comput. Graph. Stat. 7, 434–455. https://doi.org/10.1080/10618600.1998.10474787

Brown, G.P., Brooks, R.J., 1994. Characteristics of and fidelity to hibernacula in a northern population of Snapping Turtles, *Chelydra serpentina*. Copeia 1994, 222. https://doi.org/10.2307/1446689

Brown, G.P., Brooks, R.J., 1993. Sexual and seasonal differences in activity in a northern population of Snapping Turtles, *Chelydra serpentina*. Herpetologica 49, 311–318.

Bury, R.B., Wolfheim, J.H., 1973. Aggression in free-living Pond Turtles (*Clemmys marmorata*). Bioscience 23, 659–662. https://doi.org/http://dx.doi.org/10.2307/1296781

Cagle, F.R., 1939. A system of marking turtles for future identification. Copeia 1939, 170–183. https://doi.org/http://dx.doi.org/10.2307/1436818

Candolin, U., Tukiainen, I., 2015. The sexual selection paradigm: Have we overlooked other mechanisms in the evolution of male ornaments? Proc. R. Soc. London Ser. B Biol. Sci. 282. https://doi.org/10.1098/rspb.2015.1987

Ceballos, C.P., Adams, D.C., Iverson, J.B., Valenzuela, N., 2013. Phylogenetic patterns of sexual size dimorphism in turtles and their implications for Rensch's rule. Evol. Biol. 40, 194–208. https://doi.org/10.1007/s11692-012-9199-y

Clark, R.W., Schuett, G.W., Repp, R.A., Amarello, M., Smith, C.F., Herrmann, H.-W., 2014. Mating systems, reproductive success, and sexual selection in secretive species: a case study of the Western Diamond-backed Rattlesnake, *Crotalus atrox*. PLoS One 9, e90616–e90616. https://doi.org/10.1371/journal.pone.0090616

Clutton-Brock, T.H., Parker, G.A., 1995. Sexual coercion in animal societies. Anim. Behav. 49, 1345–1365. https://doi.org/10.1006/anbe.1995.0166

Collet, J.M., Dean, R.F., Worley, K., Richardson, D.S., Pizzari, T., 2014. The measure and significance of Bateman's principles. Proc. R. Soc. B-Biological Sci. 281, 20132973. https://doi.org/10.1098/rspb.2013.2973

Congdon, J.D., Gibbons, J.W., Brooks, R.J., Rollinson, N., Tsaliagos, R.N., 2012. Indeterminate growth in long-lived freshwater turtles as a component of individual fitness. Evol. Ecol. 27, 445–459. https://doi.org/10.1007/s10682-012-9595-x

Cox, R.M., Butler, M.A., John-Alder, H.B., 2007. Sex, Size and Gender Roles, Sex, Size and Gender Roles: Evolutionary Studies of Sexual Size Dimorphism. Oxford University PressOxford, Oxford, United Kingdom. https://doi.org/10.1093/acprof:oso/9780199208784.001.0001

Cox, R.M., Skelly, S.L., John-Alder, H.B., 2003. A comparative test of adaptive hypotheses for sexual size dimorphism in lizards. Evolution. 57, 1653–1669. https://doi.org/10.1554/02-227

Cunnington, D.C., Brooks, R.J., 1996. Bet-hedging theory and eigenelasticity: a comparison of the life histories of Loggerhead Sea Turtles (*Caretta caretta*) and Snapping Turtles (*Chelydra serpentina*). Can. J. Zool. 74, 291–296. https://doi.org/10.1139/z96-036

Darwin, C.R., 1871. The Descent of Man, and Selection in Relation to Sex. John Murray, London.

Davis, K.M., 2009. Sociality, Cognition and Social Learning in Turtles (Emydidae). (Doctoral Dissertation). University of Tennessee, Knoxville, Tennessee.

Dawkins, R., Krebs, J.R., 1979. Arms races between and within species. Proc. R. Soc. London. Ser. B. Biol. Sci. 205, 489–511. https://doi.org/10.1098/rspb.1979.0081

de Solla, S.R., Bishop, C.A., Van der Kraak, G., Brooks, R.J., 1998. Impact of organochlorine contamination on levels of sex hormones and external morphology of Common Snapping Turtles (*Chelydra serpentina serpentina*) in Ontario, Canada. Environ. Health Perspect. 106, 253–260. https://doi.org/10.1289/ehp.98106253

de Solla, S.R., Portelli, M., Spiro, H., Brooks, R.J., 2001. Penis displays of Snapping Turtles (*Chelydra serpentina*) in response to handling: Defensive or displacement behavior? Chelonian Conserv. Biol. 4, 187–189.

Dustman, E.A., 2013. Sex identification in the Common Snapping Turtle (*Chelydra serpentina*): A new technique and evaluation of previous methods. Herpetol. Rev. 44, 235–238.

Emlen, S.T., Oring, L.W., 1977. Ecology, sexual selection, and evolution of mating systems. Science 197, 215–223. https://doi.org/10.1126/science.327542

Enquist, M., Leimar, O., 1990. The evolution of fatal fighting. Anim. Behav. 39, 1–9. https://doi.org/10.1016/S0003-3472(05)80721-3

Enquist, M., Leimar, O., 1987. Evolution of fighting behavior: the effect of variation in resource value. J. Theor. Biol. 127, 187–205. https://doi.org/10.1016/S0022-5193(87)80130-3

Fairbairn, D.J., Blanckenhorn, W.U., Székely, T. (Eds.), 2007. Sex, Size and Gender Roles: Evolutionary Studies of Sexual Size Dimorphism. Oxford University Press, Oxford, United Kingdom. https://doi.org/10.1093/acprof:oso/9780199208784.001.0001

Fauth, J.E., Resetarits, W.J., 1999. Biting in the salamander *Siren intermedia intermedia*: Courtship component or agonistic behavior? J. Herpetol. 33, 493–496. https://doi.org/10.2307/1565651

Froese, A.D., Burghardt, G.M., 1974. Food competition in captive juvenile Snapping Turtles, *Chelydra serpentina*. Anim. Behav. 22, 735–740. https://doi.org/10.1016/S0003-3472(74)80025-4

Galbraith, D.A., Brooks, R.J., 1987. Survivorship of adult females in a northern population of Common Snapping Turtles, *Chelydra serpentina*. Can. J. Zool. 65, 1581–1586. https://doi.org/http://dx.doi.org/10.1139/z87-247

Galbraith, D.A., Chandler, M.W., Brooks, R.J., 1987. The fine structure of home ranges of male *Chelydra serpentina*: Are Snapping Turtles territorial? Can. J. Zool. 65, 2623–2629. https://doi.org/http://dx.doi.org/10.1139/z87-398

Galbraith, D.A., White, B.N., Brooks, R.J., Boag, P.T., 1993. Multiple paternity in clutches of Snapping Turtles (*Chelydra serpentina*) detected using DNA fingerprints. Can. J. Zool. 71, 318–324. https://doi.org/10.1139/z93-044

Gelman, A., Carlin, J.P., Stern, H.S., Runin, D.B., 2004. Bayesian Data Analysis. CRC/Chapman & Hall, Boca Raton, F.L.

Ghiselin, M.T., 1974. The Economy of Nature and the Evolution of Sex. The University of California Press, Berkeley, California.

Gibbons, J.W., Lovich, J.E., 1990. Sexual dimorphism in turtles with emphasis on the Slider Turtle (*Trachemys scripta*). Herpetol. Monogr. 4, 1–29. https://doi.org/http://dx.doi.org/10.2307/1466966

González-Suárez, M., Cassini, M.H., 2014. Variance in male reproductive success and sexual size dimorphism in pinnipeds: testing an assumption of sexual selection theory. Mamm. Rev. 44, 88–93. https://doi.org/10.1111/mam.12012

Gould, S.J., Vrba, E.S., 1982. Exaptation—a missing term in the subject of form. Paleobiology 8, 4–15. https://doi.org/http://dx.doi.org/10.1017/S0094837300004310

Hailey, A., 1990. Adult survival and recruitment and the explanation of an uneven sex-ratio in a tortoise population. Can. J. Zool. 68, 547–555. https://doi.org/10.1139/z90-080

Halámková, L., Schulte II, J.A., Langen, T.A., 2013. Patterns of sexual size dimorphism in Chelonia. Biol. J. Linn. Soc. 108, 396–413. https://doi.org/10.1111/j.1095-8312.2012.02015.x

Han, C.S., Jablonski, P.G., 2010. Male water striders attract predators to intimidate females into copulation. Nat. Commun. 1, 52. https://doi.org/10.1038/ncomms1051

Kaufmann, J.H., 1992. The social behavior of Wood Turtles, *Clemmys insculpta*, in central Pennsylvania. Herpetol. Monogr. 6, 1–25. https://doi.org/http://dx.doi.org/10.2307/1466959

Kéry, M., 2010. An Introduction to WinBUGS for Ecologists. Academic Press.

Kiviat, E., 1980. A Hudson River tidemarsh Snapping Turtle population. Trans. Northeast Sect. Wildl. Soc. 37, 158–168.

Kramer, M., Burghardt, G.M., 1998. Precocious courtship and play in emydid turtles. Ethology 104, 38. https://doi.org/http://dx.doi.org/10.1111/j.1439-0310.1998.tb00028.x

Kramer, M., Fritz, U., 1989. Courtship of the turtle, *Pseudemys nelsoni*. J. Herpetol. 23, 84–86. https://doi.org/http://dx.doi.org/10.2307/1564324

Krüger, O., Wolf, J.B.W., Jonker, R.M., Hoffman, J.I., Trillmich, F., 2014. Disentangling the contribution of sexual selection and ecology to the evolution of size dimorphism in pinnipeds. Evolution. 68, 1485–1496. https://doi.org/10.1111/evo.12370

Lee, P.L.M., Hays, G.C., 2004. Polyandry in a marine turtle: Females make the best of a bad job. Proc. Natl. Acad. Sci. U. S. A. 101, 6530–6535. https://doi.org/10.1073/pnas.0307982101

Legler, J.M., 1955. Observations on the sexual behavior of captive turtles. Lloydia 18, 95–99.

Lindeman, P. V, 2008. Evolution of body size in the Map Turtles and Sawbacks (Emydidae : Deirochelyinae : *Graptemys*). Herpetologica 64, 32–46. https://doi.org/10.1655/07-025.1

Lindeman, P. V, 1999. Aggressive interactions during basking among four species of emydid turtles. J. Herpetol. 33, 214–219. https://doi.org/http://dx.doi.org/10.2307/1565717

Lindenfors, P., Gittleman, J., Jones, K., 2007. Sexual size dimorphism in mammals, in: Fairbairn, D.J., Blanckenhorn, W.U., Székely, T. (Eds.), Sex, Size and Gender Roles: Evolutionary Studies of Sexual Size Dimorphism. Oxford University Press, Oxford, United Kingdom, pp. 19–26.

Litzgus, J.D., Costanzo, J.P., Brooks, R.J., Lee Jr., R.E., 1999. Phenology and ecology of hibernation in Spotted Turtles (*Clemmys guttata*) near the northern limit of their range. Can. J. Zool. 77, 1348–1357. https://doi.org/http://dx.doi.org/10.1139/z99-107

Liu, Y., Davy, C.M., Shi, H.-T., Murphy, R.W., 2013. Sex in the half-shell: a review of the functions and evolution of courtship behavior in freshwater turtles. Chelonian Conserv. Biol. 12, 84–100. https://doi.org/http://dx.doi.org/10.2744/CCB-1037.1

Liu, Y., He, B., Shi, H., Murphy, R.W., Fong, J.J., Wang, J., Fu, L., Ma, Y., 2008. An analysis of courtship behaviour in the Four-eyed Spotted Turtle, *Sacalia quadriocellata* (Reptilia : Testudines : Geoemydidae). Amphibia-Reptilia 29, 185–195. https://doi.org/10.1163/156853808784124901

Loncke, D.J., Obbard, M.E., 1977. Tag success, dimensions, clutch size and nesting site fidelity for the Snapping Turtle, *Chelydra serpentina* (Reptilia, Testudines, Chelydridae) in Algonquin Park, Ontario, Canada. J. Herpetol. 11, 243–244. https://doi.org/http://dx.doi.org/10.2307/1563158

Lovich, J.E., Gibbons, J.W., 1992. A review of techniques for quantifying sexual size dimorphism. Growth Dev. Aging 56, 269–281.

Lovich, J.E., Gibbons, J.W., Agha, M., 2014. Does the timing of attainment of maturity influence sexual size dimorphism and adult sex ratio in turtles? Biol. J. Linn. Soc. 112, 142–149. https://doi.org/10.1111/bij.12275

Madsen, T., Shine, R., Loman, J., Hakansson, T., 1993. Determinants of mating success in male Adders, *Vipera berus*. Anim. Behav. 45, 491–499. https://doi.org/10.1006/anbe.1993.1060

Maynard Smith, J., Price, G.R., 1973. The logic of animal conflict. Nature 246, 15–18. https://doi.org/10.1038/246015a0

Merrill, L., 2014. *Chelydra serpentina* (Snapping Turtle): Ritualized aggressive behavior. Herpetol. Rev. 45, 686.

Miller, J.D., 2003. Reproduction in Sea Turtles, in: Lutz, P.L., Musick, J.A., Wyneken, J. (Eds.), The Biology of the Sea Tutles. CRC Press, Boca Raton, Florida, pp. 51–81.

Moldowan, P.D., Brooks, R.J., Litzgus, J.D., 2020. Demographics of injuries indicate sexual coercion in a population of Painted Turtles (*Chrysemys picta*). Can. J. Zool. cjz-2019-0238. https://doi.org/10.1139/cjz-2019-0238

Mosimann, J., Bider, J.R., 1960. Variation, sexual dimorphism, and maturity in a Quebec population of the Common Snapping Turtle, *Chelydra serpentina*. Can. J. Zool. 38, 19–38. https://doi.org/10.1139/z60-003

Newton, E.J., Herman, T.B., 2009. Habitat, movements, and behaviour of overwintering Blanding's Turtles (*Emydoidea blandingii*) in Nova Scotia. Can. J. Zool. 87, 299–309. https://doi.org/http://dx.doi.org/10.1139/Z09-014

Obbard, M.E., Brooks, R.J., 1981. A radio-telemetry and mark-recapture study of activity in the Common Snapping Turtle, *Chelydra serpentina*. Copeia 1981, 630–637. https://doi.org/http://dx.doi.org/10.2307/1444568

Orbach, D.N., Packard, J.M., Piwetz, S., Würsig, B., 2015. Sex-specific variation in conspecific-acquired marking prevalence among dusky dolphins (*Lagenorhynchus obscurus*). Can. J. Zool. 93, 383–390. https://doi.org/10.1139/cjz-2014-0302

Paterson, J.E., Steinberg, B.D., Litzgus, J.D., 2012. Generally specialized or especially general? Habitat selection by Snapping Turtles (*Chelydra serpentina*) in central Ontario. Can. J. Zool. 90, 139–149. https://doi.org/10.1139/z11-118

Plummer, M., 2013. JAGS Version 3.4.0 User Manual.

Poschadel, J.R., Meyer-Lucht, Y., Plath, M., 2006. Response to chemical cues from conspecifics reflects male mating preference for large females and avoidance of large competitors in the European Pond Turtle, *Emys orbicularis*. Behaviour 143, 569–587. https://doi.org/10.1163/156853906776759510

R Development Core Team, 2020. R: A language and environment for statistical computing.

Rasmussen, M.L., Litzgus, J.D., 2010. Habitat selection and movement patterns of Spotted Turtles (*Clemmys guttata*): Effects of spatial and temporal scales of analyses. Copeia 2010, 86–96. https://doi.org/10.1643/CE-09-141

Rovero, F., Lebboroni, M., Chelazzi, G., 1999. Aggressive interactions and mating in wild populations of the European Pond Turtle *Emys orbicularis*. J. Herpetol. 33, 258–263. https://doi.org/10.2307/1565723

Rowe, L., 1992. Convenience polyandry in a water strider: foraging conflicts and female control of copulation frequency and guarding duration. Anim. Behav. 44, 189–202. https://doi.org/10.1016/0003-3472(92)90025-5

Schofield, G., Katselidis, K., Pantis, J., Dimopoulos, P., Hays, G., 2007. Female–female aggression: structure of interaction and outcome in Loggerhead Sea Turtles. Mar. Ecol. Prog. Ser. 336, 267–274. https://doi.org/10.3354/meps336267

Schulte-Hostedde, A.I., Millar, J.S., Gibbs, H.L., 2004. Sexual selection and mating patterns in a mammal with female-biased sexual size dimorphism. Behav. Ecol. 15, 351–356. https://doi.org/http://dx.doi.org/10.1093/beheco/arh021

Scott, E.M., Mann, J., Watson-Capps, J.J., Sargeant, B.L., Connor, R.C., 2005. Aggression in bottlenose dolphins: Evidence for sexual coercion, male-male competition, and female tolerance through analysis of tooth-rake marks and behaviour. Behaviour 142, 21–44. https://doi.org/10.1163/1568539053627712

Shine, R., 1989. Ecological causes for the evolution of sexual dimorphism: a review of the evidence. Q. Rev. Biol. 64, 419–461. https://doi.org/10.1086/416458

Snyder, B.F., Gowaty, P.A., 2007. A reappraisal of Bateman's classic study of intrasexual selection. Evolution. 61, 2457–2468. https://doi.org/10.1111/j.1558-5646.2007.00212.x

Spiegelhalter, D.J., Best, N.G., Carlin, B.P., Van Der Linde, A., 2002. Bayesian measures of model complexity and fit. J. R. Stat. Soc. Ser. B – Stat. Methodol. 64, 583–639. https://doi.org/http://dx.doi.org/10.1111/1467-9868.00353

Staub, N.L., 1993. Intraspecific agonistic behavior of the salamander *Aneides flavipunctatus* (Amphibia, Plethodontidae) with comparisons to other plethodontid species. Herpetologica 49, 271–282.

Stephens, P.R., Wiens, J.J., 2009. Evolution of sexual size dimorphisms in emydid turtles: Ecological dimorphism, Rensch's rule, and sympatric divergence. Evolution. 63, 910–925. https://doi.org/10.1111/j.1558-5646.2008.00597.x

Su, Y.-S., Yajima, M., 2014. R2jags: A Package for Running jags from R.

Teodecki, E., Brodie, E., Formanowicz, D., Nussbaum, R., 1998. Head dimorphism and burrowing speed in the African caecilian *Schistometopum thomense* (Amphibia: Gymnophiona). Herpetologica 54, 154–160.

Thomas, R.B., 2002. Conditional mating strategy in a long-lived vertebrate: ontogenetic shifts in the mating tactics of male Slider Turtles (*Trachemys scripta*). Copeia 2002, 456–461.

Tinbergen, N., 1963. On aims and methods of Ethology. Z. Tierpsychol. 20, 410–433. https://doi.org/10.1111/j.1439-0310.1963.tb01161.x

Uller, T., Olsson, M., 2008. Multiple paternity in reptiles: patterns and processes. Mol. Ecol. 17, 2566–2580. https://doi.org/10.1111/j.1365-294X.2008.03772.x

Venables, W.N., Ripley, B.D., 2001. Modern Applied Statistics with S. Springer, New York.

Wade, M.J., 1979. Sexual selection and variance in reproductive success. Am. Nat. 114, 742–747. https://doi.org/10.1086/283520

Williams, R.N., DeWoody, J.A., 2009. Reproductive success and sexual selection in wild Eastern Tiger Salamanders (*Ambystoma t. tigrinum*). Evol. Biol. 36, 201–213. https://doi.org/10.1007/s11692-009-9058-7

Wright, L.I., Fuller, W.J., Godley, B.J., McGowan, A., Tregenza, T., Broderick, A.C., 2013. No benefits of polyandry to female Green Turtles. Behav. Ecol. 24, 1022–1029. https://doi.org/10.1093/beheco/art003

Tables

Table 2.1. Sexual size dimorphism (SSD) in Snapping Turtles (*Chelydra serpentina*). We estimated SSD of mature adults using 88 males and 139 females that were a subset of the wounding study. Maturity in males was defined as a ratio of pre-cloacal tail length/length of the posterior lobe > 1. Measurements of females were only included if they were taken on or after the year of first observed nesting.

	Median		Minimum		Maximum		W	*P*
	Female	Male	Female	Male	Female	Male		
SCL (cm)	28.3	33.4	22.4*	18.95	33.3	41.5	9148	<<0.01
Mass (kg)	5.5	9.6	3.15	1.55	8.8	18.1	9512.5	<<0.01

SCL = straight-line carapace length

W is the Wilcoxon-Mann-Whitney test statistic

* The smallest nesting female by length had SCL = 22.4 cm, which misrepresents her overall body size because her carapace is deformed. Her mass was 3.8 kg. The smallest nesting female by mass (3.15 kg) had the next smallest SCL at 23.5 cm.

Table 2.2. Number and percentage of Snapping Turtle (*Chelydra serpentina*) observations scored for presence/absence of putative combat wounds. Turtles were caught in Algonquin Provincial Park from 2009 to 2013. Combat wounds were considered to be fresh (less than ~1 year old) injuries sustained to the soft tissue of the head, neck, or tail. We did not consider old, dark coloured scaring and injuries to the shell or other bony parts as recent combat wounds. Individuals with 'Unknown' sex were juveniles that did not exhibit secondary sexual characteristics.

	Turtles	Observations	Wounded
Male	93	161	27 (17%)
Female	186	330	10 (3%)
Unknown	18	19	0 (0%)
Total	297	510	37

Table 2.3. The 13 most supported binomial models (ΔDIC < 2) of wounding probability in Snapping Turtles (*Chelydra serpentina*). Also shown are three simple but poorly supported models (models 0, 1, 2, ΔDIC >> 2). Parameter values are provided as mean (SD). Beta parameters (intercept and B[1–5]) with 95% CRIs that do not overlap 0 are marked with an * and shown in bold. The full model is: logit.p[i]=Int + B[1]*sex[i] + B[2]*size[i] + B[3]*sex[i]*size[i] + B[4]*size[i]^2 + B[5]*sex[i]*size[i]^2

Parameters $asym_1 + asym_2 * sex_i$ set the asymptote of the logistic link function. If both are 0, then the asymptote is 1. sex_i is coded as 0 for females, 1 for males, $size_i$ is standardized carapace length which is straight line carapace length as a proportion of mean maximum size (males 38.19 cm, females 30.96 cm).

Model	DIC	rank	ΔDIC	Intercept	B[1]	B[2]	B[3]	B[4]	B[5]	asym[1]	asym[2]
16	186.8	1	0.00	-3.61 (0.32)*	0	0	0	0	2.62 (0.46)*	0	0
48	187.4	2	0.63	-3.34 (0.61)*	0	0	0	0	2.94 (1.21)*	0.84 (0.26)	0
5	187.6	3	0.79	-3.54 (0.33)*	-3.22 (1.78)*	0	5.85 (1.95)*	0	0	0	0
112	187.8	4	1.07	-3.36 (1.04)*	0	0	0	0	2.76 (1.06)*	0.87 (0.24)	0.03 (0.09)
18	188.0	5	1.26	-4.62 (1.47)*	0	1.16 (1.68)	0	0	2.55 (0.47)*	0	0
21	188.1	6	1.36	-3.54 (0.32)*	-1.51 (3.22)	0	1.75 (7.6)	0	2.41 (4.75)	0	0
17	188.2	7	1.38	-3.54 (0.32)*	-0.79 (1.03)	0	0	0	3.45 (1.18)*	0	0
20	188.3	8	1.50	-3.56 (0.34)*	0	0	-1.36 (2.3)	0	4.01 (2.39)	0	0
24	188.4	9	1.61	-4.05 (0.82)*	0	0	0	0.54 (1.02)	2.59 (0.47)*	0	0
6	188.4	10	1.63	-5.78 (1.56)*	0	2.4 (1.72)	2.38 (0.44)*	0	0	0	0
14	188.5	11	1.73	-6.63 (3.03)*	0	4.44 (6.97)	2.36 (0.44)*	-1.19 (4.21)	0	0	0
37	188.6	12	1.78	-2.98 (0.81)*	-3.19 (4.6)	0	7.11 (4.3)*	0	0	0.7 (0.34)	0
26	188.7	13	1.92	-5.02 (2.74)*	0	2.21 (6.22)	0	-0.68 (3.76)	2.57 (0.47)*	0	0
0	220.4	92	33.66	-2.56 (0.17)*	0	0	0	0	0	0	0
1	196.2	85	9.44	-3.54 (0.33)*	1.86 (0.39)*	0	0	0	0	0	0
2	220.3	89	33.52	-4.51 (1.38)*	0	2.17 (1.52)	0	0	0	0	0

Figures

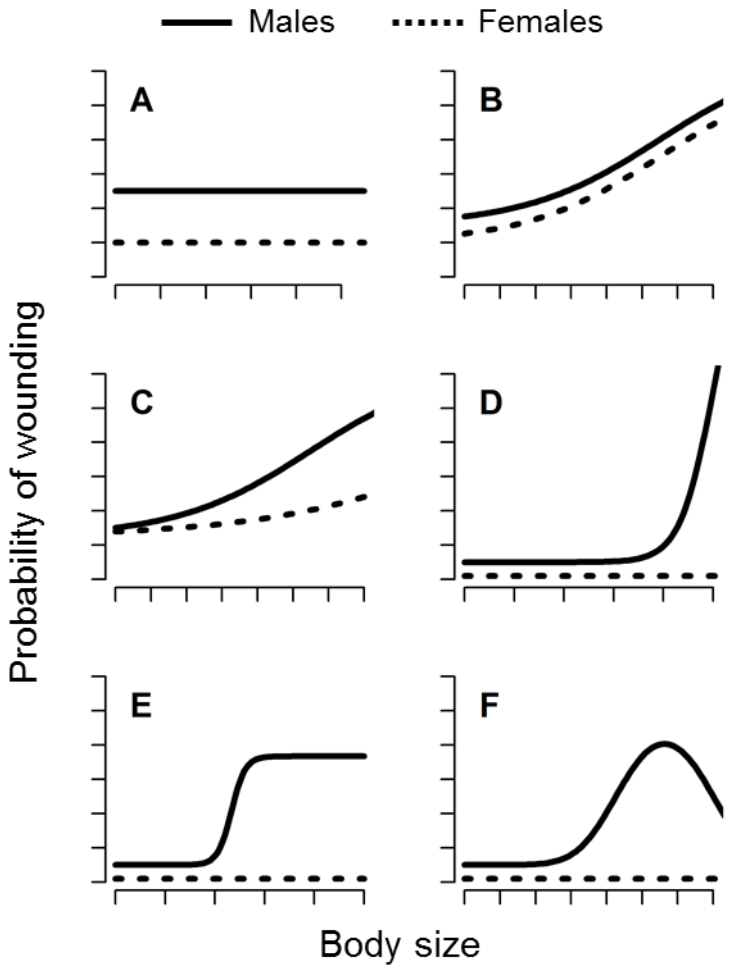

Figure 2.1. Hypothetical models of the effects of size and sex on the probability that turtles will display combat wounds. These examples correspond to plausible *a priori* biological hypotheses but are not an exhaustive enumeration of all combinations of models considered. Model A has an effect of sex but no size effect while Model B has a size effect but no sex effect. C includes a *sex*×*size* interaction in which males experience a greater rate of increase in wounding probability with body size. Models D through F have no *size* effect on wounding in females. These three models, in addition to model C, show wounding probability vs. male size under four hypotheses of male mate competition: C larger males monopolize mating opportunities to a small degree,

smaller males are less likely to fight; D the largest males fight to monopolize females and other males do not fight for access to mates; E, there is a threshold/plateau effect (added asymptote term) in which males begin to compete after maturity but fights to determine dominance are limited to individuals of similar size and all males have similar rates of injury; F, similar to E but large males fight less often to establish dominance (added polynomial term).

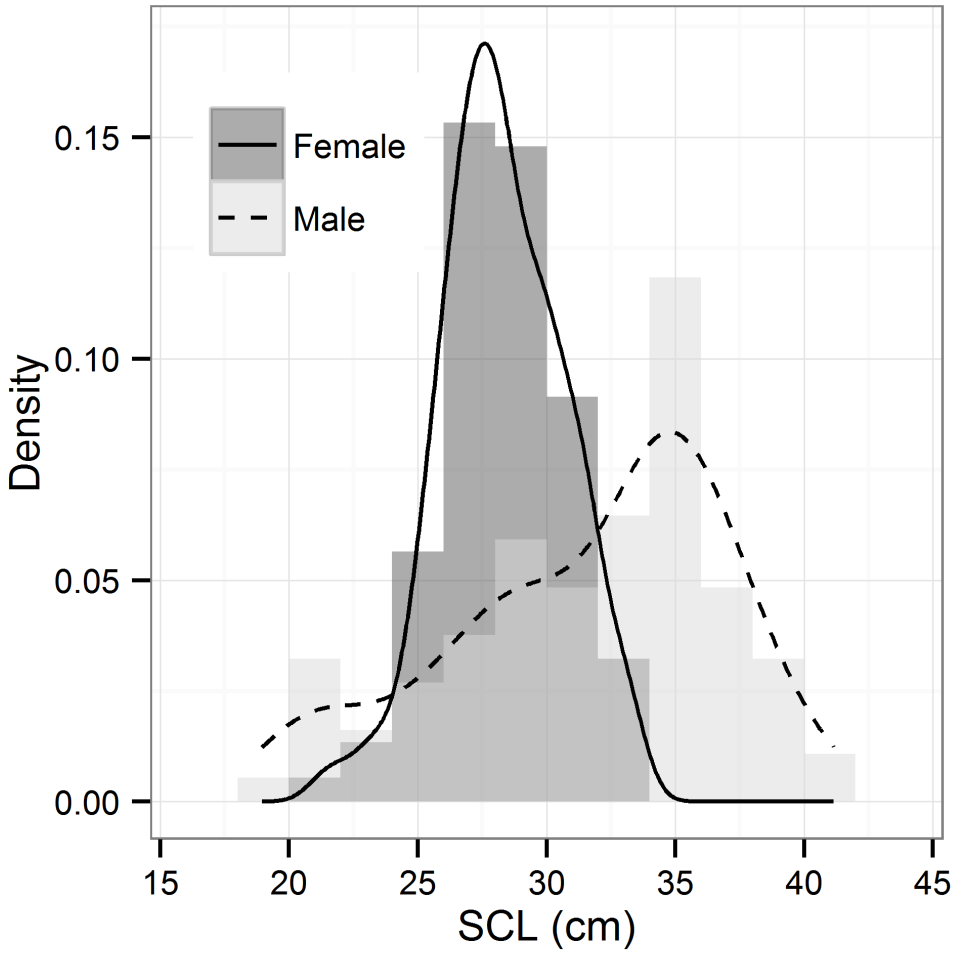

Figure 2.2. Relative frequency histogram and kernel density curves of straight line carapace length (SCL) for male (n= 93) and female (n=186) Snapping Turtles (*Chelydra serpentina*) showing sexual size dimorphism. Observations were made from 2009 to 2013. The median SCL was used for individuals measured more than once. Unsexed juveniles are excluded.

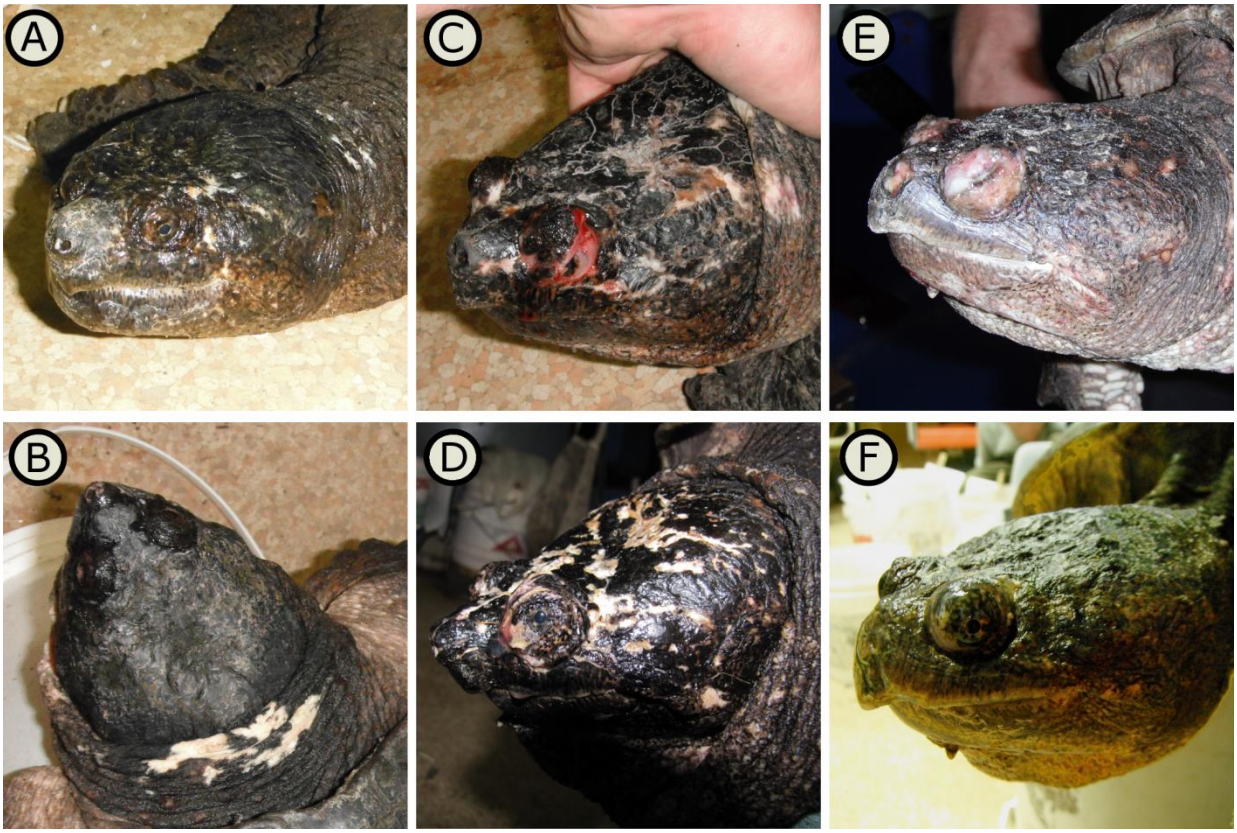

Figure 2.3. Observed putative combat wounds on Snapping Turtles (*Chelydra serpentina*). A. Male Z18, 29 May 2013, SCL = 36.8 cm, with minor potential combat wounds. B. Male A364, 14 Aug. 2011, SCL = 35.85, with white scarring on nape which was a commonly observed injury. C. Male 742, 15 July 2010, SCL = 34.0 cm, with more severe wounds including eyelid damage. Although he did not permanently lose vision, observations like these indicate that combat among Snapping Turtles has potentially permanent fitness consequences. D. Male 943, 30 May 2013, SCL = 38.5 cm. Note the inflamed left eye. E. Female 162, 13 June 2010, SCL = 27.0 cm. She is the only female that had severe injuries; other females had no wounds or minor wounds. F. Female 162 one year later (27 May 2011) showing healing progression; her wounds no longer appear fresh.

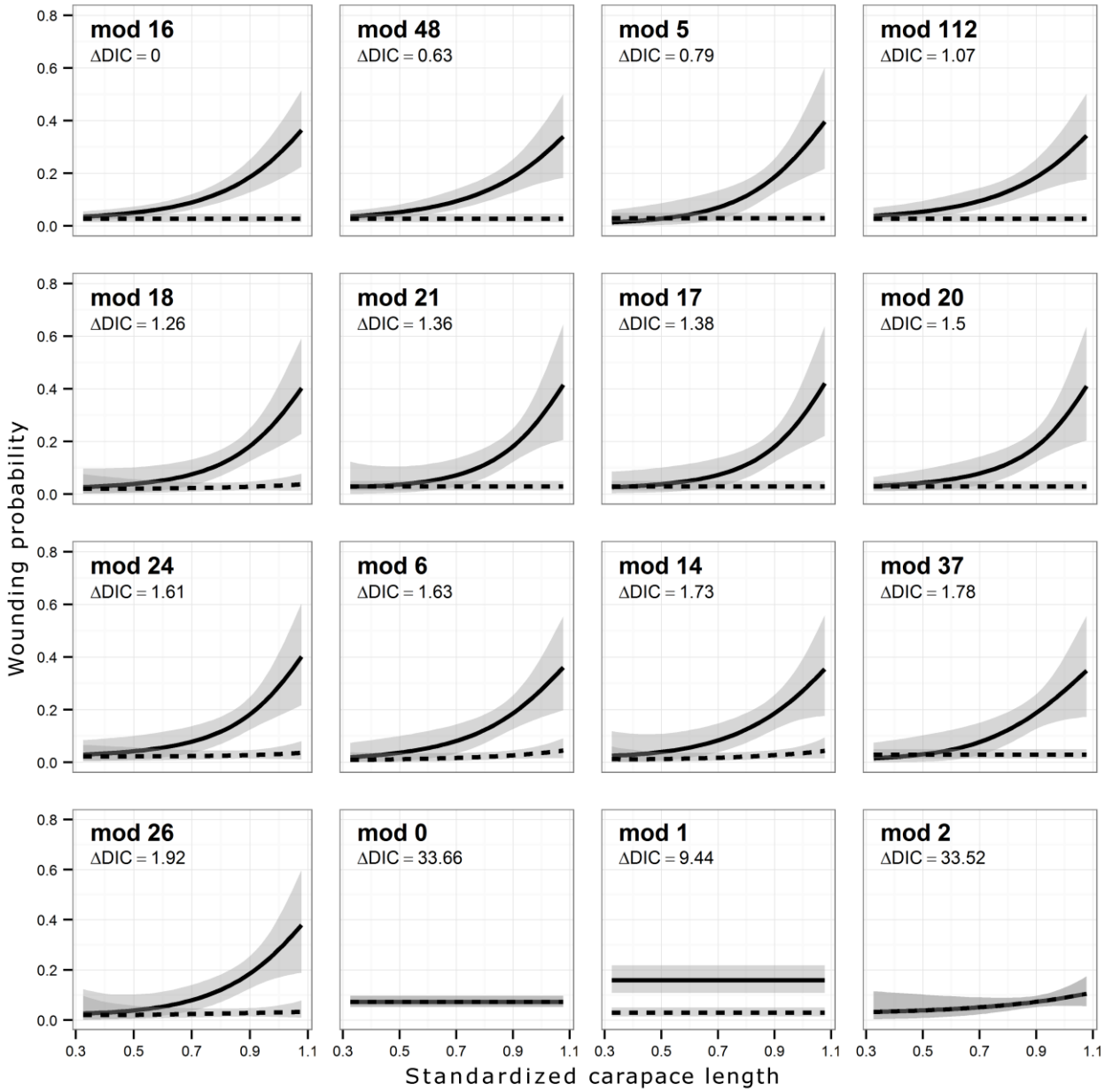

Figure 2.4. The 13 most supported models (ΔDIC < 2) of wounding probability in Snapping Turtles (*Chelydra serpentina*). Also shown are three simple but poorly supported models (models 0, 1, 2, ΔDIC >> 2). Solid lines denote males, dashed lines denote females. Standardized carapace length (x axis) is straight line carapace length as a proportion of mean maximum size (males 38.19 cm, females 30.96 cm). Model formulas and parameter estimates are given in Table 2.3.

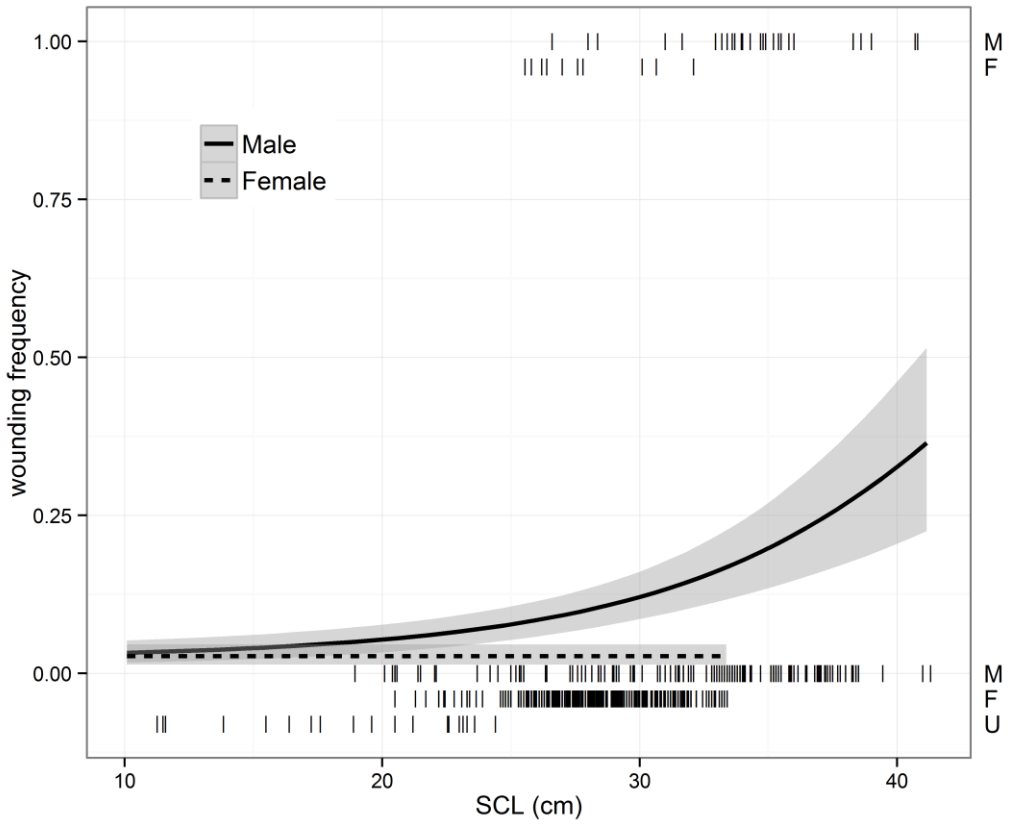

Figure 2.5. Combat wound frequency vs. sex and straight-line carapace length in Snapping Turtles (*Chelydra serpentina*). Individual observations are shown with "|" symbols. Males (marked M on the right axis) are plotted at 0 (not wounded) or 1 (wounded). Observations of females (F) and juveniles of uncertain sex (U) are adjusted downwards for visibility. The fit and 95% CRI (shaded regions) of the model receiving the most support assessed by DIC (model 16, see Table 2.3) are shown transformed to absolute size. Models were fit to sex and carapace length standardized as a proportion of mean maximum size (males 38.19 cm, females 30.96 cm) using Bayesian methods allowing for uncertainty in juvenile sex.

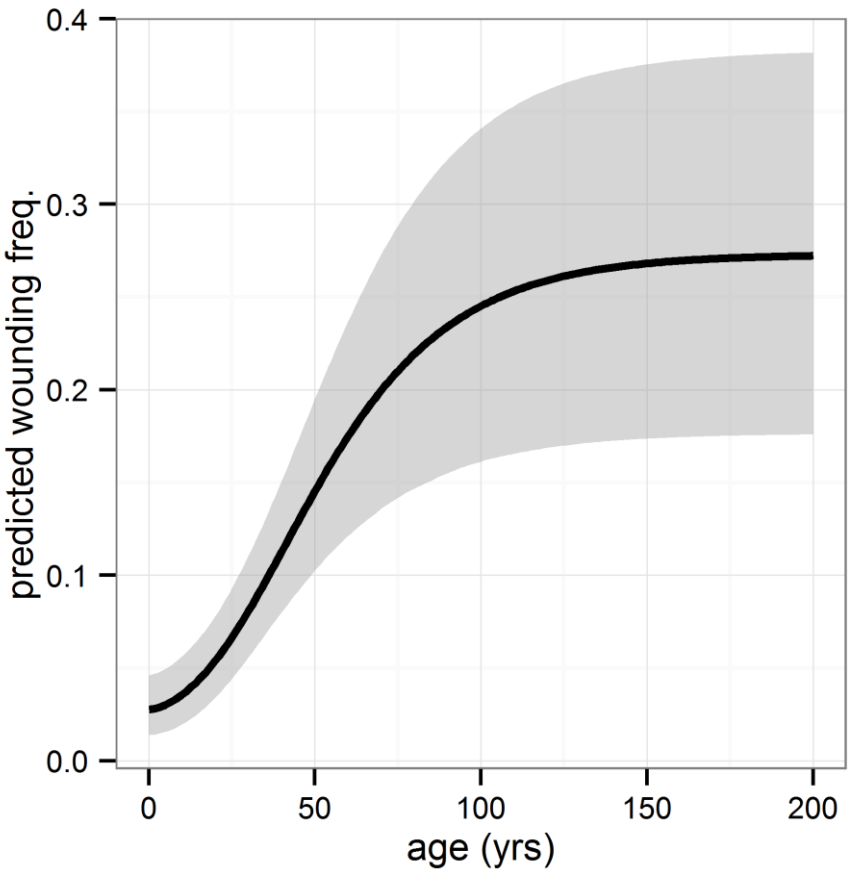

Figure 2.6. Predicted wounding probability projected onto age for a hypothetical, typically growing, male Snapping Turtle (*Chelydra serpentina*) in Algonquin Provincial Park. Age was related to size using mean parameter values of the preferred von Bertalanffy growth model estimated for males in this population by Armstrong and Brooks (2013). Wounding probability vs. size was estimated using our most supported model (model 16), $a+size^2*sex$ (see text). Shading marks the 95% CRI of wounding probabilities, ignoring uncertainty in growth model parameters.

Chapter 3

A model of seasonal variation in somatic growth rates applied to two temperate turtle species.

Published as:

Keevil, M.G., Armstrong, D.P., Brooks, R.J., Litzgus, J.D., 2021. A model of seasonal variation in somatic growth rates applied to two temperate turtle species. Ecol. Modell. 443, 109454. https://doi.org/10.1016/j.ecolmodel.2021.109454

Abstract

Modelling somatic growth of animals whose growth rates are seasonally variable is a challenge. Seasonal variation in growth reduces model fit and precision if not accounted for, and *ad hoc* adjustments to growth models may be biased or biologically unrealistic. We developed a growth phenology model (GPM) that uses a logistic function to model the cumulative proportion of total annual growth. We applied this model using two different approaches to datasets from temperate-climate populations of two freshwater turtle species that experience extended winter dormancy during which no growth occurs. The first dataset consisted of repeated intra-annual observations of sub-adult Snapping Turtles (*Chelydra serpentina*) tracked by radio telemetry, which we analyzed in a Bayesian context, focusing on growth over a single season. We then demonstrated a *post hoc* combination of the fitted GPM with a separate overall growth model. For the second application, we fully integrated the GPM into a hierarchical von Bertalanffy growth model, which we applied to a dataset of primarily inter-annual observations of juvenile Midland Painted Turtles (*Chrysemys picta marginata*). Specifying informative priors allowed us to fit the model despite the sparseness of intra-annual information in the data. We also demonstrate using the beta cumulative distribution function as an alternative to the logistic function in the GPM. We discuss incorporating prior knowledge about seasonal foraging and activity periods into growth models via a GPM as a transparent alternative to deterministic, implicit, *a priori* constructs.

Introduction

Somatic growth is influenced by environmental conditions (e.g., Kielbassa et al., 2010; Marchand et al., 2018; Ramirez et al., 2020) and growth interacts dynamically with other evolved aspects of life history such as size and age at maturity, survival, and fecundity (e.g., Armstrong et al., 2018; Congdon et al., 2018; Shine and Iverson, 1995). The link between growth and population vital

rates means that somatic growth models are critical for parameterizing many applied population models such as integral projection models (Rose et al., 2019) and allometric models (Hatch, 2019). Tests of life-history and ecological hypotheses may therefore depend on accurate estimation of growth model parameters (e.g., Bulté and Blouin-Demers, 2009; Hatch et al., 2019) or among-individual variation in growth rates (Armstrong et al., 2018; Bjorndal et al., 2019; Congdon et al., 2018).

Under standard growth models, the predicted growth of an animal over a time interval depends only on the animal's current size and the duration of the interval (Wang and Jackson, 2000). However, growth will also depend on the environmental conditions over the interval, and these are expected to vary seasonally. Therefore, modelling somatic growth in long-lived ectotherms is a challenge when growth rates are seasonally variable. Failure to account for seasonal variation in growth reduces model fit and precision (Lindeman, 1997; Spence and Turtle, 2017), seasonal biases in observation interval duration can result in biased growth estimates (Schmid, 1995), and *ad hoc* adjustments to growth models may be biologically unrealistic (Figure 3.1). Some authors resort to discarding a subset of data to avoid discrepancies due to unmodelled seasonal differences among observations (Bjorndal et al., 2013; Chessman, 2018; Krueger et al., 2011; Samson, 2003; Seminoff et al., 2002).

Approaches to handling seasonal variation can include: i) modelling growth as a function of a measured environmental covariate, such as temperature, which is integrated into the growth function itself (e.g., Arnall et al., 2019; Kielbassa et al., 2010) or indirectly by defining growing-degree-days (e.g., Snover et al., 2015), or: ii) seasonality can be handled by using a model of annual growth phenology. Within the latter general approach, specific strategies include (Figure 3.1):

- Ignore-as-error: Within-season growth rate variability is relegated to the residual error term along with other unmodelled sources of variation (e.g., Armstrong and Brooks, 2013; Bernstein et al., 2018; Caillouet et al., 2011; Lewis et al., 2018; Rose et al., 2018).
- Restricted sample period: Use only observations collected during a brief, consistent annual period (e.g., Moldowan et al., 2015; Samson, 2003) or specifically analyze recapture intervals with approximately integer year time differences (e.g., Braun-McNeill et al., 2008; Chessman, 2018).
- Implicit seasonal model: Use ancillary information to estimate the active season during which growth is assumed to be uniform (e.g., Bulté and Blouin-Demers, 2009; Litzgus and Brooks, 1998; Maida et al., 2018; Marchand et al., 2018; Wilkinson et al., 2016).
- Oscillating model: Modify the growth model by including an oscillating (sine) function (e.g., Koch et al., 2007; Ogle, 2017; Pitcher and Macdonald, 1973; Somers, 1988; reviewed in Akamine, 2009; also see technical note García-Berthou et al., 2012).

Most herpetological growth models rely on either completely implicit seasonal models or the ignore-as-error approach. In many temperate-climate ectotherm populations, feeding occurs during a limited annual window that may not be equivalent to the duration of the general activity season. An often-unstated assumption is that either the activity season or a narrower annual foraging window is an adequate proxy for the timing and duration of growth. The implicit approach makes the additional assumption that the growth rate is uniform during this period. Implicit models are typically applied by transforming observation dates into a continuous variable defined relative to the start and end of the activity season. This transformation may be implemented during initial data processing so that the implied model and its assumptions are not

usually considered part of a formal growth model. An exception is Smith et al. (2010), who include the start and end points for the non-growing season as explicit parameters, which were estimated using the growth data along with the other growth model parameters.

The use of oscillating functions in growth models is well established in fisheries science, and versions of these models are available in several stock assessment software packages such as `TropFishR` (Mildenberger et al., 2017) and `fishmethods` (Nelson, 2018). Typically, oscillating growth functions do not accommodate prolonged periods of zero growth, and fitting them to such data can result in apparent negative growth (size decreases) at certain times of year (Pauly et al., 1992). However, models adding a No Growth Time term to prevent this have been developed (Ogle, 2017; Pauly et al., 1992; Wang and Jackson, 2000). Lindeman (1997) simply rescaled the time term to exclude the winter period before fitting an oscillating model to produce a non-linear implicit model of growth in juvenile Painted Turtles (*Chrysemys picta*).

Here, we present a simple, flexible, conceptual framework for combining a model of lifetime somatic growth, such as the von Bertalanffy (vB), with a model of the seasonal timing of growth (growth phenology model (GPM)). This approach allows more precise modelling of seasonally variable growth by explicitly incorporating the timing of seasonal changes in growth rate, including prolonged dormant periods without growth, fitted to the observed data. We also demonstrate a strategy for specifying biologically meaningful priors on seasonal component parameters. We first develop and illustrate a logistic GPM, focusing only on growth within a single season, in the context of repeated intra-annual observations of juvenile Snapping Turtles (*Chelydra serpentina*). We then construct a model of growth over multiple years by fitting a combined GPM and vB model to a dataset of primarily inter-annual mark recapture observations of Midland Painted Turtles (*Chrysemys picta marginata*).

Study site and species

Both our snapping and Painted Turtle datasets were collected during long-term field studies carried out from the Algonquin Wildlife Research Station (WRS) in the western highlands of Algonquin Provincial Park, Ontario, Canada. Details of the field sites and methods are described elsewhere (Painted Turtles: Schwarzkopf and Brooks, 1985; Hughes and Brooks, 2006; Samson, 2003; Snapping Turtles: Obbard and Brooks, 1981; Brown et al., 1994; Keevil et al., 2018). Focal sites include nesting areas, wetlands, streams, and lakes in and around the WRS property and at the Arowhon study area 15 km to the west. Aquatic habitats are dystrophic or oligotrophic, often beaver regulated, and shallow areas have abundant floating vegetation and coarse woody debris. The study area has a cool regional climate with a frost-free season of approximately 110 days (Environment and Climate Change Canada, 2020). For both species, most activity occurs between early May and mid-September (Lefevre and Brooks, 1995; Obbard and Brooks, 1981; Rollinson and Brooks, 2007).

Algonquin Park female Snapping Turtles lay one clutch of eggs per year once they reach 24 cm carapace length at approximately 15 to 20 years of age (YOA) (Armstrong and Brooks, 2013; Galbraith et al., 1989; Keevil et al., 2018). Median male Snapping Turtles are 1.2 × longer and 1.8 × heavier than median females despite males initially reaching sexual maturity earlier and at a smaller size (Keevil et al., 2017). In contrast, Painted Turtles have female-biased size dimorphism. In Algonquin Park, male Painted Turtles mature at 7 to 10 YOA at a plastron length typically > 8.5 cm (Samson, 2003). Females reach maturity at an average plastron length of 13 cm between 12 and 15 YOA after which they nest approximately annually with 10 to 30% of individuals also producing a second clutch (Rollinson and Brooks, 2007; Samson, 2003). The peak of nesting for both species occurs in mid-June and the midpoint date of hatching is

approximately 15 September (Riley et al., 2014). Painted Turtle hatchlings often remain in the nest cavity after hatching to emerge in the spring (Riley et al., 2014).

A logistic growth phenology model (GPM)

In temperate-climate turtles, growth in body length within a single season has rarely been quantified but there is evidence that it may be approximately sigmoidal (Ernst, 1971; Keller et al., 1997; Lindeman, 1999, 1997; Sexton, 1965). Following Lindeman (1997), we used a logistic function (Eq. (B.1)) to model seasonal growth:

$$\Delta L_{i,j} = \frac{a_i}{1 + \exp(g^{-1}(B - s_{i,j}))} + \epsilon_{i,j} \qquad (1)$$

where $\Delta L_{i,j}$ is the change in length relative to the first measurement of the season for observation j of individual i, and $s_{i,j}$ is the fraction of the year elapsed by observation j of individual i. B, g, and a_i are parameters of the logistic function to be estimated: B is the inflection point (the fraction of the year when half the growth has occurred) and g is the logistic rate parameter that determines how quickly growth occurs. a_i is the total increase in length over the growing season relative to the initial size of individual i, so that a_i is a property of individuals rather than seasonal variation in growth rate. $\epsilon_{i,j} \sim \mathcal{N}(0,\ {\sigma_e}^2)$ is the normally distributed residual error.

Fitting the logistic GPM to seasonal growth of Snapping Turtles

We analyzed within-season growth using previously unpublished observations of juvenile and young adult Snapping Turtles tracked by VHF radio telemetry during 2013 and 2014. Snapping Turtles were captured in May from canoe by hand or dip net, in baited hoop traps, or by hand during terrestrial movements as part of sampling for the long-term Algonquin Park snapping and Painted Turtle life-history projects. Turtles were fitted with model A2480 (3.6 g) or Model

R1920 (16 g) transmitters (Advanced Telemetry Systems (ATS), Isanti, Minnesota, USA) depending on turtle size. Transmitters were attached using epoxy to the posterior-lateral portion of the carapace and the transmitter and glue combined to weigh less than 5% of body mass in all cases. Five radio-tracked adults that did not show appreciable growth were excluded from the analysis. One juvenile was excluded because it was removed for successful veterinary treatment of a suspected infection at the transmitter attachment site. The remaining 11 Snapping Turtles (carapace length (CL) range: 11.09 – 29.65 cm) were radio-located on foot or from canoe once every 14 days (mean) from May through August and once more in mid-September (2013) or early October (2014). Turtles were initially captured in or adjacent to seven different water bodies and most movements were within contiguous habitat patches. However, two individuals were initially captured during overland movements and one moved again to another water body during the active season. Three individuals transitioned to small adjacent wetlands in late August prior to hibernation. When feasible, turtles were recaptured from canoe, by wading, or by snorkelling, and straight midline CL was measured using Vernier calipers to the nearest 0.1 mm. Snapping Turtles were often unavailable for capture due to their frequent retreat to inaccessible habitat features such as beaver lodges, bank burrows, or areas under floating bog mats. We measured size on 52 of 90 observation occasions, including initial capture. We only analyzed data from one field season for each individual.

We parameterized the data as within-season growth by subtracting the first measurement of the season for each individual from subsequent measurements. First measurements were taken between 6 May and 31 May. Because we could not assume that no growth occurred before then, we modified Eq.(1) by adding a second term to account for missed growth:

$$\Delta L_{i,j} = \frac{a_i}{1 + \exp(g^{-1}(B - s_{i,j}))} - \frac{a_i}{1 + \exp(g^{-1}(B - s_{i,1}))} + \epsilon_{i,j}$$

In the JAGS model (described below), we expressed this using the equivalent formulation:

$$\begin{aligned} \Delta L_{i,j} &\sim \mathcal{N}(\mu_{\Delta_{i,j}}, {\sigma_e}^2) \\ \mu_{\Delta_{i,j}} &= \frac{a_i}{1 + \exp(g^{-1}(B - s_{i,j}))} - \frac{a_i}{1 + \exp(g^{-1}(B - s_{i,1}))} \end{aligned} \qquad (2)$$

Bayesian analysis of the logistic GPM with intra-annual data

We fitted the GPM using the Bayesian updating software JAGS version 4.2.0 (Plummer, 2003) implemented in R version 4.0.2 (R Development Core Team, 2018) using the R2jags package version 0.6-1 (Su and Yajima, 2014). We specified a_i as a fixed effect of individual i and B and g as single, population-level parameters. Additionally, we constructed a model with B_i and g_i as individually varying random effects (Appendix B), but this more complex model was not an improvement as judged by DIC (deviance information criterion; Spiegelhalter et al., 2002). A similar model can be fitted using maximum likelihood, for example by using the R package `nlme`; however, Bayesian fitting is advantageous here because it allows for informative priors to be specified based on common-sense biological and climatic constraints. Informative priors can improve precision of the posterior parameter estimates, especially when the sample size is small (e.g., Link and Barker, 2010).

Informative priors often take the form of a PERT (program evaluation and review technique) distribution (Malcolm et al., 1959), which is a beta distribution fitted to data elicited from experts on the most likely value and minimum and maximum constraints (Vose, 2000). Snapping Turtles in Algonquin Park are typically active from early May through September, with foraging occurring between late May and the end of August (Obbard and Brooks, 1981). Mean temperatures in the study area peak in mid-July (Environment and Climate Change Canada,

2020). We used this information to formulate a prior for parameter B, which corresponds to the midpoint and maximum rate of increase of the logistic function, by specifying a PERT distribution with a minimum of 15 May, a most likely value (mode) of 15 July, and maximum of 1 September, which is $B \sim PERT(0.37,\ 0.54,\ 0.67)$ on the year fraction scale.

To specify a biologically interpretable prior on parameter g, we noted that the logistic function is also the cumulative distribution function (CDF) for the logistic probability distribution, which in turn has quantile function: $\mathrm{Q}(p) = B + g \cdot \ln(p/(1-p))$ where p is the probability. The quantile function enabled us to conceptualize g in terms of the proportion of growth accumulating within a time frame. We proposed that accruing 90% of annual growth in only three weeks (21 days) would be a conservative upper limit on growth rate relative to the length of the active season, which is *ca.* 5 months (Obbard and Brooks, 1981). Therefore, $\Delta s = 21 \text{ days} = 0.0575 \text{ yr} = \mathrm{Q}(p_2 = 0.95) - \mathrm{Q}(p_1 = 0.05))$ and solving for g reveals that B cancels out and:

$$\begin{aligned} g &= \Delta s/(\ln(p_2/(1-p_2)) - \ln(p_1/(1-p_1))) \qquad (3) \\ &= (21/365.2422)/(\ln(0.95/(1-0.95) - \ln(0.05/(1-0.05))) \\ &= 0.0098 \end{aligned}$$

We used Eq.(3) to determine that when $g = 0.085$ it would take six months to complete 90% of growth, which we took as a conservative constraint on the minimum growth rate. We proposed a most likely value of $g = 0.043$, corresponding to the 76 days between 31 May and 15 August, resulting in the prior $g \sim PERT(0.0098,\ 0.043,\ 0.085)$.

We treated the individually varying annual increment parameter a_i as a fixed effect with prior $a_i \sim U(0,\ 5)$ to constrain mean annual growth between 0 and 5 cm (95% of growth trajectories are not expected to exceed *ca.* 3 cm/year (Armstrong and Brooks, 2013)). Individual growth was

highly variable in part because individuals varied in sex and starting size. We could have implemented a more informative prior along with a random effects data structure based on the model of Armstrong and Brooks (2013), but the present procedure is more generalizable to the typical case where a detailed population-specific growth model has not yet been implemented.

The directed acyclic graph of the model structure is shown in Figure 3.2A. We ran three MCMC (Markov Chain Monte Carlo) chains for 110 000 iterations and discarded the first 10 000 as burn-in. We assessed convergence using the Gelman–Rubin diagnostic ($\hat{R} \leq 1.1$; Brooks and Gelman, 1998) and inspection of trace plots of monitored parameters. We performed posterior predictive checking by calculating the sum-of-squares (SSQ) of residuals and comparing these to SSQ of datasets simulated based on the model at each MCMC iteration. We made these comparisons using a Bayesian p-value (P_B) and by visually inspecting the scatterplot (Gelman et al., 2004).

The logistic GPM parameters all showed good convergence and the posterior predictive check indicated adequate fit ($P_B = 0.475$, where values far from 0.5 suggest inadequate fit for the chosen discrepancy measure; Gelman et al., 2004).

The total annual growth, a_i, varied among individuals (range 0.26–1.84 cm; Figure 3.2B). If a_i is factored out, the fitted function describes the *proportion* of the total annual growth predicted to have occurred by time s based on parameters B and g (Table 3.1; Figure 3.2C). Figure 3.3 demonstrates that time can be rescaled to reflect the proportion of annual growth predicted to have occurred by each point in the year.

Based on the estimated parameter means (Table 3.1), 95% of annual growth was accrued by 23 July (Figure 3.2C), which is only 64% of the way through the foraging period (Figure 3.1). This differs markedly from the timing of growth predicted if growth is assumed to be linear over the presumed active or foraging periods (Figure 3.1). Several studies on this and other turtle species have reported reduced foraging activity or reduced growth later in the season despite warm temperatures (Ernst, 1971; Keller et al., 1997; Lindeman, 1997; Obbard and Brooks, 1981; Sexton, 1965). Additionally, food intake at the beginning and end of the active season may be allocated to recovering from, or preparing for, periods of negative energy balance (aphagic periods before, during, and after hibernation) rather than growth (Crawford, 1994; Jackson and Ultsch, 2010).

Adding the logistic GPM to a von Bertalanffy growth function

To this point we have not modelled a within-year effect of body size on growth rate. That is, we assumed that, over a single season, slower growth with increasing size was adequately accommodated by among-individual/year differences in annual growth increment, a_i. This simplification is reasonable as a starting point for Snapping Turtles in Algonquin Park because each growing season comprises only a small fraction of individuals' lifetime growth trajectory (Armstrong and Brooks, 2013). To explicitly integrate the seasonal model into an overall somatic growth model, we conceptualized the logistic GPM as a scaling modification for time. This suggests an intuitive way to incorporate the logistic GPM into a somatic growth model like the von Bertalanffy (vB) model, by including it within the time term. Spence and Turtle (2017) take a similar approach (but without defining a continuous seasonal model) and they point out that the Somers (1988) version of the seasonal vB model can also be conceived this way. A typical formulation of the length-at-age vB model is that of Beverton and Holt (1957):

$$L_{i,j} = L_{\infty}(1 - \exp(-k(t.s_{i,j} - t_0))) \qquad (4)$$

where L_{∞} is the asymptotic size parameter, k is the rate parameter, $t.s_{i,j}$ is age at observation j of individual i, and t_0 is the hypothetical age before birth when length is 0, which we treated as a population-level parameter. In our notation, we used $y.s$ for time variables measured in decimal calendar years and $t.s$ for age measured in decimal years-of-age (Table 3.2).

We symbolized the seasonal logistic GPM as function f(s) applied to year fraction $0 \leq s > 1$ and as function F($y.s$) applied to $y.s$, which includes whole number years (Table 3.2; see Appendix B for derivations). To add the seasonal model, we focused on the time term of Eq.(4), $\Delta t = t.s_{i,j} - t_0$, which we modified to apply the logistic GPM using function F so that the time difference is quantified on the GPM scale. Therefore, an integrated vB and logistic GPM model is:

$$L_{i,j} = L_\infty(1 - \exp(-k[\mathrm{F}(t.s_{i,j} + s_H) - \mathrm{F}(t_0 + s_H)])) \qquad (5)$$

where s_H is year fraction at hatching. We have made the simplifying assumption that all hatching occurs at the same time every year (September 15, which is the middle of the hatching period; Riley et al., 2014), in which case s_H is a population-level parameter. Because each year-of-age begins at s_H instead of 0 on the calendar scale, the function of this parameter is to shift age variables so that a fraction of a year-of-age aligns with fractions of a calendar year before applying the logistic GPM transformation. See Appendix A: Section 2 for details of our derivation.

Figure 3.3C and D show a version of the combined vB and logistic GPM model plotted using different scales, with years the same in both cases but fractions of years represented as either linear age ($t.s$) or as growth phenology age (expected proportion of annual growth accrued), which we denoted as $t.p$ (Eq.(B.9), Table 3.2). Figure 3.3 illustrates that the form and parameters of the overall growth model can be treated independently from the particulars of the GPM.

Incorporating seasonal growth into the interval form of the von Bertalanffy model

The interval parameterization of the vB model (Fabens, 1965) can be written (using notation as in Table 3.2):

$$L_{i,j} = L_\infty - (L_\infty - L_{i,j-1})\exp(-k[y.s_{i,j} - y.s_{i,j-1}]) \qquad (6)$$

This form is also called the recapture parameterization and is used to fit the vB model to recapture data without relying on known age. As we did for the size-at-age vB function, we modified the time terms to incorporate the logistic GPM:

$$L_{i,j} = L_\infty - (L_\infty - L_{i,j-1})\exp(-k[\mathrm{F}(y.s_{i,j}) - \mathrm{F}(y.s_{i,j-1})])$$

which we can express in the *y.p* notation (Table 3.2) signifying the logistic GPM scale:

$$L_{i,j} = L_\infty - (L_\infty - L_{j-1})\exp(-k[y.p_{i,j} - y.p_{i,j-1}]) \qquad (7)$$

Enforcing intercepts

Within our conception of the seasonal model, it is desirable that the proportion of annual growth, p, approaches 0 at the start and 1 at the end of each annual period ($s = 0$ and $s = 1$ respectively). This is approximately satisfied for the fitted logistic model of seasonal growth in Snapping Turtles. However, in some situations, such as a frequentist analysis or Bayesian analysis with more diffuse priors, it is conceivable that the unmodified logistic GPM could produce unanticipated or unrealistic output under certain parameter combinations (Figure B.1). We have applied two approaches to this problem. In Appendix C we replace the logistic function with the beta CDF which is constrained to return values from 0 to 1 over the range [0,1]. This gave very similar results to the approach presented here, which is to rescale the logistic function. Given a

linear proportion of year s, the following modification of the logistic GPM f(s) standardizes the output so that p intersects 0 at the start and 1 at the end of each annual period:

$$\begin{aligned} \mathrm{f}'(s) &= \frac{\mathrm{f}(s) - \mathrm{f}(0)}{\mathrm{f}(1) - \mathrm{f}(0)} \\ &= p \end{aligned} \quad \text{and} \quad \begin{aligned} \mathrm{F}'(y.s) &= y + \mathrm{f}'(s) \\ &= y.p \end{aligned} \tag{8}$$

where function F′ accommodates year fractions (s) combined with whole years (y). The standardized and unstandardized versions of the logistic GPM function are compared in Figure B.1.

Fitting the combined model to Painted Turtle recaptures

For the Snapping Turtle dataset above, we added the seasonal logistic GPM component to an overall growth model after estimating the GPM parameters g and B separately using an ancillary data set. Here we demonstrate fitting the combined model to a primarily inter-annual recapture dataset for a different species of freshwater turtle, Painted Turtles, also living in Algonquin Park. Compared to the vB model without an explicit seasonal component, this comes at the cost of an increase in model complexity due to having to estimate two additional parameters (B and g) in the frequentist framework; however, incorporating prior information can reduce the increase in complexity in Bayesian analysis (Spiegelhalter et al., 2002).

Painted Turtle dataset

The recapture dataset was collected in Algonquin Provincial Park as part of a long-term life-history study. To focus on illustrating the seasonal component, we only included observations of juveniles (L < 8.6 cm) to avoid complicating the model by incorporating effects of sex and

maturity. We excluded unknown-age individuals with only one juvenile observation because these cases were not informative for the model. One pronounced outlier, which had a residual that was more than double the next largest value, was detected after fitting the model. We removed this observation, which was inconsistent with other observations of the same individual, before refitting the model. The remaining data consist of 658 midline plastron length observations of 158 juvenile Painted Turtles collected between 1991 and 2017 with a median interval of 1 year (min = 3 days, max = 3 years). Aquatic sampling for the Painted Turtle project is primarily conducted during the pre-nesting period and focuses on among-year recaptures. As a consequence, of the 658 juvenile observations we analyzed, only 13 were made in the same year as a previous observation of the same individual, and only 44 were made after 31 May. By fitting a seasonal model to these data, we endeavoured to assess whether our approach could be applied in cases without directed within-year sampling.

Juvenile Painted Turtles can be confidently aged using scute rings for a few years after hatching (Brooks et al., 1997; Lindeman, 1997). We incorporated known-age information for 28 individuals whose age could be determined at first capture and for which contemporaneous photographs verifying growth-ring counts were available. We also applied a separate dataset of hatchling observations to estimate variation in size-at-hatch (described below).

Hierarchical von Bertalanffy model

We adapted the Armstrong and Brooks (2013) hierarchical formulation of the vB model, which differs from the conventional vB model (Eq.(4) and (6)) by including among-individual variation in parameter estimates. Armstrong and Brooks (2013) also replaced k_i with k_i/L_{∞_i} which decouples individual variation in growth rate and asymptotic size. Because we did not include adult size observations, among-individual variation in L_{∞_i} was not well estimated (the MCMC

chains for hierarchical mean and SD parameters did not converge in preliminary runs), so we treated L_∞ as a single parameter without individual variation. Incorporating these features along with the logistic GPM into the vB interval formulation (Eq.(7)) results in the model:

$$L_{i,j} = L_\infty - (L_\infty - L_{i,j-1})\exp[-(\frac{k_i}{L_\infty})(y.p_{i,j} - y.p_{i,j-1})] + \epsilon_{i,j}$$

where $k_i \sim \ln\mathcal{N}(\mu_k,\ {\sigma_k}^2)$ is the individually varying rate parameter, $\epsilon_{i,j}$ is the residual error with distribution $\mathcal{N}(0,\ {\sigma_e}^2)$ and $y.p_{i,j} = \mathrm{F}'(y.s_{i,j})$ (Eq.(8)) is time of observation j of individual i adjusted using the standardized logistic GPM function with parameters B and g, which are estimated from the data along with the vB parameters. In the JAGS code we used the equivalent parameterization:

$$\begin{aligned} L_{i,j} &\sim \mathcal{N}(\mu_{L_{i,j}}, {\sigma_e}^2) \\ \mu_{L_{i,j}} &= L_\infty - (L_\infty - L_{i,j-1})\exp[-(\frac{k_i}{L_\infty})(y.p_{i,j} - y.p_{i,j-1})] \end{aligned} \quad (9)$$

Seasonal model parameters

The Painted Turtle activity season is similar in timing to that experienced by Snapping Turtles as both populations occur in Algonquin Park, with foraging occurring primarily between late May and the end of August (Lefevre and Brooks, 1995; Rollinson and Brooks, 2007). We therefore used the same priors $B \sim PERT(0.37,\ 0.54,\ 0.67)$ and $g \sim PERT(0.0098,\ 0.043,\ 0.085)$ for the Painted Turtle data. To assess identifiability and prior sensitivity of the seasonal component parameters, we refitted the model using uniform priors constrained over the same ranges: $B \sim U(0.37,\ 0.67)$ and $g \sim U(0.0098,\ 0.085)$. We did not model individual variation in these parameters because most individuals were not captured more than once per season.

Known-age individuals and hatching size data

For known-age individuals, we used the same interval formulation that we applied to the recapture data (Eq.(9)), with the first observation paired with inferred size and time of hatching to create the first interval. In these cases, $L_{i,j-1} = L_{H_i}$ (unobserved hatching plastron length for individual i) and $y.p_{i,j-1} = \mathrm{F}'(y_H.s_{H_i})$ (time of hatch incorporating the logistic GPM). We assumed a standard hatching date of 15 September ($s_H = 0.706$), which is in the middle of the hatching period. Although Painted Turtle hatchlings often delay emergence from the nest chamber until the following spring, fall emergence is not uncommon in Algonquin Park populations (Riley et al., 2014). Fall and spring emergence episodes are separated by the cold period when significant somatic growth is not expected regardless of overwintering strategy, so we do not anticipate substantial differences in growth rates between strategies.

L_{H_i} was not observed for any of the individuals in our growth dataset, so we assumed that for each individual, L_{H_i} was drawn from a random distribution of hatchling sizes. We used size-at-hatching data from the Algonquin Park study populations (Hughes and Brooks, 2006; Riley et al., 2014; Riley and Litzgus, 2013) to estimate the parameters of the hatchling size distribution. We used a hierarchical model fit to plastron length observations of 632 hatchlings from 140 clutches where the length of hatchling h within in each clutch c is normally distributed around the within-clutch mean as $hL_h \sim \mathcal{N}(\mu_{H_c}, {\sigma_H}^2)$ and clutch means are themselves normally distributed across the population as $\mu_{H_c} \sim \mathcal{N}(\mu_C, {\sigma_C}^2)$. Therefore, applying the law of total variance, we modelled the distribution of L_{H_i} as:

$$L_{H_i} \sim \mathcal{N}(\mu_C, {\sigma_H}^2 + {\sigma_C}^2)$$

Because we used the interval formulation, the vB parameter t_0 is not part of the likelihood and does not need to be estimated during model fitting. However, some form of t_0 is necessary for plotting the length-at-age or length vs. time vB curve. For known-age individuals, we calculated individual $\widetilde{t_{0_i}}$ (t_{0_i} on the GPM transformed age scale) as a derived parameter (Appendix A: Section 3).

Integrated model

We combined the hierarchical vB, hatchling size, and seasonal components into an integrated model. The directed acyclic graph of the model structure is shown in Figure 3.4. We specified uninformative priors for all parameters except B and g in the seasonal component. We ran the model in JAGS to sample 110 000 MCMC draws for each of three chains before discarding 10 000 as burn-in and thinning by 10. We assessed convergence using the Gelman–Rubin diagnostic ($\hat{R} \leq 1.1$; Brooks and Gelman, 1998) and inspection of trace plots of monitored parameters. We performed posterior predictive checking by calculating the sum-of-squares (SSQ) of residuals and comparing these to SSQ of datasets simulated based on the model at each MCMC iteration. We made these comparisons using a Bayesian p-value (P_B) and by visually inspecting the scatterplot (Gelman et al., 2004). We assessed identifiability of the GPM parameters by estimating prior/posterior overlap ($\hat{\tau}$) for B and g (Gimenez et al., 2009; calculated as in Keevil, 2020).

Painted Turtles: fitted model results

Convergence was achieved for all monitored parameters (Table 3.3) and the posterior predictive check indicated adequate fit based on the SSQ discrepancy measure ($P_B = 0.497$). Under the less informative uniform distribution, GPM parameter B was identifiable ($\hat{\tau}_B = 0.224$) while g was

weakly identifiable ($\hat{\tau}_g = 0.368$) based on the the $\tau > 0.35$ threshold of Garrett and Zeger (2000) (Appendix A: Section 4). Weak identifiability suggests that the posterior estimates may be informed substantially by the priors (Garrett and Zeger, 2000; Gimenez et al., 2009); however, the differences in posterior distributions estimated under different prior specifications were negligible (Figure B.2).

The logistic GPM for Painted Turtles (Figure 3.5) was estimated with less precision than the GPM for the intra-annual observations of Snapping Turtles (Figure 3.2C). This is unsurprising because, while the Snapping Turtle dataset consisted of repeated observations of individuals within a growing season, only a small subset of the Painted Turtle observations was informative for the seasonal component because the sampling was primarily annual. Nevertheless, the GPM parameters were at least weakly identifiable even under a less informative uniform prior (Figure B.3).

Our estimate of the length of the 90% growing season, which we defined as the annual interval between 5% and 95% growth accumulation, was substantially longer for Painted Turtles compared to Snapping Turtles (Table 3.4). We interpret this comparison with caution because these estimates were made using somewhat different models applied to data collected at different temporal scales. However, the direction of the difference is consistent with ecological differences between the two species. Painted Turtles bask throughout the open water season to raise their body temperature and metabolic rate (Edwards and Blouin-Demers, 2007; Rollinson et al., 2008; Rowe et al., 2017). Aerial basking by Snapping Turtles is comparatively infrequent (albeit more common in Algonquin Park than at warmer sites; Obbard and Brooks, 1979) and Snapping Turtles often choose microhabitats that are cooler than the available maximum environmental temperatures (Brown et al., 1990; Rowe et al., 2020). In Michigan, Rowe et al. (2020, 2017) found that Snapping Turtles were less precise thermoregulators and that Painted Turtles maintained higher rates of thermal exploitation over a greater proportion of the active season. The between-species difference in the onset of growth, quantified as 5% accumulated growth (Table 3.4), was a substantial component of the difference in overall growing season length that we

estimated. Although male Snapping Turtles in Algonquin Park are very active in May while seeking mating opportunities, females are significantly less active in May than in June, July, and August (Brown and Brooks, 1993), which is consistent with a late onset of feeding and growth that we inferred for Snapping Turtles. In general, if these differences in activity and thermal ecology are reflected in the timing of feeding, assimilation, and growth, then they are congruent with the phenological differences implied by our fitted models.

Advantages of a Bayesian GPM approach

The integrated seasonal vB model is plotted for an example individual Painted Turtle with two observations in 2013 (Figure 3.6). On the standard time scale, an observation made on 18 August 2013 is plotted near an earlier observation made 02 May in the same year (Figure 3.6A), but on the GPM-corrected scale, the August observation is much closer to the third observation made on 12 May of the following spring (Figure 3.6B). This example illustrates the seasonality correction provided by the logistic GPM component. The horizontal error bars on observations in Figure 3.6B indicate the quantification and propagation of uncertainty around the effect of season on growth (i.e., growth phenology), providing an advantage over implicit models, which may afford some ability to correct for seasonality, but cannot account for uncertainty in phenology.

Relative to the common approaches to handle seasonal growth rate variation identified in the Introduction (ignore-as-error, implicit, oscillating/sine, etc.), using the logistic GPM to model seasonal variation in somatic growth has benefits that include:

- Quantification and propagation of uncertainty in growth phenology to somatic growth models.

- Biological realism due to gradual increase and decrease in growth rate at the beginning and end of the growing season.
- Accommodation of prolonged winter dormancy without appreciable growth.
- Incorporation of commonly available basic ancillary information about timing and duration of the active/foraging season (in the Bayesian context).
- Does not require additional environmental covariates.
- Can be fitted to data with few intra-annual observations given sufficiently informative Bayesian priors.
- Timing and rate of growth are fit to data rather than being fixed before analysis.

Although some of these features are present, or can be added, in some of the alternative approaches, the logistic GPM (or the beta GPM) has the advantage of including them all within a fairly simple two-parameter model. The informative priors for the GPM parameters relied only on ancillary information about growth season duration because this type of information is frequently available and is already commonly used for implicit seasonal models in growth studies.

Many ecologists avoid incorporating prior information, especially when doing so may directly impact conclusions about focal hypotheses, preferring instead to use vague priors or purely likelihood-based methods (Banner et al., 2020). However, for many applications of somatic growth models, seasonal variation in growth rate is not a theoretical focus; instead, the focus may be on estimating life-history parameters or assessing effects of site or phenotype on growth over multiple years. In this context, growth phenology can be thought of as a nuisance component that,

nevertheless, must be modelled to understand the overall growth process. Furthermore, many applications already rely implicitly on prior information by defining growth time based on values chosen for the start and end of the growing season. These implicit models further assume that growth is uniform within these rigid bounds. We propose that formally including prior information into an explicit seasonal model such as the logistic GPM is a better approach because it is more transparent, allows the observed data to influence the seasonal component, and quantifies uncertainty and propagates it to the rest of the model.

Conclusions

Our analysis of within-year Snapping Turtle growth indicated that the phenology of somatic growth in our study population differed substantially from the phenology inferred from the activity season, which suggests that activity season delineations may not adequately characterize the somatic growth period. This illustrates an advantage of our approach, which allows observed data to influence the model of seasonal variation in growth rather than fixing it *a priori* as in implicit models. Our application of the logistic GPM to inter-annual observations of Painted Turtle growth demonstrates integration of the seasonal model with an overall somatic growth model, and illustrates that such a model can be fitted in the context of sparse seasonal growth data if prior information is included.

Potential extensions

Our application of the logistic GPM is flexible, facilitating extensions to other situations. One possibility is to apply our logistic GPM component to growth functions other than the vB model. We do not anticipate any barrier to applying the GPM to the age or time interval term of somatic growth models such as Richards, Gompertz, or Schnute. A second possible extension is to replace the logistic function with a different cumulative proportion function in the GPM. We

illustrate this using the beta CDF in Appendix C. Another possibility is the inverse probit function, which also has two parameters to estimate and would behave similarly to the logistic function but with a slightly more abrupt increase and decrease. Because the probit is the corresponding quantile function, the probit function can be applied to determine prior constraints based on proportions of the growth period, as we did for the logistic and beta distributions. Distributions with other features such as asymmetry (e.g., Gompertz, beta, Kumaraswamy) or flexible tails (e.g., the t-distribution) could also be used, although these typically require estimation of more than two parameters or additional assumptions (Appendix C).

It is important to note that we applied the GPM in the context of northern hemisphere animals with winter dormancy, for which it is reasonable to assume that no growth is occurring at year boundaries (31 December/01 January). This assumption may also apply to species that experience winter cessation of growth in the absence of hibernation, such as some marine turtles (Snover and Hohn, 2004), and species undergoing obligate aestivation during the austral summer (e.g., Western Swamp Turtles, *Pseudemydura umbrina*; Arnall et al., 2019). Other populations, for which calendar year boundaries occur during the active season, could be accommodated by modifying our approach to include a phase-shift constant within the time terms.

References

Akamine, T., 2009. Non-linear and graphical methods for fish stock analysis with statistical modeling. Aqua-BioScience Monogr. 2, 1–45. https://doi.org/10.5047/absm.2009.00203.0001

Armstrong, D.P., Brooks, R.J., 2013. Application of hierarchical biphasic growth models to long-term data for Snapping Turtles. Ecol. Modell. 250, 119–125. https://doi.org/10.1016/j.ecolmodel.2012.10.022

Armstrong, D.P., Keevil, M.G., Rollinson, N., Brooks, R.J., 2018. Subtle individual variation in indeterminate growth leads to major variation in survival and lifetime reproductive output in a long-lived reptile. Funct. Ecol. 32, 752–761. https://doi.org/10.1111/1365-2435.13014

Arnall, S.G., Mitchell, N.J., Kuchling, G., Durell, B., Kooijman, S.A.L.M., Kearney, M.R., 2019. Life in the slow lane? A dynamic energy budget model for the Western Swamp Turtle, *Pseudemydura umbrina*. J. Sea Res. 143, 89–99. https://doi.org/10.1016/j.seares.2018.04.006

Banner, K.M., Irvine, K.M., Rodhouse, T.J., 2020. The use of Bayesian priors in ecology: The good, the bad and the not great. Methods Ecol. Evol. 11, 882–889. https://doi.org/10.1111/2041-210X.13407

Bernstein, N.P., Todd, R.G., Baloch, M.Y., McCollum, S.A., Skorczewski, T., Mickael, K.A., Eastham, J.E.M., 2018. Morphometric models of growth in Ornate Box Turtles (*Terrapene ornata ornata*) as related to growth rings. Chelonian Conserv. Biol. 17, 197–205. https://doi.org/10.2744/CCB-1281.1

Beverton, R.J.H., Holt, S., 1957. On the dynamics of exploited fish populations. Fisheries Investigations (Series 2), vol 19. United Kingdom Ministry of Agriculture and Fisheries, London.

Bjorndal, K.A., Bolten, A.B., Chaloupka, M.Y., 2019. Green Turtle somatic growth dynamics: Distributional regression reveals effects of differential emigration. Mar. Ecol. Prog. Ser. 616, 185–195. https://doi.org/10.3354/meps12946

Bjorndal, K.A., Schroeder, B.A., Foley, A.M., Blair, Witherington, E., Bresette, M., Clark, D., Herren, R.M., Arendt, M.D., Schmid, J.R., Meylan, A.B., Meylan, P.A., Provancha, J.A., Hart, K.M., Lamont, M.M., Carthy, R.R., Bolten, A.B., 2013. Temporal, spatial, and body

size effects on growth rates of Loggerhead Sea Turtles (*Caretta caretta*) in the Northwest Atlantic. Mar. Biol. 160, 2711–2721. https://doi.org/10.1007/s00227-013-2264-y

Braun-McNeill, J., Epperly, S., Avens, L., Snover, M., Taylor, J., 2008. Growth rates of Loggerhead Sea Turtles (*Caretta caretta*) from the western North Atlantic. Herpetol. Conserv. Biol. 3, 273–281.

Brooks, R.J., Krawchuk, M.A., Cameron, S., Koper, N., 1997. Testing the precision and accuracy of age estimation using lines in scutes of *Chelydra serpentina* and *Chrysemys picta*. J. Herpetol. 31, 521–529.

Brooks, S.P., Gelman, A., 1998. General methods for monitoring convergence of iterative simulations. J. Comput. Graph. Stat. 7, 434–455. https://doi.org/10.1080/10618600.1998.10474787

Brown, G.P., Bishop, C.A., Brooks, R.J., 1994. Growth rate, reproductive output, and temperature selection of Snapping Turtles in habitats of different productivities. J. Herpetol. 28, 405–410.

Brown, G.P., Brooks, R.J., 1993. Sexual and seasonal differences in activity in a northern population of Snapping Turtles, *Chelydra serpentina*. Herpetologica 49, 311–318.

Brown, G.P., Brooks, R.J., Layfield, J.A., 1990. Radiotelemetry of body temperatures of free-ranging Snapping Turtles (*Chelydra serpentina*) during summer. Can. J. Zool. 68, 1659–1663. https://doi.org/10.1139/z90-246

Bulté, G., Blouin-Demers, G., 2009. Does sexual bimaturation affect the cost of growth and the operational sex ratio in an extremely size-dimorphic reptile? Ecoscience 16, 175–182. https://doi.org/10.2980/16-2-3243

Caillouet, C.W., Shaver, D.J., Landry, A.M., Owens, D.W., Pritchard, P.C.H., 2011. Kemp's Ridley Sea Turtle (*Lepidochelys kempii*) age at first nesting. Chelonian Conserv. Biol. 10, 288–293. https://doi.org/10.2744/CCB-0836.1

Chessman, B.C., 2018. Slow and unsteady: Growth of the Australian Eastern Long-necked Turtle near the southern end of its natural range. Aust. J. Zool. 66, 77–83. https://doi.org/10.1071/ZO18001

Congdon, J.D., Nagle, R.D., Kinney, O.M., 2018. Front-loading life histories: The enduring influence of juvenile growth on age, size, and reproduction of primiparous female freshwater turtles. Evol. Ecol. Res. 19, 353–364.

Crawford, K.M., 1994. Patterns of energy substrate utilization in overwintering Painted Turtles, *Chrysemys picta*. Comp. Biochem. Physiol. Part A Physiol. 109, 495–502. https://doi.org/10.1016/0300-9629(94)90155-4

Edwards, A.L., Blouin-Demers, G., 2007. Thermoregulation as a function of thermal quality in a northern population of Painted Turtles *Chrysemys picta*. Can. J. Zool. 85, 526–535.

Environment and Climate Change Canada, 2020. Canadian Climate Normals 1981-2010 Station Data. https://climate.weather.gc.ca/climate_normals/index_e.html. Accessed December 2020.

Ernst, C.H., 1971. Growth of the Painted Turtle, *Chrysemys picta*, in southeastern Pennsylvania. Herpetologica 27, 135–141. https://doi.org/10.2307/3891068

Fabens, A.J., 1965. Properties and fitting of the von Bertalanffy growth curve. Growth 29, 265–289.

Galbraith, D.A., Brooks, R.J., Obbard, M.E., 1989. The influence of growth rate on age and body size at maturity in female Snapping Turtles (*Chelydra serpentina*). Copeia 1989, 896–904. https://doi.org/10.2307/1445975

García-Berthou, E., Carmona-Catot, G., Merciai, R., Ogle, D.H., 2012. A technical note on seasonal growth models. Rev. Fish Biol. Fish. 22, 635–640. https://doi.org/10.1007/s11160-012-9262-x

Garrett, E.S., Zeger, S.L., 2000. Latent class model diagnosis. Biometrics 56, 1055–1067. https://doi.org/10.1111/j.0006-341X.2000.01055.x

Gelman, A., Carlin, J.P., Stern, H.S., Runin, D.B., 2004. Bayesian Data Analysis. CRC/Chapman & Hall, Boca Raton, F.L.

Gimenez, O., Morgan, B.J.T., Brooks, S.P., 2009. Weak identifiability in models for mark-recapture-recovery data, in: Thomson, D.L., Cooch, E.G., Conroy, M.J. (Eds.), Modeling Demographic Processes in Marked Populations. Springer, New York, pp. 1055–1067.

Hatch, J.M., Haas, H.L., Richards, P.M., Rose, K.A., 2019. Life-history constraints on maximum population growth for Loggerhead Turtles in the northwest Atlantic. Ecol. Evol. 9, 9442–9452. https://doi.org/10.1002/ece3.5398

Hughes, E.J., Brooks, R.J., 2006. The good mother: Does nest-site selection constitute parental investment in turtles? Can. J. Zool. 84, 1545–1554.

Jackson, D.C., Ultsch, G.R., 2010. Physiology of hibernation under the ice by turtles and frogs. J. Exp. Zool. Part A Ecol. Genet. Physiol. 313A, 311–327. https://doi.org/10.1002/jez.603

Keevil, M.G., 2022. Joint estimation of growth and survival from mark-recapture data to improve estimates of senescence in wild populations: Comment. Ecology 103, e03232. https://doi.org/10.1002/ecy.3232

Keevil, M.G., Brooks, R.J., Litzgus, J.D., 2018. Post-catastrophe patterns of abundance and survival reveal no evidence of population recovery in a long-lived animal. Ecosphere 9, e02396. https://doi.org/10.1002/ecs2.2396

Keevil, M.G., Hewitt, B.S., Brooks, R.J., Litzgus, J.D., 2017. Patterns of intraspecific aggression inferred from injuries in an aquatic turtle with male-biased size dimorphism. Can. J. Zool. 95, 393–403. https://doi.org/10.1139/cjz-2016-0182

Keller, C., Díaz-Paniagua, C., Andreu, A.C., 1997. Post-emergent field activity and growth rates of hatchling Spur-thighed Tortoises, *Testudo graeca*. Can. J. Zool. 75, 1089–1098. https://doi.org/10.1139/z97-131

Kielbassa, J., Delignette-Muller, M.L., Pont, D., Charles, S., 2010. Application of a temperature-dependent von Bertalanffy growth model to Bullhead (*Cottus gobio*). Ecol. Modell. 221, 2475–2481. https://doi.org/10.1016/j.ecolmodel.2010.07.001

Koch, V., Brooks, L.B., Nichols, W.J., 2007. Population ecology of the Green/Black Turtle (*Chelonia mydas*) in Bahía Magdalena, Mexico. Mar. Biol. 153, 35–46. https://doi.org/10.1007/s00227-007-0782-1

Krueger, B.H., Chaloupka, M.Y., Leighton, P.A., Dunn, J.A., Horrocks, J.A., 2011. Somatic growth rates for a Hawksbill Turtle population in coral reef habitat around Barbados. Mar. Ecol. Ser. 432, 269–276. https://doi.org/10.3354/meps09125

Kruschke, J.K., 2015. Doing Bayesian Data Analysis: A Tutorial with R, JAGS, and Stan, 2nd ed. Academic Press/Elsevier, Burlington, MA.

Lefevre, K., Brooks, R.J., 1995. Effects of sex and body size on basking behavior in a northern population of the Painted Turtle, *Chrysemys picta*. Herpetologica 51, 217–224.

Lewis, E.L., Iverson, J.B., Smith, G.R., Rettig, J.E., 2018. Body size and growth in the Red-eared Slider (*Trachemys scripta elegans*) at the northern edge of its range: Does Bergmann's rule apply? Herpetol. Conserv. Biol. 13, 700–710.

Lindeman, P. V, 1999. Growth curves for *Graptemys*, with a comparison to other emydid turtles. Am. Midl. Nat. 142, 141–151. https://doi.org/10.2307/2426900

Lindeman, P. V, 1997. Contributions toward improvement of model fit in nonlinear regression modelling of turtle growth. Herpetologica 53, 179–191.

Link, W.A., Barker, R.J., 2010. Bayesian Inference: with Ecological Applications. Academic Press, Amsterdam.

Litzgus, J.D., Brooks, R.J., 1998. Growth in a cold environment: Body size and sexual maturity in a northern population of Spotted Turtles, *Clemmys guttata*. Can. J. Zool. 76, 773–782.

Maida, J.R., Kirk, D.A., McKibbin, O., Row, J.R., Larsen, K.W., Stringam, C., Bishop, C.A., 2018. Population estimate, survivorship, and generation time of the Northern Pacific Rattlesnake (*Crotalus o. oreganus*) at its northern-most range limits. Herpetol. Conserv. Biol. 13, 662–672.

Malcolm, D.G., Roseboom, J.H., Clark, C.E., Fazar, W., 1959. Application of a technique for research and development program evaluation. Oper. Res. 7, 646–669. https://doi.org/10.1287/opre.7.5.646

Marchand, K.A., Hughes, G.N., Litzgus, J.D., 2018. Geographic variation in somatic growth rate of Wood Turtles (*Glyptemys insculpta*). Copeia 106, 477–484. https://doi.org/10.1643/ch-18-022

Mildenberger, T.K., Taylor, M.H., Wolff, M., 2017. TropFishR: an R package for fisheries analysis with length-frequency data. Methods Ecol. Evol. 8, 1520–1527. https://doi.org/10.1111/2041-210X.12791

Moldowan, P.D., Keevil, M.G., Koper, N., Brooks, R.J., Litzgus, J.D., 2015. Growth, sexual maturity, and reproduction of a female Midland Painted Turtle (*Chrysemys picta marginata*) afflicted with kyphosis. Chelonian Conserv. Biol. 14, 157–160. https://doi.org/10.2744/CCB-1147.1

Nelson, Gary, A., 2018. fishmethods: Fishery Science Methods and Models.

Obbard, M.E., Brooks, R.J., 1981. A radio-telemetry and mark-recapture study of activity in the Common Snapping Turtle, *Chelydra serpentina*. Copeia 1981, 630–637. https://doi.org/http://dx.doi.org/10.2307/1444568

Obbard, M.E., Brooks, R.J., 1979. Factors affecting basking in a northern population of the Common Snapping Turtle *Chelydra serpentina*. Can. J. Zool. 57, 435–440.

Ogle, D.H., 2017. An algorithm for the von Bertalanffy seasonal cessation in growth function of Pauly et al. (1992). Fish. Res. 185, 1–5. https://doi.org/10.1016/j.fishres.2016.09.020

Pauly, D., Soriano-Bartz, M., Mor Eauc, J., Jarre-Teichmann, A., 1992. A new model accounting for seasonal cessation of growth in fishes. Mar. Freshw. Res. 43, 1151–1156. https://doi.org/10.1071/MF9921151

Pitcher, T.J., MacDonald, P.D.M., 1973. Two models for seasonal growth in fishes. J. Appl. Ecol. 10, 599–606. https://doi.org/10.2307/2402304

Plummer, M., 2003. JAGS: a program for analysis of Bayesian graphical models using Gibbs sampling, in: Hornik, K., Leisch, F., Zeileis, A. (Eds.), Proceedings of the 3rd International Workshop on Distributed Statistical Computing (DSC 2003), Vienna, Austria, March 20–22, 2003. Austrian Association for Statistical Computing (AASC) and the R Foundation for Statistical Computing, Vienna, Austria, pp. 1–10.

R Development Core Team, 2020. R: A language and environment for statistical computing.

Ramirez, M.D., Avens, L., Goshe, L.R., Snover, M.L., Cook, M., Heppell, S.S., 2020. Regional variation in Kemp's Ridley Sea Turtle diet composition and its potential relationship with somatic growth. Front. Mar. Sci. 7, 253. https://doi.org/10.3389/fmars.2020.00253

Riley, J.L., Freedberg, S., Litzgus, J.D., 2014. Incubation temperature in the wild influences hatchling phenotype of two freshwater turtle species. Evol. Ecol. Res. 16, 397–416.

Riley, J.L., Litzgus, J.D., 2013. Evaluation of predator-exclusion cages used in turtle conservation: Cost analysis and effects on nest environment and proxies of hatchling fitness. Wildl. Res. 40, 499–511. https://doi.org/10.1071/WR13090

Rollinson, N., Brooks, R.J., 2007. Proximate constraints on reproductive output in a northern population of Painted Turtles: An empirical test of the bet-hedging paradigm. Can. J. Zool. 85, 177–184.

Rollinson, N., Tattersall, G.J., Brooks, R.J., 2008. Overwintering habitats of a northern population of Painted Turtles (*Chrysemys picta*): Winter temperature selection and dissolved oxygen concentrations. J. Herpetol. 42, 312–321. https://doi.org/10.1670/07-1422.1

Rose, J.P., Ersan, J.S.M., Wylie, G.D., Casazza, M.L., Halstead, B.J., 2019. Demographic factors affecting population growth in Giant Gartersnakes. J. Wildl. Manage. 83, 1540–1551. https://doi.org/10.1002/jwmg.21728

Rose, J.P., Halstead, B.J., Wylie, G.D., Casazza, M.L., 2018. Spatial and temporal variability in growth of Giant Gartersnakes: Plasticity, precipitation, and prey. J. Herpetol. 52, 40–49. https://doi.org/10.1670/17-055

Rowe, J.W., Mulligan, W.P., Martin, C.E., Goerge, T.M., Bunce, M.A., 2020. Spatial and thermal ecology of Snapping Turtles (*Chelydra serpentina*) in a small, dystrophic lake in central Michigan. Chelonian Conserv. Biol. 19, 22. https://doi.org/10.2744/CCB-1358.1

Rowe, J.W., Nawrot, M.L., Clark, D.L., 2017. Thermoregulation in a north temperate population of Midland Painted Turtles (*Chrysemys picta marginata*): Temporal patterns and intersexual differences. Copeia 105, 765–780. https://doi.org/10.1643/CP-16-507

Samson, J., 2003. The Life History Strategy of a Northern Population of Midland Painted Turtles, *Chrysemys picta marginata*. (Master's Thesis). University of Guelph.

Schmid, J.R., 1995. Marine turtle populations on the east-central coast of Florida: Results of tagging studies at Cape Canaveral, Florida, 1986-1991. Fish. Bull. 93, 139–151.

Schwarzkopf, L., Brooks, R.J., 1985. Application of operative environmental temperatures to analysis of basking behavior in *Chrysemys picta*. Herpetologica 41, 206–212.

Seminoff, J.A., Resendiz, A., Nichols, W.J., Jones, T.T., 2002. Growth rates of wild Green Turtles (*Chelonia mydas*) at a temperate foraging area in the Gulf of California, México. Copeia 610–617. https://doi.org/10.1643/0045-8511(2002)002[0610:GROWGT]2.0.CO;2

Sexton, O.J., 1965. The annual cycle of growth and shedding in the Midland Painted Turtle, *Chrysemys picta marginata*. Copeia 1965, 314–318. https://doi.org/10.2307/1440793

Shine, R., Iverson, J.B., 1995. Patterns of survival, growth and maturation in turtles. Oikos 72, 343–348. https://doi.org/10.2307/3546119

Smith, J.J., Amarello, M., Goode, M., 2010. Seasonal growth of free-ranging Gila Monsters (*Heloderma suspectum*) in a southern Arizona population. J. Herpetol. 44, 484–488. https://doi.org/10.1670/09-104.1

Snover, M.L., Adams, M.J., Ashton, D.T., Bettaso, J.B., Welsh, H.H., 2015. Evidence of counter-gradient growth in western Pond Turtles (*Actinemys marmorata*) across thermal gradients. Freshw. Biol. 60, 1944–1963. https://doi.org/10.1111/fwb.12623

Snover, M.L., Hohn, A.A., 2004. Validation and interpretation of annual skeletal marks in Loggerhead (*Caretta caretta*) and Kemp's Ridley (*Lepidochelys kempii*) sea turtles. Fish. Bull. 102, 682–692.

Somers, I.F., 1988. On a seasonally oscillating growth function. Fishbyte 6, 8–11.

Spence, M.A., Turtle, A.J., 2017. Making the most of survey data: Incorporating age uncertainty when fitting growth parameters. Ecol. Evol. 7, 7058–7068. https://doi.org/10.1002/ece3.3280

Spiegelhalter, D.J., Best, N.G., Carlin, B.P., Van Der Linde, A., 2002. Bayesian measures of model complexity and fit. J. R. Stat. Soc. Ser. B – Stat. Methodol. 64, 583–639. https://doi.org/http://dx.doi.org/10.1111/1467-9868.00353

Su, Y.-S., Yajima, M., 2014. R2jags: A Package for Running jags from R.

Vose, D., 2000. Risk Analysis: A Quantitative Guide. John Wiley & Sons, Chichester, U.K.

Wang, Y., Jackson, C.J., 2000. Growth curves with time-dependent explanatory variables. Environmetrics 11, 597–605. https://doi.org/10.1002/1099-095X(200009/10)11:5<597::AID-ENV418>3.0.CO;2-I

Wilkinson, P.M., Rainwater, T.R., Woodward, A.R., Leone, E.H., Carter, C., 2016. Determinate growth and reproductive lifespan in the American Alligator (*Alligator mississippiensis*): Evidence from long-term recaptures. Copeia 104, 843–852. https://doi.org/10.1643/ch-16-4

Tables

Table 3.1. Parameters of the logistic growth phenology model fit to intra-annual growth observations of Snapping Turtles in Algonquin Provincial Park in 2013 and 2014. Columns labeled 2.5% and 97.5% show 95% credible intervals.

Parm.	**Description**	**In code**	**Mean**	**SD**	**2.5%**	**Median**	**97.5%**
B	inflection point, median	`B`	0.485	0.005	0.476	0.485	0.495
g	rate/shape parameter	`g`	0.026	0.003	0.019	0.026	0.033
σ_e	SD of residual error	`sigma.e`	0.048	0.006	0.038	0.047	0.061

Table 3.2. Notation and description of time variables and functions and their relationships. Fractions of a calendar year and fractions of a growth year are defined relative to 01 January while fractions of a year of age are defined relative to date of hatching. Therefore, age fractions are phase-shifted relative to calendar-year fractions and this must be accounted for when applying a non-linear transformation such as the logistic GPM (growth phenology model).

Notation	Description	Definition/relationships
Functions		
$\lfloor x \rfloor$	floor function	greatest integer $\leq x$
$\mathrm{f}(s)$	GPM transformation of s^*	$= (1 + \exp(g^{-1}(B - s)))^{-1}$
$\mathrm{F}(y.s)$	GPM transformation of $y.s$ accounting for year y	$= \lfloor y.s \rfloor + \mathrm{f}(y.s - \lfloor y.s \rfloor)$ $= y + \mathrm{f}(s)$
$\mathrm{f}'(s)$	$\mathrm{f}(s)$ with enforced intercepts†	$= (\mathrm{f}(s) - \mathrm{f}(0))/(\mathrm{f}(1) - \mathrm{f}(0))$
$\mathrm{F}'(y.s)$	$\mathrm{F}(y.s)$ with enforced intercepts†	$= y + \mathrm{f}'(s)$
Variables		
$y.s$	decimal calendar year	$= y + s;\ y.s \in \mathbb{R}$
y	integer calendar year	$= \lfloor y.s \rfloor;\ y \in \mathbb{Z}$
s	linear scale year fraction	$= y.s - \lfloor y.s \rfloor;\ 0 \leq s < 1$
p	GPM rescaled year fraction‡	$= \mathrm{f}(s);\ 0 \leq p < 1$
$y.p$	GPM rescaled decimal year‡	$= \mathrm{F}(y.s)$
$t.s$	decimal age (years)	$= y.s - y_H.s_H$
t	integer age (years)	$= \lfloor t.s \rfloor$
$y_H.s_H$	date of hatch (decimal year)	$= y_H + s_H$
s_H	year fraction at date of hatch	$= y_H.s_H - \lfloor y_H.s_H \rfloor$
$t.p$	GPM rescaled age‡	$= \mathrm{F}(t.s + s_H) - \mathrm{F}(s_H)$
t_0	theoretical age at length 0	
$\tilde{t}_0$	GPM scale age at length 0‡	$= \mathrm{F}(t_0 + s_H) - \mathrm{F}(s_H)$

* Applies the GPM logistic function with parameters B and g to be estimated.

† See text for explanation of enforced intercepts.

‡ May also be calculated using GPM modified to enforce intercepts.

Table 3.3. Parameters estimated in the Algonquin Park Painted Turtle hierarchical growth model with seasonal and size-at-hatch components. Posterior parameter distribution statistics are shown for population-level parameters and are omitted for individual- and observation-level parameters. In the descriptions 'hL' denotes length at hatching, 'vB' is the hierarchical von Bertalanffy model, 'GPM' is the logistic growth phenology model, and indices are $\boldsymbol{i}$ = recaptured individual, $\boldsymbol{j}$ = observation of $\boldsymbol{i}$, $\boldsymbol{h}$ = hatchling, and $\boldsymbol{c}$ = clutch. 2.5% and 97.5% are the upper and lower limits of the 95% CRI.

Parm.	Description	In code	Mean	SD	2.5%	Median	97.5%
L_∞	vB asymptote	`Lmax`	12.1	0.428	11.3	12.1	13.0
μ_k	logmean vB rate	`mu.k`	0.727	0.0407	0.646	0.727	0.806
σ_k	logsd vB rate	`sigma.k`	0.154	0.0214	0.112	0.154	0.196
k_i	indiv. vB rate	`k[i]`					
σ_e	SD of residual error	`sigma.e`	0.297	0.0109	0.277	0.297	0.320
$\mu_{L_{i,j}}$	expected length at obs. i,j	`mu[i,j]`					
μ_C	among-clutch mean hL	`mu.c`	2.47	0.0141	2.45	2.47	2.50
σ_C	among-clutch sd of hL	`sigma.c`	0.160	0.0110	0.140	0.159	0.183
μ_{H_c}	mean hL for clutch c	`mu.h[c]`					
σ_H	within-clutch sd of hL	`sigma.h`	0.0882	0.00286	0.0829	0.0881	0.0941
hL_h	observed hL of hatchling h	`hL[h]`					
L_{H_i}	unobserved hL for i	`LH[i]`					
B	GPM inflection point	`B`	0.475	0.0135	0.450	0.475	0.503
g	GPM rate	`g`	0.0469	0.00585	0.0356	0.0468	0.0584
$y.p_{i,j}$	GPM date of i,j	`y.p[i,j]`					
$y_H.p_{H_i}$	GPM date of hatch of i	`yH.pH[i]`					
$\widetilde{t_{0_i}}$	derived GPM age at $L = 0$	`t0.tld[i]`					
mean($\widetilde{t_0}$)	derived mean of $\widetilde{t_0}$	`mean.t0.tld`	-1.33	0.0562	-1.44	-1.33	-1.23
sd($\widetilde{t_0}$)	derived SD of $\widetilde{t_0}$	`sd.t0.tld`	0.221	0.0371	0.154	0.219	0.300

Table 3.4. Phenology of Snapping Turtle and Painted Turtle growth in Algonquin Park as year fraction (**s**) and date-of-year at three levels of accumulated proportion of annual growth (**p**). The logistic GPM seasonal models were fitted to within-year observations of Snapping Turtles and as a seasonal component of a von Bertalanffy model of growth fitted to among-year observations of Painted Turtles. **s** was calculated for each level of **p** at each MCMC iteration using the inverse of the logistic GPM function (Snapping Turtles: Eq.(B.2), Painted Turtles Eq.(B.13)). Values are medians with 95% HDI (highest density intervals).

Cumulative growth		Snapping Turtles		Painted Turtles	
p	%	*s* (95% HDI)	Date* (95% HDI)	*s* (95% HDI)	Date* (95% HDI)
0.05	5%	0.409 (0.383 – 0.433)	29 May (20 May – 07 Jun)	0.337 (0.299 – 0.378)	03 May (19 Apr – 18 May)
0.50	50%	0.485 (0.476 – 0.495)	26 Jun (22 Jun – 29 Jun)	0.475 (0.45 – 0.503)	22 Jun (13 Jun – 02 Jul)
0.95	95%	0.561 (0.544 – 0.58)	23 Jul (17 Jul – 30 Jul)	0.613 (0.569 – 0.661)	11 Aug (26 Jul – 29 Aug)
0.05 to 0.95	5 to 95	0.152† (0.113 – 0.192)	56 days (41 – 70)	0.276† (0.209 – 0.343)	101 days (76 – 125)

* Date during non-leap years

† Duration as a proportion of year

Figures

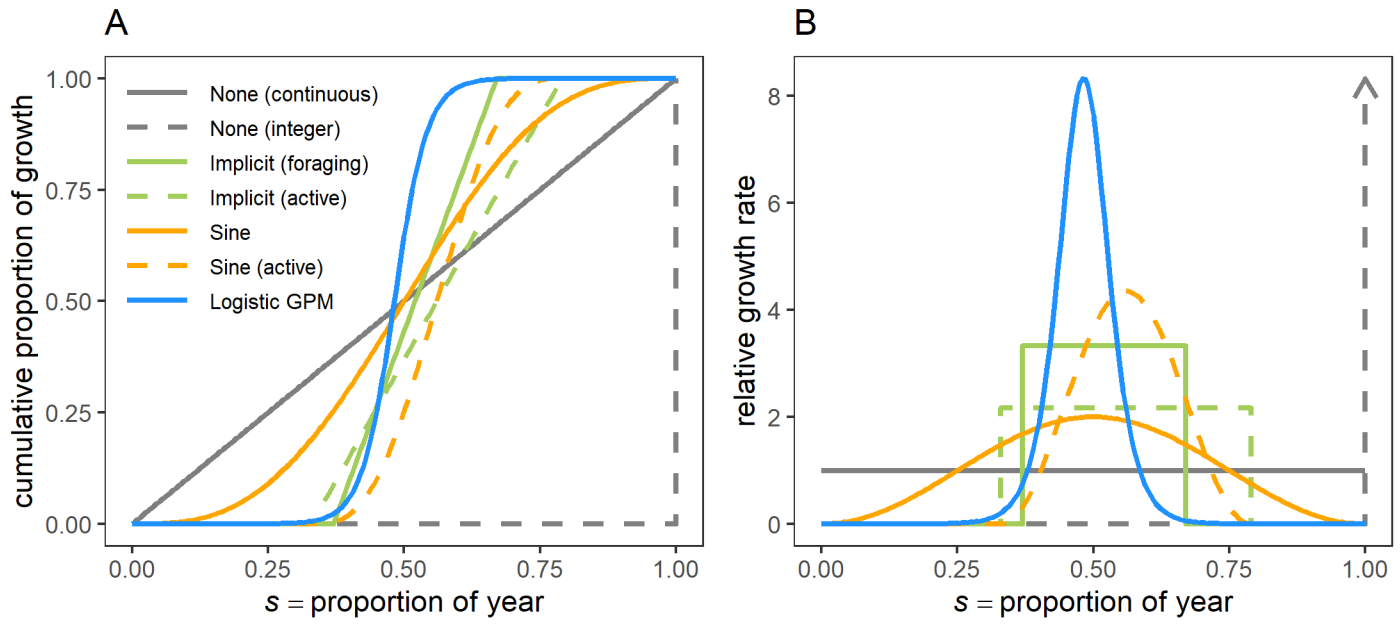

Figure 3.1. Approaches to modelling seasonal variation in growth rate comparing (A) cumulative functions of proportion of annual growth and (B) the corresponding instantaneous rate functions. Non-seasonal model (None) implies that all seasonal growth variation will be ignored-as-error and is plotted for continuous time and for integer years. Implicit models are plotted for foraging and activity periods for Snapping Turtles (Chelydra serpentina) in Algonquin Provincial Park, Ontario (Obbard and Brooks, 1981). Sine models (Somers, 1988) assume no negative growth with a minimum of zero at the start of the annual period of one year or the active season (Lindeman, 1997). This sine model implementation is also implicit because parameters were determined by initial assumptions and time scaling rather than being fitted to growth data. The logistic growth phenology model (GPM) is fitted to intra-annual observations of Snapping Turtles in Algonquin (this study).

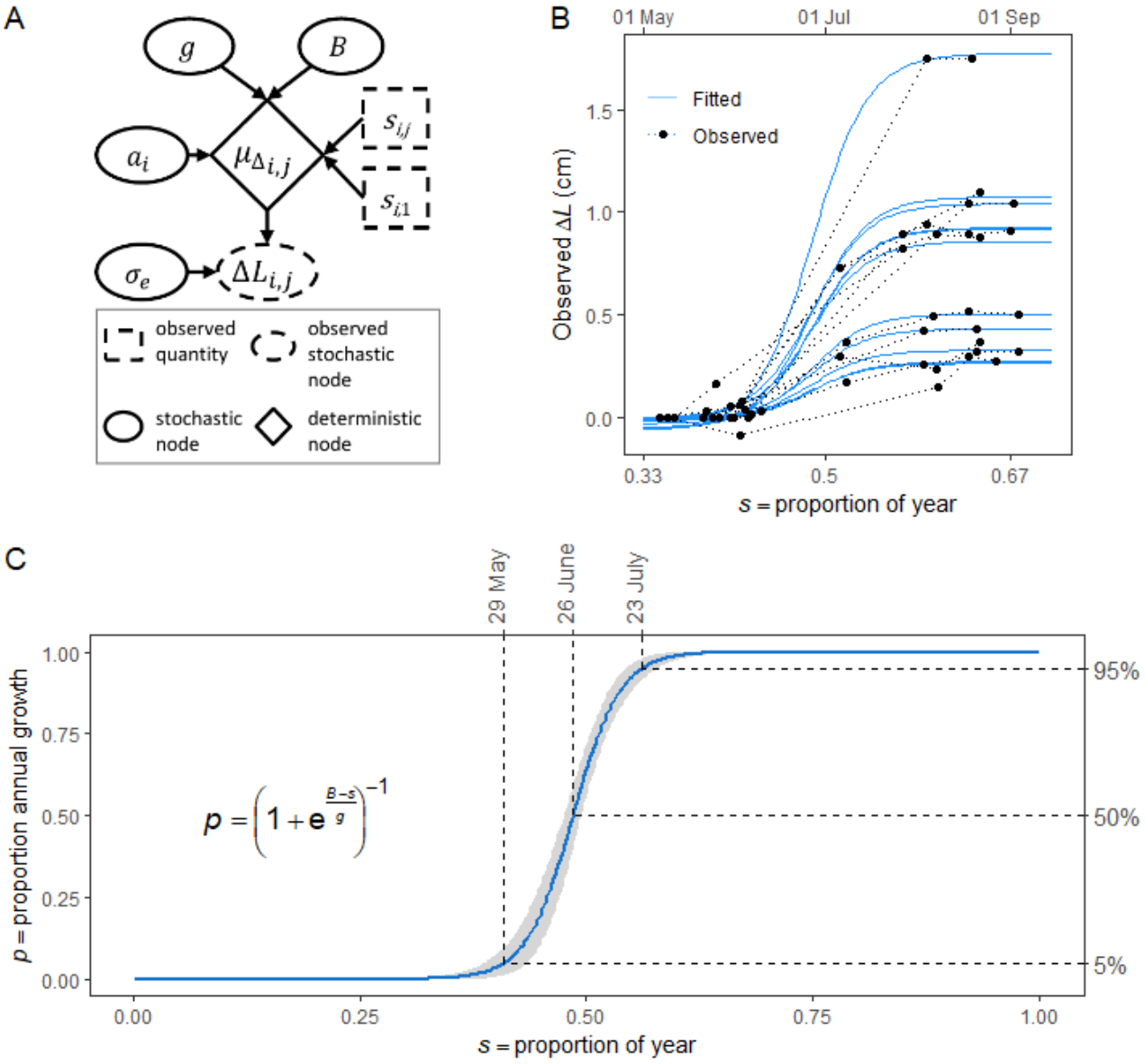

Figure 3.2. (A) Directed acyclic graph of model structure for the logistic growth phenology model (GPM) of intra-annual observations of Snapping Turtles (see Table 3.1 for notation). (B) Individual within-season trajectories of observed growth in midline carapace length (***ΔL***, cm) for 11 Snapping Turtles plotted with fitted curves from the GPM. (C) Shared seasonal component of the GPM as the proportion of annual growth accrued vs. proportion of year. The shaded region indicates the 95% HDI (highest density interval, the narrowest interval containing 95% of the probability density; Kruschke, 2015). In panel B, ***ΔL*** is quantified relative to observed initial size

by subtracting the first measurement of the season for each individual from subsequent observations. Negative apparent growth increments were presumably due to measurement error and were not excluded because measurement error is an expected component of the residual error variance.

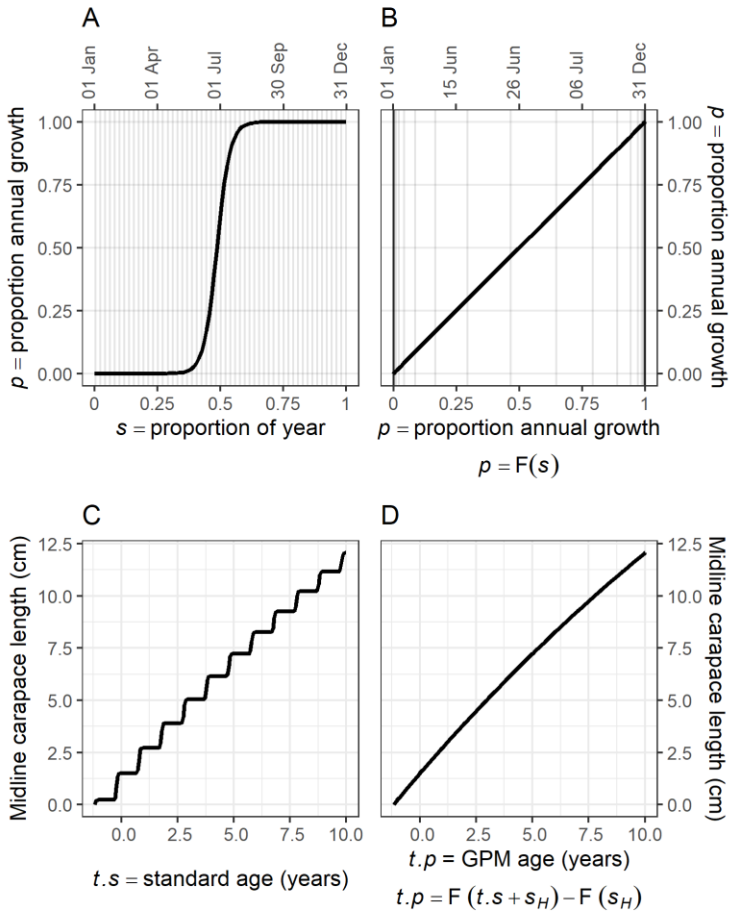

Figure 3.3. Proportion of annual growth p within a year predicted by a logistic GPM (growth phenology model) plotted against proportion of year (A) and against itself (B). The GPM is extended over multiple years as the seasonal component of a von Bertalanffy (vB) model (C), which can be plotted against GPM adjusted age (D). Vertical gridlines are spaced at one-week intervals in panels A and B. Comparing the gridline spacing among A and B illustrates the conceptual shift of the GPM from an estimate of growth to a scaling function for time. The vB component follows Armstrong and Brooks' (2013) analysis of growth in Algonquin Park Snapping Turtles. Function **F** applies the logistic GPM. Parameter $\boldsymbol{s_H}$ is the annual timing of hatching on the standard time scale, which was set as 0.706 corresponding to 15 September (Eq. (B.9)).

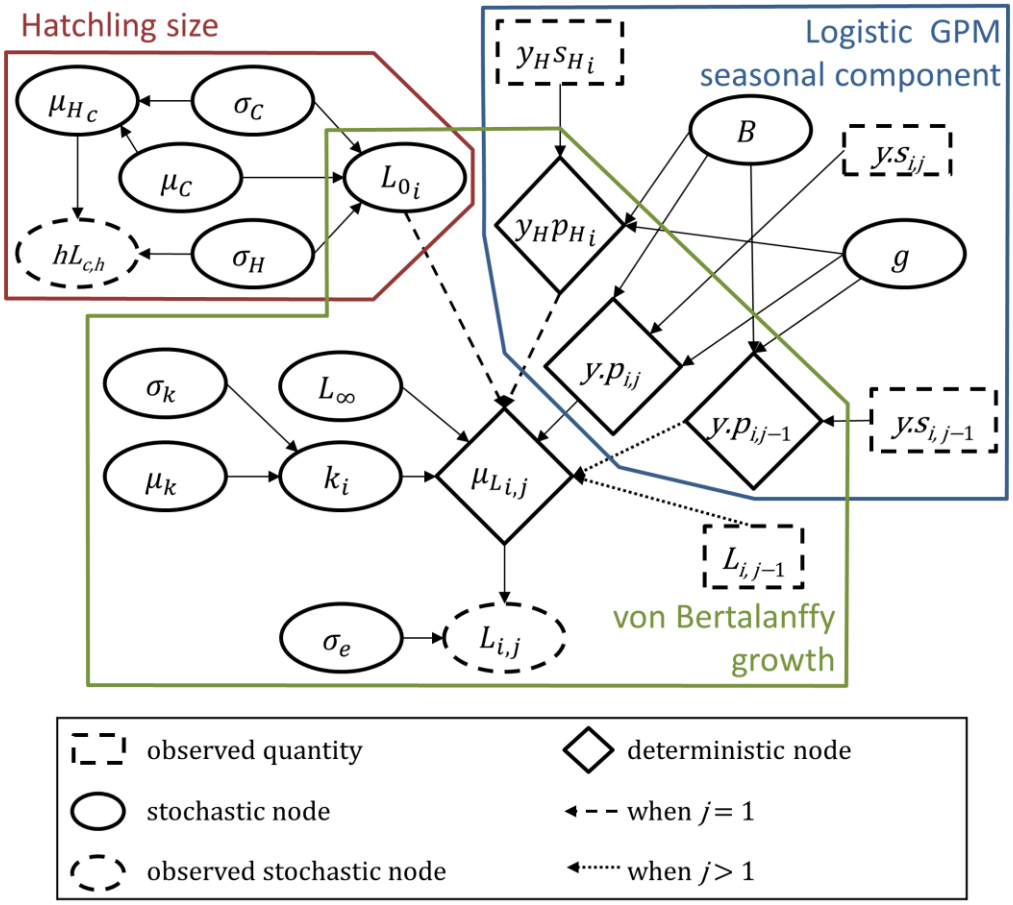

Figure 3.4. Directed acyclic graph of model structure for the integrated model of juvenile Painted Turtle growth combining the logistic GPM, a hierarchical von Bertalanffy component, and a model of size-at-hatching. For known-age individual $\boldsymbol{i}$ with $\boldsymbol{J_i}$ observations, index $\boldsymbol{j = 1, \ldots, J_i}$. For individual $\boldsymbol{i}$ with unknown age, $\boldsymbol{j = 2, \ldots, J_i}$. Notation of variables is paired with descriptions in Table 3.3.

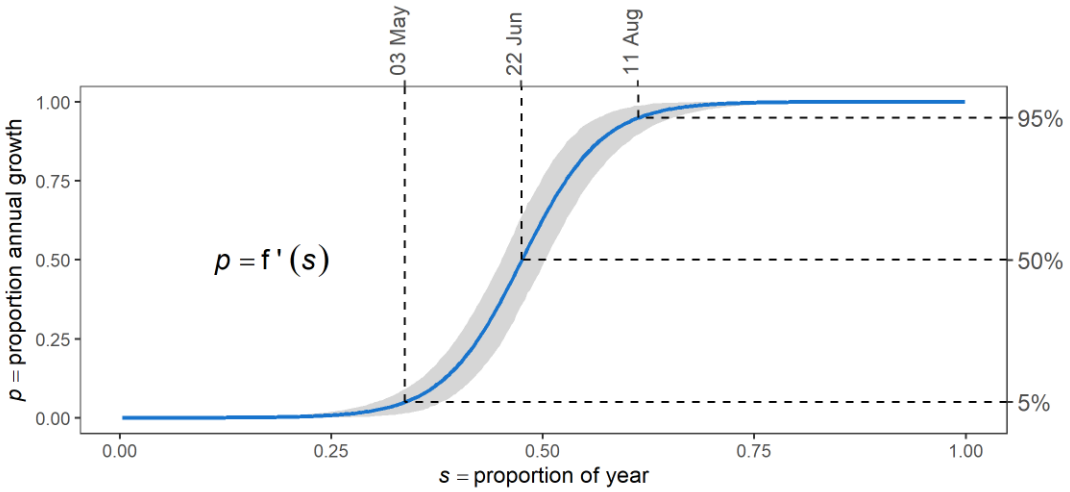

Figure 3.5. Fitted logistic growth phenology model (GPM) as a proportion of annual growth. The model was combined with a hierarchical von Bertalanffy growth model and fitted to primarily inter-annual observations of juvenile and subadult Painted Turtles in Algonquin Park. The shaded region indicates the 95% HDI. $p = \mathrm{f}'(s)$ indicates the GPM function (modified to enforce intercepts, see text).

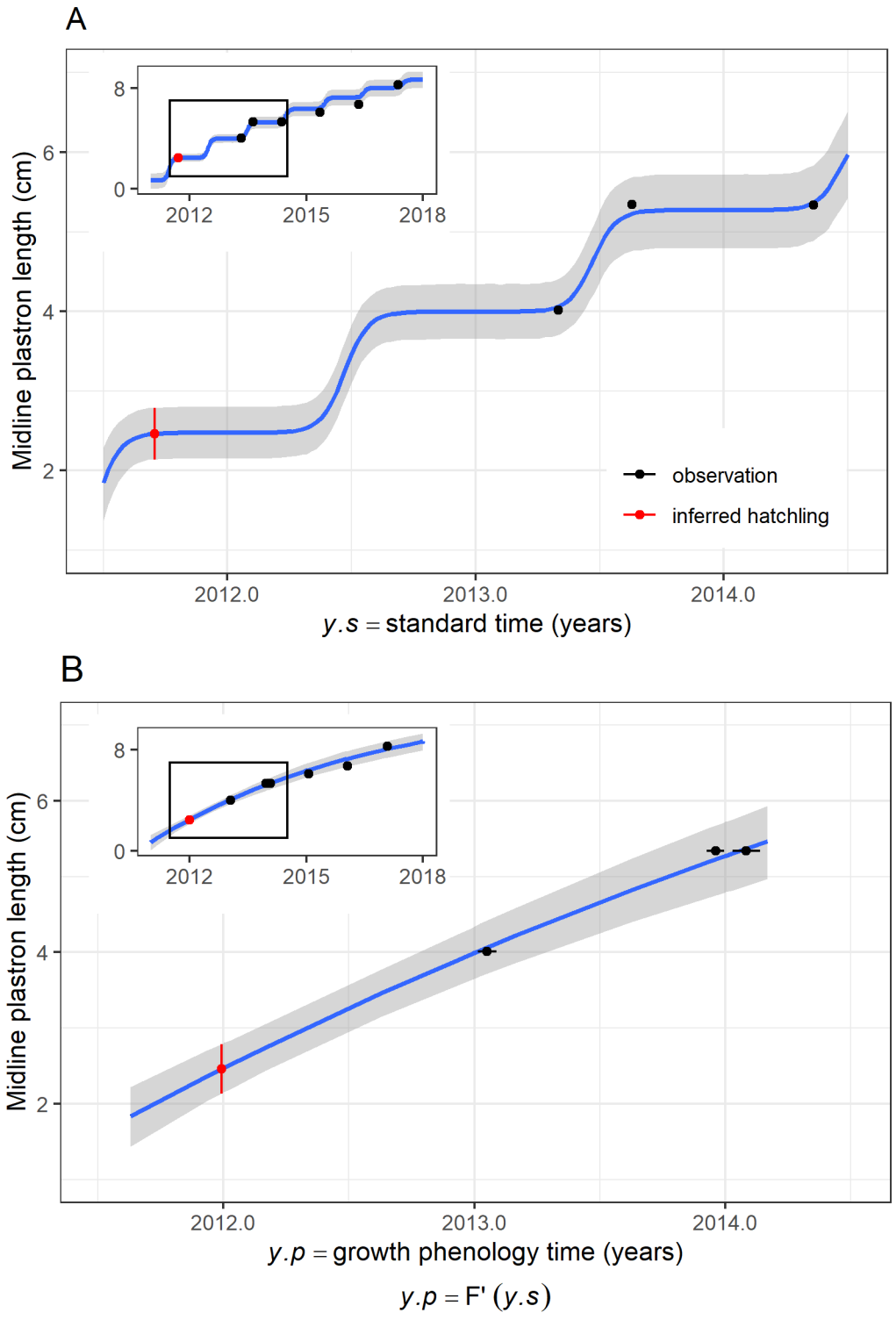

Figure 3.6. Seasonal hierarchical von Bertalanffy model of juvenile growth of Painted Turtles in Algonquin Park showing an example fit for a single known-age individual plotted against

standard linear time as decimal years (**A**) and time adjusted using the posterior mean parameter estimates of the logistic GPM (growth phenology model; **B**). The individual's observation history is shown by the inset plots; the occasion of hatching and subsequent three observations are shown at larger scale. Uncertainty in the unobserved size at hatching is expressed by vertical 95% HDI error bars (highest density interval, the narrowest interval containing 95% of the probability density; Kruschke, 2015). In (**B**), uncertainty in the timing of observations with respect to growth phenology is expressed via horizontal error bars; in (**A**), growth phenology uncertainty is included in the 95% HDI band of the fitted curve.

Chapter 4

Lost reproductive value reveals a high burden of juvenile road mortality in a long-lived species

Published as:

Keevil, M.G., Lesbarrères, D., Noble, N., Boyle, S.P., Brooks, R.., Litzgus, J.D., 2023. Lost reproductive value reveals a high burden of juvenile road mortality in a long-lived species. Ecol. Appl. e2789. https://doi.org/10.1002/eap.2789

Open Research Statement: On-road observation data supporting the results, along with novel R and JAGS code for all non-standard analyses, are archived at Figshare https://doi.org/10.6084/m9.figshare.19123163.v1 (Keevil et al., 2022).

Abstract

Adult mortality is often the most sensitive vital rate affecting at-risk wildlife populations. Therefore, road ecology studies often focus on adult mortality despite the possibility for roads to be hazardous to juvenile individuals during natal dispersal. Failure to quantify concurrent variation in mortality risk and population sensitivity across demographic states can mislead efforts to understand and mitigate the effects of population threats. To compare relative population impacts from road mortality among demographic classes, we weighted mortality observations by applying reproductive value analysis to quantify expected stage-specific contributions to population growth. We demonstrate this approach for Snapping Turtles (*Chelydra serpentina*) observed on roads at two focal sites in Ontario, Canada, where we collected data for both live and dead individuals observed on roads. We estimated reproductive values using stage-classified matrix models to compare relative population-level impacts of adult and juvenile mortality. Reproductive value analysis is a tractable approach to assessing demographically variable effects for applications covering large spatial scales, non-discrete populations, or where abundance data are lacking. For one site with long-term life-history data, we compared demographic frequency on roads to expected general population frequencies predicted by the matrix model. Our application of reproductive value is sex-specific but, as juvenile Snapping Turtles lack external secondary sex characters, we estimated the sex ratio of road-crossing juveniles after dissecting and sexing carcasses collected on roads at five sites across central Ontario. Juveniles were more abundant on roads than expected, suggesting a substantial dispersal contribution, and road-killed juvenile sex ratio approached 1:1. A higher proportion of juveniles were also found dead compared to adults, and cumulative juvenile mortality had similar population-level importance as adult mortality. This suggests that the

impact of roads needs to be considered across all life stages, even in wildlife species with slow life histories, such as Snapping Turtles, that are particularly sensitive to adult mortality.

Introduction

Vulnerability to patchy hazards, such as transportation corridors, differs within and among species because of differences in life-history, spatial ecology, and behavioural or physical interactions with those hazards (Rytwinski and Fahrig, 2013). Within populations, individual vulnerability varies demographically when morphological and behavioural risk factors depend on age and sex (Bulté et al., 2010; Roosenburg et al., 1997; Steen et al., 2006). Species differ in their sensitivity to how mortality is distributed among demographic classes because of population differences in life-history traits and mating system (Cunnington and Brooks, 1996; Rytwinski and Fahrig, 2012; Warden et al., 2015). Specifically, populations of iteroparous organisms with slow life-histories are particularly vulnerable to increased adult mortality, while semelparous species with fast life-histories are comparatively sensitive to juvenile mortality (Jonsson et al., 2001). Animal populations are often more sensitive to female mortality than male mortality, although this varies with operational sex ratio and mating system (Fahrig, 2007; Lindström, 1998). Therefore, impacts of hazards are population-specific and depend on both the magnitude and demographic distribution of mortality burdens.

Natal dispersal is associated with heightened mortality risk for wildlife (Rittenhouse et al., 2009; Sergio et al., 2021), and roads and other hazards can be a major source of mortality for dispersing juveniles (Bonnet et al., 1999; Kim et al., 2019; Massemin et al., 1998; Storm et al., 1976). Sex bias among dispersers mediates the demographic consequences of dispersal mortality, and road effects on populations are expected to be more severe when dispersal is frequent and includes females (Fahrig, 2007). Therefore, disperser sex ratio is a critical component of estimating the

impact of elevated dispersal mortality. Although the magnitude and direction of sex bias in natal dispersal varies among taxa, disperser sex bias is poorly known for many taxa outside of birds and mammals (Trochet et al., 2016). Further, juvenile dispersal stages are often overlooked in road ecology research (Petrovan and Schmidt, 2019). Quantifying the relative risks across sexes and life stages is necessary to understand the impact of hazards on natural history processes such as natal dispersal and on populations more generally.

Turtles are particularly vulnerable to road effects because they mature slowly, depend on high adult survivorship (Fahrig, 2007; Howell et al., 2019; Piczak et al., 2019), and they are slow-moving and behaviourally vulnerable to traffic (Rytwinski and Fahrig, 2012). Concern about road effects on freshwater turtle populations often focuses on adult females because roads attract or intercept females during nesting migrations (Steen et al., 2012, 2006) and adult female survivorship is the most sensitive vital rate affecting population growth rate (Congdon et al., 1994; Cunnington and Brooks, 1996; Enneson and Litzgus, 2008; Heppell, 1998). Sex-biased road mortality in turtles is evidenced by male-skewed populations (Patrick and Gibbs, 2010; Steen et al., 2006; Steen and Gibbs, 2004), although some studies question the strength of this phenomenon (Bowne et al., 2018; Carstairs et al., 2018; Dorland et al., 2014), resulting in controversy (Bowne et al., 2019; Lambert and Steen, 2019). In addition to nesting migrations, primarily aquatic turtles move through terrestrial habitats in response to habitat changes such as pond drying (Aresco, 2005; Gibbons et al., 1983; Mali et al., 2016), for dispersal or mating opportunities (Bowne et al., 2006; Tuberville et al., 1996), or, for semi-terrestrial species, to exploit seasonal resources within a multi-patch home range (Edge et al., 2010). In particular, natal dispersal could bring juveniles into terrestrial habitats and contact with roads. Few studies explicitly investigate natal dispersal patterns of turtles and their interaction with roads; however,

evidence indicating a lower proportion of juveniles in turtle populations in disturbed habitats is consistent with higher juvenile mortality at anthropogenically impacted sites (Howell et al., 2019; Marchand and Litvaitis, 2004; Saumure and Bider, 1998). The consequences of juvenile dispersal mortality for turtle populations are further obscured because juvenile sex cannot usually be determined genetically or by external morphology, so sex is rarely reported.

Approach and objectives

We assessed the relative importance of road mortality among demographic classes, including dispersing juveniles, of Snapping Turtles (*Chelydra serpentina*), in Ontario, Canada where they are listed as a species of Special Concern and where roads constitute a major threat (COSEWIC, 2008; Environment and Climate Change Canada, 2020; Piczak et al., 2019). To quantify relative demographic importance of sex and body size, we estimated reproductive values (RV, expected contribution of individuals to population growth based on their demographic class; Caswell, 2001). In contrast to population viability analyses, reproductive value analysis evaluates demographically variable impacts without defining a discrete population or estimating abundance. Further, reproductive value analysis does not depend on quantifying effects as changes to absolute population vital rates, which would be required for elasticity analysis. Therefore, the RV approach is applicable to impacts occurring at wide spatial scales or affecting diffuse populations.

Our approach had three components with the following objectives:

1. Estimate sex ratio of juveniles killed on roads by dissecting carcasses collected at multiple sites.
2. Estimate reproductive values (RV) to quantify the relative importance of road mortality among demographic classes at two focal study sites.

3. Compare on-road demographic frequencies to expected frequencies based on stage distributions to assess which demographic classes were over-represented on roads.

We constructed deterministic stage-classified matrix population models to estimate RV (objective 2) and to generate expected demographic frequencies as stable stage distributions (objective 3). Estimating sex ratio of juveniles killed on roads (objective 1) allowed us to infer expected RV for individuals that could not be sexed and to assess predictions of sex-biased dispersal. Because juveniles lack external secondary sex characters, sex was identified by dissection of carcasses.

Predictions

We expected that juvenile or sub-adult dispersers and nesting females would be more frequent on roads than other demographic classes because other phases of Snapping Turtle natural history—such as foraging, mating, and hibernating—occur in aquatic habitats. Because adult females are likely to encounter roads (Steen et al., 2006) and contribute more to population growth than males (Cunnington and Brooks, 1996), we predicted adult female road mortality would contribute most of the total road mortality burden as quantified by RV.

Consideration of the selective forces that favour potentially costly dispersal, which include inbreeding avoidance and kin competition for resources (local resource competition) and mates (local mate competition) (Gandon, 1999; Hamilton and May, 1977; Li and Kokko, 2019a; Perrin and Mazalov, 2000), informed our prediction of sex-biased dispersal. Inbreeding avoidance promotes sex-biased dispersal but does not intrinsically determine the more dispersive sex (Gandon, 1999; Li and Kokko, 2019a; Perrin and Mazalov, 2000). Theory suggests that the sex experiencing the most intense local competition is expected to be more dispersive (Leturque and Rousset, 2004; Perrin and Mazalov, 2000). Snapping Turtles have a polygamous mating system (Galbraith et al., 1993) with frequent conflict among males (Keevil et al., 2017) suggesting high

rates of mate competition. Additionally, Snapping Turtles lack paternal care and do not defend exclusive territories (Galbraith et al., 1987) and so lack elements of social systems that favour male philopatry among other taxa (Greenwood, 1980; Trochet et al., 2016). Finally, limited data suggest that male-biased dispersal predominates in non-avian reptiles (Trochet et al., 2016). Therefore, we hypothesized that natal dispersal in Snapping Turtles would be male-biased, resulting in male-biased juvenile or sub-adult road mortality. A corollary is that if dispersal functions to reduce mate competition and inbreeding after maturity, and if predation risk and energetic costs are lower for larger individuals, then dispersal may be deferred (Li and Kokko, 2019b) leading us to predict that older juveniles and subadults would be more overrepresented on roads than younger and smaller juveniles.

Methods

Sex ratio of road-killed juveniles

We obtained carcasses of dead-on-road (DOR) juvenile Snapping Turtles and determined sex by dissection. Carcasses were collected along roads during 2013–2015 in five areas across south and central Ontario: Presqu'ile Provincial Park (PQP), Algonquin Provincial Park (APP), Highway 69/400 along eastern Georgian Bay, the Muskoka region, and three specimens were collected opportunistically in eastern Ontario (Figure 4.1). We identified sex of juvenile carcasses collected over a wider geographic region beyond and including our two focal study sites (Figure 4.1) to obtain a larger, more generalized sample with which to infer sex ratio of road-crossing juveniles. Roads at study sites ranged from high-volume provincial highways to unpaved access roads. Carcasses were collected during opportunistic encounters and regular surveys, and were frozen until dissection. Site descriptions and survey methods at eastern Georgian Bay (Baxter-Gilbert et al., 2018, 2015), and Muskoka (McCurdy-Adams, 2016) are provided elsewhere. At PQP, two

wetland-adjacent 1250 m road transects were surveyed daily three times by bicycle and once by walking from May to August (Boyle et al., 2021, 2017). Traffic volumes at PQP were 161–212 vehicles/hour during field work (Boyle et al., 2021). Field work at APP was undertaken as part of a long-term turtle life history project, which has been previously described (Keevil et al., 2021, 2018; Riley and Litzgus, 2013) but here we analyze opportunistic on-road observations collected from a larger area of APP, beyond marked study populations, that includes a 60 km length of highway corridor bisecting the park. Summer average annual daily traffic volumes vary by highway segment and were 1250–4050 vehicles/day in 2016 (Ontario Ministry of Transportation, 2016). This highway and associated access roads, which were also sampled, traverse multiple watersheds and the associated sample does not correspond to a specific, discrete population.

We determined juvenile sex by identification of gonads. We did not base sex determination on penis presence because that would induce a female bias among indeterminate cases. We excluded hatchlings (juveniles less than one year old) from this and subsequent analyses to avoid conflating initial migration away from terrestrial nests with dispersal between aquatic habitats. Additionally, hatchling emergence dates extend into the autumn beyond the regular survey period, so we did not attempt to quantify hatchling interactions with roads. We measured straight midline plastron (PL) and carapace (CL) lengths to the nearest 0.1 mm using Vernier callipers. In instances of severe carapace damage, CL was inferred by linear regression of CL on PL of intact specimens ($\widehat{CL} = 1.32 \times PL + 0.37$, $n_{intact} = 86$, $R^2_{\text{adj}} = 0.98$, $P < 0.001$). We pooled juveniles across sites and obtained the binomial likelihood confidence interval for sex ratio. To assess evidence for size or site effects on sex ratios, we used AICc (Burnham and Anderson 2002) to rank binomial linear models with and without these covariates. We used the results of this model to predict expected sex for unsexed individuals.

Demographic comparison to marked population

In addition to salvageable juvenile carcasses, we recorded all alive-on-road (AOR) and DOR Snapping Turtles encountered in APP (2013–2015) and PQP (2013–2017). All turtles observed on roads in APP were recorded, including those encountered opportunistically outside of long-term study sites with marked populations.

Stage-based matrix model

We constructed variable-duration stage-based matrix demographic models (Caswell 2001; Stubben and Milligan 2007; Figure 1.2; Appendix D) based on the long term life-history study at APP to estimate reproductive value (RV) and stable stage distributions. To parameterize stage transitions, we used the hierarchical growth model of Armstrong and Brooks (2013) modified to accommodate seasonal variation (Keevil et al., 2021), which we refit for observations up to 2018 (Appendix S2). This model estimated somatic growth variation within the APP population. Adult survivorship (Armstrong et al., 2018; Brooks et al., 1991b; Galbraith and Brooks, 1987; Keevil et al., 2018) and the fertility and body size relationship (Armstrong et al., 2018) have been previously estimated for this population. Published nest survival and hatching success estimates (Bobyn and Brooks, 1994a; Brooks et al., 1988, 1991a; Riley and Litzgus, 2013; Rouleau et al., 2019) were combined with previously unpublished observations from 2014 and 2015 by weighted averaging according to sample size (Table D.2).

Because juvenile survivorship is largely unmeasured in Snapping Turtles, we calculated stable stage distributions for three sets of plausible values defined by different relationships between juvenile size and survivorship. Each scenario was constrained to result in a stable population ($\lambda = 1$), which is a common strategy to interpolate missing vital rates (Congdon et al., 1994; Pike et al., 2008; Wallace et al., 2008). Additionally, we assumed that juvenile survival approaches

adult survival as juveniles approach adult size. Within these constraints, we varied the size-survival relationship across the scenarios to estimate a range of three stable stage distributions (Figure D.1, Table D.4, Figure 4.2). Scenario 1 is intermediate between Scenario 2, which is sigmoidal with an abrupt increase in survival with size, and Scenario 3, which is a gradual linear increase. These scenarios qualitatively resemble juvenile survival patterns in other chelonians (Arsovski et al., 2018; Fernández-Chacón et al., 2011; Loehr, 2017; McGovern et al., 2020).

Reproductive value (RV) of DOR Snapping Turtles

We tested differences in the AOR/DOR ratio between pooled juvenile and pooled adult stages at PQP and APP using Fisher's exact tests. To compare road mortality impacts among stages, we summed RVs of road-killed individuals in each stage. RVs were calculated as the left eigenvector of the projection matrices using R package `popbio` (Stubben and Milligan, 2007; Appendix S1). We also applied the stage-specific RVs developed for APP to road-killed individuals at PQP.

Stable stage distribution

We compared the size distribution of live and dead Snapping Turtles observed on roads in APP to the expected distribution in the population estimated as the stable stage distribution, which we computed as right eigenvectors of our matrix models (Caswell, 2001; Stubben and Milligan, 2007). Hatchlings were excluded to focus on potential dispersal movements between aquatic habitats. For this portion of the analysis, we also excluded nesting females (adult females observed on roads between first and last nesting observations) to focus on non-nesting movements. Our matrix model is female-only, so we assumed a 1:1 sex ratio to add males to the expected stage distributions (surveys in APP have not shown significantly biased sex ratios; Galbraith et al. 1988, Keevil et al. 2018). We compared the distributions graphically and by using χ^2 goodness-of-fit tests. Because some expected counts were < 5, we used simulated p-values, as

implemented in R's `chisq.test` function, to avoid violating asymptotic approximation assumptions of traditional χ^2 tests (R Development Core Team, 2020). We repeated this analysis using only AOR observations to assess whether our inferences were robust to differences in detectability resulting from among-stage differences in road mortality risk. All analyses were performed in R version 4.0.2 (R Development Core Team, 2020).

Results

Sex ratio of road-killed juveniles

Sex was identified for 51 of 122 road-killed juvenile Snapping Turtles collected from multiple sites in central and southern Ontario (Table 4.1). Upon dissection, many apparently intact carcasses were found to have had the viscera ejected, in which case sex was non-identifiable. Because this resulted in an absence of gonads, we do not suspect that it caused a bias in our ability to confirm sex of males or females. Of those that could be sexed, sex ratios did not differ from 1:1 (N = 51, proportion female = 0.51, P = 1) but with some uncertainty because of low sample size (95% binomial CI 0.348−0.634; Figure 4.3). The null (intercept only) model was the top-ranked model of sex ratio (ΔAICc > 2 for all other models) indicating that sex ratio was not appreciably related to body size or site.

Demographic distribution and reproductive value

We observed 164 Snapping Turtles on roads at APP and 293 at PQP. The demographic distributions of all AOR and DOR Snapping Turtles observed on roads in APP and PQP had modes of juveniles between 6 cm and 12 cm CL and a larger peak of nesting females (Figure 4.4). Most Snapping Turtles killed on roads in APP and PQP were juveniles (pooled DOR proportion juvenile 0.965; 95% binomial CI 0.902–0.993; Table 4.2). Conditional on being

detected on a road, and pooled across site and sex, juveniles had 70 times higher odds of being observed dead than adults (odds ratio = 70.4; 95% CI 22.5−354.0).

The estimated RV of juvenile stages was strongly affected by juvenile survivorship, thus RV differed among the survivorship scenarios (Figure 4.2B; Figure D.2). Differences among scenarios were less pronounced for very small juveniles (which have yet to move through most stages) and for those approaching maturity (which have already survived most stages) because the cumulative survivorship at the end of the juvenile period was similar among scenarios to satisfy the imposed stable population constraint. RV continued to increase with size after maturity because larger body size is associated with higher survival and greater reproductive output (Galbraith et al. 1989; Armstrong et al. 2018).

The cumulative RV of juveniles killed either exceeded or was equivalent to the cumulative RV of adult females killed in PQP (cumulative lost juvenile RV was 1.79×, 5.18×, or 0.94× that of adults under scenarios 1, 2, and 3, respectively) and APP (lost juvenile RV was 1.02×, 2.41× adult RV for scenario 1 and 2) except under scenario 3 in APP (0.54×; Figure 4.5).

Stable stage distribution

The estimated stable-stage distributions predicted high frequencies of early stages (eggs and small juveniles) relative to adults, which is typical of turtle population models (Enneson and Litzgus 2008; Salice et al. 2014; Knoerr et al. 2021). The stage distribution of non-nesting Snapping Turtles observed on roads in APP differed from expected distributions under each of the three juvenile survival scenarios ($\chi^2 = 119.4, 224.3, 78.5$, all $P \leq 0.001$). Adult males and small juveniles (CL < 6 cm, stage 2) were under-represented whereas mid-sized juveniles, especially stages 3–5 (6–15 cm CL), were over-represented (Figure 4.6). The results were similar

when we repeated the analysis while excluding dead individuals to account for differential mortality risk (Appendix S4 of Keevil et al., 2023). Stage 8 (the largest juvenile/sub-adult stage) was also over-represented and all six observed individuals were male. However, this pattern was not observed at PQP nor was it apparent in the dissected carcass sample (Figure 4.3).

Discussion

Stage distribution and reproductive value

Adult females and mid-sized juveniles were the most abundant demographic classes on roads. However, juveniles were much more likely to be killed than adults. While nesting female turtles frequently encounter roads, many complete nesting on road shoulders without crossing traffic lanes, in which case road mortality risk is reduced (Crawford et al., 2018). Mid-sized juveniles were more abundant on roads in APP than expected from the stable stage distribution. The smallest post-hatchling juvenile stage (stage 2) was under-represented at APP (Figure 4.6). Although this may have been influenced by lower detectability of small individuals (Steen and Smith, 2006), a similar pattern was observed at PQP where surveys were conducted systematically by foot and bicycle, and where carcass persistence times are longer than sampling intervals (Boyle et al., 2021). More generally, to the extent that detection or carcass persistence biases may have affected comparisons between adult and juvenile frequencies on roads, we expect the direction would be biased against juveniles due to their smaller size resulting in an underestimation of the juvenile proportion of road mortality (Barrientos et al., 2018; Steen and Smith, 2006). Hatchling (stage 1) interactions with roads were outside of the scope of our analysis, but nothing suggests that road mortality of hatchlings is negligible or is unimportant for populations. In fact, including DOR hatchlings would have increased the RV-weighted juvenile mortality burden relative to that of adults.

While the burden of juvenile road mortality, weighted by RV, was comparable to that of adult females, there were few adults killed during the observation periods. Because mean adult female RV is substantially higher than mean juvenile RV, the relative proportion of RV-weighted road mortality burden attributed to juveniles is very sensitive to the number of road-killed adults. Thus, the demographic proportions of RV-weighted mortality burden that we observed were highly contingent—one more (or fewer) observation of a dead adult female would result in a large change to the impact of road mortality and the relative contributions of juveniles compared to adults.

Uncertainty in the juvenile survivorship schedule also contributed substantially to uncertainty in relative RV lost among demographic classes (Figure 4.5). More generally, missing survivorship data reduces the ability of any demographic modeling approach to make relevant distinctions among life-history stages. Accurate juvenile survivorship estimates are difficult to obtain and are biased or lacking for many species for which other vital rates are well estimated (Pike et al., 2008). Improved estimates are probably achievable by specifically focusing efforts towards understanding juvenile survival, along with advancements in modeling approaches and survey or monitoring technology such as telemetry devices. Promising modeling approaches include the use of informative Bayesian priors to increase precision of estimates (Rankin et al., 2016) and parametric modeling of survival as a function of continuous age or size covariates (Arsovski et al., 2018).

Juvenile dispersal

We predicted that nesting females and dispersers would be over-represented on roads relative to their proportion in the population. After accounting for nesting females, the next most frequent stages observed on roads included male and female juveniles 6–15 cm in carapace length, which

were significantly more frequent on roads than expected. This peak of juveniles probably corresponds to dispersal movements.

For a species whose population growth and persistence depend primarily on females (Congdon et al., 1994; Cunnington and Brooks, 1996; Salice et al., 2014), unbiased dispersal implies greater population-level consequences from dispersal mortality compared to male-biased dispersal (Fahrig, 2007). Contrary to our predictions, we found no sex-bias in road-killed juveniles. We had predicted that Snapping Turtle dispersal would be male-biased because of high mate competition among males involving strongly male-biased sexual size dimorphism and frequent combat (Keevil et al., 2017). Mate competition is associated with male-biased juvenile dispersal in other taxa (Dobson, 1982; Greenwood, 1980; Mabry et al., 2013; Trochet et al., 2016) and sex-biased dispersal in the few non-avian reptiles studied to date is frequently male-biased (Trochet et al., 2016). However, mate competition does not always entail selection for male dispersal (Li and Kokko, 2019a). Tucker et al. (1998) reported unbiased natal dispersal in freshwater crocodiles (*Crocodylus johnstoni*), which have a similar life history to Snapping Turtles in that they are long-lived, late-maturing, iteroparous reptiles with a polygynous mating system.

The cost of dispersal in Snapping Turtles, as mortality risk and relative energetic cost, is likely to be inversely related to body size. If so, then it would be adaptive for individuals to defer dispersal, in which case the absence of the smallest stage class from our sample would be expected. However, most of the juveniles observed were still less than halfway to maturity. A possible explanation for early juvenile dispersal is kin competition for resources (local resource competition), which favours dispersal through inclusive fitness effects that begin to accrue prior to maturity (Hamilton and May, 1977; Li and Kokko, 2019b). Other selective forces that also favour potentially costly dispersal—local mate competition and inbreeding avoidance—do not

affect fitness until reproductive maturity and tend to be sex-biased (Li and Kokko, 2019a; Perrin and Mazalov, 2000). Of these forces, only local resource competition favours unbiased dispersal (Gandon, 1999). Juvenile Snapping Turtle growth rates vary both among individuals and among years resulting in variable time to maturity affecting cumulative survival to maturity (Armstrong et al., 2018; Armstrong and Brooks, 2013; Salice et al., 2014). Consequently, resource competition among kin that affects growth rates has potentially large fitness consequences. Spatial and temporal clumping of related juveniles is expected for Snapping Turtles because nesting habitat is limited to specific areas used by the same mothers year after year (Francis et al., 2019; Keevil et al., 2018) and clutches typically succeed or fail as a unit (Bobyn and Brooks, 1994b; Riley and Litzgus, 2014). Iteroparity and clumping of relatives may increase local resource competition, which favours the evolution of dispersal to reduce kin competition (Duputié and Massol, 2013; Parvinen et al., 2003).

Reproductive value analysis as a conservation tool

The RV analysis allowed us to compare population impacts across demographic classes. RV-weighted counts have been used to quantify impacts of marine fisheries targeting sharks of different age classes (Gallucci et al., 2006) and to by-catch effects on marine turtles (Haas, 2010; Wallace et al., 2008; Warden et al., 2015). In contexts with adequate data and discrete populations, population viability analyses (PVAs) are often used to compare conservation scenarios (e.g., Enneson and Litzgus 2009, Howell and Seigel 2019). When data are limited, simpler models may outperform complicated ones (Rueda-Cediel et al., 2015). For conservation questions focused on alternatives that differ in the demographic distribution of their effects, RV analysis can provide a salient comparison without producing tangential and potentially spurious estimates of population growth rates and extinction probability. Estimating RV requires some of

the same data necessary for a stage-based PVA (e.g., schedules of survivorship and fecundity), but does not require difficult-to-obtain data about population size, density dependence, or environmental stochasticity. Unlike elasticity analysis, RV can be used to compare impacts across demographic classes without quantifying absolute change in vital rates. RV approaches compare demographic impacts without defining discrete populations, which is an advantage when phenomena of interest occur over wide spatial extents, data are limited, or populations are diffuse.

Juveniles represented approximately half of the overall road mortality burden that we observed; therefore, our primary recommendation is that juveniles should be explicitly considered in data collection and reporting and in the application of demographic analyses evaluating road effects and their mitigation. Selection of site and seasonal timing of road surveys for freshwater turtles to focus on nesting can introduce demographic biases in road mortality data, which can result in males and juveniles being under-represented in empirical data (Carstairs et al., 2018; Crawford et al., 2014; Haxton, 2000). Juvenile mortality is frequently omitted when applying demographic models to evaluate road impacts or mitigation measures (e.g., Howell and Seigel 2019, Piczak et al. 2019, Murphy et al. 2022; but see Sterrett et al. 2019), and this issue is not limited to studies on turtles (Petrovan and Schmidt, 2019). Accounting for juvenile road mortality will reduce bias in estimates of total road mortality burden and may be especially salient when assessing road effects and mitigation that may be demographically biased. While a lack of juvenile sex ratio, abundance, and vital rate data is a frequent challenge for fully incorporating juveniles into demographic analyses, collection of juvenile data in road surveys can be improved and the RV approach lowers the requirements for data and assumptions.

A limiting factor for conservation action is funding availability for work or mitigation infrastructure, particularly for road ecology, where road construction, exclusion fencing, and crossing structures can be prohibitively expensive (Lesbarrères and Fahrig, 2012; Rytwinski et al., 2015). Demographic-specific RVs have potential to guide mitigation planning. Mitigation may be demographically biased because of location or details of construction. Some mitigation strategies, such as constructed nesting areas or time- and season-specific interventions (Beaudry et al., 2010; Crawford et al., 2018), target specific demographic classes, which, in our study system, likely represented less than half of the road mortality burden. Even for long-lived species dependent on high adult survival, interventions targeting juveniles may provide the greatest conservation benefit when adult-focused interventions achieve diminishing returns (Bennett et al., 2017; Crawford et al., 2014; Cunnington and Brooks, 1996; Knoerr et al., 2021; Sergio et al., 2021). Similar to prioritizing areas with the most conservation value (Boyle et al., 2017; Laurance et al., 2014), life-history stage-specific mitigation planning informed by demographic vulnerabilities standardized by RV can help to optimize the value of conservation resources.

Conclusions

Roads can increase natal dispersal mortality (Bonnet et al., 1999; Case, 1978; Kim et al., 2019; Massemin et al., 1998), which has more severe effects when dispersal is frequent and includes females (Fahrig, 2007). However, juveniles tend to be overlooked in road ecology studies (Petrovan and Schmidt, 2019). Among freshwater turtles, for which adult female survivorship is the most sensitive vital rate, roads attract or intercept nesting females and so road impacts mediated through other demographic classes are frequently deemphasized in research and conservation planning (e.g., see discussions in Bowne et al. 2019, Carstairs et al. 2019, Lambert and Steen 2019). The sex ratio of juvenile Snapping Turtles killed on roads in Ontario was

approximately 1:1, and mid-sized juveniles were over-represented on roads. Juvenile Snapping Turtles were more likely to be killed on roads than adults, and the cumulative impact of juvenile road mortality was similar or greater compared to that of adults when quantified using reproductive value. Our results highlight the importance of considering juveniles in road ecology and other conservation scenarios, even in long-lived species for which sensitivity to adult mortality is very high. A single-minded focus on one demographic category and class of behaviour runs the risk of oversimplifying a complex conservation problem, biasing impact assessments, and overlooking potential mitigation challenges and opportunities.

References

Aresco, M.J., 2005. Mitigation measures to reduce highway mortality of turtles and other herpetofauna at a north Florida lake. J. Wildl. Manage. 69, 549–560. https://doi.org/10.2193/0022-541X(2005)069[0549:MMTRHM]2.0.CO;2

Armstrong, D.P., Brooks, R.J., 2013. Application of hierarchical biphasic growth models to long-term data for Snapping Turtles. Ecol. Modell. 250, 119–125. https://doi.org/10.1016/j.ecolmodel.2012.10.022

Armstrong, D.P., Keevil, M.G., Rollinson, N., Brooks, R.J., 2018. Subtle individual variation in indeterminate growth leads to major variation in survival and lifetime reproductive output in a long-lived reptile. Funct. Ecol. 32, 752–761. https://doi.org/10.1111/1365-2435.13014

Arsovski, D., Olivier, A., Bonnet, X., Drilholle, S., Tomović, L., Béchet, A., Golubović, A., Besnard, A., 2018. Covariates streamline age-specific early life survival estimates of two chelonian species. J. Zool. 306, 223–234. https://doi.org/10.1111/jzo.12585

Barrientos, R., Martins, R.C., Ascensão, F., D'Amico, M., Moreira, F., Borda-de-Água, L., 2018. A review of searcher efficiency and carcass persistence in infrastructure-driven mortality

assessment studies. Biol. Conserv. 222, 146–153. https://doi.org/10.1016/J.BIOCON.2018.04.014

Baxter-Gilbert, J.H., Riley, J.L., Boyle, S.P., Lesbarrères, D., Litzgus, J.D., 2018. Turning the threat into a solution: Using roadways to survey cryptic species and to identify locations for conservation. Aust. J. Zool. 66, 50–56. https://doi.org/10.1071/ZO17047

Baxter-Gilbert, J.H., Riley, J.L., Lesbarrères, D., Litzgus, J.D., 2015. Mitigating reptile road mortality: Fence failures compromise ecopassage effectiveness. PLoS One 10, e0120537. https://doi.org/10.1371/journal.pone.0120537

Beaudry, F., Demaynadier, P.G., Hunter, M.L., 2010. Identifying hot moments in road-mortality risk for freshwater turtles. J. Wildl. Manage. 74, 152–159. https://doi.org/10.2193/2008-370

Bennett, A.M., Steiner, J., Carstairs, S., Gielens, A., Davy, C.M., 2017. A question of scale: Replication and the effective evaluation of conservation interventions. FACETS 2, 892–909. https://doi.org/10.1139/FACETS-2017-0010

Bobyn, M.L., Brooks, R.J., 1994a. Interclutch and interpopulation variation in the effects of incubation conditions on sex, survival and growth of hatchling turtles (*Chelydra serpentina*). J. Zool. 233, 233–257. https://doi.org/10.1111/j.1469-7998.1994.tb08586.x

Bobyn, M.L., Brooks, R.J., 1994b. Incubation conditions as potential factors limiting the northern distribution of Snapping Turtles, *Chelydra serpentina*. Can. J. Zool. 72, 28–37. https://doi.org/http://dx.doi.org/10.1139/z94-005

Bonnet, X., Naulleau, G., Shine, R., 1999. The dangers of leaving home: Dispersal and mortality in snakes. Biol. Conserv. 89, 39–50. https://doi.org/10.1016/S0006-3207(98)00140-2

Bowne, D.R., Bowers, M.A., Hines, J.E., 2006. Connectivity in an agricultural landscape as reflected by interpond movements of a freshwater turtle. Conserv. Biol. 20, 780–791. https://doi.org/10.1111/j.1523-1739.2006.00355.x

Bowne, D.R., Cosentino, B.J., Anderson, L.J., Bloch, C.P., Cooke, S., Crumrine, P.W., Dallas, J., Doran, A., Dosch, J.J., Druckenbrod, D.L., Durtsche, R.D., Garneau, D., Genet, K.S., Fredericksen, T.S., Kish, P.A., Kolozsvary, M.B., Kuserk, F.T., Lindquist, E.S., Mankiewicz, C., March, J.G., Muir, T.J., Murray, K.G., Santulli, M.N., Sicignano, F.J., Smallwood, P.D., Urban, R.A., Winnett-Murray, K., Zimmermann, C.R., 2018. Effects of urbanization on the population structure of freshwater turtles across the United States. Conserv. Biol. 32, 1150–1161. https://doi.org/10.1111/cobi.13136

Bowne, D.R., Cosentino, B.J., Anderson, L.J., Cooke, S., Dosch, J.J., Garneau, D., Fredericksen, T.S., Kolozsvary, M.B., Lindquist, E.S., March, J.G., Urban, R.A., Zimmermann, C.R., 2019. A broader approach to understanding urbanization effects on freshwater turtles: reply to Lambert and Steen 2019. Conserv. Biol. 33, 1197–1199. https://doi.org/10.1111/cobi.13398

Boyle, S.P., Keevil, M.G., Litzgus, J.D., Tyerman, D., Lesbarrères, D., 2021. Road-effect mitigation promotes connectivity and reduces mortality at the population-level. Biol. Conserv. 261, 109230. https://doi.org/10.1016/J.BIOCON.2021.109230

Boyle, S.P., Litzgus, J.D., Lesbarrères, D., 2017. Comparison of road surveys and circuit theory to predict hotspot locations for implementing road-effect mitigation. Biodivers. Conserv. 26, 3445–3463. https://doi.org/10.1007/s10531-017-1414-9

Brooks, R.J., Bobyn, M.L., Galbraith, D.A., Layfield, J.A., Nancekivell, E.G., 1991a. Maternal and environmental influences on growth and survival of embryonic and hatchling Snapping Turtles (*Chelydra sepentina*). Can. J. Zool. 69, 2667–2676. https://doi.org/10.1139/z91-375

Brooks, R.J., Brown, G.P., Galbraith, D.A., 1991b. Effects of a sudden increase in natural mortality of adults on a population of the Common Snapping Turtle (*Chelydra serpentina*). Can. J. Zool. 69, 1314–1320. https://doi.org/10.1139/z91-185

Brooks, R.J., Galbraith, D.A., Nancekivell, E.G., Bishop, C.A., 1988. Developing management guidelines for Snapping Turtles, in: Management of Amphibians. Reptiles and Small Mammals in North America; Proceedings of the Symposium. Flagstaff, AZ, pp. 174–179.

Bulté, G., Carrière, M.-A., Blouin-Demers, G., 2010. Impact of recreational power boating on two populations of Northern Map Turtles (*Graptemys geographica*). Aquat. Conserv. Mar. Freshw. Ecosyst. 20, 31–38. https://doi.org/10.1002/aqc.1063

Burnham, K.P., Anderson, D.R., 2002. Model Selection and Multimodel Inference: A Practical Information-Theoretic Approach. Springer-Verlag, New York, New York, USA.

Carstairs, S., Dupuis-Desormeaux, M., Davy, C.M., 2018. Revisiting the hypothesis of sex-biased turtle road mortality. Can. Field-Naturalist 132, 289–295. https://doi.org/10.22621/cfn.v132i3.1908

Case, R.M., 1978. Interstate highway road-killed animals: A data source for biologists. Wildl. Soc. Bull. 6, 8–13. https://doi.org/10.2307/3781058

Caswell, H., 2001. Matrix Population Models : Construction, Analysis, and Interpretation, 2nd ed. Sinauer Associates, Sunderland, MA. USA.

Congdon, J.D., Dunham, A.E., van Loben Sels, R.C., 1994. Demographics of Common Snapping Turtles (*Chelydra serpentina*): Implications for conservation and management of long-lived organisms. Am. Zool. 34, 397–408.

COSEWIC, 2008. COSEWIC Assessment and Status Report on the Snapping Turtle *Chelydra serpentina* in Canada. Committee on the Status of Endangered Wildlife in Canada.

Crawford, B.A., Maerz, J.C., Nibbelink, N.P., Buhlmann, K.A., Norton, T.M., 2014. Estimating the consequences of multiple threats and management strategies for semi-aquatic turtles. J. Appl. Ecol. 51, 359–366. https://doi.org/10.1111/1365-2664.12194

Crawford, B.A., Moore, C.T., Norton, T.M., Maerz, J.C., 2018. Integrated analysis for population estimation, management impact evaluation, and decision-making for a declining species. Biol. Conserv. 222, 33–43. https://doi.org/10.1016/j.biocon.2018.03.023

Cunnington, D.C., Brooks, R.J., 1996. Bet-hedging theory and eigenelasticity: a comparison of the life histories of Loggerhead Sea Turtles (*Caretta caretta*) and Snapping Turtles (*Chelydra serpentina*). Can. J. Zool. 74, 291–296. https://doi.org/10.1139/z96-036

Dobson, F.S., 1982. Competition for mates and predominant juvenile male dispersal in mammals. Anim. Behav. 30, 1183–1192. https://doi.org/doi:10.1016/S0003-3472(82)80209-1

Dorland, A., Rytwinski, T., Fahrig, L., 2014. Do roads reduce Painted Turtle (*Chrysemys picta*) populations? PLoS One 9, e98414. https://doi.org/10.1371/journal.pone.0098414

Duputié, A., Massol, F., 2013. An empiricist's guide to theoretical predictions on the evolution of dispersal. Interface Focus 3, 1–14.

Edge, C.B., Steinberg, B.D., Brooks, R.J., Litzgus, J.D., 2010. Habitat selection by Blanding's Turtles (*Emydoidea blandingii*) in a relatively pristine landscape. Ecoscience 17, 90–99. https://doi.org/10.2980/17-1-3317 ER

Enneson, J.J., Litzgus, J.D., 2009. Stochastic and spatially explicit population viability analyses for an endangered freshwater turtle, *Clemmys guttata*. Can. J. Zool. 87, 1241–1254. https://doi.org/10.1139/Z09-112

Enneson, J.J., Litzgus, J.D., 2008. Using long-term data and a stage-classified matrix to assess conservation strategies for an endangered turtle (*Clemmys guttata*). Biol. Conserv. 141, 1560–1568. https://doi.org/10.1016/j.biocon.2008.04.001

Environment and Climate Change Canada, 2020. Management Plan for the Snapping Turtle (*Chelydra serpentina*) in Canada.

Fahrig, L., 2007. Non-optimal animal movement in human-altered landscapes. Funct. Ecol. 21, 1003–1015. https://doi.org/10.1111/j.1365-2435.2007.01326.x ER

Fernández-Chacón, A., Bertolero, A., Amengual, A., Tavecchia, G., Homar, V., Oro, D., 2011. Spatial heterogeneity in the effects of climate change on the population dynamics of a Mediterranean Tortoise. Glob. Chang. Biol. 17, 3075–3088. https://doi.org/10.1111/j.1365-2486.2011.02469.x

Francis, E.A., Moldowan, P.D., Greischar, M.A., Rollinson, N., 2019. Anthropogenic nest sites provide warmer incubation environments than natural nest sites in a population of oviparous reptiles near their northern range limit. Oecologia 190, 511–522. https://doi.org/10.1007/s00442-019-04383-3

Galbraith, D.A., Bishop, C.A., Brooks, R.J., Simser, W.L., Lampman, K.P., 1988. Factors affecting the density of populations of Common Snapping Turtles (*Chelydra serpentina serpentina*). Can. J. Zool. 66, 1233–1240. https://doi.org/http://dx.doi.org/10.1139/z88-178

Galbraith, D.A., Brooks, R.J., 1987. Survivorship of adult females in a northern population of Common Snapping Turtles, *Chelydra serpentina*. Can. J. Zool. 65, 1581–1586. https://doi.org/http://dx.doi.org/10.1139/z87-247

Galbraith, D.A., Chandler, M.W., Brooks, R.J., 1987. The fine structure of home ranges of male *Chelydra serpentina*: Are Snapping Turtles territorial? Can. J. Zool. 65, 2623–2629. https://doi.org/http://dx.doi.org/10.1139/z87-398

Galbraith, D.A., White, B.N., Brooks, R.J., Boag, P.T., 1993. Multiple paternity in clutches of Snapping Turtles (*Chelydra serpentina*) detected using DNA fingerprints. Can. J. Zool. 71, 318–324. https://doi.org/10.1139/z93-044

Gallucci, V.F., Taylor, I.G., Erzini, K., 2006. Conservation and management of exploited shark populations based on reproductive value. Can. J. Fish. Aquat. Sci. 63, 931–942. https://doi.org/10.1139/f05-267

Gandon, S., 1999. Kin competition, the cost of inbreeding and the evolution of dispersal. J. Theor. Biol. 200, 345–364. https://doi.org/10.1006/jtbi.1999.0994

Gibbons, J.W., Greene, J.L., Congdon, J.D., 1983. Drought-related responses of aquatic turtle populations. J. Herpetol. 17, 242–246.

Greenwood, P.J., 1980. Mating systems, philopatry and dispersal in birds and mammals. Anim. Behav. 28, 1140–1162. https://doi.org/10.1016/S0003-3472(80)80103-5

Haas, H.L., 2010. Using observed interactions between sea turtles and commercial bottom-trawling vessels to evaluate the conservation value of trawl gear modifications. Mar. Coast. Fish. 2, 263–276. https://doi.org/10.1577/C09-013.1

Hamilton, W.D., May, R.M., 1977. Dispersal in stable habitats. Nature 269, 578–581.

Haxton, T., 2000. Road mortality of Snapping Turtles, *Chelydra sperpentina*, in central Ontario during their nesting period. Can. F. Nat. 114, 106–110.

Heppell, S.S., 1998. Application of life-history theory and population model analysis to turtle conservation. Copeia 1998, 367–375. https://doi.org/10.2307/1447430

Howell, H.J., Legere, R.H., Holland, D.S., Seigel, R.A., 2019. Long-term turtle declines: Protected is a verb, not an outcome. Copeia 107, 493–501. https://doi.org/10.1643/ch-19-177

Howell, H.J., Seigel, R.A., 2019. The effects of road mortality on small, isolated turtle populations. J. Herpetol. 53, 39. https://doi.org/10.1670/18-022

Jonsson, A., Ebenman, B., 2001. Are certain life histories particularly prone to local extinction? J. Theor. Biol. 209, 455–463. https://doi.org/10.1006/jtbi.2001.2280

Keevil, M.G., Armstrong, D.P., Brooks, R.J., Litzgus, J.D., 2021. A model of seasonal variation in somatic growth rates applied to two temperate turtle species. Ecol. Modell. 443, 109454. https://doi.org/10.1016/j.ecolmodel.2021.109454

Keevil, M.G., Brooks, R.J., Litzgus, J.D., 2018. Post-catastrophe patterns of abundance and survival reveal no evidence of population recovery in a long-lived animal. Ecosphere 9, e02396. https://doi.org/10.1002/ecs2.2396

Keevil, M.G., Hewitt, B.S., Brooks, R.J., Litzgus, J.D., 2017. Patterns of intraspecific aggression inferred from injuries in an aquatic turtle with male-biased size dimorphism. Can. J. Zool. 95, 393–403. https://doi.org/10.1139/cjz-2016-0182

Keevil, M.G., Lesbarrères, D., Noble, N., Boyle, S.P., Brooks, R.., Litzgus, J.D., 2023. Lost reproductive value reveals a high burden of juvenile road mortality in a long-lived species. Ecol. Appl. e2789. https://doi.org/10.1002/eap.2789

Keevil, M.G., Noble, N., Boyle, S.P., Lesbarrères, D., Brooks, R.J., Litzgus, J.D., 2022. Demographic characteristics of Snapping Turtles (*Chelydra serpentina*) observed on roads in Ontario, Canada. Figshare data repository. https://doi.org/10.6084/m9.figshare.19123163.v1

Kim, K., Serret, H., Clauzel, C., Andersen, D., Jang, Y., 2019. Spatio-temporal characteristics and predictions of the endangered Leopard Cat *Prionailirus bengalensis euptilura* road-kills in the Republic of Korea. Glob. Ecol. Conserv. 19, e00673. https://doi.org/10.1016/j.gecco.2019.e00673

Knoerr, M.D., Tutterow, A.M., Graeter, G.J., Pittman, S.E., Barrett, K., 2021. Population models reveal the importance of early life-stages for population stability of an imperiled turtle species. Anim. Conserv. 25, 53–64. https://doi.org/10.1111/acv.12718

Lambert, M.R., Steen, D.A., 2019. Reexamining effects of urbanization on population structure of freshwater turtles: response to Bowne et al. 2018. Conserv. Biol. 33, 1193–1196. https://doi.org/10.1111/cobi.13397

Laurance, W.F., Clements, G.R., Sloan, S., O'Connell, C.S., Mueller, N.D., Goosem, M., Venter, O., Edwards, D.P., Phalan, B., Balmford, A., Van Der Ree, R., Arrea, I.B., 2014. A global strategy for road building. Nature 513, 229–232. https://doi.org/10.1038/nature13717

Lesbarrères, D., Fahrig, L., 2012. Measures to reduce population fragmentation by roads: What has worked and how do we know? Trends Ecol. Evol. 27, 374–380. https://doi.org/10.1016/J.TREE.2012.01.015

Leturque, H., Rousset, F., 2004. Intersexual competition as an explanation for sex-ratio and dispersal biases in polygynous species. Evolution. 58, 2398–2408. https://doi.org/10.1554/04-186

Li, X.Y., Kokko, H., 2019a. Sex-biased dispersal: a review of the theory. Biol. Rev. 94, 721–736. https://doi.org/10.1111/brv.12475

Li, X.Y., Kokko, H., 2019b. Intersexual resource competition and the evolution of sex-biased dispersal. Front. Ecol. Evol. 7, 111. https://doi.org/10.3389/FEVO.2019.00111/BIBTEX

Lindström, J., 1998. Harvesting and sex differences in demography. Wildlife Biol. 4, 213–221. https://doi.org/10.2981/wlb.1998.024

Loehr, V.J.T., 2017. Unexpected decline in a population of Speckled Tortoises. J. Wildl. Manage. 81, 470–476. https://doi.org/10.1002/jwmg.21217

Mabry, K.E., Shelley, E.L., Davis, K.E., Blumstein, D.T., Van Vuren, D.H., 2013. Social mating system and sex-biased dispersal in mammals and birds: a phylogenetic analysis. PLoS One 8, e57980. https://doi.org/10.1371/journal.pone.0057980

Mali, I., Weckerly, F.W., Simpson, T.R., Forstner, M.R.J., 2016. Small scale-high resolution terrestrial activity of *Trachemys scripta elegans*, harvest intensity, and immediate movement responses following harvest events. Copeia 104, 677–682. https://doi.org/10.1643/ch-15-367

Marchand, M.N., Litvaitis, J.A., 2004. Effects of habitat features and landscape composition on the population structure of a common aquatic turtle in a region undergoing rapid development. Conserv. Biol. 18, 758–767.

Massemin, S., Maho, Y. Le, Handrich, Y., 1998. Seasonal pattern in age, sex and body condition of Barn Owls *Tyto alba* killed on motorways. Ibis. 140, 70–75. https://doi.org/10.1111/j.1474-919X.1998.tb04543.x

McCurdy-Adams, H.L., 2016. Anthropogenic effects on chronic stress and nest predation patterns in freshwater turtles. MSc Thesis. Laurentian University.

McGovern, P.A., Buhlmann, K.A., Todd, B.D., Moore, C.T., Peaden, J.M., Hepinstall-Cymerman, J., Daly, J.A., Tuberville, T.D., 2020. The effect of size on postrelease survival of head-started Mojave Desert Tortoises. J. Fish Wildl. Manag. 11, 494–506. https://doi.org/10.3996/JFWM-20-014

Murphy, R.E., Martin, A.E., Fahrig, L., 2022. Reduced predation on roadside nests can compensate for road mortality in road-adjacent turtle populations. Ecosphere 13, e3946. https://doi.org/10.1002/ECS2.3946

Ontario Ministry of Transportation, 2016. Provincial Highways Traffic Volumes 1988–2016. Ontario Ministry of Transportation.

Parvinen, K., Dieckmann, U., Gyllenberg, M., Metz, J.A.J., 2003. Evolution of dispersal in metapopulations with local density dependence and demographic stochasticity. J. Evol. Biol. 16, 143–153. https://doi.org/10.1046/j.1420-9101.2003.00478.x

Patrick, D., Gibbs, J.P., 2010. Population structure and movements of freshwater turtles across a road-density gradient. Landsc. Ecol. 25, 791–801. https://doi.org/10.1007/s10980-010-9459-0

Perrin, N., Mazalov, V., 2000. Local competition, inbreeding, and the evolution of sex-biased dispersal. Am. Nat. 155, 116–127. https://doi.org/10.1086/303296

Petrovan, S.O., Schmidt, B.R., 2019. Neglected juveniles; a call for integrating all amphibian life stages in assessments of mitigation success (and how to do it). Biol. Conserv. 236, 252–260. https://doi.org/10.1016/j.biocon.2019.05.023

Piczak, M.L., Markle, C.E., Chow-Fraser, P., 2019. Decades of road mortality cause severe decline in a Common Snapping Turtle (*Chelydra serpentina*) population from an urbanized wetland. Chelonian Conserv. Biol. 18, 231–240. https://doi.org/10.2744/CCB-1345.1

Pike, D.A., Pizzatto, L., Pike, B.A., Shine, R., 2008. Estimating survival rates of uncatchable animals: the myth of high juvenile mortality in reptiles. Ecology 89, 607–611. https://doi.org/10.2307/27651583

R Development Core Team, 2020. R: A language and environment for statistical computing.

Rankin, R.W., Nicholson, K.E., Allen, S.J., Krützen, M., Bejder, L., Pollock, K.H., 2016. A full-capture hierarchical Bayesian model of Pollock's closed robust design and application to dolphins. Front. Mar. Sci. 3, 25. https://doi.org/10.3389/fmars.2016.00025

Riley, J.L., Litzgus, J.D., 2014. Cues used by predators to detect freshwater turtle nests may persist late into incubation. Can. Field-Naturalist 128, 179. https://doi.org/10.22621/cfn.v128i2.1583

Riley, J.L., Litzgus, J.D., 2013. Evaluation of predator-exclusion cages used in turtle conservation: Cost analysis and effects on nest environment and proxies of hatchling fitness. Wildl. Res. 40, 499–511. https://doi.org/10.1071/WR13090

Rittenhouse, T.A.G., Semlitsch, R.D., Thompson, F.R., 2009. Survival costs associated with wood frog breeding migrations: effects of timber harvest and drought. Ecology 90, 1620–1630. https://doi.org/10.1890/08-0326.1

Roosenburg, W.M., Cresko, W., Modesitte, M., Robbins, M.B., 1997. Diamondback Terrapin (*Malaclemys terrapin*) mortality in crab pots. Conserv. Biol. 11, 1166–1172. https://doi.org/10.1046/j.1523-1739.1997.95443.x

Rouleau, C.J., Massey, M.D., Rollinson, N., 2019. Temperature does not affect hatch timing in Snapping Turtles (*Chelydra serpentina*). J. Herpetol. 53, 165–169.

Rueda-Cediel, P., Anderson, K.E., Regan, T.J., Franklin, J., Regan, H.M., 2015. Combined influences of model choice, data quality, and data quantity when estimating population trends. PLoS One 10, e0132255. https://doi.org/10.1371/journal.pone.0132255

Rytwinski, T., Fahrig, L., 2013. Why are some animal populations unaffected or positively affected by roads? Oecologia 173, 1143–1156. https://doi.org/10.1007/s00442-013-2684-x

Rytwinski, T., Fahrig, L., 2012. Do species life history traits explain population responses to roads? A meta-analysis. Biol. Conserv. 147, 87–98. https://doi.org/10.1016/j.biocon.2011.11.023

Rytwinski, T., van der Ree, R., Cunnington, G.M., Fahrig, L., Findlay, C.S., Houlahan, J., Jaeger, J.A.G., Soanes, K., van der Grift, E.A., 2015. Experimental study designs to improve the evaluation of road mitigation measures for wildlife. J. Environ. Manage. 154, 48–64. https://doi.org/10.1016/J.JENVMAN.2015.01.048

Salice, C.J., Rowe, C.L., Eisenreich, K.M., 2014. Integrative demographic modeling reveals population level impacts of PCB toxicity to juvenile Snapping Turtles. Environ. Pollut. 184, 154–160. https://doi.org/10.1016/j.envpol.2013.08.031

Saumure, R.A., Bider, J.R., 1998. Impact of agricultural development on a population of Wood Turtles (*Clemmys insculpta*) in southern Quebec, Canada. Chelonian Conserv. Biol. 3, 37–45.

Sergio, F., Tavecchia, G., Blas, J., Tanferna, A., Hiraldo, F., 2021. Demographic modeling to fine-tune conservation targets: Importance of pre-adults for the decline of an endangered raptor. Ecol. Appl. e2266. https://doi.org/10.1002/eap.2266

Steen, D.A., Aresco, M.J., Beilke, S.G., Compton, B.W., Condon, E.P., Dodd Jr., C.K., Forrester, H., Gibbons, J.W., Greene, J.L., Johnson, G., Langen, T.A., Oldham, M.J., Oxier, D.N., Saumure, R.A., Schueler, F.W., Sleeman, J.M., Smith, L.L., Tucker, J.K., Gibbs, J.P., 2006. Relative vulnerability of female turtles to road mortality. Anim. Conserv. 9, 269–273. https://doi.org/10.1111/j.1469-1795.2006.00032.x

Steen, D.A., Gibbs, J.P., 2004. Effects of roads on the structure of freshwater turtle populations. Conserv. Biol. 18, 1143–1148. https://doi.org/10.1111/j.1523-1739.2004.00240.x

Steen, D.A., Gibbs, J.P., Buhlmann, K.A., Carr, J.L., Compton, B.W., Congdon, J.D., Doody, J.S., Godwin, J.C., Holcomb, K.L., Jackson, D.R., Janzen, F.J., Johnson, G., Jones, M.T., Lamer, J.T., Langen, T.A., Plummer, M. V., Rowe, J.W., Saumure, R.A., Tucker, J.K., Wilson, D.S., 2012. Terrestrial habitat requirements of nesting freshwater turtles. Biol. Conserv. 150, 121–128. https://doi.org/10.1016/j.biocon.2012.03.012

Steen, D.A., Smith, L.L., 2006. Road surveys for turtles: Consideration of possible sampling biases. Herpetol. Conserv. Biol. 1, 9–15.

Sterrett, S.C., Katz, R.A., Fields, W.R., Campbell Grant, E.H., 2019. The contribution of road-based citizen science to the conservation of pond-breeding amphibians. J. Appl. Ecol. 56, 988–995. https://doi.org/10.1111/1365-2664.13330

Storm, G.L., Andrews, R.D., Phillips, R.L., Bishop, R.A., Siniff, D.B., Tester, J.R., 1976. Morphology, reproduction, dispersal, and morality of midwestern Red Fox populations. Wildl. Monogr. 49, 3–82.

Stubben, C., Milligan, B., 2007. Estimating and analyzing demographic models using the popbio package in R. J. Stastistical Softw. 22, 1–23. https://doi.org/10.18637/jss.v022.i11

Trochet, A., Courtois, E.A., Stevens, V.M., Baguette, M., Chaine, A., Schmeller, D.S., Clobert, J., Wiens, J.J., 2016. Evolution of sex-biased dispersal. Q. Rev. Biol. 91, 297–320. https://doi.org/10.1086/688097

Tuberville, T.D., Gibbons, J.W., Greene, J.L., 1996. Invasion of new aquatic habitats by male freshwater turtles. Copeia 1996, 713–715. https://doi.org/10.1175/1520-0469(1960)017<0084:sc>2.0.co;2

Tucker, A.D., McCallum, H.I., Limpus, C.J., McDonald, K.R., 1998. Sex-biased dispersal in a long-lived polygynous reptile (*Crocodylus johnstoni*). Behav. Ecol. Sociobiol. 44, 85–90. https://doi.org/10.1007/s002650050519

Wallace, B.P., Heppell, S.S., Lewison, R.L., Kelez, S., Crowder, L.B., 2008. Impacts of fisheries bycatch on Loggerhead Turtles worldwide inferred from reproductive value analyses. J. Appl. Ecol. 45, 1076–1085. https://doi.org/10.1111/j.1365-2664.2008.01507.x

Warden, M.L., Haas, H.L., Rose, K.A., Richards, P.M., 2015. A spatially explicit population model of simulated fisheries impact on Loggerhead Sea Turtles (*Caretta caretta*) in the Northwest Atlantic Ocean. Ecol. Modell. 299, 23–39. https://doi.org/10.1016/J.ECOLMODEL.2014.11.025

Tables

Table 4.1. Juvenile Snapping Turtles killed on roads and dissected to determine sex (male (M), female (F), or unknown (U)) tabulated by collection area: Algonquin Provincial Park (APP), Eastern Ontario (EON), Hwy 69/400 in the eastern Georgian Bay region, the Muskoka region, and Presqu'ile Provincial Park (PQP).

Site	F	M	U	Total
APP	7	8	19	34
EON	0	2	1	3
Hwy69/40	6	4	6	16
Muskoka	7	3	16	26
PQP	6	8	29	43
Total	26	25	71	122

Table 4.2. Snapping Turtles (*Chelydra serpentina*) observed on roads in Algonquin Provincial Park (APP) and Presqu'ile Provincial Park (PQP) tabulated by coarse demographic category (adult male = AdM, adult female = AdF, or juvenile = Juv) and whether they were alive (AOR) or dead-on-road (DOR). Nesting females are included. At both sites, the proportion observed as DOR differed significantly among categories (Fisher's exact tests).

Site	**Juv**		**AdF**		**AdM**		***P***
	AOR	**DOR**	**AO**	**DOR**	**AOR**	**DOR**	
APP	45	39	75	2	3	0	<0.001
PQP	59	44	176	1	13	0	<0.001

Figures

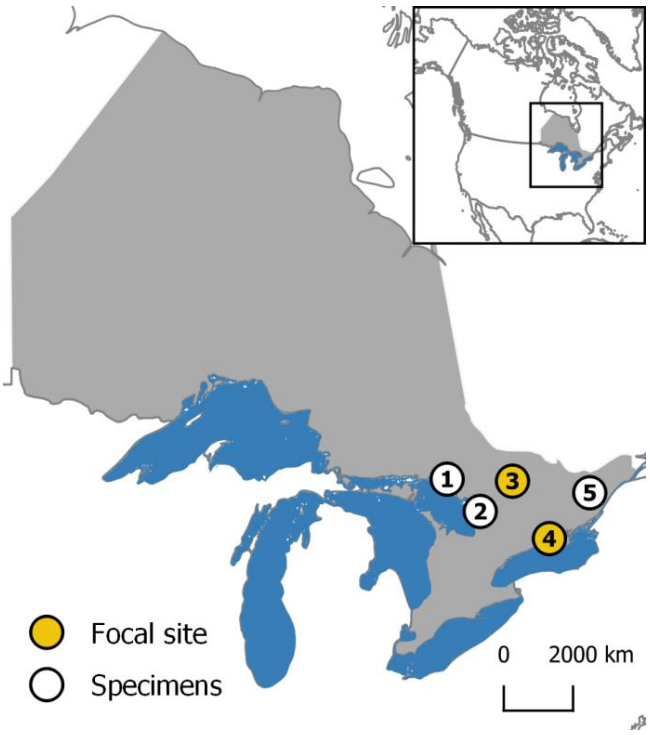

Figure 4.1. Study sites in Ontario, Canada where juvenile Snapping Turtle (Chelydra serpentina) carcasses were collected during road surveys: 1. Eastern Georgian Bay, 2. Muskoka, 3. Algonquin Provincial Park (APP), 4. Presqu'ile Provincial Park (PQP), 5. Eastern Ontario. Carcasses were used to estimate sex ratio of juveniles killed on roads. At the two focal sites (yellow dots), we analyzed demographic data for all live and dead individuals observed on roads.

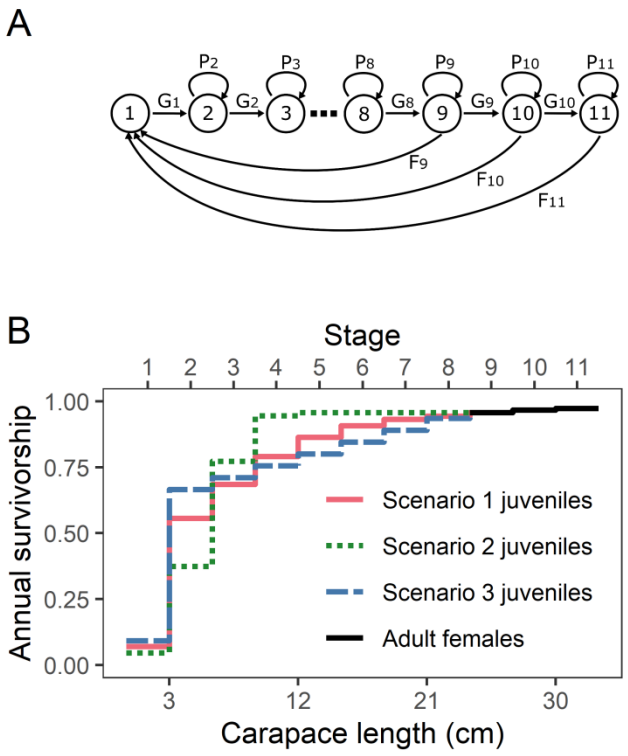

Figure 4.2. A) Life-cycle graph for stage-based matrix models of Snapping Turtles (*Chelydra serpentina*) in Algonquin Provincial Park. Stage 1: egg/hatchling; Stages 2–8: growth to maturity; Stages 9–11: mature females. Stages 2–11 are variable-duration 3 cm carapace length (CL) size classes. Arcs are G_i = probability of growth from stage i to $i + 1$, P_i = probability of remaining in i, and F_i = fertility of stage i. B) Stage-based survival under three juvenile survival scenarios. Stage 1 is the product of nest survival, hatching success, and scenario-specific hatchling survival and has duration of 1 year. Survival of mature females (CL > 24 cm) is independent of scenario.

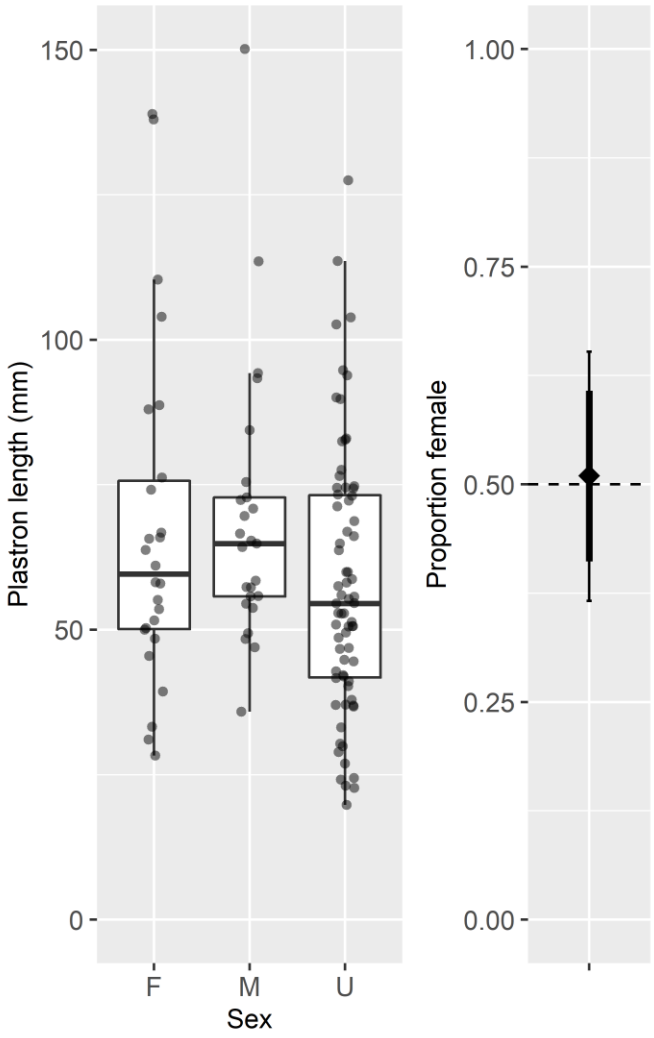

Figure 4.3. Sex ratios and size distributions of road-killed juvenile Snapping Turtles dissected to determine sex. Observed sizes are plotted as points (jittered horizontally for visibility) and size distributions are summarized with box plots showing the median, inter-quartile range, and range (excluding outliers). Error bars on the sex ratio denote 95% (thin line) and 80% (thick line) binomial likelihood confidence intervals.

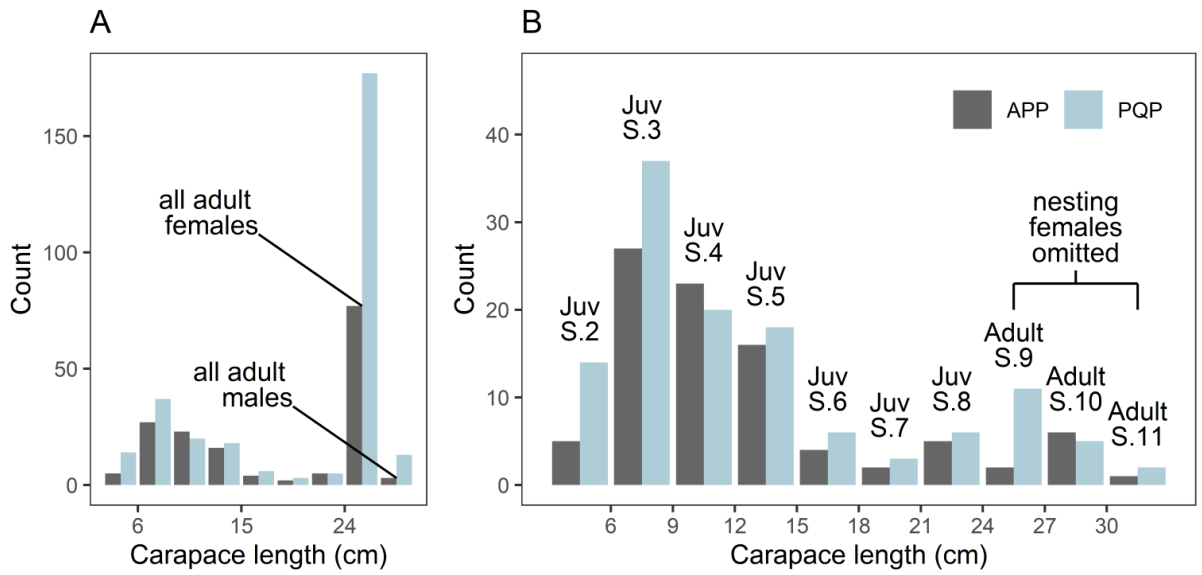

Figure 4.4. Demographic distributions of Snapping Turtles (*Chelydra serpentina*) observed on roads at two sites in Ontario. A) Juveniles partitioned by size and adults by sex (including nesting females). B) Adults and juveniles partitioned by size. Nesting females—71 out of 164 total observations in Algonquin Provincial Park (APP), 171 out of 293 in Presqu'ile Provincial Park (PQP)—are omitted from panel B to facilitate comparisons among other stages. Bar labels indicate matrix model stages (S). In PQP, eight nesting females with carapace length < 24 cm were assigned as adults (S.9). Hatchlings less than one year old (S.1) were omitted from both panels.

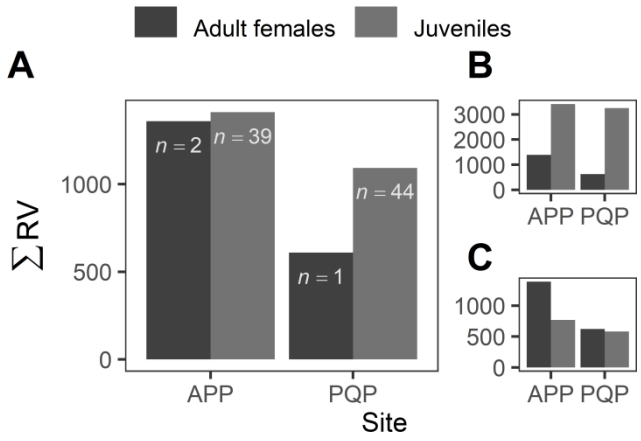

Figure 4.5. Cumulative reproductive value (RV) of Snapping Turtles (*Chelydra serpentina*) killed on roads in Algonquin Provincial Park (APP; 2013–2015) and Presqu'ile Provincial Park (PQP; 2013–2017). RV was calculated using A) the APP intermediate juvenile survival scenario 1; B) scenario 2, which has an abrupt increase in survival with size; and C) scenario 3, which has a gradual, linear relationship between juvenile size and survival (Figure D.1). RV is scaled relative to one female egg (RV = 1) and was set to 0 for males, which are not plotted, and discounted by half for juveniles of unknown sex.

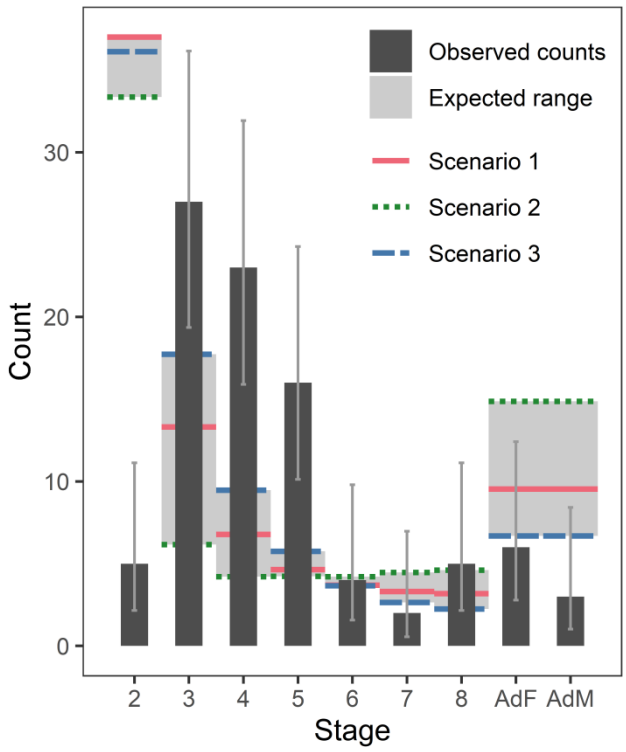

Figure 4.6. Snapping Turtles (*Chelydra serpentina*) by demographic stage expected and observed on roads in Algonquin Provincial Park 2013–2015. The first stage (egg/hatchling) is excluded, three adult female (AdF) size classes are pooled, and expected counts for juvenile stages 2–8 and adult males (AdM) are adjusted to include males by assuming a 1:1 sex ratio. N = 93 after excluding 71 females that were observed during nesting season. Expected range was calculated from stable stage distributions of a matrix population model using three different scenarios of juvenile survivorship (see text). Error bars indicate 95% binomial confidence intervals scaled relative to the total number observed.

General Discussion and Conclusion

Chapter summaries

Each of the chapters of this dissertation investigate demographic and behavioural aspects of the ecology and life history of Snapping Turtles (*Chelydra serpentina*) by building upon the previous body of work comprising the long-term Snapping Turtle life-history project in Algonquin Provincial Park (APP).

Chapter 1 summary

The first chapter (Keevil et al., 2018) examined population response to a catastrophic perturbation—a mass mortality of adult turtles caused by River Otter (*Lontra canadensis*) predation during overwintering—using a mark-recapture approach to analyze survivorship and abundance before, during, and after the mortality event. I focused on adult females nesting at the Lake Sasajewun dam or at nearby alternate sites from 1980 to 2013. I employed a Bayesian framework using a multi-state design to account for switching between nesting areas and temporary emigration due to skipped reproduction or use of nesting sites outside the study area. During the three years of the predation event, annual survivorship declined from 0.94 to 0.76 for females nesting at the dam, and from 0.94 to 0.86 for females using alternate sites, which resulted in a population decline of 36% overall, and 49% at the dam nesting site. Mean total abundance (combining both sites) was 42 females over the five years following the catastrophe (1989–1993). During the most recent five years analyzed (2009–2013), mean abundance was 40 females, indicating a lack of recovery over the 23 years following the mortality event.

Abundance in Lake Sasajewun itself was assessed using aquatic survey observations collected during hoop trapping and canoe-capture surveys. I used a simple robust design mark-recapture

approach to analyze observations of male and female adult Snapping Turtles from 2009 to 2013. Mean abundance was 13 for males and 10 for females, which indicates that abundance in the lake, like that at the nesting sites, showed no recovery relative to abundance observed by Brooks et al. (1991) who estimated 31 adults remained immediately following the mortality event. Assessing aquatic habitats served to demonstrate that the broad abundance trend was consistent across survey methods and sex, and therefore is not likely to be confounded by changes in the use of particular nest sites.

Chapter 2 summary

Mating systems are linked to many other aspects of ecology and life history, including spatial ecology and dispersal (Dobson, 1982; Greenwood, 1980), growth, maturity, and survivorship (Golubovic et al., 2018; Toïgo and Gaillard, 2003). However, the mating system of Snapping Turtles has received little empirical investigation and remains poorly known, so I pursued this topic in Chapter 2 (Keevil et al., 2017). Multiple hypotheses have been applied to explain observations of sexual size dimorphism and intraspecific interactions observed opportunistically in the wild. In particular, male-biased size dimorphism has been explained as an adaptation for coercive mating (Berry and Shine, 1980), male combat (Kiviat, 1980), or due to earlier maturation and the cost of reproduction for females (Gibbons and Lovich, 1990; Lovich et al., 2014). Because Snapping Turtle behaviour is difficult to observe in natural habitats, I attempted to resolve these ambiguities by inferring aspects of interspecific interactions indirectly using wounds observed on captured individuals.

A preliminary step in this investigation was quantifying sexual size dimorphism, which I explored using both body mass and straight-line carapace length (CL) to calculate and index of sexual dimorphism (Lovich and Gibbons, 1992). I found that adult body size had more variation

in males than in females because males matured at a smaller size but grew to a larger size, and that population-scale size dimorphism was substantially male biased.

I developed predictions for multiple hypotheses of the relationship between sex, size, and wounding probability by formulating these as models that could be tested using an information-theoretic model selection. Hypotheses differed in their predicted distribution of wounds across sex and body size. Male-biased wounding is predicted if mating is mediated primarily by male-male combat (Baxter-Gilbert and Whiting, 2019; Brown et al., 2022) as opposed to coercion by males, which results in female-biased wounding (Golubovic et al., 2018; Moldowan et al., 2020). In many taxa, wound frequencies are similar in males and females (Brown et al., 2022), suggesting similar rates of agonistic encounters that may be related to resource competition or to the presence of both competitive and coercive behaviours (Burgess et al., 2013; Scott et al., 2005).

Observations were scored in collaboration with Brittainy Hewitt, who presented a preliminary analysis in an undergraduate thesis, using photos and field notes collected during 2009–2013. We parameterized injury observations as a wounded/not wounded binomial variable. While some wounds were observed on females, most occurred on males despite the preponderance of female observations in the dataset. I conducted the final analysis in a Bayesian framework, so that juveniles with missing sex could be included by defining a Bayesian prior on sex. Model selection revealed strong support for sex and size effects, and indicated that males were far more likely to be wounded than females and juveniles, and that wounding probability was low for small males and increased with size with no evidence for a decline at the largest sizes. These results are consistent with a hypothesis that agonistic interactions occur primarily between males

(but not exclusively so) and that mate competition is more intense for larger males, suggesting some ability for large males to monopolize mating opportunities.

Chapter 3 summary

Somatic growth interacts dynamically with other components of life history that include age and size at maturity, and helps determine survival to first reproduction, fecundity, and generation time (Armstrong et al., 2018; Congdon et al., 2018; Shine and Iverson, 1995). Because somatic growth is intrinsically linked to population growth by its effect on vital rates, accurate and precise somatic growth modelling is an important component for parameterizing demographic models that inform broad-scale assessments of ecological or conservation problems, so improving growth model precision was the objective I pursued in Chapter 3 (Keevil et al., 2021).

Snapping Turtles in APP experience a strongly seasonal climate, and growth will therefore vary seasonally. Individuals may be observed at any point during the active season, which means that growth interval lengths vary in both absolute duration and seasonal timing. Accounting for this required a model of the relative effect of season on growth rate.

My initial assessment of seasonal growth patterns was made using a sample of 11 juvenile Snapping Turtles that I tracked by radio telemetry so that they could be measured multiple times during the active season. These data revealed that absolute growth across the active season varied substantially among individuals but that relative growth rate was approximately sigmoidal. I developed a new model to account for this seasonal constraint on growth, which I called the logistic growth phenology model (GPM). The GPM can be conceived of as a model of effective growth time because it estimates the point of the year when any arbitrary fraction of annual growth has accumulated. This insight allowed me to incorporate the GPM into any model of overall somatic growth, such as the von Bertalanffy model, by using the GPM to transform the

time term(s). One advantage of this approach is that the parameters can be made to correspond to simple biological concepts, which not only aids in interpretation, but also makes it possible to propose informative Bayesian priors based on existing knowledge.

A potential issue for my initial formulation of the logistic GPM is that it does not necessarily approach 0 and 1 at the start and end, respectively, of each year. Although this effect is likely to be negligible over the parameter space that I explored in this application, in other circumstances it could be problematic. Therefore, I added a step to the logistic GPM function to scale the results so to intersect 0 and 1. A second solution was to use the cumulative distribution function for the beta distribution (beta CDF) instead of the logistic function in the GPM. I explored both avenues.

I applied a combined logistic GPM and von Bertalanffy model to observations juvenile Painted Turtles (*Chrysemys picta*) in APP to assess the ability of the combined model to be fitted to a dataset that had few observations of intra-annual growth intervals. Because individuals were rarely observed more than once per year, seasonal information in that dataset was limited primarily to the effect of inconsistent seasonal timing of capture in different years and to the information included in the priors. Despite the fact that the data were collected with no intention of informing seasonal growth effect estimation, the seasonal model parameters were seemingly estimated, although with less precision than was the case for radio-tracked Snapping Turtles with repeated intra-annual observations.

I repeated the analysis of the Painted Turtle dataset using the beta CDF as the basis for the GPM and recovered very similar growth phenology estimates. Although the two models achieved similar results in this application, in other circumstances one approach may be more preferable than the other under depending on whether the shape of GPM is expected to be symmetrical or if

a prior is elicited more easily based on the timing of maximal seasonal growth rate or based on the midpoint of growth accumulation.

Modelling Snapping Turtle growth with a joint von Bertalanffy and seasonal model

Estimating rate and variability of fine-scale demographic stage transitions requires an individually varying model of somatic growth. Therefore, I developed a model of somatic growth that builds upon previous analyses of Snapping Turtle growth in APP (Armstrong and Brooks, 2014, 2013) by including more observations and by improving the precision and accuracy of model predictions by accounting for seasonality using the beta GPM that I developed in Chapter 3. I used the top model selected by Armstrong and Brooks (2013), but expanded the amount of data by including observations collected up to 2018 (Armstrong and Brooks (2014, 2013) fit data collected up to 2005) and I entered records from pre-2000 datasheets that had not been previously included in the database and which were primarily observations of juveniles. In combination, these updates resulted in more than a 50% increase in both the number of individuals and the number of observations, over almost twice as many 'turtle years', and 2.6 times more observed growth.

The seasonal model parameters were successfully estimated and all the von Bertalanffy parameters, which were common to both the Armstrong and Brooks (2013) and my updated model, were estimated with higher precision in the updated model. The most appreciable difference was that the population-level mean growth rate parameter was higher and the estimated amount of individual variation was lower. This resulted in an estimated female median age at maturity of 17.4 years, 10.6 years younger with the updated data and model than the original estimate of Armstrong and Brooks (2013).

Chapter 4 summary

In Chapter 4 (Keevil et al., 2023), I integrated the results and methods from the previous three chapters into an investigation of how relative road encounter and mortality risk differed among Snapping Turtle demographic stages, and compared the road mortality burden across stages that differ in reproductive value (RV; expected contribution of individuals to population growth based on their demographic class; Caswell, 2001). Carcasses of road-killed juvenile Snapping Turtles were collected and dissected to determine sex. Natasha Noble dissected these specimens and presented a preliminary analysis in her undergraduate thesis; she found that the sex ratio of juveniles killed on roads was essentially even (26 females, 25 males). This chapter also included observations of alive-on-road and dead-on-road Snapping Turtles that were collected as components of other projects.

I constructed a variable-duration stage-based matrix demographic model to calculate RV and estimate the stage distribution. The model used 11 stages, with the first stage defined as an egg or hatchling less than one year of age and each subsequent stage defined as a 3 cm carapace length classes. To parameterize stage transitions, I used results from earlier chapters (growth rate and adult female survivorship) and other previously published analyses from the APP long term project (adult female survivorship, fecundity, nest survival and hatching success). In 2014 and 2015, I monitored nest survival at several sites in APP and these previously unpublished data also informed the model.

There were no size-specific estimates of juvenile Snapping Turtle survival available. Therefore, I generated a range of plausible survivorship values for each juvenile stage by proposing three scenarios for the relationship between size and survivorship and used these scenarios to interpolate missing survivorship values. The scenarios were constrained to be consistent with a

stable population (i.e., $\lambda = 1$) and so that juvenile survival approached adult survival as juveniles approached adult size.

I compared the demographic distribution of Snapping Turtles on roads in APP to the expected distribution predicted for the population based on the stable stage distribution calculated from the matrix model for each juvenile survival scenario. Interestingly, juveniles were much less likely to be observed alive on roads than adults. Observed road mortalities in each demographic stage were weighted by RV to compare cumulative impact among demographic categories. The total cumulative RV lost due to road mortality of juveniles was greater than, or similar to, the total RV lost due to adult mortality. Adult females are critical for population persistence, and adult mortality is frequently the focus of freshwater turtle road ecology (Crawford et al., 2018; Murphy et al., 2022), so finding that juvenile road mortality represents a burden of similar magnitude has important implications for future studies and mitigation planning.

Uniting themes across chapters

In Chapter 4 I investigated the demographic distribution of Snapping Turtles on roads and used a matrix population model to estimate the relative road mortality burden across demographic classes. The matrix model was parameterized, in part, using survivorship estimates from Chapter 1 and growth rate and variability based on the growth modelling developed in Chapter 3. My predictions for the demographic distribution of individuals encountering roads were based, in part, on hypotheses informed by the mating system inferred in Chapter 2.

The lack of recovery following catastrophe that was revealed by the Chapter 1 analyses suggests weak or absent density dependent compensation. This was predicted by Brooks et al. (1991) based on constraints that limited the amount of compensation that would be feasible for relevant vital rates. In particular, adult survivorship in non-catastrophe years was already high with little

room to respond (Cunnington and Brooks, 1996), and growth, fertility, and nest survival are limited by the cool climate and short growing season. However, compensatory, density-dependent dispersal is a conceivable mechanism for population recovery that was not realized, despite apparent opportunities. In particular, Lake Sasajewun and adjacent nest sites are situated along the North Madawaska River and tributaries, which connect multiple habitat patches via routes that nesting females frequently traverse (Obbard and Brooks, 1980). Additionally, adults switching to new nest sites occurred with some frequency, estimated as the state transition probability in the multistate analysis in Chapter 1. Anecdotally, some individuals have been observed to switch between sites separated by several kilometers. Apparently transient nesters—individuals that are only observed nesting once—are not uncommon (Brooks et al., 1991).

Because apparent dispersal was observed but failed to mitigate local decline, I hypothesized that dispersal was not conditional on density, and proceeded to consider unconditional dispersal and the circumstances of ecology and life history that might imply. The development of dispersal theory has suggested a limited number of selective forces that favour unconditional, individually costly dispersal. These include inbreeding avoidance and kin competition for resources (local resource competition) and mates (local mate competition). However, the relative role of these factors in the evolution of dispersal is closely tied to mating system (Dobson, 1982; Greenwood, 1980), which has not been well studied in Snapping Turtles. I approached this question in Chapter 2 by analyzing sexual size dimorphism and the demographic distribution of wounding probability to make inferences about the Snapping Turtle mating system. I observed strongly male-biased sexual size dimorphism and a demographic pattern of wounding suggesting that intense agonistic interactions primarily involved larger males, implying a high level of male mate competition.

The prominence of male mate competition informed my hypothesis of sex-biased dispersal, which I applied in Chapter 4 to make predictions about the demography of individuals encountering roads during overland movement. Inbreeding avoidance promotes sex-biased dispersal but does not intrinsically determine the more dispersive sex (Gandon, 1999; Li and Kokko, 2019; Perrin and Mazalov, 2000). Theory suggests that dispersal will be biased towards the sex experiencing the most intense local kin competition (Leturque and Rousset, 2004; Perrin and Mazalov, 2000). I hypothesized that dispersal is adaptive because it alleviates local kin competition for mates and, therefore, I predicted that natal dispersal would be male biased and deferred until males approached sexual maturity. Neither of these predictions was supported, and the observed unbiased dispersal of comparatively young juveniles instead suggests that local kin competition for resources mediates dispersal.

Conservation implications

Lack of recovery following catastrophe

Turtles' slow life history, low and variable juvenile recruitment, and reliance on high adult survivorship makes them vulnerable to anthropogenic threats resulting in turtles being disproportionately imperilled (Böhm et al., 2013; Gibbons et al., 2000; McCallum, 2021; Stanford et al., 2020).

Adult female survivorship is typically the most sensitive vital rate among turtle populations (Congdon et al., 1994; Cunnington and Brooks, 1996; Enneson and Litzgus, 2008). This is typical for populations with slow life histories, which are very sensitive to changes in adult survivorship (Jonsson and Ebenman, 2001) and are slower to recover from depletion (Hutchings and Reynolds, 2004; Neubauer et al., 2013; Roff, 2002). Following the Otter mortality event that approximately halved the adult Snapping Turtle population at Lake Sasajewun, Brooks et al.

(1991) predicted that recovery would be extremely slow. Conversely, species with slower life histories may have stronger per-generation strength of density-dependent compensation as observed in birds (Sæther et al., 2005), marine fishes (Bjørkvoll et al., 2012), and freshwater fishes (Vélez-Espino and Koops, 2012). However, up to the last year analyzed (2013, 23 years after the mortality event) little recovery of adult abundance was evident.

The pattern of recovery following the Otter mortality event was confounded by a second, lesser, mortality event caused by flooding, dam failure, and an abrupt draw down of the water in Lake Sasajewun. While the dam was an anthropogenic structure, failure of beaver dams is not infrequent and can result in similar drawdowns affecting sizable areas of habitat. The occurrence of a second even illustrates that, while infrequent and stochastic, potentially catastrophic events are an important consideration for conservation planning. While their timing is unpredictable, the fact that catastrophes occur is an important facet of population ecology. The probability of catastrophes in vertebrate populations has been estimated as 14% per generation (Gerber and Hilborn 2001, Reed et al. 2003, Ward et al. 2007) and they have a disproportionately large impact on population persistence and may be the most important factor driving local extinctions (Mangel and Tier, 1994; Menges, 1990)

The frequency of immigration to this population has not clearly compensated for the decreased abundance despite being well connected to other patches. This suggests that movement between patches did not mitigate local depletion. This is concerning because managers of commercially exploited Snapping Turtle populations have assumed that localized depletion will be compensated for by *ex situ* recruitment from less exploited patches (Cain, 2010).

This study provided a unique opportunity to empirically test the ability of a turtle population to recover over a long time series following a perturbation. I did not find convincing evidence of

timely recovery, and the second mortality event suggests an apparent risk of additional catastrophes. These results strongly support prioritizing protection of existing populations rather than relying on recovery after declines have already occurred. In this case the perturbation was a natural catastrophe, but the slow or absent recovery also has implications for populations recovering following acute or chronic anthropogenic threats.

Juvenile road mortality

Because of the sensitivity of turtle populations to adult female mortality, and because females of many species frequently encounter roads during nesting (Steen et al., 2006), mortality of nesting females has been a focus of conservation and road ecology studies of freshwater turtles (Aresco, 2005; Crawford et al., 2018; Murphy et al., 2022). However, I found that a large proportion of Snapping Turtles observed on roads were juveniles, and these were much more likely to be dead than adult females were, and so juveniles made up a large majority of turtles that were found dead on roads. Although individual RV of adult females was much higher than for juveniles in size classes that were most frequently encountered, the cumulative RV of juveniles lost to road mortality rivalled or exceeded that of adults. Sex-biased road mortality has been implicated as a cause of sex bias in road-adjacent turtle populations, which is itself often interpreted as a proxy or indicator of road effects (Patrick and Gibbs, 2010; Steen et al., 2006; Steen and Gibbs, 2004). However, some recent studies have not detected such sex bias (Bowne et al., 2018; Carstairs et al., 2018; Vanek and Glowacki, 2019) or have obtained ambiguous results (Piczak et al., 2019). Conflicting results have recently stirred controversy (Bowne et al., 2019; Lambert and Steen, 2019). High rates of juvenile mortality that is not sex-biased, as we observed, could potentially overwhelm any signal of sex bias caused by biased adult road mortality. Importantly, high juvenile mortality implies more severe road impacts on populations while simultaneously

obscuring the detectability of effects of biased adult mortality. Therefore, failure to detect biased sex ratios does not, on its own, suggest absence of a strong road mortality effect.

Conclusions

Organisms with slow life histories are subjected to impacts that are realized over longer time scales caused by either chronic effects that manifest gradually, or by intermittent perturbations widely spaced in time. Long-term field studies are needed to reveal the effects of both chronic threats (Garber and Burger, 1995; Howell and Seigel, 2019; Piczak et al., 2019) and infrequent events (Fleischer et al., 2017) and to assess population responses (Keevil et al., 2018; Mullin et al., 2020).

Even with the benefit of long-term field studies, understanding behavioural ecology and quantifying life-history traits of cryptic, long-lived organisms remains challenging but this information is necessary to assess threats and implement conservation action. I approached data gaps using several strategies. I made inferences about the Snapping Turtle mating system using indirect evidence in the form of wounding patterns, I used opportunistic observations of road-killed turtles to estimate the sex ratio of dispersing juveniles killed on roads, and I used deterministic modelling to interpolate juvenile survivorship. Finally, I integrated this information into a demographic model that I applied to estimate the relative effects of road mortality across demographic classes and that revealed unexpected importance of juveniles to the overall road mortality burden.

References

Aresco, M.J., 2005. The effect of sex-specific terrestrial movements and roads on the sex ratio of freshwater turtles. Biol. Conserv. 123, 37–44. https://doi.org/10.1016/j.biocon.2004.10.006

Armstrong, D.P., Brooks, R.J., 2014. Estimating ages of turtles from growth data. Chelonian Conserv. Biol. 13, 9–15. https://doi.org/http://dx.doi.org/10.2744/CCB-1055.1

Armstrong, D.P., Brooks, R.J., 2013. Application of hierarchical biphasic growth models to long-term data for Snapping Turtles. Ecol. Modell. 250, 119–125. https://doi.org/10.1016/j.ecolmodel.2012.10.022

Armstrong, D.P., Keevil, M.G., Rollinson, N., Brooks, R.J., 2018. Subtle individual variation in indeterminate growth leads to major variation in survival and lifetime reproductive output in a long-lived reptile. Funct. Ecol. 32, 752–761. https://doi.org/10.1111/1365-2435.13014

Baxter-Gilbert, J.H., Whiting, M.J., 2019. Street fighters: Bite force, injury rates, and density of urban Australian Water Dragons (*Intellagama lesueurii*). Austral Ecol. 44, 255–264. https://doi.org/10.1111/aec.12670

Berry, J.F., Shine, R., 1980. Sexual size dimorphism and sexual selection in turtles (Order Testudines). Oecologia 44, 185–191. https://doi.org/http://dx.doi.org/10.1007/BF00572678

Bjørkvoll, E., Grøtan, V., Aanes, S., Sæther, B.-E., Engen, S., Aanes, R., 2012. Stochastic population dynamics and life-history variation in marine fish species. Am. Nat. 180, 372–387. https://doi.org/10.1086/666983

Böhm, M., Collen, B., Baillie, J.E.M., Bowles, P., Chanson, J., Cox, N., Hammerson, G., et al. 2013. The conservation status of the world's reptiles. Biol. Conserv. 157, 372–385. https://doi.org/10.1016/j.biocon.2012.07.015

Bowne, D.R., Cosentino, B.J., Anderson, L.J., Bloch, C.P., Cooke, S., Crumrine, P.W., Dallas, J., Doran, A., Dosch, J.J., Druckenbrod, D.L., Durtsche, R.D., Garneau, D., Genet, K.S.,

Fredericksen, T.S., Kish, P.A., Kolozsvary, M.B., Kuserk, F.T., Lindquist, E.S., Mankiewicz, C., March, J.G., Muir, T.J., Murray, K.G., Santulli, M.N., Sicignano, F.J., Smallwood, P.D., Urban, R.A., Winnett-Murray, K., Zimmermann, C.R., 2018. Effects of urbanization on the population structure of freshwater turtles across the United States. Conserv. Biol. 32, 1150–1161. https://doi.org/10.1111/cobi.13136

Bowne, D.R., Cosentino, B.J., Anderson, L.J., Cooke, S., Dosch, J.J., Garneau, D., Fredericksen, T.S., Kolozsvary, M.B., Lindquist, E.S., March, J.G., Urban, R.A., Zimmermann, C.R., 2019. A broader approach to understanding urbanization effects on freshwater turtles: reply to Lambert and Steen 2019. Conserv. Biol. 33, 1197–1199. https://doi.org/10.1111/cobi.13398

Brooks, R.J., Brown, G.P., Galbraith, D.A., 1991. Effects of a sudden increase in natural mortality of adults on a population of the Common Snapping Turtle (*Chelydra serpentina*). Can. J. Zool. 69, 1314–1320. https://doi.org/10.1139/z91-185

Brown, C.M., Currie, P.J., Therrien, F., 2022. Intraspecific facial bite marks in tyrannosaurids provide insight into sexual maturity and evolution of bird-like intersexual display. Paleobiology 48, 12–43. https://doi.org/10.1017/pab.2021.29

Burgess, E.A., Brown, J.L., Lanyon, J.M., 2013. Sex, scarring, and stress: understanding seasonal costs in a cryptic marine mammal. Conserv. Physiol. 1, 1–14. https://doi.org/10.1093/conphys/cot014

Cain, P.W., 2010. The Cost Of Soup: An Assessment of The Commercial Harvest of Snapping Turtles (*Chelydra serpentina*) in Maryland. (Master's Thesis). Townsend University, Townsend, Maryland.

Carstairs, S., Dupuis-Desormeaux, M., Davy, C.M., 2018. Revisiting the hypothesis of sex-biased turtle road mortality. Can. Field-Naturalist 132, 289–295. https://doi.org/10.22621/cfn.v132i3.1908

Caswell, H., 2001. Matrix Population Models : Construction, Analysis, and Interpretation, 2nd ed. Sinauer Associates, Sunderland, MA. USA.

Congdon, J.D., Dunham, A.E., van Loben Sels, R.C., 1994. Demographics of Common Snapping Turtles (*Chelydra serpentina*): Implications for conservation and management of long-lived organisms. Am. Zool. 34, 397–408.

Congdon, J.D., Nagle, R.D., Kinney, O.M., 2018. Front-loading life histories: The enduring influence of juvenile growth on age, size, and reproduction of primiparous female freshwater turtles. Evol. Ecol. Res. 19, 353–364.

Crawford, B.A., Moore, C.T., Norton, T.M., Maerz, J.C., 2018. Integrated analysis for population estimation, management impact evaluation, and decision-making for a declining species. Biol. Conserv. 222, 33–43. https://doi.org/10.1016/j.biocon.2018.03.023

Cunnington, D.C., Brooks, R.J., 1996. Bet-hedging theory and eigenelasticity: A comparison of the life histories of Loggerhead Sea Turtles (*Caretta caretta*) and Snapping Turtles (*Chelydra serpentina*). Can. J. Zool. 74, 291–296. https://doi.org/10.1139/z96-036

Dobson, F.S., 1982. Competition for mates and predominant juvenile male dispersal in mammals. Anim. Behav. 30, 1183–1192. https://doi.org/doi:10.1016/S0003-3472(82)80209-1

Enneson, J.J., Litzgus, J.D., 2008. Using long-term data and a stage-classified matrix to assess conservation strategies for an endangered turtle (*Clemmys guttata*). Biol. Conserv. 141, 1560–1568. https://doi.org/10.1016/j.biocon.2008.04.001

Fleischer, T., Gampe, J., Scheuerlein, A., Kerth, G., 2017. Rare catastrophic events drive population dynamics in a bat species with negligible senescence. Sci. Rep. 7, 7370. https://doi.org/10.1038/s41598-017-06392-9

Gandon, S., 1999. Kin competition, the cost of inbreeding and the evolution of dispersal. J. Theor. Biol. 200, 345–364. https://doi.org/10.1006/jtbi.1999.0994

Garber, S.D., Burger, J., 1995. A 20-yr study documenting the relationship between turtle decline and human recreation. Ecol. Appl. 5, 1151–1162. https://doi.org/10.2307/2269362

Gibbons, J.W., Lovich, J.E., 1990. Sexual dimorphism in turtles with emphasis on the Slider Turtle (*Trachemys scripta*). Herpetol. Monogr. 4, 1–29. https://doi.org/http://dx.doi.org/10.2307/1466966

Gibbons, J.W., Scott, D.E., Ryan, T.J., Buhlmann, K.A., Tuberville, T.D., Metts, B.S., Greene, J.L., Mills, T., Leiden, Y., Poppy, S., Winne, C.T., 2000. The global decline of reptiles, déjà vu amphibians. Bioscience 50, 653–666.

Golubovic, A., Arsovski, D., Tomovic, L., Bonnet, X., 2018. Is sexual brutality maladaptive under high population density? Biol. J. Linn. Soc. 124, 394–402. https://doi.org/10.1093/biolinnean/bly057

Greenwood, P.J., 1980. Mating systems, philopatry and dispersal in birds and mammals. Anim. Behav. 28, 1140–1162. https://doi.org/10.1016/S0003-3472(80)80103-5

Howell, H.J., Seigel, R.A., 2019. The effects of road mortality on small, isolated turtle populations. J. Herpetol. 53, 39. https://doi.org/10.1670/18-022

Hutchings, J.A., Reynolds, J.D., 2004. Marine fish population collapses: Consequences for recovery and extinction risk. Bioscience 54, 297–309. https://doi.org/10.1641/0006-3568(2004)054[0297:MFPCCF]2.0.CO;2

Jonsson, A., Ebenman, B., 2001. Are certain life histories particularly prone to local extinction? J. Theor. Biol. 209, 455–463. https://doi.org/10.1006/jtbi.2001.2280

Keevil, M.G., Armstrong, D.P., Brooks, R.J., Litzgus, J.D., 2021. A model of seasonal variation in somatic growth rates applied to two temperate turtle species. Ecol. Modell. 443, 109454. https://doi.org/10.1016/j.ecolmodel.2021.109454

Keevil, M.G., Brooks, R.J., Litzgus, J.D., 2018. Post-catastrophe patterns of abundance and survival reveal no evidence of population recovery in a long-lived animal. Ecosphere 9, e02396. https://doi.org/10.1002/ecs2.2396

Keevil, M.G., Hewitt, B.S., Brooks, R.J., Litzgus, J.D., 2017. Patterns of intraspecific aggression inferred from injuries in an aquatic turtle with male-biased size dimorphism. Can. J. Zool. 95, 393–403. https://doi.org/10.1139/cjz-2016-0182

Keevil, M.G., Lesbarrères, D., Noble, N., Boyle, S.P., Brooks, R.., Litzgus, J.D., 2023. Lost reproductive value reveals a high burden of juvenile road mortality in a long-lived species. Ecol. Appl. e2789. https://doi.org/10.1002/eap.2789

Kiviat, E., 1980. A Hudson River tidemarsh Snapping Turtle population. Trans. Northeast Sect. Wildl. Soc. 37, 158–168.

Lambert, M.R., Steen, D.A., 2019. Reexamining effects of urbanization on population structure of freshwater turtles: response to Bowne et al. 2018. Conserv. Biol. 33, 1193–1196. https://doi.org/10.1111/cobi.13397

Leturque, H., Rousset, F., 2004. Intersexual competition as an explanation for sex-ratio and dispersal biases in polygynous species. Evolution 58, 2398–2408. https://doi.org/10.1554/04-186

Li, X.Y., Kokko, H., 2019. Sex-biased dispersal: a review of the theory. Biol. Rev. 94, 721–736. https://doi.org/10.1111/brv.12475

Lovich, J.E., Gibbons, J.W., 1992. A review of techniques for quantifying sexual size dimorphism. Growth Dev. Aging 56, 269–281.

Lovich, J.E., Gibbons, J.W., Agha, M., 2014. Does the timing of attainment of maturity influence sexual size dimorphism and adult sex ratio in turtles? Biol. J. Linn. Soc. 112, 142–149. https://doi.org/10.1111/bij.12275

Mangel, M., Tier, C., 1994. Four facts every conservation biologists should know about persistence. Ecology 75, 607–614. https://doi.org/10.2307/1941719

McCallum, M.L., 2021. Turtle biodiversity losses suggest coming sixth mass extinction. Biodivers. Conserv. 30, 1257–1275. https://doi.org/10.1007/s10531-021-02140-8

Menges, E.S., 1990. Population viability analysis for an endangered plant. Conserv. Biol. 4, 52–62. https://doi.org/10.1111/j.1523-1739.1990.tb00267.x

Moldowan, P.D., Brooks, R.J., Litzgus, J.D., 2020. Demographics of injuries indicate sexual coercion in a population of Painted Turtles (*Chrysemys picta*). Can. J. Zool. cjz-2019-0238. https://doi.org/10.1139/cjz-2019-0238

Mullin, D.I., White, R.C., Lentini, A.M., Brooks, R.J., Bériault, K.R., Litzgus, J.D., 2020. Predation and disease limit population recovery following 15 years of headstarting an endangered freshwater turtle. Biol. Conserv. 245, 108496. https://doi.org/10.1016/j.biocon.2020.108496

Murphy, R.E., Martin, A.E., Fahrig, L., 2022. Reduced predation on roadside nests can compensate for road mortality in road-adjacent turtle populations. Ecosphere 13, e3946. https://doi.org/10.1002/ECS2.3946

Neubauer, P., Jensen, O.P., Hutchings, J.A., Baum, J.K., 2013. Resilience and recovery of overexploited marine populations. Science 340, 347–349. https://doi.org/10.1126/science.1230441

Obbard, M.E., Brooks, R.J., 1980. Nesting migrations of the Snapping Turtle (*Chelydra serpentina*). Herpetologica 36, 158–162.

Patrick, D., Gibbs, J.P., 2010. Population structure and movements of freshwater turtles across a road-density gradient. Landsc. Ecol. 25, 791–801. https://doi.org/10.1007/s10980-010-9459-0

Perrin, N., Mazalov, V., 2000. Local competition, inbreeding, and the evolution of sex-biased dispersal. Am. Nat. 155, 116–127. https://doi.org/10.1086/303296

Piczak, M.L., Markle, C.E., Chow-Fraser, P., 2019. Decades of road mortality cause severe decline in a Common Snapping Turtle (*Chelydra serpentina*) population from an urbanized wetland. Chelonian Conserv. Biol. 18, 231–240. https://doi.org/10.2744/CCB-1345.1

Roff, D.A., 2002. Life History Evolution. Sinauer, Sunderland, MA.

Sæther, B.-E., Lande, R., Engen, S., Weimerskirch, H., Lillegard, M., Altwegg, R., Becker, P.H., Bregnballe, T., Brommer, J.E., McCleery, R.H., Merila, J., Nyholm, E., Rendell, W., Robertson, R.R., Tryjanowski, P., Visser, M.E., 2005. Generation time and temporal scaling of bird population dynamics. Nature 436, 99–102. https://doi.org/10.1038/nature03666

Scott, E.M., Mann, J., Watson-Capps, J.J., Sargeant, B.L., Connor, R.C., 2005. Aggression in bottlenose dolphins: Evidence for sexual coercion, male-male competition, and female tolerance through analysis of tooth-rake marks and behaviour. Behaviour 142, 21–44. https://doi.org/10.1163/1568539053627712

Shine, R., Iverson, J.B., 1995. Patterns of survival, growth and maturation in turtles. Oikos 72, 343–348. https://doi.org/10.2307/3546119

Stanford, C.B., Iverson, J.B., Rhodin, A.G.J., Paul van Dijk, P., Mittermeier, R.A., Kuchling, G., Berry, K.H., Bertolero, A., Bjorndal, K.A., Blanck, T.E.G., Buhlmann, K.A., Burke, R.L., Congdon, J.D., Diagne, T., Edwards, T., Eisemberg, C.C., Ennen, J.R., Forero-Medina, G., Frankel, M., Fritz, U., Gallego-García, N., Georges, A., Gibbons, J.W., Gong, S., Goode, E. V., Shi, H.T., Hoang, H., Hofmeyr, M.D., Horne, B.D., Hudson, R., Juvik, J.O., Kiester, R.A., Koval, P., Le, M., Lindeman, P. V., Lovich, J.E., Luiselli, L., McCormack, T.E.M., Meyer, G.A., Páez, V.P., Platt, K., Platt, S.G., Pritchard, P.C.H., Quinn, H.R., Roosenburg,

W.M., Seminoff, J.A., Shaffer, H.B., Spencer, R., Van Dyke, J.U., Vogt, R.C., Walde, A.D., 2020. Turtles and tortoises are in trouble. Curr. Biol. 30, R721–R735. https://doi.org/10.1016/j.cub.2020.04.088

Steen, D.A., Aresco, M.J., Beilke, S.G., Compton, B.W., Condon, E.P., Dodd Jr., C.K., Forrester, H., Gibbons, J.W., Greene, J.L., Johnson, G., Langen, T.A., Oldham, M.J., Oxier, D.N., Saumure, R.A., Schueler, F.W., Sleeman, J.M., Smith, L.L., Tucker, J.K., Gibbs, J.P., 2006. Relative vulnerability of female turtles to road mortality. Anim. Conserv. 9, 269–273. https://doi.org/10.1111/j.1469-1795.2006.00032.x

Steen, D.A., Gibbs, J.P., 2004. Effects of roads on the structure of freshwater turtle populations. Conserv. Biol. 18, 1143–1148. https://doi.org/10.1111/j.1523-1739.2004.00240.x

Toïgo, C., Gaillard, J.M., 2003. Causes of sex-biased adult survival in ungulates: Sexual size dimorphism, mating tactic or environment harshness? Oikos 101, 376–384. https://doi.org/10.1034/j.1600-0706.2003.12073.x

Vanek, J.P., Glowacki, G.A., 2019. Assessing the impacts of urbanization on sex ratios of Painted Turtles (*Chrysemys picta*). Diversity 11, 72. https://doi.org/10.3390/D11050072

Vélez-Espino, L.A., Koops, M.A., 2012. Capacity for increase, compensatory reserves, and catastrophes as determinants of minimum viable population in freshwater fishes. Ecol. Modell. 247, 319–326. https://doi.org/10.1016/j.ecolmodel.2012.09.022

Appendix A: Details of mark-recapture model construction and analysis

This appendix was first published as Appendix S1 in supplemental materials of

Keevil, M.G., Brooks, R.J., Litzgus, J.D., 2018. Post-catastrophe patterns of abundance and survival reveal no evidence of population recovery in a long-lived animal. Ecosphere 9, e02396. https://doi.org/10.1002/ecs2.2396

Methods

Mark-recapture analysis I: Nesting females (1980-2013)

Initial multistate model construction — The CMR data of nesting females were analysed using Arnason-Schwartz multistate models with nesting on the Sasajewun dam as one state and nesting at pooled alternate sites as another state to allow for transitions and differential survival and detection probability between sites (Brownie et al., 1993). Arnason-Schwarz models are strictly 1st order Markovian and individual survival and transition probabilities from *t* to *t* + 1 depend only on the state at time t and not on previous states (i.e., there is no 'memory') nor dependence on subsequent states (i.e., individuals survive, then move; Brownie et al. 1993). All multistate models that we fitted in the Bayesian and information-theoretic contexts share these assumptions. Initial model fitting and exploration was conducted in Program MARK (White, 2011; White et al., 2006; White and Burnham, 1999). We included *period* as a categorical time effect on survival and movement to reflect *a priori* hypotheses about the effects of the otter predation event (before, during = *otter*, after, presumptively called *low dens*) and the temporary failure of the Sasajewun dam during the spring of 1998 (*blowout*) (Table A.1).

Goodness-of-fit (GOF) — Program U-CARE (Choquet et al., 2005) was used to test (GOF) of the fully parameterized standard "Jolly Move" multistate model (Pradel et al., 2003). Because some parameters of the full state and time effects model were unidentifiable in a preliminary analysis in Program MARK, we also tested GOF of a reduced parameter model ($S_{site*period}p_{site+t}\psi^{S\cdot}$) using the parametric bootstrap GOF procedure implemented in MARK (White and Burnham 1999, White et al. 2006; notation adapted from Lebreton et al. 2009)

Development of m-array models for implementation in Program JAGS — An m-array is a summary of recapture data using minimally sufficient statistics that tabulates number released and the occasions of next recapture across release occasions (Burnham et al., 1987). Construction of m-arrays for multiple states is reviewed in Lebreton et al. (2009) and Brownie et al. (1993). The m-array parameterization of mark-recapture models uses a multinomial likelihood in contrast to the binomial likelihood of state-space parameterizations.

We chose the m-array parameterization for model selection and GOF analysis because it was better-suited than state-space models for posterior predictive checking and comparing among candidate models. This is because DIC (deviance information criterion; Spiegelhalter et al. 2002) and posterior predictive checks are available for the multinomial likelihood used in the m-array parameterization but not for the binary responses of state-space models (Kéry and Schaub, 2012;

McCullagh and Nelder, 1989). Additionally, state-space models run more slowly (Kéry and Schaub, 2012) making variable selection impractical with our data.

The nesting female dataset consisted of $T = 34$ occasions corresponding to the years 1980:2013 over $s = 2$ observable states. There were 1:33 release occasions and 2:34 recapture occasions. The multistate m-array consisted of a $T - 1 \times s$ matrix **R** of released individuals at each site over occasions 1:33 and a four-dimensional triangular recapture array **M** with $T - 1$ rows and columns over occasions 2:34 where each cell contains an $s \times s$ matrix $\mathbf{m}_{t,j}$ where $t - 1$ is the release occasion and j is the recapture occasion. For example, cell $m_{9,9}^{AB}$ stores the number of individuals released at occasion 8 in state A that were next recaptured at occasion 9 in state B. In our analysis, superscript *A* denotes the Sasajewun dam and *B* denotes alternate sites. The $T - 1 \times s$ matrix of individuals released on each occasion that were never recaptured can be calculated from **R** and **M**.

As summarised in Brownie et al. (1993) and Lebreton et al. (2009), we used a vector of $s \times s$ transition matrices to store the probabilities of survival and state transitions between occasions:

$$\boldsymbol{\varphi}_t = \begin{bmatrix} S_t^A(1-\psi_t^{AB}) & S_t^A\psi_t^{AB} \\ S_t^B\psi_t^{BA} & S_t^B(1-\psi_t^{BA}) \end{bmatrix}$$

where S_t^s are survivorships, ψ_t^{AB} is movement from state *A* to *B* conditional on survival in *A* from $t - 1$ to t. Vectors of $1 \times T - 1$ diagonal matrices $D(\mathbf{p}_t)$ and $D(\mathbf{q}_t)$ are constructed from $1 \times s$ vectors of recapture probabilities $\mathbf{p}_t$ and $\mathbf{q}_t$, = $\mathbf{1}_s$ - $\mathbf{p}_t$ where $\mathbf{1}_s$ is a vector of ones of length s. Cell probabilities for release occasion i and recapture occasion j are stored in a $1 \times T$ vector of $s \times s$ matrices $\boldsymbol{\pi}_{ij}$. Cell probabilities correspond to m-array cells. On the diagonal (time t for animals released at $t - 1$) $\boldsymbol{\pi}_{t,t} = \boldsymbol{\varphi}_t \times D(\mathbf{p}_t)$ and above the diagonal

$$\boldsymbol{\pi}_{t,t+1} = \boldsymbol{\varphi}_t \times D(\mathbf{q}_t) \times \boldsymbol{\varphi}_{t+1} \times D(\mathbf{p}_{t+1})$$

for the animals released at time $t - 1$, surviving to, but not detected at, t, and surviving to and being recaptured at $t + 1$. The final column of cell probabilities, the probability of never being recaptured for an individual released into site s at time $t - 1$, is 1 minus the probability of being recaptured on any previous occasion:

$$\pi_{t,T+1}^{s\ Final} = 1 - \sum_{j=t:T}^{T} \pi_{tj}^{sA} + \pi_{tj}^{sB}$$

where T is the number of recapture occasions. The multinomial likelihood relates counts in the m-array to cell probabilities multiplied by the number released at each occasion and state. The likelihood is, like the corresponding Cormack-Joly-Seber model for a single state, conditional on first capture and this class of models are therefore referred to as Conditional Arnason–Schwarz (CAS) models (Lebreton et al., 2009). Specific information on the likelihood function can be found in Brownie et al. (1993) and Lebreton et al. (2009).

Unlike the simpler single-state case, cell probability calculations for multistate m-arrays require matrix multiplication, which is not available in Program WinBUGS, and therefore we performed the analysis using Program JAGS (Plummer, 2013) implemented through the R2jags package (Su and Yajima, 2014).

Model with temporary emigration (TE) — We modified the CAS framework to account for temporary emigration (TE) by adding unobservable states (Fujiwara and Caswell, 2002; Kendall and Nichols, 2002; Schaub et al., 2004). We used two unobservable states: C1 for individuals that have transitioned into temporary unavailability from the Sasajewun dam (A) and C2 for individuals temporarily unavailable from the alternate sites (B). In this model, individuals could not transition between C1 and C2, B and C1, or A and C2. Survival in C1 was the same for A, and C2 survival was the same as B. Thus the transition matrix is:

$$\boldsymbol{\varphi}_t = \begin{bmatrix} S_t^A(1-\psi_t^{AB}-\psi_t^{AC1}) & S_t^A\psi_t^{AB} & S_t^A\psi_t^{AC1} & 0 \\ S_t^B\psi_t^{BA} & S_t^B(1-\psi_t^{BA}-\psi_t^{BC2}) & 0 & S_t^B\psi_t^{BC2} \\ S_t^A\psi_t^{C1A} & 0 & S_t^A(1-\psi_t^{C1A}) & 0 \\ 0 & S_t^B\psi_t^{C2B} & 0 & S_t^B(1-\psi_t^{C2B}) \end{bmatrix}$$

The cell probabilities, $\pi_{ij}^{1:4,1:4}$ are now calculated with dimensions 4×4 for each pair of release (i) and recapture occasions (j) but only an $i \times j$ array of 2×2 matrices with cells $\pi_{ij}^{1:2,1:2}$ is used in the likelihood because the probabilities of being released or recaptured in unobserved states is 0 by definition. Thus the format of the m-array and the likelihood does not need to be changed from the 2-state case.

Prior constraints on transition parameters, ψ_t^{uv}, must be adjusted from the two-state case (where we used $U[0,1]$ priors and obtained fidelity — the probability of not switching states — by subtraction) to ensure that they sum to 1. We did this by applying the multinomial logit constraint (Kéry and Schaub, 2012). We retained the random effects structure from the CAS model with $U[0,1]$ priors for mean transition probabilities between observable states. Including unobservable states causes Identifiability problems in unconstrained open population models (Kendall and Nichols, 2002). Since our dataset is relatively sparse we made the decision to model transition probabilities involving unobservable states as time-invariant fixed effects.

Multinomial m-array with observation effects — To account for *observation* effects (OE) of capture, we focused on cell probabilities along the diagonal ($\boldsymbol{\pi}_{t,t}$) which correspond to transition, survival, and recapture probabilities on the occasion immediately following each release for each release-cohort. We included a series of $1 \times s$ vectors $\mathbf{p}^B{}_t$ and $\mathbf{q}^B{}_t$ containing the probability of being recaptured or not recaptured at each site after release in addition to the recapture vectors $\mathbf{p}_t$ and $\mathbf{q}_t$ described for the CAS model. We therefore apply $D(\mathbf{p}^B{}_t)$ to calculations on the diagonal for $\boldsymbol{\pi}_{t,t}$

and $D(\mathbf{q}^B_t)$ for calculations on the diagonal for ($\pi_{t,j>t}$) and $D(\mathbf{p}_t)$ and $D(\mathbf{q}_t)$ for above-diagonal calculations. Thus, for example, $\boldsymbol{\pi}_{t,t} = \boldsymbol{\varphi}_t \times D(\mathbf{p}^B_t)$ and

$$\boldsymbol{\pi}_{t,t+2} = \boldsymbol{\varphi}_t \times D(\mathbf{q}^{\boldsymbol{B}}_t) \times \boldsymbol{\varphi}_{t+1} \times D(\mathbf{q}_{\boldsymbol{t+1}}) \times \boldsymbol{\varphi}_{t+2} \times D(\mathbf{p}_{t+2}).$$

We modeled the observational effect, *obs*, on the logistic scale so that

$$\text{logit}(p_{B,t}) = \text{obs} * \text{site} + \text{occasion}$$

where $p_{1,t}$ is recapture probability at occasion t for individuals recaptured on the previous occasion, $t-1$, and $p_{0,t}$ is the recapture probability for individuals not detected at $t-1$. *obs* is the magnitude of the *observation effect* and varies with *site* but is additive (on the logit scale) across occasions. Estimated probability of recapture at occasion *t* depended only on site at *t* and whether an individual was captured at $t-1$ but not site at $t-1$. We did not model a *site* * *occasion* interaction because the resulting parameters would not be intrinsically identifiable (Gimenez et al., 2003).

Variable selection. — We used a generalized linear model (GLM) parameterization for *S* and *p* in order to examine the effects of individual parameters and for variable selection. The general model (omitting the design matrix) for survival is

$$\text{logit}(S) = \beta_0 + \beta_1 + \beta_2 + \beta_3 + \beta_4 + \beta_5 + \beta_6 + \beta_7 + \epsilon_T$$

where β_0 = intercept, $\beta_{1\ldots3}$ are the effects for three of the four levels of *period* (the first level is the intercept), β_4 is the effect of site and $\beta_{5\ldots7}$ are the interactions of *site* and *period*, and ϵ_T is the random time effect. Since *period* effects are non-overlapping, this means that the prior induced on mean survivorship within a period and site is a sum of priors for 1 to 4 parameters on the logistic scale, which is not flat on the probability scale (King et al., 2010). In order to induce a minimally informative prior for mean survivorship, we used a $\mu_i = 0$ for the mean and an inverse gamma hyperprior (King et al., 2010) for the variance, $\sigma_i^2 \sim \Gamma^{-1}(4,5)$, as β_i priors. This produces an approximately flat prior for sums of three parameters, but somewhat inflated at 0 and 1 for sums of four parameters and somewhat concentrated around 0.5 for sums of two or one parameters (Figure A.1). We used the same prior for each parameter in our general model of recapture probability *p*:

$$\text{logit}(p) = \beta_{site} + \beta_{T(1)} + \ldots + \beta_{T(T)} + \beta_{site*T(1)} + \ldots + \beta_{site*T(T)}$$

(again, omitting the design matrix), or

$$\text{logit}(p_{site,t}) = \beta_{site} + \beta_{T(t)} + \beta_{site*T(t)}$$

where β_{site} is the fixed site effect, $\beta_{T(t)}$ is the fixed effect of occasion *t*, and $\beta_{site*T(t)}$ is the interaction of *site* and occasion *t*.

We used Gibbs variable selection (GVS) (Dellaportas et al., 2000) to assess support for the inclusion of parameters on *S* and *p*. In GVS each variable of interest, v_i, is multiplied by an inclusion parameter g_i which takes values of 0 or 1. On iterations when $g_i = 0$, the product $g_i v_i = 0$ and v_i drops out of the likelihood (Dellaportas et al., 2000). The mean value of g_i in the MCMC output is the marginal posterior probability averaged across models in which v_i is included (O'Hara and Sillanpää, 2009). When $g_i = 0$, v_i does not affect the likelihood but is drawn from a pseudoprior distribution (informed by the posteriors of a pilot run of the full model) in order to improve mixing (Dellaportas et al., 2000; Ntzoufras, 2002; Tenan et al., 2014).

We used GVS to assess effects of *site*, *occasion*, and their interaction on recapture probability. The 33 occasion parameters were assigned a single inclusion parameter (g_2) as were the 33 interaction parameters (g_3) with the result that these variables were selected (or not) as single blocks. In addition, we only considered nested submodels so that models with an interaction always included both *occasion* and *site* main effects. This resulted in five possible sub models which were (adapting the notation of Lebreton et al. (1992)): *p*(.), *p*(*t*), *p*(*site*), *p*(*site*+*t*), and *p*(*site***t*). Variable selection was limited to selection among the five recapture submodels using the procedure outlined by Ntzoufras (2002).

We used dam = 1, alternate sites = 0 dummy coding in the design matrix of the survivorship GLM so that the interaction *site* * $period_i$ without one or both of the corresponding main effects parameters implies a model in which the effect of $period_i$ applies only to the dam nesting females. We view such models as potentially meaningful and biologically plausible. Therefore, we did not limit variable selection of the seven survivorship parameters to nested submodels, which results in $2^7 = 127$ combinations of survivorship parameters (Ntzoufras, 2002). Combining survival and recapture submodels results in a total model space of $5 \times 127 = 635$ models. The model proposed at each iteration of the MCMC chain was encoded in JAGS as

$$mdl = 1 + \sum_{n=1}^{P} g_n^{n-1}$$

for $n = 1{:}P$ inclusion parameters. This form of bookkeeping reduces the number of parameters that need to be monitored in WinBUGS or JAGS because converting *mdl* to binary notation reveals the status of each inclusion parameter and allows calculation of marginal probabilities outside of a BUGS environment which improves speed (Ntzoufras, 2002).

Data augmented state-space model — To estimate abundance, we modified our preferred model, TE, identified using the procedure described above, to implement it in a state-space formulation with parameter-expanded data augmentation. State-space CMR models separate the observation (captured in A, captured in B, not captured) and population (recruitment, survival, and site transitions) processes (Gimenez et al., 2007; Royle and Dorazio, 2008).

Data augmentation (Tanner and Wong, 1987) for capture-recapture models involves creating an augmented encounter history dataset **M** (**M** in this case does not refer to an m-array and is used for consistency with published literature), by adding all-zero encounter histories (Royle and Dorazio, 2012, 2008; Schofield and Barker, 2011). In the multi-state formulation described in Royle and Dorazio (2012), the removal entry probability, $\gamma_{t,s}$, is the probability that an individual M_i in the pre-entry state will be recruited into an alive state s (in our case, one of two nesting areas: A = dam and B = alternate) on occasion t. It is required to implement data augmentation but does not have direct biological meaning (Kéry and Schaub, 2012; Royle and Dorazio, 2012). A dummy occasion is added before the first occasion (with the consequence that indexing differs between m-array and state-space models; Table A.1) and thus $\gamma_{1,s}$ becomes the proportions of individuals present on the first real occasion at each site and the multi-state model becomes conditional on individuals being present rather than conditional on initial capture, allowing abundance to be estimated (Kéry and Schaub, 2012).

We assigned an uninformative Dirichlet prior to constrain $\sum_{s=1}^{3} \gamma_{ts} = 1$. The latent state variable, $z_{i,t}$, stores the process state of individual i at occasion t. Individual state changes from t to $t + 1$ through the following transition matrix, whose entries are constraints and transition probabilities to be estimated:

state	not entered = 1	A = 2	B = 3	C1 = 4	C2 = 5	dead = 6
not entered	$1-(\gamma_t^A+\gamma_t^B)$	γ_t^A	γ_t^B	0	0	0
A	0	$S_t^A(1-\psi_t^{AB}-\psi_t^{AC1})$	$S_t^A\psi_t^{AB}$	$S_t^A\psi_t^{AC1}$	0	$1-S_{A,t}$
B	0	$S_t^B\psi_t^{BA}$	$S_t^B(1-\psi_t^{BA}-\psi_t^{BC2})$	0	$S_t^B\psi_t^{BC1}$	$1-S_{B,t}$
C1	0	$S_t^A\psi_t^{C1A}$	0	$S_t^A(1-\psi_t^{AC1})$	0	$1-S_{A,t}$
C2	0	0	$S_t^B\psi_t^{C2B}$	0	$S_t^B(1-\psi_t^{C2B})$	$1-S_{B,t}$
dead	0	0	0	0	0	1

where the 'from' state is listed on the left margin and 'to' state on the top along with index values used in z.

The latent state variable is related to the encounter history data through the following observation matrix $\mathbf{y}_{i,t}$ whose entries also contain constraints and encounter probabilities to be estimated:

State	obs. in A	obs. in B	Not observed

	y_{it}=1	y_{it}=2	y_{it}=3
not entered, z_{it}= 1	0	0	1
A, z_{it}= 2	$p_{A,t}$	0	$1 - p_{A,t}$
B, z_{it}= 3	0	$p_{B,t}$	$1 - p_{B,t}$
C1, z_{it}= 4	0	0	1
C2, z_{it}= 5	0	0	1
Dead, z_{it}= 6	0	0	1

Following Kéry and Schaub (2012), with modifications for more than one site, we calculated abundance estimates for each observable state *s* at occasion *t* from the state variable $z_{s,t}$: $N_{t,s} = \sum_{i=1}^{M} \mathrm{I}(z_{i,t} = s)$ where I() is an indicator function. The number of new recruits at each site and occasion is $B_{t,s} = \sum_{i=1}^{M} \mathrm{I}(\mathrm{z_{i,t}} = s)\, \mathrm{I}\left(1 - \left(z_{i,t-1} = s\right)\right)$ where *s* is either dam (*s* = 2) or alternate sites (*s* = 3) and the superpopulation size (Schwarz and Arnason, 1996) is $N_{super} = \sum_{s=2}^{5} \sum_{t=1}^{T} B_{t,s}$ which is the number of individuals that ever enter an alive state. The choice of *M* sets an upper limit on N_{super} which occurs only as a derived parameter and so does not have an explicit Bayesian prior (Kéry and Schaub, 2012). To assess whether our choice of *M* had undue influence on the posterior distribution of N_{super}(and thereby other parameters), we used a histogram to check the posterior distribution of N_{super} and ensure that it did not extend to *M* (Kéry and Schaub, 2012). We augmented the dataset so that *M* = 400.

Results

Goodness-of-fit of multi-state CMR models. — Two components of the U-CARE GOF tests showed a significant lack of fit for the basic CAS model. Test WBWA indicated a significant 'memory' effect on transitions (χ^2 = 56.3, *df* = 26, *P* = 0.001) and component Test M.ITEC indicated a 'trap-happiness' or analogous observation effect (χ^2 = 60.4, *df* = 32, *P* = 0.002) (Choquet et al., 2005; Pradel et al., 2003). None of the other U-CARE component tests and the omnibus GOF test were significant (*P* > 0.05). The overdispersion parameter based on the omnibus test statistic was $\hat{c} = \chi^2/df$= 214 /218 = 1.055. There was no significant lack of fit of a reduced parameter CAS model detected by a Bootstrap GOF test with 100 iterations implemented in Program MARK (*P* = 0.67) which produced an estimate of the overdispersion parameter $\hat{c} =$ 1.02.

Multinomial m-array models CAS, TE, and TR were fitted in Program JAGS and all achieved convergence based on visual inspection of MCMC chains and $\hat{R} \leq 1.1$ for all parameters (Brooks and Gelman, 1998). Posterior predictive checking yielded Bayesian p-values of 0.11 for CAS, 0.44 for TE, and 0.44 for TR (Figure A.2). We rejected the basic CAS model because of its relative lack of fit and proceeded with analysis of the TE and TR models.

Observation effects. — The o*bservation effects* model estimated separate observation effects parameters for each site: mean (95% CRI) β_{dam} = 0.061 (-0.71, 0.77) and β_{alt} = 1.3 (0.76, 1.7) (Figure 1.3, Figure A.3). There was support for a trap-happy type of response of turtles nesting at the alternate sites ($\beta_{alt} > 0$) but not for those at the dam as the 95% CRI overlapped 0 and the effect size was close to 0 (Figure 1.3). Because the OE effect was modeled as additive on the logistic scale, the effect on estimated recapture probabilities decreased as p approached 0 or 1 but, averaged over all occasions, individuals at the alternate sites were 33.8% more likely to be captured if they were captured on the most recent prior occasion (Figure A.3). Model OE produced similar apparent survival estimates to the TE model results described in the main text (Figure 1.3).

Model selection. — We considered DIC when comparing TE (pD = 115, DIC = 972.1) and TR (pD = 111, DIC = 978.0) in order to choose a general model from which to conduct variable selection. The difference in DIC values was 5.9, suggesting moderate support for model TE. This combined with our judgement that temporary emigration was likely to be more biologically important than trap response, led us to choose the general TE model for further analysis. GVS model selection results are given in the main text.

Patterns of abundance of nesting females. — Our multi-state model of abundance using data augmentation achieved convergence based on visual inspection of MCMC chains and $\hat{R} \leq 1.1$ for all parameters. A graphical comparison of parameter estimates between the state-space abundance model and the conditional multinomial m-array showed estimates were very similar (Figure 1.5) with slightly higher precision of apparent survivorship in the state-space model, likely because it did not include model uncertainty.

Discussion

Model performance — Both temporary emigration and observation effects can induce patterns of autocorrelation of recapture events in which the probability of recapture varies depending on whether an individual was captured on a previous occasion (Pradel and Sanz-Aguilar, 2012). Temporary emigration is commonly observed in populations surveyed during reproductive events because individuals that skip reproduction are unavailable for recapture (Kendall et al., 1997; Sanz-Aguilar et al., 2011; Schmidt et al., 2002). Likewise, some form of observation effect is frequent in mark-recapture studies (Pradel and Sanz-Aguilar, 2012). Although most often thought of as, a behavioural response to baited traps or handling, observation effects encompass a host of phenomena in which recapture probability changes permanently (permanent observation effect) or transiently (immediate observation effect) following detection (reviewed in Pradel and Sanz-Aguilar, 2012). Such responses can include changes in observer behaviour, such as when locations of recent detections are more likely to be revisited (Schaub et al., 2005).

Accounting for trap effects in closed (Otis et al., 1978) or robust designs (Kendall et al., 1997) has long been standard practice, and the short intervals intrinsic to these designs tends to increase the magnitude of trap dependence (Pradel and Sanz-Aguilar, 2012). Immediate observation

effects over the sampling frequencies typical of open designs are also quite commonly detected but are modeled explicitly less often (Pradel and Sanz-Aguilar, 2012). Temporary emigration is also more likely to be modeled in robust designs because the inclusion of unobserved states is very data-hungry and often results in identifiability problems for other parameters in open designs (Kendall and Nichols, 2002). Our starting general model of temporary emigration was constrained and did not include time effects on transitions to unobservable states in recognition of these limitations.

Modeling either temporary emigration or observation effects produced similar and pronounced improvements in model fit as assessed using posterior predictive checking. There were also similar effects of *site* in both types of model, with a stronger correlation between successive encounters at the alternate sites compared to the dam. The choice of which type of model to proceed with was based partly on higher DIC support for temporary emigration and partly on our assessment of which model is most biologically plausible for our study system. Because our detections of females at nest sites does not involve bait or traps, we reasoned that if an observation effect had actually occurred, it was likely to be either a result of changes in observer behaviour or a 'trap shy' response to capture and handling in which females avoid monitored nesting areas. The latter can be ruled out because the direction of the response is towards 'trap happiness' (Fig. S4). We cannot exclude a role of observer behavioural effects but our observations of nest site switching means that temporary emigration definitely occurs in our population. In addition to transitions between the dam and alternate sites, turtles also periodically change nest sites among alternate sites and some individuals have been observed nesting at sites outside the study area as defined for the present analysis. In recent years, two females experienced 5 and 6 consecutive years without observed nesting in association with apparent illness: one with severe scute infection, and another who laid grossly malformed, unviable eggs for the first two clutches after her hiatus. We suspect that such illnesses or injury can cause females to temporarily forgo reproduction for one or more occasions. These observations support our inference that individuals are occasionally unavailable for capture at nest sites. These phenomena are best modeled using temporary emigration so that models more closely approach biological realism.

A subtest for 'memory' effects (transition probabilities that are non-Markovian and depend on state on previous occasions in addition to present state) was also significant. A significant memory effect implies that individuals that had been observed to transition between sites on a prior occasion were more likely to transition again on a future occasion. Lebreton et al. (2009) emphasize that memory models are extremely data-hungry and difficult to implement in most situations and they suggest adjusting for overdispersion instead. The overdispersion parameter estimated was already close to one ($\hat{c} = 1.055$) and overall fit was acceptable as assessed by the U-CARE omnibus test statistic and the bootstrap GOF test in MARK. We therefore focussed further model development on accounting for temporary emigration/trap dependence followed by using posterior predictive checks to reassess model fit.

Abundance and survival of nesting females. — We defined entry into the study as the event of an individual first being observed at a monitored nest site with the consequence that we did not model recruitment into unobservable states. This implies that any individuals that had been present but happened to be unavailable for capture in the early occasions and then subsequently returned would be classified as new recruits instead of returning temporary emigrants; this

modelling artefact, rather than real recruitment, may account for the observed higher recruitment during early intervals as compared to later intervals.

References

Brooks, S.P., Catchpole, E.A., Morgan, B.J.T., Barry, S.C., 2000. On the Bayesian analysis of ring-recovery data. Biometrics 56, 951–956. https://doi.org/10.1111/j.0006-341X.2000.00951.x

Brooks, S.P., Gelman, A., 1998. General methods for monitoring convergence of iterative simulations. J. Comput. Graph. Stat. 7, 434–455. https://doi.org/10.1080/10618600.1998.10474787

Brownie, C., Hines, J.E., Nichols, J.D., Pollock, K.H., Hestbeck, J.B., 1993. Capture-recapture studies for multiple strata including non-Markovian transitions. Biometrics 49, 1173–1187. https://doi.org/10.2307/2532259 ER

Burnham, K.P., Anderson, D.R., White, G.C., Brownie, C., Pollock, K.H., 1987. Design and analysis methods for fish survival experiments based on release-recapture. Am. Fish. Soc. Monogr. 5, 1–437.

Choquet, R., Reboulet, A.M., Lebreton, J.-D., Gimenez, O., Pradel, R., 2005. U-Care 2.2 User's Manual.

Dellaportas, P., Forster, J., Ntzoufras, I., 2000. Bayesian variable selection using the Gibbs sampler., in: Dey, D., Ghosh, S., Mallick, B. (Eds.), Generalized Linear Models: A Bayesian Perspective, Vol. 5. CRC Press, New York, USA, pp. 273–286.

Fujiwara, M., Caswell, H., 2002. A general approach to temporary emigration in mark-recapture analysis. Ecology 83, 3266–3275. https://doi.org/10.2307/3072077 ER

Gelman, A., Carlin, J.P., Stern, H.S., Runin, D.B., 2004. Bayesian Data Analysis. CRC/Chapman & Hall, Boca Raton, F.L.

Gimenez, O., Choquet, R., Lebreton, J.-D., 2003. Parameter redundancy in multistate capture-recapture models. Biometrical J. 45, 704–722.

Gimenez, O., Morgan, B.J.T., Brooks, S.P., 2009. Weak identifiability in models for mark-recapture-recovery data, in: Thomson, D.L., Cooch, E.G., Conroy, M.J. (Eds.), Modeling Demographic Processes in Marked Populations. Springer, New York, pp. 1055–1067.

Gimenez, O., Rossi, V., Choquet, R., Dehais, C., Doris, B., Varella, H., Vila, J.-P., Pradel, R., 2007. State-space modelling of data on marked individuals. Ecol. Modell. 206, 431–438. https://doi.org/10.1016/j.ecolmodel.2007.03.040 ER

Kendall, W.L., Nichols, J.D., 2002. Estimating state-transition probabilities for unobservable states using capture-recapture/resighting data. Ecology 83, 3276–3284. https://doi.org/10.2307/3072078 ER

Kendall, W.L., Nichols, J.D., Hines, J.E., 1997. Estimating temporary emigration using capture-recapture data with Pollock's robust design. Ecology 78, 563–578.

Kéry, M., Schaub, M., 2012. Bayesian Population Analysis Using WinBUGS: A Hierarchical Perspective. Academic Press, Waltham, Massachussets, USA.

King, R., Morgan, B.J.T., Gimenez, O., Brooks, S.P., 2010. Bayesian Analysis for Population Ecology. CRC Press, Boca Raton, FL.

Lebreton, J.-D., Burnham, K.P., Clobert, J., Anderson, D.R., 1992. Modeling survival and testing biological hypotheses using marked animals: a unified approach with case studies. Ecol. Monogr. 62, 67–118. https://doi.org/10.2307/2937171

Lebreton, J.-D., Nichols, J.D., Barker, R.J., Pradel, R., Spendelow, J.A., 2009. Modeling Individual Animal Histories with Multistate Capture-Recapture Models, in: Caswell, H. (Ed.), Advances in Ecological Research. Elsevier, San Diego, pp. 87–173. https://doi.org/10.1016/S0065-2504(09)00403-6 ER

McCullagh, C., Nelder, J., 1989. Generalized Linear Models. Chapman & Hall, London.

Ntzoufras, I., 2002. Gibbs variable selection using BUGS. J. Stat. Softw. 7, 1–19.

O'Hara, R.B., Sillanpää, M.J., 2009. A review of Bayesian selection methods: What, how, and which? Bayesian Anal. 4, 85–118.

Otis, D.L., Burnham, K.P., White, G.C., Anderson, D.R., 1978. Statistical inference from capture data on closed animal populations. Wildl. Monogr. 1–135.

Plummer, M., 2013. JAGS Version 3.4.0 User Manual.

Pradel, R., Sanz-Aguilar, A., 2012. Modeling trap-awareness and related phenomena in capture-recapture studies. PLoS One 7, e32666. https://doi.org/10.1371/journal.pone.0032666 ER

Pradel, R., Wintrebert, C.M.A., Gimenez, O., 2003. A proposal for a goodness-of-fit test to the Arnason-Schwarz multisite capture-recapture model. Biometrics 59, 43–53. https://doi.org/10.1111/1541-0420.00006 ER

Royle, J.A., Dorazio, R.M., 2012. Parameter-expanded data augmentation for Bayesian analysis of capture-recapture models. J. Ornithol. 152, S521–S537. https://doi.org/10.1007/s10336-010-0619-4 ER

Royle, J.A., Dorazio, R.M., 2008. Heirarchical models of animal abundance and occurrence in ecology: the analysis of data from populations, metapopulations and communities. Academic Press, SanDiego, California, USA. https://doi.org/10.1007/s10336-010-0619-4 ER

Sanz-Aguilar, A., Tavecchia, G., Genovart, M., Manuel Igual, J., Oro, D., Rouan, L., Pradel, R., 2011. Studying the reproductive skipping behavior in long-lived birds by adding nest inspection to individual-based data. Ecol. Appl. 21, 555–564. https://doi.org/10.1890/09-2339.1 ER

Schaub, M., Gimenez, O., Schmidt, B.R., Pradel, R., 2004. Estimating survival and temporary emigration in the multistate capture-recapture framework. Ecology 85, 2107–2113. https://doi.org/10.1890/03-3110 ER

Schaub, M., Kania, W., Koeppen, U., 2005. Variation of primary production during winter induces synchrony in survival rates in migratory white storks *Ciconia ciconia*. J. Anim. Ecol. 74, 656–666. https://doi.org/10.1111/j.1365-2656.2005.00961.x

Schmidt, B.R., Schaub, M., Anholt, B.R., 2002. Why you should use capture-recapture methods when estimating survival and breeding probabilities: On bias, temporary emigration, overdispersion, and Common Toads. Amphibia-Reptilia 23, 375–388. https://doi.org/10.1163/15685380260449234

Schofield, M.R., Barker, R.J., 2011. Full open population capture-recapture models with individual covariates. J. Agric. Biol. Environ. Stat. 16, 253–268. https://doi.org/10.1007/s13253-010-0052-4

Schwarz, C.J., Arnason, A.N., 1996. A general methodology for the analysis of capture-recapture experiments in open populations. Biometrics 52, 860–873. https://doi.org/10.2307/2533048

Spiegelhalter, D.J., Best, N.G., Carlin, B.P., Van Der Linde, A., 2002. Bayesian measures of model complexity and fit. J. R. Stat. Soc. Ser. B – Stat. Methodol. 64, 583–639. https://doi.org/http://dx.doi.org/10.1111/1467-9868.00353

Su, Y.-S., Yajima, M., 2014. R2jags: A Package for Running jags from R.

Tanner, M.A., Wong, W.H., 1987. The Calculation of Posterior Distributions by Data Augmentation. J. Am. Stat. Assoc. 82, 528–540. https://doi.org/10.1080/01621459.1987.10478458

Tenan, S., O'Hara, R.B., Hendriks, I., Tavecchia, G., 2014. Bayesian model selection: The steepest mountain to climb. Ecol. Modell. 283, 62–69. https://doi.org/10.1016/j.ecolmodel.2014.03.017

White, G.C., 2011. Program MARK 6.1.

White, G.C., Burnham, K.P., 1999. Program MARK: Survival estimation from populations of marked animals. Bird Study 46, S120–S139.

White, G.C., Kendall, W.L., Barker, R.J., 2006. Multistate survival models and their extensions in Program MARK. J. Wildl. Manage. 70, 1521–1529. https://doi.org/10.2193/0022-541X(2006)70[1521:MSMATE]2.0.CO;2

Tables

Table A.1. Indexing and corresponding years, sampling occasions (occ), and intervals (inter) for selected parameters from WinBUGS (state-space) and JAGS (m-array) code for multistate mark-recapture models of nesting female Snapping Turtles in Algonquin Park. Shaded columns denote intervals of high mortality from otter predation (1986/87−1988/89) and dam failure (1997/98).

Year	dummy occ	Inter	1980 occ	inter	1981 occ	… …	1986 occ	inter	1987 occ	inter	1988 occ	inter	1989 occ	… …	1997 occ	inter	1998 occ	… …	2012 occ	inter	2013 occ
state-space			pA[1]		pA[2]	…	pA[7]		pA[8]		pA[9]		pA[10]	…	pA[18]		pA[19]	…	pA[33]		pA[34]
			pB[1]		pB[2]	…	pB[7]		pB[8]		pB[9]		pB[10]	…	pB[18]		pB[19]	…	pB[33]		pB[34]
	z[i,1]		z[i,2]		z[i,3]	…	z[i,8]		z[i,9]		z[i,10]		z[i,11]	…	z[i,19]		z[i,20]	…	z[i,34]		z[i,35]
	y[i,1]		y[i,2]		y[i,3]	…	y[i,8]		y[i,9]		y[i,10]		y[i,11]	…	y[i,19]		y[i,20]	…	y[i,34]		y[i,35]
		SA[1]*		SA[2]		…		SA[8]		SA[9]		SA[10]		…		SA[19]		…		SA[34]	
		SB[1]*		SB[2]		…		SB[8]		SB[9]		SB[10]		…		SB[19]		…		SB[34]	
		psiAB[1]*		psiAB[2]		…		psiAB[8]		psiAB[9]		psiAB[10]		…		psiAB[19]		…		psiAB[34]	
		psiBA[1]*		psiBA[2]		…		psiBA[8]		psiBA[9]		psiBA[10]		…		psiBA[19]		…		psiBA[34]	
		psiAC1[1]*		psiAC1[2]		…		psiAC1[8]		psiAC1[9]		psiAC1[10]		…		psiAC1[19]		…		psiAC1[34]	
		psiBC2[1]*		psiBC2[2]		…		psiBC2[8]		psiBC2[9]		psiBC2[10]		…		psiBC2[19]		…		psiBC2[34]	
		psiC1A[1]*		psiC1A[2]		…		psiC1A[8]		psiC1A[9]		psiC1A[10]		…		psiC1A[19]		…		psiC1A[34]	
		psiC2B[1]*		psiC2B[2]		…		psiC2B[8]		psiC2B[9]		psiC2B[10]		…		psiC2B[19]		…		psiC2B[34]	
		gamma1[1]		gamma1[2]		…		gamma1[8]		gamma1[9]		gamma1[10]		…		gamma1[19]		…		gamma1[34]	
		gammaA[1]		gammaA[2]		…		gammaA[8]		gammaA[9]		gammaA[10]		…		gammaA[19]		…		gammaA[34]	
		gammaB[1]		gammaB[2]		…		gammaB[8]		gammaB[9]		gammaB[10]		…		gammaB[19]		…		gammaB[34]	
m-array					pA[1]	…	pA[6]		pA[7]		pA[8]		pA[9]	…	pA[17]		pA[18]	…	pA[32]		pA[33]
					pB[1]	…	pB[6]		pB[7]		pB[8]		pB[9]	…	pB[17]		pB[18]	…	pB[32]		pB[33]
				SA[1]		…		SA[7]		SA[8]		SA[9]		…		SA[18]		…		SA[33]	
				SB[1]		…		SB[7]		SB[8]		SB[9]		…		SB[18]		…		SB[33]	
				psiBA[1]		…		psiBA[7]		psiBA[8]		psiBA[9]		…		psiBA[18]		…		psiBA[33]	
				psiAB[1]		…		psiAB[7]		psiAB[8]		psiAB[9]		…		psiAB[18]		…		psiAB[33]	
				psiAC1[1]		…		psiAC1[7]		psiAC1[8]		psiAC1[9]		…		psiAC1[18]		…		psiAC1[33]	
				psiBC2[1]		…		psiBC2[7]		psiBC2[8]		psiBC2[9]		…		psiBC2[18]		…		psiBC2[33]	
				psiC1A[1]		…		psiC1A[7]		psiC1A[8]		psiC1A[9]		…		psiC1A[18]		…		psiC1A[33]	
				psiC2B[1]		…		psiC2B[7]		psiC2B[8]		psiC2B[9]		…		psiC2B[18]		…		psiC2B[33]	
				phi[1,,]		…		phi[7,,]		phi[8,,]		phi[9,,]		…		phi[18,,]		…		phi[33,,]	
					Dp[1,,]	…	Dp[6,,]		Dp[7,,]		Dp[8,,]		Dp[9,,]	…	Dp[17,,]		Dp[18,,]	…	Dp[32,,]		Dp[33,,]
					Dq[1,,]	…	Dq[6,,]		Dq[7,,]		Dq[8,,]		Dq[9,,]	…	Dq[17,,]		Dq[18,,]	…	Dq[32,,]		Dq[33,,]

* denotes empty parameters not informed by occasion-specific data but estimable via hyperparameter

Figures

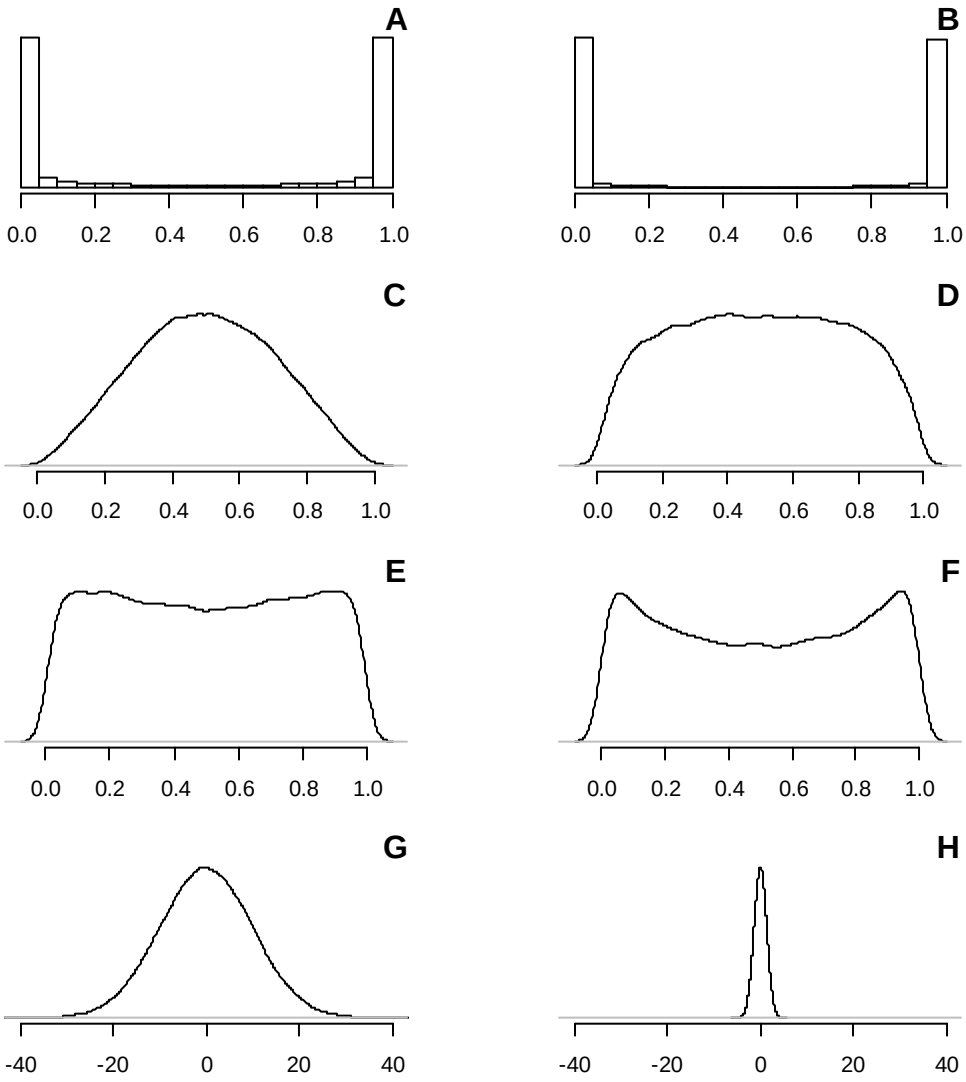

Figure A.1 Induced prior distributions on the probability scale (A-F) of parameters that are estimated as the logit sum of categorical GLM effects with normal priors (G,H). A and B are histograms, C-H are density kernels and each plot is based on 10^5 simulations. A is function of a prior that is $N(0, 10)$ distributed (G) which is vague on the logit scale but induces a strongly informative distribution on the probability scale. B is the resulting induced prior on survivorship given a hypothetical GLM with four $N(0, 10)$ parameters. C-F show induced prior distributions of mean survivorship on the probability scale resulting from linear models defined on the logit scale with 1 (C), 2 (D), 3 (E), and 4 (F) parameters. In C-F each parameter has a prior distribution of $N(0, \sigma_i^2)$ where σ_i^2 is given an inverse gamma hyperprior $\Gamma^{-1}(4,5)$. The resulting prior is less diffuse on the logit scale (H) but results in more appropriate induced priors on the probability scale. See King et al. (2010) *pp.* 245-247.

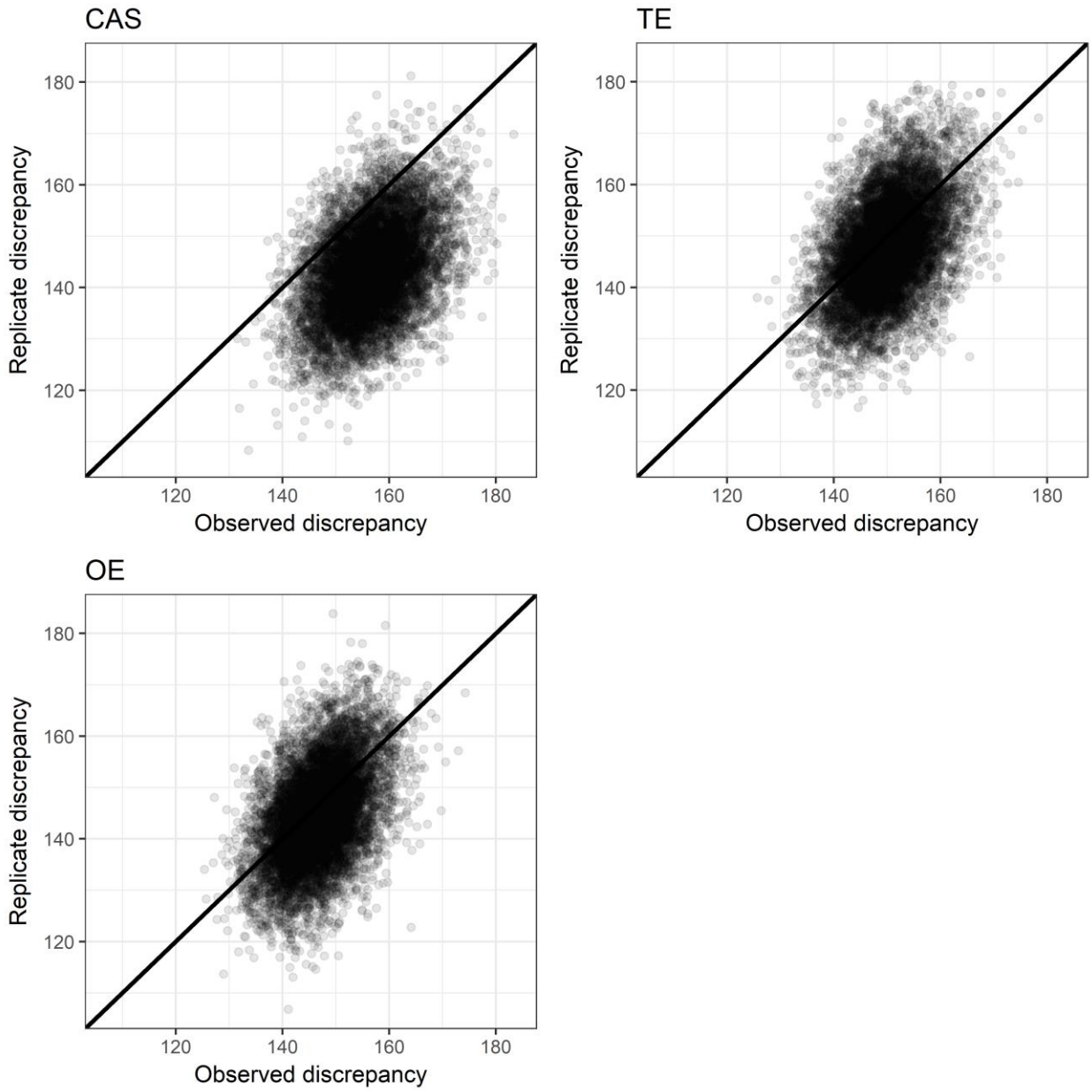

Figure A.2. Scatterplots of replicate and observed discrepancy plotted as a visual posterior predictive check (Gelman et al., 2004) for a constrained Conditional Arnason–Schwarz model (CAS), and similar models including temporary emigration (TE) or immediate observation effect (OE). All are multistate models of nesting Snapping Turtles in Algonquin Park 1980-2013. Discrepancies were calculated for each MCMC iteration in JAGS using the Freeman-Tukey statistic (Brooks et al., 2000; Kéry and Schaub, 2012). Bayesian P-values are calculated as the proportion of points above and below the 1:1 line of equality (Gelman et al., 2004) and were 0.11 for CAS, 0.438 for TE, and 0.441 for OE. Values closer to 0.5 indicate adequate fit as assessed using the chosen discrepancy measure.

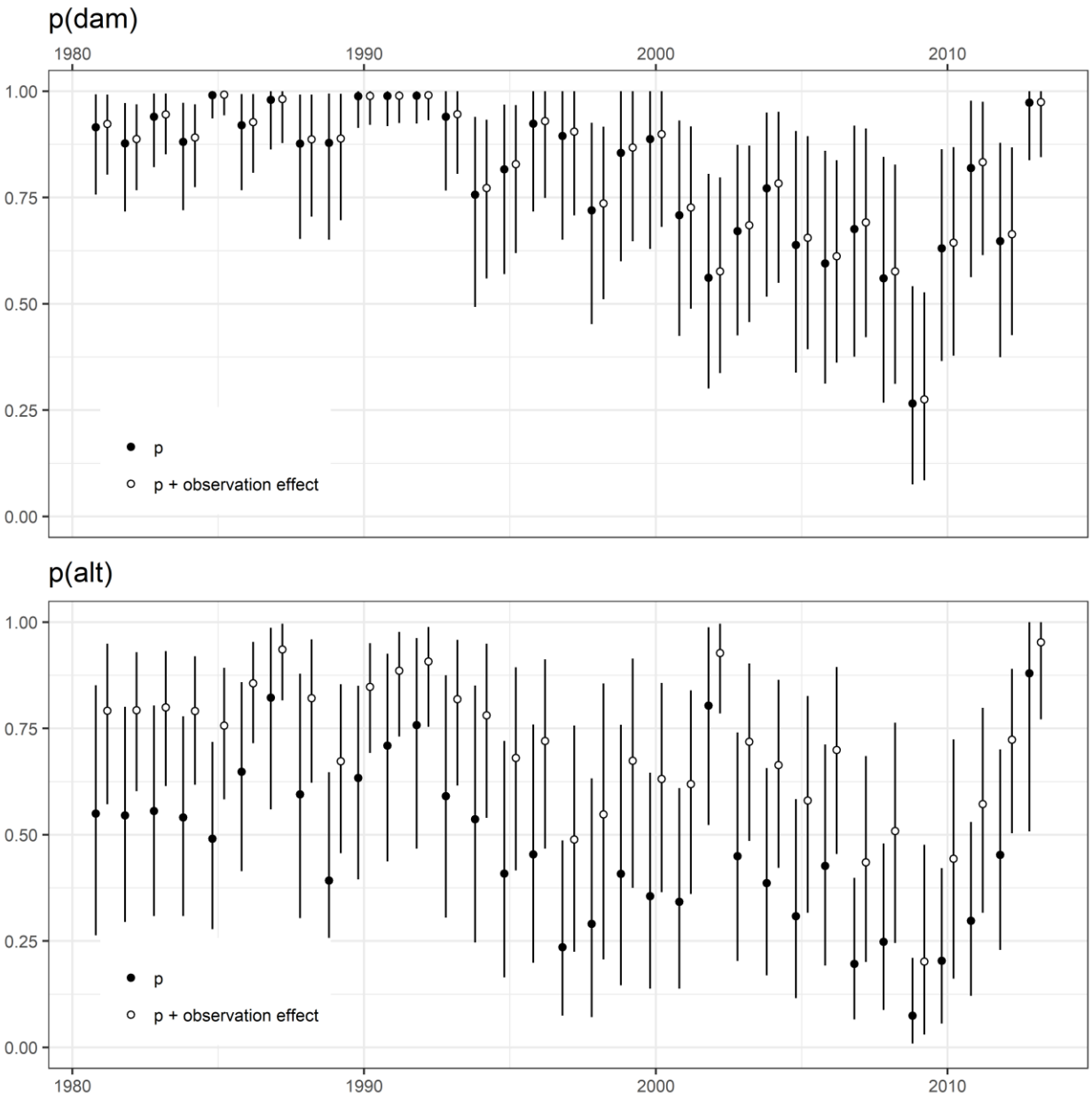

Figure A.3. Recapture parameter estimates and 95% CRI of a multinomial m-array multistate mark recapture model of nesting Snapping Turtles over 33 occasions with observation effects and two sites: Sasajewun Dam (top) and alternate sites (bottom). Hollow circles are recapture probabilities for occasion *t* when an individual was last captured on occasion $t - 1$ and filled circles are recapture probabilities for individuals not captured on occasion $t - 1$.

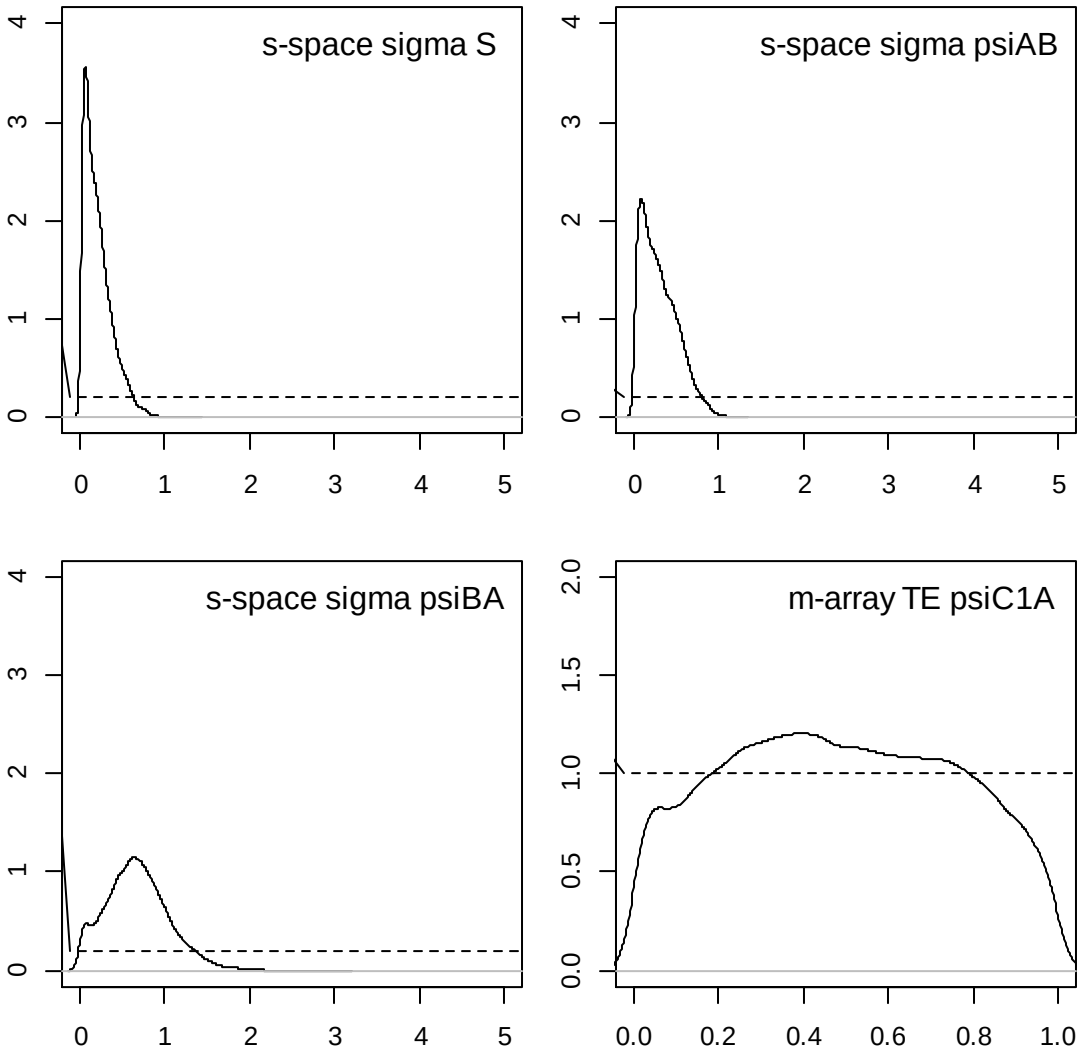

Figure A.4. Distributions of some parameters from state-space or m-array (*psiC1A*) models of nesting female Snapping Turtles. These parameters were suspected of being weakly identifiable. The prior distribution is shown by the dotted line. Only *psiC1A*, the constant probability of return from unobservable state C1 to observable state A (nesting on the dam) on the bottom right is unidentifiable (Gimenez et al., 2009). In the subsequent state space parameterization for abundance estimation this parameter was constrained to U[0.3,0.7] to allow for convergence of the other parameters. See Kéry and Schaub (2012) *p*. 219.

Appendix B: Applying the seasonal growth model over multiple years

This appendix was first published as Appendix A in supplemental materials of

Keevil, M.G., Armstrong, D.P., Brooks, R.J., Litzgus, J.D., 2021. A model of seasonal variation in somatic growth rates applied to two temperate turtle species. Ecol. Modell. 443, 109454. https://doi.org/10.1016/j.ecolmodel.2021.109454

Enforcing intercepts

In the simple case where seasonal growth is modeled without among-individual, site, or year variation, the logistic GPM (growth phenology model) applied to fraction of a calendar year, s, is:

$$\begin{aligned} \mathrm{f}(s) &= \left[1 + \exp\left(\frac{B - s}{g}\right)\right]^{-1} \\ &= p \end{aligned} \qquad \text{(B1)}$$

where g and B are parameters to be estimated and p is the proportion of annual growth accumulated by s.

Note that the inverse of $\mathrm{f}(s) = p$ is $\mathrm{f}^{-}(p) = s$ and is given by:

$$\begin{aligned} \mathrm{f}^{-}(p) &= B + g \cdot \ln\left(\frac{p}{1 - p}\right) \\ &= s \end{aligned} \qquad \text{(B2)}$$

Time, quantified in decimal calendar years, is denoted as $y.s$ and we use $y \in \mathbb{Z}$ to symbolize the integer component and $0 \leq s < 1$ is the remaining fractional component (notation for variables measuring time on different scales are summarized in Table 3.2). Therefore, $y.s = y + s$. Function F separates the integer year from the fractional component, applies the logistic GPM function f (Eq. (B.1)), and returns the sum of year and expected proportion of annual growth accumulated:

$$\begin{aligned} \mathrm{F}(y.s) &= \lfloor y.s \rfloor + \mathrm{f}(y.s - \lfloor y.s \rfloor) \\ &= y + \mathrm{f}(s) \\ &= y + p \\ &= y.p \end{aligned} \qquad \text{(B.3)}$$

where $y.p$ is the expected growth phenology time and $\lfloor y.s \rfloor$ symbolizes the $\mathrm{floor}(y.s)$ function which rounds down to the nearest integer $y \leq y.s$. For example, on 10 Aug 2016, the decimal

year date is $y.s = 2016.61$ and $y = \lfloor y.s \rfloor = \lfloor 2016.61 \rfloor = 2016$ and $s = y.s - y = 2016.61 - 2016 = 0.61$. Our notation is based on the shorthand that y is the component to the left of the decimal point in $y.s$ and s is the component to the right of the decimal. This notation is intuitive when applied to positive decimal year values but must be interpreted more carefully for negative values (for example, the von Bertalanffy parameter t_0 (theoretical age when size = 0) is expected to be negative)[1].

A modification of the logistic GPM is described in the main text using Eq.(8), which we reproduce here as:

$$\begin{aligned} \mathrm{f}'(s) &= \frac{\mathrm{f}(s) - \mathrm{f}(0)}{\mathrm{f}(1) - \mathrm{f}(0)} \\ &= p \end{aligned}$$

and

$$\begin{aligned} \mathrm{F}'(y.s) &= y + \mathrm{f}'(s) \\ &= y.p \end{aligned}$$

This change rescales the response, p, in order to constrain it to so that $p = 0$ at $s = 0$ and p approaches 1 as s approaches 1. This makes little difference over the range of values of B and g that we have considered in our applications, but the unmodified logistic GPM could produce unanticipated or unrealistic output when subjected to a wider range of proposed parameter combinations without this constraint (Figure B.1).

[1] For negative decimal year value $x.s$, $\mathrm{F}(x.s)$ still applies and the equalities $x.s = x + s,\ x = \lfloor x.s \rfloor$, and $s = x.s - \lfloor x.s \rfloor$ are also still valid. Note, however, that when $x < 0$, $x = \lfloor x.s \rfloor$ is not equivalent to truncating $x.s$ at the decimal point. For example, given a hypothetical negative value $x.s = -1.2$, $x = \lfloor x.s \rfloor = -2$ rather than -1, and $s = x.s - \lfloor x.s \rfloor = 0.8$ rather than 0.2. Therefore, $\mathrm{F}(-1.2) = -2 + \mathrm{f}(0.8)$.

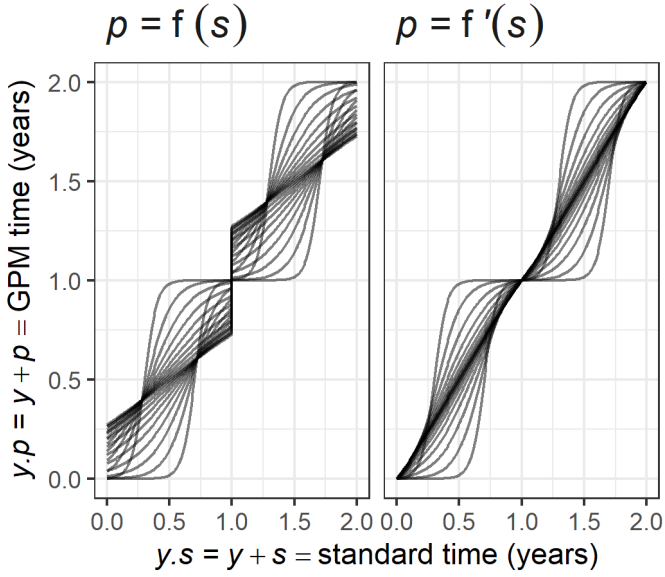

Figure B.1. Comparison of the unmodified logistic GPM (f(s); Eq.(B.1))) to the rescaled version (f′(s); Eq.(8)). Rescaling ensures the proportion of annual growth, p, approaches 0 at the start ($s = 0$) and 1 at the end ($s = 1$) of each annual period. Output is shown over $y = 2$ years across a range of logistic GPM parameter values ($B = 0.3{:}\,0.7$, $g = 0.05{:}\,0.5$).

In addition to the rescaling approach , we have also demonstrated a model using the beta cumulative distribution function instead of the logistic function for the GPM, which avoids this problem (Appendix C).

Adding the logistic GPM to a von Bertalanffy growth function

We denoted age quantified as decimal years-of-age as $t.s$ to distinguish it from decimal calendar years. This distinction is necessary because because age is measured relative to date of birth (or date of hatch in the case of turtles) which is not expected to fall at a transition between calendar years. Therefore, fractions of a year of age are phase-shifted relative to fractions of a calendar year and this must be accounted for when applying a non-linear transformation such as the logistic GPM.

Given this notation, the length-at-age von Bertalanffy (vB) model is given in the main text as Eq. (4):

$$L_{i,j} = L_\infty \left(1 - \exp\left(-k\left(t.s_{i,j} - t_0\right)\right)\right)$$

where L_∞ is the asymptotic size parameter, k is the rate parameter, $t.s_{i,j}$ is age at observation j of individual i, and t_0 is the hypothetical age before birth when length is 0, which we treated as a population-level parameter. We incorporated the logistic GPM using function F (Eq. (B.3)) within the time term as main text Eq. (5):

$$L_{i,j} = L_\infty \left(1 - \exp\left(-k\left[\mathrm{F}\left(t.s_{i,j} + s_H\right) - \mathrm{F}(t_0 + s_H)\right]\right)\right)$$

where s_H is a phase shift parameter corresponding to the year fraction on the date of hatch. We arrived at this equation by focusing on the vB time term, $\Delta t = t.s_{i,j} - t_0$ and expanding age into a difference of calendar decimal year values by observing that:

$$\begin{aligned} t.s_{i,j} &= y.s_{i,j} - y_H.s_{H_i} \\ t_0 &= y_0.s_{0_i} - y_H.s_{H_i} \end{aligned} \qquad (\mathrm{B}.4)$$

where $y.s_{i,j}$ is time at observation j of individual i, $y_H.s_{H_i}$ is individual time of hatching, and $y_0.s_{0_i}$ is the time when $L = 0$. Substituting Eq. (B.4) into the vB time term yields:

$$\begin{aligned} \Delta t &= \left(y.s_{i,j} - y_H.s_{H_i}\right) - \left(y_0.s_{0_i} - y_H.s_{H_i}\right) \\ &= y.s_{i,j} - y_0.s_{0_i} \end{aligned} \qquad (\mathrm{B}.5)$$

Because the time variables are now on the decimal calendar year scale, the logistic GPM as function F (Eq. (B.3)) can then be applied to Eq. (B.5) :

$$\Delta t' = \mathrm{F}\left(y.s_{i,j}\right) - \mathrm{F}\left(y_0.s_{0_i}\right) \qquad (B.6)$$

Finally, we rearranged the equalities in Eq. (B.4) and substituted them into Eq. (B.6). In order to simplify, we noted that $\mathrm{F}(x.s) = \mathrm{F}(x + s) = x + \mathrm{F}(s)$ when x is an integer ($x \in \mathbb{Z}$):

$$\begin{aligned} \Delta t' &= \mathrm{F}\left(t.s_{i,j} + y_H.s_{H_i}\right) - \mathrm{F}\left(t_0 + y_H.s_{H_i}\right) \\ &= \left(\mathrm{F}\left(t.s_{i,j} + s_{H_i}\right) + y_{H_i}\right) - \left(\mathrm{F}\left(t_0 + s_{H_i}\right) + y_{H_i}\right) \\ &= \mathrm{F}\left(t.s_{i,j} + s_{H_i}\right) - \mathrm{F}\left(t_0 + s_{H_i}\right) \end{aligned} \qquad (B.7)$$

For our analyses, we have assumed that hatching occurs at the same time each year so that there is no individual variation in s_H and so no index i in Eq.(5) in the main text.

Plotting length-at-age on the GPM scale

In order to plot the length-at-age vB curve on the GPM effective time scale (Figure 3.3D) we reorganized the time term as:

$$\Delta t' = t.p_{i,j} - \widetilde{t_0} \qquad (B.8)$$

where $t.p_{i,j}$ is age of individual i at occasion j on the GPM time scale. $\widetilde{t_0}$ is the GPM time scale counterpart of t_0, defined as the theoretical age when $L = 0$. To relate $t.p$ to age on the linear time scale ($t.s$), we defined age on the GPM scale and then substituted from Eq. (B.4):

$$\begin{aligned} t.p_{i,j} &= \mathrm{F}\left(y.s_{i,j}\right) - \mathrm{F}\left(y_H.s_{H_i}\right) \\ &= \mathrm{F}\left(t.s_{i,j} + y_H.s_{H_i}\right) - \mathrm{F}\left(y_H.s_{H_i}\right) \\ &= \mathrm{F}\left(t.s_{i,j} + s_H\right) + y_{H_i} - \left(\mathrm{F}(s_H) + y_{H_i}\right) \\ &= \mathrm{F}\left(t.s_{i,j} + s_H\right) - \mathrm{F}(s_H) \end{aligned} \qquad (B.9)$$

By the same logic, it can be shown that:

$$\widetilde{t_0} = \mathrm{F}(t_0 + s_H) - \mathrm{F}(s_H)$$

Deriving t_0 from the Painted Turtle interval model

The combined vB and GPM model was fitted to juvenile Painted Turtles using the vB interval formulation for recapture data. The interval formulation does not include t_0 in the likelihood so t_0 does not need to be estimated during model fitting. However, some form of this parameter is necessary for plotting the length-at-age or length vs. time vB curve (Figure 3.6). To calculate individual $\widetilde{t_{0_i}}$ as a derived parameter we substituted Eq. (B.8) into the time term of the modified Armstrong and Brooks (2013) formulation of the length-at-age vB equation:

$$L_{i,j} = L_\infty \left(1 - \exp\left(-\frac{k_i}{L_\infty}\left(t.p_{i,j} - \widetilde{t_{0_i}}\right)\right)\right) \qquad (B.10)$$

In addition to incorporating the GPM via the time term, this model differs from that of Armstrong and Brooks (2013) because L_∞ is modeled without individual variation. We set $L_{i,j} = L_{H_i}$, where L_{H_i} is the unobserved size at hatching for known-age individual i, and specified GPM age at hatching as $t.p = 0$ and rearranged to solve for $\widetilde{t_{0_i}}$:

$$\widetilde{t_{0_i}} = \frac{L_\infty}{k_i} \cdot \ln\left(1 - \frac{L_{H_i}}{L_\infty}\right) \qquad (B.11)$$

Note that the equation for $\widetilde{t_0}$ would be slightly different for the standard vB parameterization in that $1/k$ would replace L_∞/k_i.

3.1 Recovering linear-scale t_0

In order to recover t_0, Eq. (B.9) can be modified by substituting F' (function F rescaled to enforce intercepts; Eq. (8)) for F and rearranged:

$$t_{0_i} = \mathrm{F}'^{-}\left(\widetilde{t_{0_i}} + \mathrm{F}'(s_H)\right) - s_H \qquad (B.12)$$

where $\mathrm{F}'^{-}(x.p) = x.s$ is the inverse of $\mathrm{F}'(x.s) = x.p$ so:

$$\begin{aligned} \mathrm{F}'^{-}(x.p) &= \lfloor x.p \rfloor + \mathrm{f}^{-}\Big((x.p - \lfloor x.p \rfloor)\big(\mathrm{f}(1) - \mathrm{f}(0)\big) + \mathrm{f}(0)\Big) \\ &= x.s \end{aligned} \qquad (B.13)$$

where f^{-} is given by Eq. (B.2).

Identifiability of B and g

Parameters B and g of the logistic GPM for Painted Turtles (Table 3.3, Figure 3.5) were estimated with less precision than they were for the GPM fitted to intra-annual observations of Snapping Turtles (Table 3.1, Figure 3.2C) because only a small subset of the Painted Turtle observations was informative for the seasonal component. We assessed the sensitivity of B and g estimated for Painted Turtles to prior specification by comparing the posterior distributions given either a uniform prior distribution or given our initial PERT prior specification (Figure B.2).

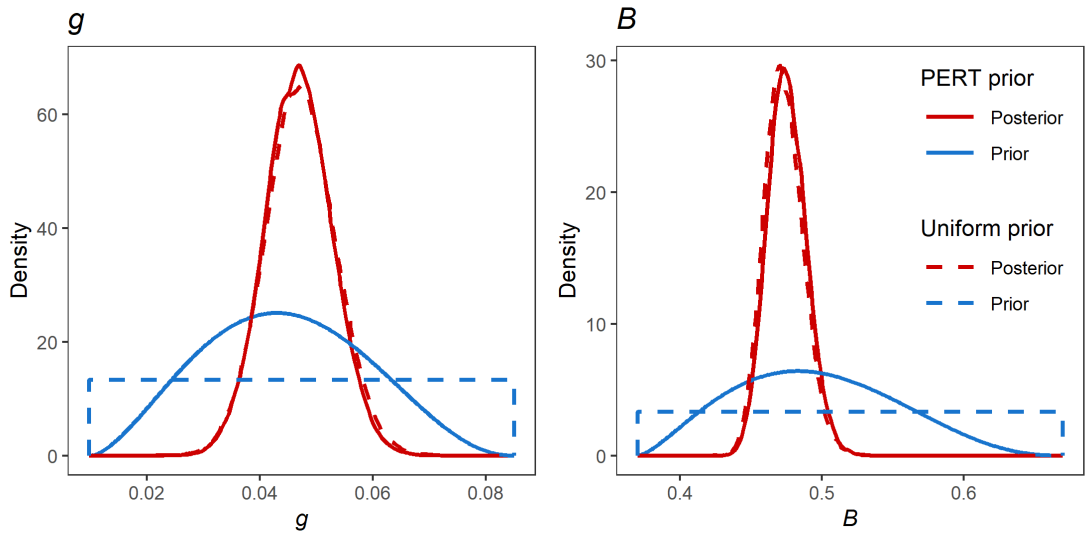

Figure B.2. Estimated marginal posterior and prior densities of Painted Turtle logistic seasonal model parameters g and B. Posteriors were estimated using either uniform or PERT prior distributions. The modes of the PERT prior distributions were chosen to reflect our prior assessment of the most likely values. These were $B = 0.54$ (corresponding to an annual growth accumulation midpoint at 15 July) and $g = 0.043$ (corresponding to 90% of annual growth accumulating in 76 days which is the time between 31 May and 15 August).

We assessed identifiability of the Painted Turtle seasonal GPM parameters B and g fitted using uniform priors by estimating τ (Garrett and Zeger, 2000), which quantifies the overlap between

the prior and posterior distributions. Garrett and Zeger (2000) suggest an *ad hoc* threshold for τ of 0.35. Given a uniform prior, if $\tau > 0.35$ then there is evidence that the corresponding parameter is weakly identifiable, which implies that the data provide limited information about the parameter and the prior has a strong influence over the posterior distribution (Garrett and Zeger, 2000; Gimenez et al., 2009). The method of Gimenez et al. (2009) is specific to $U(0,1)$ priors, so we followed Keevil (2020) in calculating an MCMC estimate of τ based on overlap estimator $\widehat{OVL_4}$ in Schmid and Schmidt (2006) as:

$$\hat{\tau} = \frac{1}{n}\sum_{i=1}^{n} \min\left[1, \frac{p(x_i)}{\hat{d}(x_i)}\right] \qquad (B.14)$$

where $p(x_i)$ is the prior density at x_i and $\hat{d}(x_i)$ is an estimate of the posterior density using a kernel density estimator applied to MCMC samples $x_i,\ i = 1, \ldots, n$ for each seasonal model parameter (Gimenez et al., 2009). We only considered estimates using a uniform prior because the $\tau > 0.35$ threshold may not apply for other prior distributions (Gimenez et al., 2009).

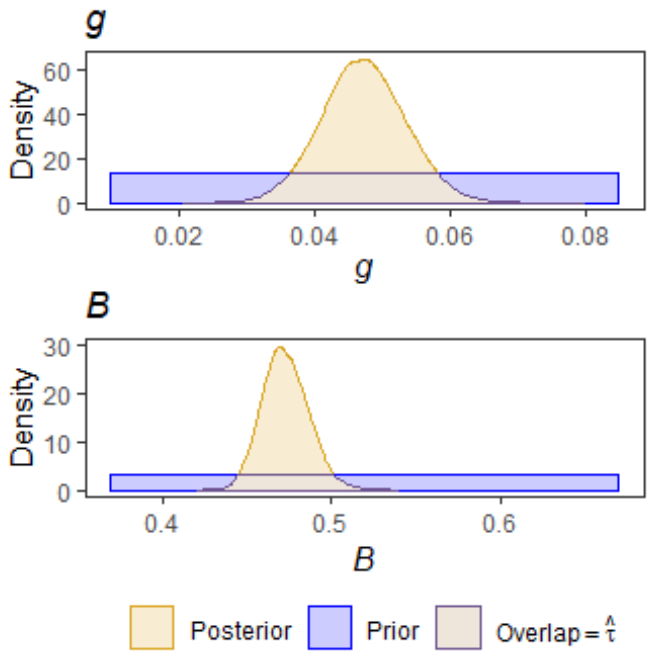

Figure B.3. Uniform prior and resulting posterior densities for parameters of the seasonal component of the juvenile Painted Turtle somatic growth model. The estimated identifiability parameters $\hat{\tau}_g = 0.368$ and $\hat{\tau}_B = 0.224$, which describe the proportional overlap of prior and posterior distributions (Eq.(B.14)), suggest that g may be only weakly identifiable (Garrett and Zeger, 2000; Gimenez et al., 2009).

Our estimates of $\hat{\tau}$ suggest weak identifiability for parameter g (Figure B.3), but the posterior distributions remained similar across two different prior specifications (Figure B.2).

References

Armstrong, D.P., Brooks, R.J., 2013. Application of hierarchical biphasic growth models to long-term data for Snapping Turtles. Ecological Modelling 250, 119–125. https://doi.org/10.1016/j.ecolmodel.2012.10.022

Garrett, E.S., Zeger, S.L., 2000. Latent class model diagnosis. Biometrics 56, 1055–1067. https://doi.org/10.1111/j.0006-341X.2000.01055.x

Gimenez, O., Morgan, B.J.T., Brooks, S.P., 2009. Weak identifiability in models for mark-recapture-recovery data, in: Thomson, D.L., Cooch, E.G., Conroy, M.J. (Eds.), Modeling Demographic Processes in Marked Populations. Springer, New York, pp. 1055–1067.

Keevil, M.G., 2020. Joint estimation of growth and survival from mark-recapture data to improve estimates of senescence in wild populations: Comment. Ecology. https://doi.org/10.1002/ecy.3232

Schmid, F., Schmidt, A., 2006. Nonparametric estimation of the coefficient of overlapping—theory and empirical application. Computational Statistics and Data Analysis 50, 1583–1596. https://doi.org/10.1016/j.csda.2005.01.014

Appendix C: Beta growth phenology model of Painted Turtle seasonal growth

This appendix was first published as Appendix C in supplemental materials of

Keevil, M.G., Armstrong, D.P., Brooks, R.J., Litzgus, J.D., 2021. A model of seasonal variation in somatic growth rates applied to two temperate turtle species. Ecol. Modell. 443, 109454. https://doi.org/10.1016/j.ecolmodel.2021.109454

Introduction and methods

The beta distribution is a continuous probability distribution defined over values between 0 and 1. Therefore, the cumulative distribution function (CDF) of the standard form of the beta distribution returns 0 at the start of the interval [0,1] and 1 at the end. This function can be used instead of the logistic function in the growth phenology model (GPM), thereby removing the need for rescaling to enforce intercepts at 0 and 1 at the start and end of each annual period (Eq.(8)).

We denoted the beta CDF of s as $\mathrm{betaCDF}(s|\alpha,\beta)$ conditional on shape parameters α and β. We used a reparameterization that defines the beta distribution in terms of ω and κ: $\mathrm{betaCDF}'(s|\omega,\kappa)$ (Kruschke, 2015). This parameterization is more intuitive for eliciting priors and interpreting the parameters. ω is the inflection point of the CDF and the mode of the probability distribution function (PDF); in the context of the GPM, ω corresponds to the annual point of maximum growth. κ is the concentration parameter, which affects the dispersion of the PDF. In the context of the GPM, κ controls the rate of change of growth and the effective length of the growing season. As κ increases, the CDF becomes steeper and the effective length of the growing season shortens. These parameters are related to the shape parameters as follows (Kruschke, 2015):

$$\begin{aligned}\alpha &= \omega(\kappa-2)+1\\ \beta &= (1-\omega)(\kappa-2)+1\end{aligned}$$

An invertible, closed-form of the beta CDF is not available (the inverse of the CDF is the quantile function) but both R (R Development Core Team, 2020) and JAGS (Plummer, 2003) provide functions `dbeta`, `pbeta`, and `qbeta` to calculate the PDF, CDF, and QF (quantile function), respectively, making a model based on the beta CDF tractable in these environments.

We specified the same PERT prior on ω as we have used on B (the median = mode of the logistic distribution as applied in the main text) so that ω was constrained between 15 May and 1 September with a mode at 15 July: $\omega \sim PERT(0.37,\ 0.54,\ 0.67)$. To determine a biologically interpretable prior on κ, we based it on the time taken to complete 90% of annual growth with a minimum of 21 days, a maximum of six months, and a most likely value (mode) of 2.5 months (corresponding to 30 May – 15 August). This is the same strategy that we used to specify the prior on the logistic GPM g parameter. However, because of the lack of a closed-form QF, we

did not construct an analytic solution for κ analogous to Eq.(3) for g. Additionally, the beta CDF and PDF is not necessarily symmetrical, so the time difference between quantiles also depends on the location of ω because the beta distribution becomes highly skewed as the mode approaches either boundary. Because we constrained the mode, ω, away from 0 and 1, we could make the simplifying assumption that the effect of ω on the distance between quantiles was small enough to be ignored in the context of prior specification on κ. Therefore, we held ω constant at 0.5 and used the `optimize` function in R to solve for κ numerically at the specified time and quantile intervals. We found that this produced a highly skewed prior distribution (Figure C.1). We reduced the skew by specifying the prior on the transformation κ^{-1} resulting in the prior $\kappa^{-1} \sim PERT(0.0012,\ 0.024,\ 0.101)$. Inverting κ also reverses the parameter so that short effective growing seasons are associated with low values of κ^{-1} and κ^{-1} has the same direction and a similar scale to parameter g of the logistic GPM over the range of plausible values that we considered.

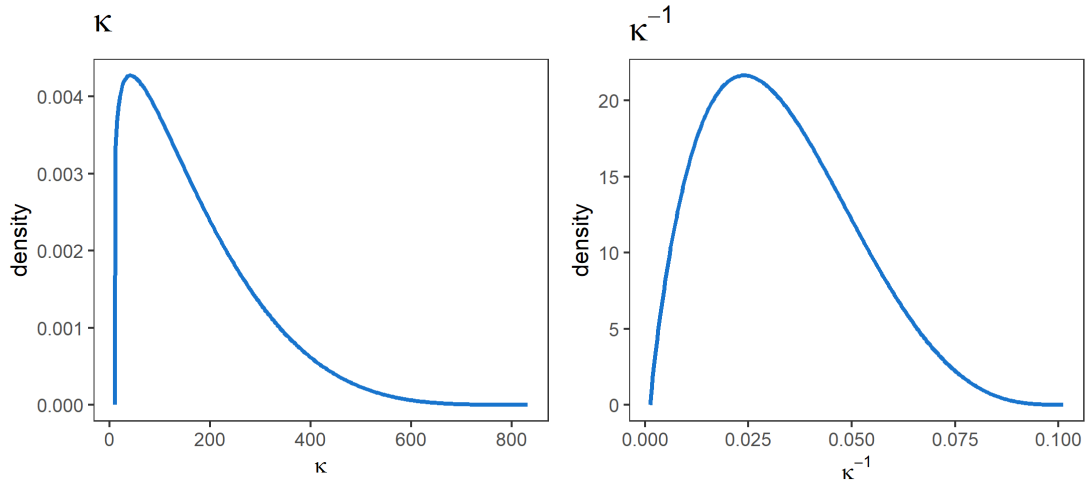

Figure C.1. Comparison of PERT prior distributions specified on the concentration parameter κ and its inverse, κ^{-1}. On the time difference scale, the most likely prior value (mode) occurs 43.9% of the interval between the minimum and maximum values specified in the prior. On the κ scale the mode is at 3.9% of the interval. Specifying the prior on κ^{-1} results in a less skewed distribution with the mode at the 22.8% of the interval.

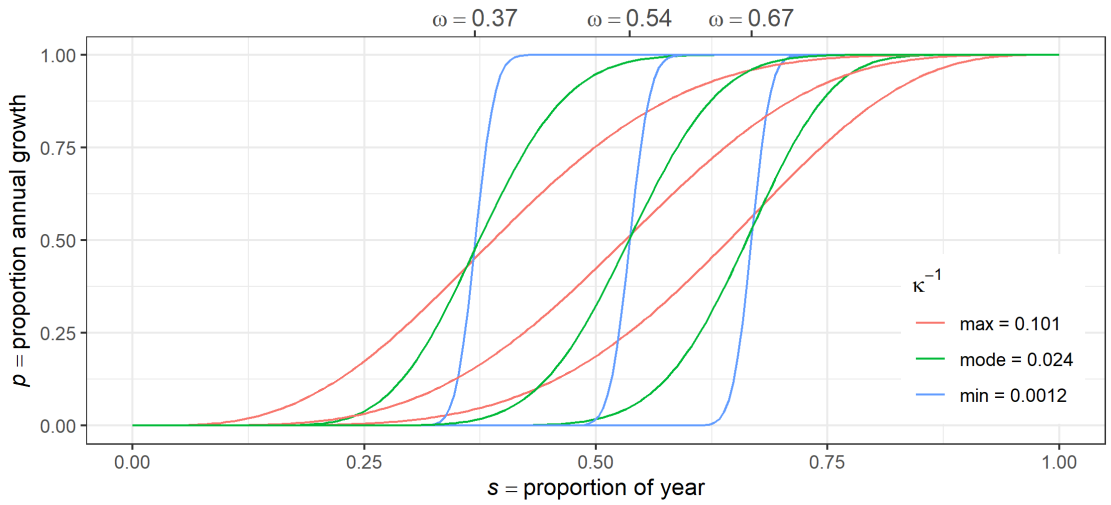

Figure C.2. betaCDF growth phenology model (GPM) calculated at the minimum, mode, and maximum of the PERT distributions specified as priors on parameters ω and κ^{-1}.

We applied the beta GPM to the juvenile Painted Turtle data set described in the main text as a component of the joint model combing the GPM, von Bertalanffy growth, and hatchling size. We fitted the joint model using the Bayesian updating software JAGS version 4.2.0 (Plummer, 2003) implemented in R version 4.0.2 (R Development Core Team, 2020) using the R2jags package version 0.6-1 (Su and Masanao Yajima, 2020). We ran three MCMC (Markov Chain Monte Carlo) chains for 110000 iterations and discarded the first 1000 as burn-in.

R and JAGS code

Data handling

R Code to prepare the data set for analysis is given in Appendix D of Keevil et al. (2021).

JAGS model

```
cat("
model {
  ## Variables passed as data
  # Growth data:
  # I = scalar number of individuals
  # J = vector of length I containing number of observations/individual
  # L = I x max(J) matrix of carapace length observations in cm
  # y = I x max(J) matrix of integer year values
  # yH = vector of hatch years for known-age individuals
  # s = I x max(J) matrix of fraction of year values (0 < s[i] < 1)
  # sH = scalar standardized fraction of year at typical hatch date
  # nKA = scalar, individuals indexed 1:nKA have known ages
```

```
# mult = scalar, individuals indexed mult:I have more than one observation

# Size-at-hatch data:
# H = scalar number of measured hatchlings
# C = scalar number of clutches
# hL = vector of length H of observed hatchling lengths
# ci = vector of length H of clutch indices (for nested indexing)

# pert = PERT prior params for GPM parameters kappa and omega

### Priors and constraints
Lmax ~ dnorm(0, 1.0E-6) # uniformative prior for mean max size
mu.k ~ dnorm(0, 1.0E-6)  # uniformative prior for mean log of k
sigma.k ~ dunif(0,100) # uninformative prior for s.d. of log of k
sigma.e ~ dunif(0,100) # uninformative prior for s.d. of residual error

# Hatchling size distribution priors
mu.c ~ dnorm(0, 1.0E-6) # among clutch mean hatchling L
sigma.c ~ dunif(0,100) # s.d. of among clutch mean hatchling L
sigma.h ~ dunif(0,100) # s.d. of within clutch hatchling L
sigma.t <- (sigma.c^2 + sigma.h^2)^0.5 # Law of total variance

# Beta-PERT priors for growth phenology parameters
# pert[1,] == invkap: min, mode, max, k
# pert[2,] == omega: min, mode, max, k
for(i in 1:2){
  m[i] <- (pert[i,1] + pert[i,4]*pert[i,2] + pert[i,3]) / (pert[i,4] + 2)
  a[i] <- (m[i]-pert[i,1])*(2*pert[i,2]-pert[i,1]-pert[i,3])
          / ((pert[i,2]-m[i])*(pert[i,3]-pert[i,1]))
  b[i] <- a[i]*(pert[i,3]-m[i])/(m[i]-pert[i,1])
  bpert[i] ~ dbeta(a[i], b[i])
}
invkap <- bpert[1] * (pert[1,3] - pert[1,1]) + pert[1,1]
kappa <- 1/invkap
omega <- bpert[2] * (pert[2,3] - pert[2,1]) + pert[2,1]

# precisions from s.d.
tau.k <- 1/(sigma.k*sigma.k)
tau.e <- 1/(sigma.e*sigma.e)
tau.c <- 1/(sigma.c*sigma.c)
tau.h <- 1/(sigma.h*sigma.h)
tau.t <- 1/(sigma.t*sigma.t)
```

```
for(i in 1:I){
  logk[i] ~ dnorm(mu.k, tau.k) # distribution for individual logk
  k[i] <- exp(logk[i]) # individual k
}

### Likelihood
## Size at hatch
# Among clutches
for (c in 1:C){
  mu.h[c] ~ dnorm(mu.c, tau.c) # clutch mean hatchling length
}
# Within clutches
for(h in 1:H){
  hL[h] ~ dnorm(mu.h[ci[h]], tau.h) # nested indexing
}

## GPM model
alpha <- omega*(kappa - 2) + 1
beta <- (1 - omega)*(kappa - 2) + 1
pH <- pbeta(sH, alpha, beta)
for(i in 1:I){
  for(j in 1:J[i]){
    y.p[i,j] <- y[i,j] + pbeta(s[i,j], alpha, beta)
  }
}

## vB Model
# First observation of known age individuals
for(i in 1:nKA){
  LH[i] ~ dnorm(mu.c, tau.t) # unobserved L at hatching
  yH.pH[i] <- yH[i] + pH # date of hatch
  mu[i,1] <- Lmax - (Lmax-LH[i]) * exp((-k[i]/Lmax) * (y.p[i,1]-yH.pH[i]))
  L[i,1] ~ dnorm(mu[i,1], tau.e)

  # calculate t0.tld[i] as a derived parameter
  t0.tld[i] <- log(1 - LH[i]/Lmax) * Lmax/k[i]
}
mean.t0.tld <- mean(t0.tld) # derived parameter
sd.t0.tld <- sd(t0.tld) # derived parameter

# Subsequent observations
for(i in mult:I){ # Loop through individuals with >1 observation
  for(j in 2:J[i]){
```

```
      mu[i,j] <- Lmax - (Lmax-L[i,j-1]) * exp((-k[i]/Lmax) * (y.p[i,j]-y.p[i,
j-1]))
      L[i,j] ~ dnorm(mu[i,j], tau.e)
    }
  }
} # end of model code",
file = "pt_beta.bug", fill = TRUE)
```

Choose PERT priors and run in R using R2jags

```
## Wrapper functions to implement mode and concetration reparameterization
#   of R functions pbeta, dbeta, qbeta
dBeta2 <- function(x, mode, kappa){
  # PDF
  alpha <- mode*(kappa - 2) + 1
  beta <- (1 - mode)*(kappa - 2) + 1
  return(dbeta(x, alpha, beta))
}

pBeta2 <- function(x, mode, kappa){
  # CDF
  alpha <- mode*(kappa - 2) + 1
  beta <- (1 - mode)*(kappa - 2) + 1
  return(pbeta(x, alpha, beta))
}

qBeta2 <- function(p, mode, kappa){
  # Quantile function
  alpha <- mode*(kappa - 2) + 1
  beta <- (1 - mode)*(kappa - 2) + 1
  return(qbeta(p, alpha, beta))
}

## Calculate inverse kappa values for pert prior
priorkfun <- function(mode, delta.s, minp, maxp){
  # compute inverse kappa for given prob range [minp,maxp], mode,
  #   and year fraction difference (delta.s)
  opt <- function(kinv){(qBeta2(maxp, mode, 1/kinv) - qBeta2(minp, mode, 1/ki
nv)-delta.s)^2}
  optimize(opt, c(0, 10))$minimum
}

ds <- c( # delta s for min, mode, and max time to 90% of annual growth
  21/365.2422,  # min: 90% in 3 weeks
```

```
  (jday("15-08-2019") - jday("31-05-2019"))/365.2422, # mode: 90% in ~2.5mo
  0.5)# max = 90% in ~6 months

# PERT prior min, mode, max for inverse kappa and omega
pert <- rbind(
  # inverse kappa = 1/concentration
  c(priorkfun(0.5, ds[1], 0.05, 0.95),
    priorkfun(0.5,  ds[2], 0.05, 0.95),
    priorkfun(0.5,  ds[3], 0.05, 0.95)),

  # omega = beta pdf mode
  jday(c("2019-05-15", "2019-07-15", "2019-09-01"))/365.2422
)
pert <- cbind(pert, c(4, 4)) # Default PERT k parameter = 4

require(R2jags)
# Specify data and initial values for JAGS
jags.data <- list(
  H = H, C = C, ci = ci, hL = hL, # hatchling data
  L = L, y = y, s = s, #matrices
  I = I, sH = sH, mult = mult, nKA = nKA, #scalars
  yH = ptj.i$yob, J = ptj.i$J, #vectors
  pert = pert # 2*4 matrix of parameters for PERT prior on kappa and omega
)
inits <- function(){list(Lmax=runif(1,5,20),
                         logk=runif(I,-1,1),  mu.k=runif(1,0,1),
                         sigma.k=runif(1,0,5),
                         sigma.e=runif(1,0,10)
)}
#specify which parameters to monitor
params <- c("Lmax", "mu.k", "sigma.k",
            "sigma.e",
            "mu.c", "sigma.h", "sigma.c",
            "mean.t0.tld", "sd.t0.tld",
            "kappa", "invkap", "omega")

# run JAGS model
out.ptbeta <- jags(data=jags.data, inits=inits, parameters.to.save=params,
                   model.file="pt_beta.bug", n.thin=10, n.chains=3,
                   n.burnin=1000, n.iter=101000, working.directory=getwd())

saveRDS(out.ptbeta,  "pt_beta.RDS")
```

Results and Discussion

The beta GPM component recovered essentially the same growing season timing and duration (Figure C.3, Table C.2) as was estimated by the logistic GPM (Figure 3.5) and the GPM mode parameter estimates were also similar (ω vs. B) (Table C.1, Table 3.3).

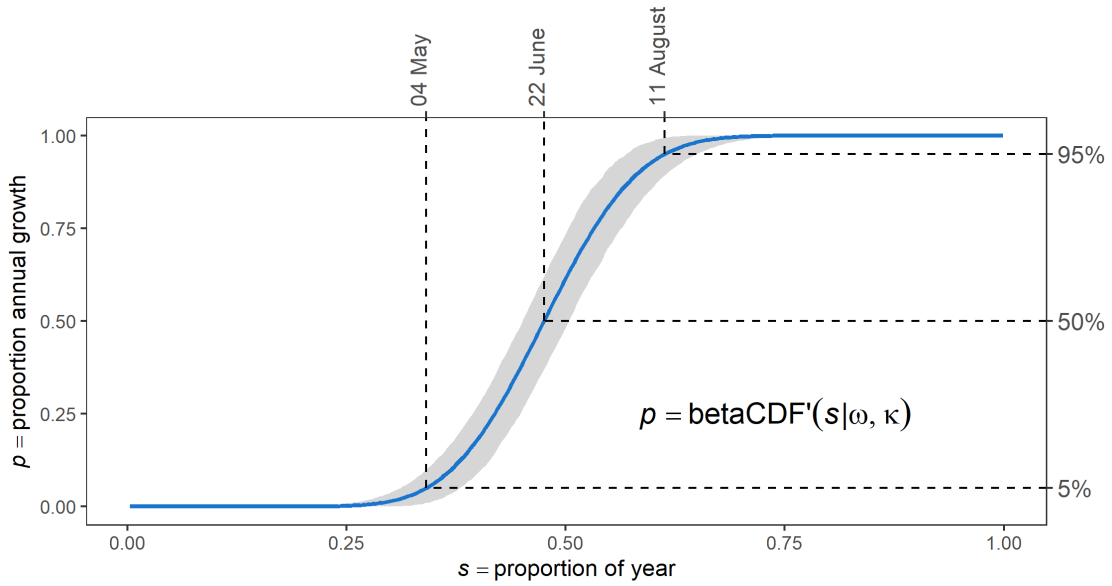

Figure C.3. Beta growth phenology component of the combined hierarchical von Bertalanffy growth model and fitted to primarily inter-annual observations of juvenile and subadult Painted Turtles in Algonquin Provincial Park, Ontario. The shaded region indicates the 95% HDI. $betaCDF'$ denotes the beta cumulative distribution function parameterized in terms of ω (the mode/inflection point) and κ (the concentration, which is a measure of dispersion).

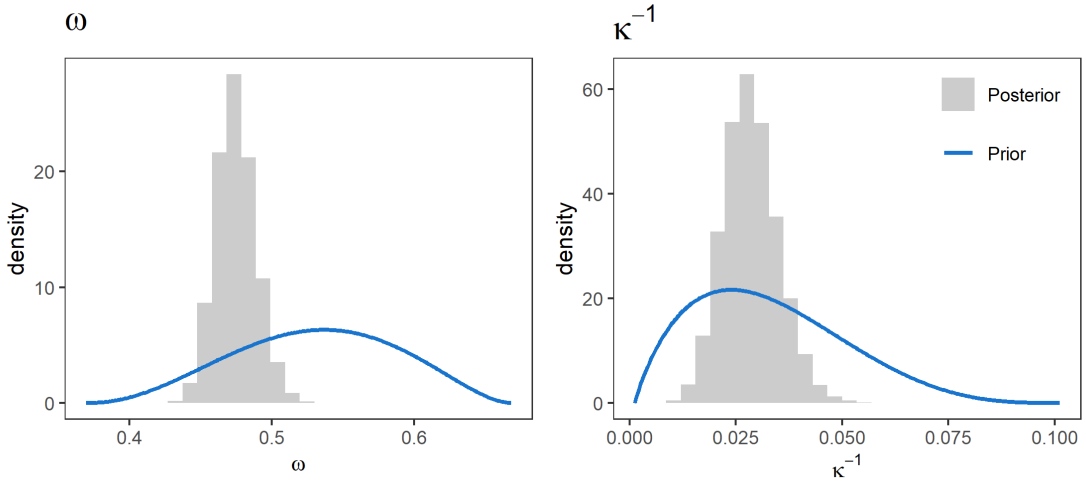

Figure C.4. Comparison of marginal posterior and PERT distribution prior densities for ω and κ^{-1}, which are the parameters of the beta CDF growth phenology model (GPM). The GPM was integrated with a hierarchical model von Bertalanffy model of growth in juvenile Painted Turtles in Algonquin Park.

Potential modifications

We parameterized the beta GPM in terms of the mode rather than the median because there is no closed-form function to specify the median of a beta distribution. In some circumstances, it may be desirable to use a function that can be formulated in terms of the median, for example, if a prior can be elicited more readily for the annual midpoint of growth rather than the timing of maximum growth. In this case the CDF of the Kumaraswamy distribution might be more appropriate. The Kumaraswamy distribution is very similar to the beta distribution but is more analytically tractable and it can be parameterized in terms of median and dispersion (Mitnik and Baek, 2013). In our implementation, the constraints on the parameters ensured the PDF (which, in the GPM, represents the relative growth rate in contrast to the accumulation of growth represented by the CDF) is approximately symmetrical across sampled parameter values; therefore, the mode and the median are approximately the same. However, in applications in which the GPM is potentially asymmetrical, the distinction between median and mode will be more important.

Due to the prior constraints that we placed on the parameters, our application of the beta distribution produced approximately symmetrical output because the 'probability mass' (recognizing that it is relative growth rather than probability that is being modeled) was concentrated away from the boundaries. The four-parameter beta distribution is a version of the beta distribution with two additional parameters specifying the upper (max) and lower (min) boundaries, which rescale the distribution from the interval [0,1] to [min, max] (the PERT distribution is a particular parameterization of the four-parameter beta distribution) (Vose, 2000). A potential modification of the GPM would be to apply a four parameter beta with the boundary parameters specified at the start and end of the growing season. This could allow for asymmetry in the seasonal growth function, such as a rapid springtime increase in growth rate followed by a gradual slow-down in late summer and autumn. This approach entails some additional

considerations, including the difficulty in eliciting a biologically meaningful, informative prior for κ^{-1} when its effect growing season length is strongly mediated by varying skewness. Another consideration is that the choice of boundary parameters affects the shape of function, which could introduce subjectivity that is not transparently included in the priors and does not contribute to the quantified uncertainty. This is one of the drawbacks of implicit seasonal models that we intended the our approach to rectify. A possible solution is to treat the boundary parameters as uncertain, assign priors, and estimate them from the data. Another strategy that might offer a partial solution is to use multimodel inference techniques to compare models with and without specified boundary parameters and incorporate model uncertainty into the posterior predictions and estimates of parameters.

Table C.1. Parameters estimated in the Algonquin Painted Turtle hierarchical growth model with a beta GPM (growth phenology model) seasonal component. Posterior parameter distribution statistics are shown for population-level parameters and are omitted for individual and observation level parameters. In the descriptions 'hL' denotes length at hatching, 'vB' is the hierarchical von Bertalanffy model, 'GPM' is the beta GPM, and indices are *i* = recaptured individual, *j* = observation of *i*, *h* = hatchling, and *c* = clutch.

Parm.	Description	In code	Mean	SD	2.5%	Median	97.5%
L_∞	vB asymptote	`Lmax`	12.1	0.423	11.3	12	13.0
μ_k	logmean vB rate	`mu.k`	0.728	0.0407	0.648	0.728	0.807
σ_k	logsd vB rate	`sigma.k`	0.154	0.0216	0.111	0.154	0.196
k_i	indiv. vB rate	`k[i]`					
σ_e	SD of residual error	`sigma.e`	0.298	0.0109	0.277	0.298	0.32
$\mu_{L_{i,j}}$	expected length at obs. i, j	`mu[i,j]`					
μ_C	among-clutch mean hL	`mu.c`	2.47	0.0142	2.45	2.47	2.5
σ_C	among-clutch sd of hL	`sigma.c`	0.16	0.011	0.14	0.159	0.183
μ_{H_c}	mean hL for clutch c	`mu.h[c]`					
σ_H	within-clutch sd of hL	`sigma.h`	0.0882	0.00283	0.0829	0.0881	0.094
hL_h	observed hL of hatchling h	`hL[h]`					
L_{Hi}	unobserved hL for i	`LH[i]`					
ω	beta mode, GPM inflection point	`omega`	0.475	0.014	0.449	0.474	0.504
κ^{-1}	beta concentration, GPM rate	`invkap`	0.0285	0.00643	0.0169	0.0281	0.0419
$y.p_{i,j}$	GPM date of i, j	`y.p[i,j]`					
$y_H.p_{Hi}$	GPM date of hatch of i	`yH.pH[i]`					
$\tilde{t_{0i}}$	derived GPM age at $L = 0$	`t0.tld[i]`					
mean($\tilde{t_0}$)	derived mean of $\tilde{t}_0$	`mean.t0.tld`	-1.33	0.0566	-1.45	-1.33	-1.22
sd($\tilde{t_0}$)	derived SD of $\tilde{t}_0$	`sd.t0.tld`	0.221	0.0368	0.154	0.219	0.298

Table C.2. Phenology of Painted Turtle growth in Algonquin Park estimated using the fitted beta GPM (growth phenology model) and presented at three scales: s (proportion of year), Julian day-of-year, and date. The model was fitted as proportion of cumulative annual growth p = $\text{betaCDF}'(s|\omega,\kappa)$ and the estimated seasonal timing of a given value of p is given by the inverse: s = $\text{betaQF}'(\text{p}|\,\omega,\kappa)$, where betaQF0 is the quantile function of the beta distribution reparameterized in terms of mode and concentration (ω and κ). Values are medians with 95% HDI (highest density intervals).

Cumulative growth	p	s (95% HDI)	Julian day (95% HDI)	Date* (95% HDI)
5%	0.05	0.341 (0.306 – 0.379)	124 (112 – 138)	04 May (21 Apr – 18 May)
50%	0.50	0.475 (0.449 – 0.502)	174 (164 – 183)	22 Jun (13 Jun – 02 Jul)
95%	0.95	0.613 (0.573 – 0.655)	224 (209 – 239)	11 Aug (28 Jul – 27 Aug)
5 to 95%	0.05 to 0.95	0.272 (0.212 – 0.33)†	99 (77 – 121) days	

* In non-leap years

† Duration as a proportion of year

References

Keevil, M.G., Armstrong, D.P., Brooks, R.J., Litzgus, J.D., 2021. A model of seasonal variation in somatic growth rates applied to two temperate turtle species. Ecol. Modell. 443, 109454. https://doi.org/10.1016/j.ecolmodel.2021.109454

Kruschke, J.K., 2015. Doing Bayesian Data Analysis: A Tutorial with R, JAGS, and Stan, 2nd ed. Academic Press/Elsevier, Burlington, MA.

Mitnik, P.A., Baek, S., 2013. The Kumaraswamy distribution: Median-dispersion reparameterizations for regression modeling and simulation-based estimation. Statistical Papers 54, 177–192. https://doi.org/10.1007/s00362-011-0417-y

Plummer, M., 2003. JAGS: a program for analysis of Bayesian graphical models using Gibbs sampling, in: Hornik, K., Leisch, F., Zeileis, A. (Eds.), Proceedings of the 3rd International Workshop on Distributed Statistical Computing. Vienna, Austria.

R Development Core Team, 2020. R: A language and environment for statistical computing.

Su, Y.-S., Masanao Yajima, 2020. R2jags: Using R to Run 'JAGS'.

Vose, D., 2000. Risk Analysis: A Quantitative Guide. John Wiley & Sons, Chichester, U.K.

Appendix D: Details of the stage-based matrix model for Algonquin Snapping Turtles

This appendix was first published as Appendix S1 in supplemental materials of

Keevil, M.G., Lesbarrères, D., Noble, N., Boyle, S.P., Brooks, R.., Litzgus, J.D., 2023. Lost reproductive value reveals a high burden of juvenile road mortality in a long-lived species. Ecol. Appl. e2789. https://doi.org/10.1002/eap.2789

Stages 2–11 are size-based and correspond to 3 cm intervals of midline carapace length (Table D.1). The first stage is egg to overwintered hatchling. The final three stages (9, 10, 11) were mature females. Intervening stages (2–8) were juveniles. The projection interval was one year.

Table D.1. Upper and lower carapace length (cm) delineating stages of the demographic model of female Snapping Turtles in Algonquin Provincial Park and the midpoint of each stage used to assign survival and fertility values. Stages 9–11 are adults. Stage 1 is egg to overwintered hatchling with midpoint as typical hatchling carapace length.

Stage	Carapace length (cm)		
	lower	upper	midpoint
1	NA	NA	2.9
2	3	6	4.5
3	6	9	7.5
4	9	12	10.5
5	12	15	13.5
6	15	18	16.5
7	18	21	19.5
8	21	24	22.5
9	24	27	25.5
10	27	30	28.5
11	30	Inf	31.5

We parameterized fertility as the number of female eggs per adult female per year which we estimated as half the expected clutch size. In Algonquin Provincial Park, clutch frequency is approximately annual (Keevil et al., 2018). Expected clutch size was predicted as the average clutch size from the long-term life history dataset for females within each stage size range.

Survivorship from stage 1 to stage 2 is survivorship from egg to overwintered hatchling, which is egg survival × hatchling survival over fall, winter, and spring. Egg survival is nest survival × hatching success, which we estimated from published and unpublished data from Algonquin Provincial Park (Table D.2).

Previously unpublished nest survival observations were made at multiple sites in western Algonquin Provincial Park. Monitored nesting areas were located in and around the North Madawaska catchment (sites described in Keevil, Brooks, and Litzgus 2018), sites near Whitefish Lake (described in Brooks, Brown, and Galbraith 1991) 4–6 km SE, and Arowhon (Riley and Litzgus, 2013) about 15 km W. Nests were marked with wire stakes and monitored daily until the end of nesting season, then approximately bi-weekly until September. Nests were checked again in October and remaining nests were excavated in November (nests laid in 2015) or the following spring (nests laid in 2014) to determine final fate. Final fate was uncertain in many cases because foxes (*Vulpes vulpes*) often excavate nests around the time of emergence before (Riley and Litzgus 2014) or after [pers. obs.] hatchlings leave the nest. Nest success in 2014 was between 0.045–0.38 and was 0.12–0.24 in 2015.

Table D.2. Nest survival (NS; the proportion of nests with successful emergence) and hatching success (HS; the proportion of eggs producing viable hatchlings) of Snapping Turtles in Algonquin Provincial Park. Average NS and NS×HS were weighted by the number of nests. HS was weighted by number of eggs. The weighted average NS×HS estimate was used as a component of stage 1 survival. Values in gray were borrowed from the corresponding weighted average. Previously unpublished nest survival was between 0.045–0.38 in 2014 and 0.12–0.24 in 2015. We used the midpoints of these ranges in this analysis. Some hatching success data was obtained from eggs incubated in a lab over the entire embryonic period (Brooks et al. 1991; Bobyn and Brooks 1994) but most comes from eggs incubated in situ for all (Riley and Litzgus 2013) or most (Rouleau, Massey, and Rollinson 2019) of development.

Source	Year	Nests	NS	Eggs	HS	NS×HS
Brooks et al 1988	<1983	142				0.0635
Brooks et al 1991b	1986	6		227	0.819	
Bobyn and Brooks 1994	1988	6		217	0.892	
Riley and Litzgus 2013	2010–2011	29	0.62	2513	0.794	0.492
Rouleau et al 2019	2017			86	0.895	
Prev. unpublished	2014	66	0.21		0.806	0.169
Prev. unpublished	2015	78	0.18		0.806	0.145
Weighted average			0.265		0.806	**0.145**

Table D.3. Recent estimates of annual survivorship of adult female Snapping Turtles in Algonquin Provincial Park as applied to parameterize the matrix model.

Source	Stage 9	Stage 10	Stage 11
Armstrong et al 2018	0.939	0.958	0.97
Keevil *et al.* 2018 Dam nesters 1990 to 2013	0.976	0.976	0.976
Mean	**0.958**	**0.967**	**0.973**

Annual adult female survivorship of Snapping Turtles from Algonquin Provincial Park has been estimated several times (Armstrong et al., 2018; Brooks et al., 1991; Galbraith and Brooks, 1987; Keevil et al., 2018). We averaged estimates from Armstrong et al. (2018) and Keevil et al. (2018) for the present analysis (Table D.3). Keevil et al. (2018) stratified survival among sites and time periods while Armstrong et al. (2018) estimated the relationship between size and survivorship. We used the Keevil et al. (2018) model-averaged estimate for dam nesting females after 1990 because it represents the most intensively sampled sub-population over a period of population stability while accounting for emigration. We combined this with size-based estimates from Armstrong et al. (2018) to obtain stage-specific values (Table D.3).

Individual growth rates are variable, which results in varying residence times within size-structured stages. To accommodate this we used estimates of population level variation in growth parameters (Appendix S2) to implement variable stage durations (Caswell, 2001, 1983). We approximated the mean $\overline{T}_i$ and variance $V(T_i)$ of residence time for each stage by sampling 1000 random growth trajectories from the growth parameter distributions.

The cells of the projection matrix are fertility (F_i) (top row), P_i, on the diagonal, is the probability of remaining in i and G_i, below the diagonal, is the probability of growth from stage i to $i+1$. Residence times are linked to the values of the projection matrix by parameter γ_i which is the probability of moving to the next stage conditional on surviving: $G_i = S_i \times \gamma_i$ and $P_i = S_i(1-\gamma_i)$ where S_i is survivorship in stage i. We estimated γ as

$$\gamma_i \approx \frac{1}{\overline{T}_i} \exp\left[-\ln\left(\frac{\lambda}{S_i}\right)\left(\frac{\overline{T}_i}{2} - \frac{V(T_i)}{2\overline{T}_i}\right)\right]$$

(Caswell, 2001; Keyfitz, 1977).

The three scenarios of juvenile survivorship as a function of size that we chose to represent a range of plausible relationships are shown in Figure D.1. These relationships determined survivorship values for the juvenile stages 2–8. We also used them to set the survival of hatchlings (mean CL ~ 29 mm; Riley et al. 2014) from fall through spring, which is multiplied by egg survival (Table D.2) to obtain a survivorship value for stage 1. Although the hatchling

survival period is less than one full year (the projection interval) we do not feel it is necessary to correct for this given the overall level of uncertainty of juvenile survivorship.

Using the projection matrices, we calculated λ as the dominant eigenvalue, stage-specific reproductive values (RVs) as the left eigenvector, and the stable stage distributions as the right eigenvector (Table D.4) using the `popbio` package (Stubben and Milligan, 2007) in program `R`.

The projection matrices were constructed as female-only. Therefore, the final expected stage distribution was adjusted according to the assumed sex ratio by adding missing males to each of the juvenile stages (including the egg stage). Males and females grow at a similar rate before females mature at about 24 cm, after which female growth is much slower than same-age males (Armstrong and Brooks, 2013). Therefore, males >24 cm were pooled into a separate adult male stage proportional to the sum of the three adult female size classes.

Table D.4. Snapping Turtle female reproductive value and stable stage distribution across stages calculated from the projection matrices for each juvenile survivorship scenario (Figure D.1). Reproductive values (RV) are scaled so that one female egg has RV = 1. Stage distributions sum to one and do not include males.

Stage	Reproductive value			Stable stage dist.		
	Scenario: 1	2	3	1	2	3
1	1.0	1.0	1.0	0.789	0.851	0.723
2	14.1	21.8	10.7	0.086	0.053	0.110
3	44.6	149.2	23.6	0.031	0.010	0.054
4	98.2	251.7	48.4	0.016	0.007	0.029
5	168.4	285.4	92.1	0.010	0.007	0.017
6	241.7	319.0	163.6	0.009	0.007	0.011
7	318.9	362.4	264.7	0.008	0.007	0.008
8	402.5	418.7	390.1	0.007	0.008	0.007
9	510.3	501.1	515.9	0.015	0.016	0.014
10	614.5	601.1	619.9	0.018	0.021	0.017
11	751.0	741.4	764.6	0.011	0.011	0.009

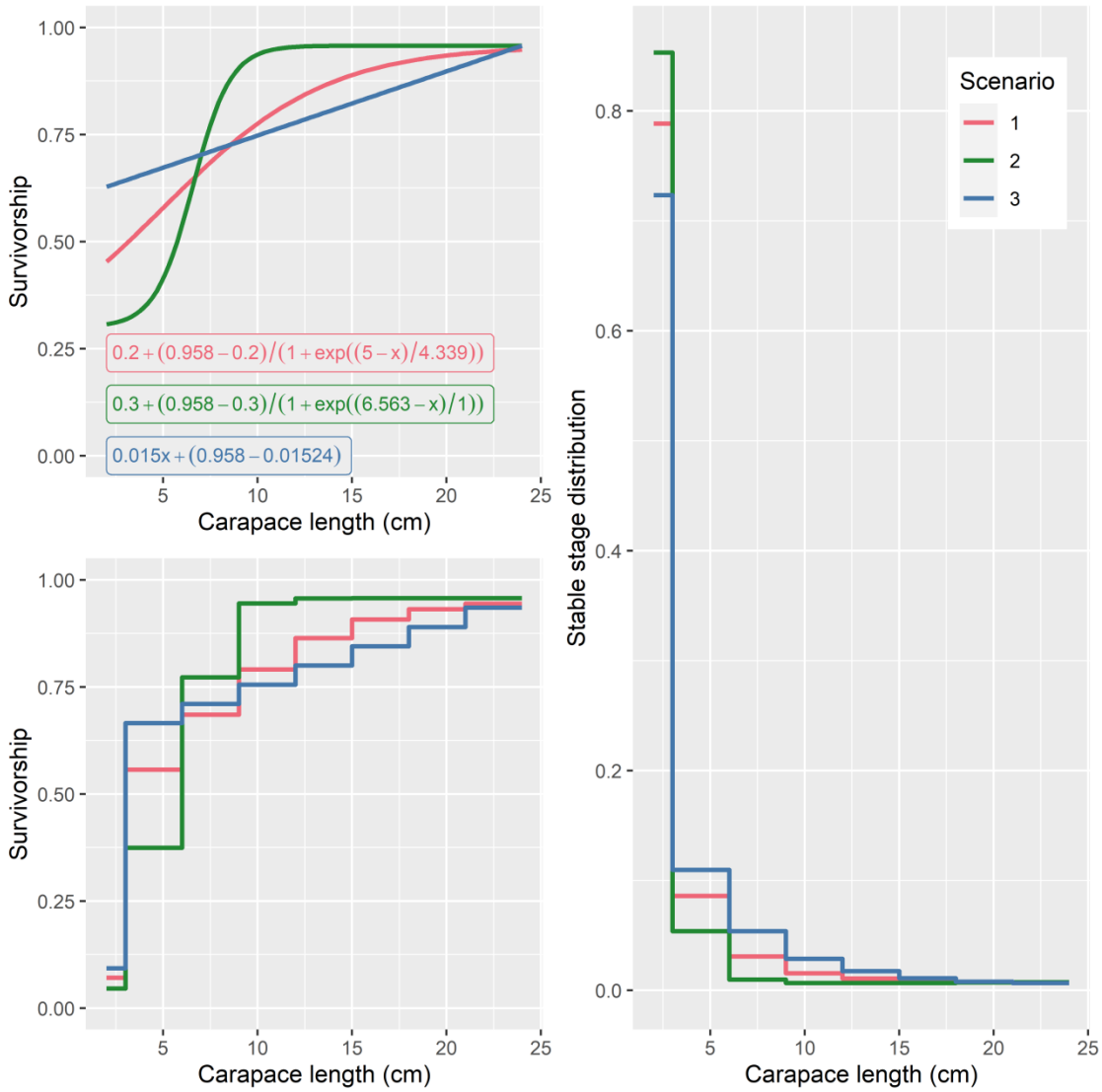

Figure D.1. Three scenarios defining the relationship between juvenile size and survivorship shown as continuous functions (top left), discretized into stages based on stage midpoint (bottom left), and the resulting stable stage distribution (right) as population proportion shown over the juvenile stages (stages 2:8) and the egg/hatchling stage (stage 1). Stage 1 survival is the product of egg survival (independent of scenario) and size-based survival determined by the scenario assuming that hatchling carapace length = 2.9 cm. Each scenario is constrained by two conditions: 1) juvenile survival approaches adult survival as juvenile size approaches adult size and 2) the resulting overall population growth rate is stable ($\lambda = 1$).

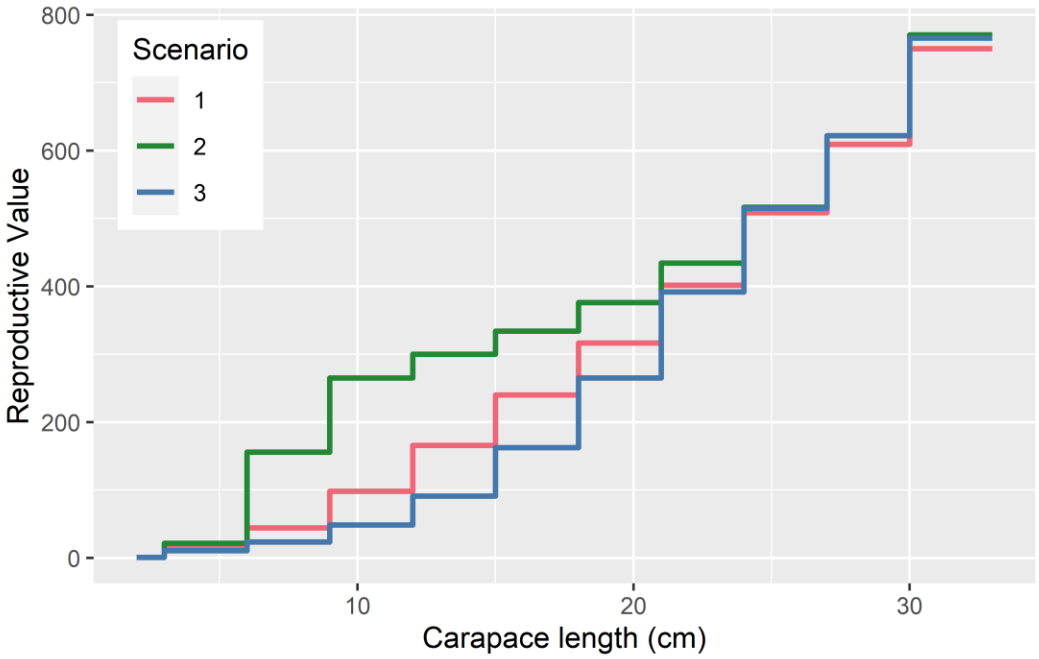

Figure D.2. Reproductive value (RV) of females by stage calculated for each of the intermediate juvenile survival scenarios. RV is scaled so that one female egg has RV = 1.

Projection matrices

Scenario 1

$$\begin{bmatrix} 0 & 0 & 0 & 0 & 0 & 0 & 0 & 0 & 15.51 & 18.14 & 20.37 \\ 0.071 & 0.351 & 0 & 0 & 0 & 0 & 0 & 0 & 0 & 0 & 0 \\ 0 & 0.206 & 0.424 & 0 & 0 & 0 & 0 & 0 & 0 & 0 & 0 \\ 0 & 0 & 0.261 & 0.501 & 0 & 0 & 0 & 0 & 0 & 0 & 0 \\ 0 & 0 & 0 & 0.291 & 0.554 & 0 & 0 & 0 & 0 & 0 & 0 \\ 0 & 0 & 0 & 0 & 0.311 & 0.62 & 0 & 0 & 0 & 0 & 0 \\ 0 & 0 & 0 & 0 & 0 & 0.288 & 0.673 & 0 & 0 & 0 & 0 \\ 0 & 0 & 0 & 0 & 0 & 0 & 0.259 & 0.737 & 0 & 0 & 0 \\ 0 & 0 & 0 & 0 & 0 & 0 & 0 & 0.207 & 0.898 & 0 & 0 \\ 0 & 0 & 0 & 0 & 0 & 0 & 0 & 0 & 0.06 & 0.951 & 0 \\ 0 & 0 & 0 & 0 & 0 & 0 & 0 & 0 & 0 & 0.016 & 0.973 \end{bmatrix}$$

Scenario 2

$$\begin{bmatrix} 0 & 0 & 0 & 0 & 0 & 0 & 0 & 0 & 15.51 & 18.14 & 20.37 \\ 0.046 & 0.268 & 0 & 0 & 0 & 0 & 0 & 0 & 0 & 0 & 0 \\ 0 & 0.107 & 0.446 & 0 & 0 & 0 & 0 & 0 & 0 & 0 & 0 \\ 0 & 0 & 0.329 & 0.531 & 0 & 0 & 0 & 0 & 0 & 0 & 0 \\ 0 & 0 & 0 & 0.414 & 0.587 & 0 & 0 & 0 & 0 & 0 & 0 \\ 0 & 0 & 0 & 0 & 0.37 & 0.642 & 0 & 0 & 0 & 0 & 0 \\ 0 & 0 & 0 & 0 & 0 & 0.316 & 0.681 & 0 & 0 & 0 & 0 \\ 0 & 0 & 0 & 0 & 0 & 0 & 0.276 & 0.739 & 0 & 0 & 0 \\ 0 & 0 & 0 & 0 & 0 & 0 & 0 & 0.218 & 0.897 & 0 & 0 \\ 0 & 0 & 0 & 0 & 0 & 0 & 0 & 0 & 0.06 & 0.953 & 0 \\ 0 & 0 & 0 & 0 & 0 & 0 & 0 & 0 & 0 & 0.014 & 0.973 \end{bmatrix}$$

Scenario 3

$$\begin{bmatrix} 0 & 0 & 0 & 0 & 0 & 0 & 0 & 0 & 15.51 & 18.14 & 20.37 \\ 0.093 & 0.388 & 0 & 0 & 0 & 0 & 0 & 0 & 0 & 0 & 0 \\ 0 & 0.278 & 0.435 & 0 & 0 & 0 & 0 & 0 & 0 & 0 & 0 \\ 0 & 0 & 0.276 & 0.486 & 0 & 0 & 0 & 0 & 0 & 0 & 0 \\ 0 & 0 & 0 & 0.269 & 0.544 & 0 & 0 & 0 & 0 & 0 & 0 \\ 0 & 0 & 0 & 0 & 0.257 & 0.596 & 0 & 0 & 0 & 0 & 0 \\ 0 & 0 & 0 & 0 & 0 & 0.25 & 0.659 & 0 & 0 & 0 & 0 \\ 0 & 0 & 0 & 0 & 0 & 0 & 0.231 & 0.735 & 0 & 0 & 0 \\ 0 & 0 & 0 & 0 & 0 & 0 & 0 & 0.2 & 0.898 & 0 & 0 \\ 0 & 0 & 0 & 0 & 0 & 0 & 0 & 0 & 0.06 & 0.953 & 0 \\ 0 & 0 & 0 & 0 & 0 & 0 & 0 & 0 & 0 & 0.014 & 0.973 \end{bmatrix}$$

References

Armstrong, D.P., Brooks, R.J., 2013. Application of hierarchical biphasic growth models to long-term data for Snapping Turtles. Ecol. Modell. 250, 119–125. https://doi.org/10.1016/j.ecolmodel.2012.10.022

Armstrong, D.P., Keevil, M.G., Rollinson, N., Brooks, R.J., 2018. Subtle individual variation in indeterminate growth leads to major variation in survival and lifetime reproductive output in a long-lived reptile. Funct. Ecol. 32, 752–761. https://doi.org/10.1111/1365-2435.13014

Brooks, R.J., Brown, G.P., Galbraith, D.A., 1991. Effects of a sudden increase in natural mortality of adults on a population of the Common Snapping Turtle (*Chelydra serpentina*). Can. J. Zool. 69, 1314–1320. https://doi.org/10.1139/z91-185

Caswell, H., 2001. Matrix Population Models : Construction, Analysis, and Interpretation, 2nd ed. Sinauer Associates, Sunderland, MA. USA.

Caswell, H., 1983. Phenotypic plasticity in life-history traits: demographic effects and evolutionary consequences. Am. Zool. 23, 35–46.

Galbraith, D.A., Brooks, R.J., 1987. Survivorship of adult females in a northern population of Common Snapping Turtles, *Chelydra serpentina*. Can. J. Zool. 65, 1581–1586. https://doi.org/http://dx.doi.org/10.1139/z87-247

Keevil, M.G., Brooks, R.J., Litzgus, J.D., 2018. Post-catastrophe patterns of abundance and survival reveal no evidence of population recovery in a long-lived animal. Ecosphere 9, e02396. https://doi.org/10.1002/ecs2.2396

Keyfitz, N., 1977. Applied mathematical demography. Wiley, New York, New York, USA.

Riley, J.L., Freedberg, S., Litzgus, J.D., 2014. Incubation temperature in the wild influences hatchling phenotype of two freshwater turtle species. Evol. Ecol. Res. 16, 397–416.

Riley, J.L., Litzgus, J.D., 2013. Evaluation of predator-exclusion cages used in turtle conservation: Cost analysis and effects on nest environment and proxies of hatchling fitness. Wildl. Res. 40, 499–511. https://doi.org/10.1071/WR13090

Stubben, C., Milligan, B., 2007. Estimating and analyzing demographic models using the popbio package in R. J. Stastistical Softw. 22, 1–23. https://doi.org/10.18637/jss.v022.i11

Appendix E: Snapping Turtle somatic growth model

This appendix was first published as Appendix S2 in supplemental materials of

Keevil, M.G., Lesbarrères, D., Noble, N., Boyle, S.P., Brooks, R.., Litzgus, J.D., 2023. Lost reproductive value reveals a high burden of juvenile road mortality in a long-lived species. Ecol. Appl. e2789. https://doi.org/10.1002/eap.2789

Introduction and Methods

The somatic growth model is a critical component of the stage-based population matrix model because it determines the estimates of how long individuals spend in each stage. This in turn determines how many juveniles survive to maturity because survival through a stage is the product of stage-specific-survivorship and the time spent in the stage. This has a large effect on stage-specific reproductive values and the stable stage distribution.

Armstrong and Brooks (2013) developed a set of hierarchical, biphasic von Bertalanffy growth models for the Algonquin Snapping Turtle population. These models estimate the distribution of individual variation in growth trajectory. We used the top-performing model identified in their model selection procedure, which has a fixed effect on the asymptote parameter for females after maturity (defined as $L' = 24$ cm), and re-fit it to our updated data set.

Armstrong and Brooks (2013) used data up to and including 2005. We included a further 13 years of data (up to and including 2018) as well as additional data extracted from old field books so that the updated dataset is substantially larger (Table E.1).

Table E.1. Approximate comparison of Snapping Turtle growth data available up to and including 2005 to data including 2018 used in the present analysis. $\sum \Delta CL$ (cm) is the observed change in carapace length summed across individuals and is an indication of the amount of growth observed along with the growth time, $\sum \Delta turtle\ years$. To approximate the information added because of known-age individuals, we supposed an extra hatchling-sized (3 cm CL) observation for the year hatched for each known-age turtle.

Year	Turtles	Observations	$\sum \Delta CL\ (cm)$	$\sum \Delta turtle\ years$
2005	325	2032	709	3197
2018	520	3201	1861	6148
Ratio	**1.6**	**1.6**	**2.6**	**1.9**

Seasonality adjustment

We accounted for time-of-year by including a model of seasonal growth (GPM, growth phenology model) that rescales fraction of year into fraction of the growing season—effective growth time—for each observation date using the cumulative distribution function (CDF) for the beta distribution as a phenomenological model. This approach is described in detail in Keevil et al. (2021) and outlined below. Accounting for seasonal growth this way reduces error variation due to uncorrected seasonal differences between observations but does not fundamentally change the scaling or interpretation of the von Bertalanffy model parameters.

The beta distribution is a continuous probability distribution defined over values between 0 and 1. Therefore, the beta CDF returns 0 at the start of the interval [0,1] and 1 at the end and is usually defined using the shape parameters α and β. For this application of the beta CDF as the GPM given year fraction s, we used a reparameterization that defines the beta distribution in terms of the mode, ω, and concentration, κ (Kruschke 2015), which we have denoted as $\mathrm{betaCDF}'(s|\omega,\kappa)$. These parameters are related to the shape parameters as follows (Kruschke 2015):

$$\begin{aligned}\alpha &= \omega(\kappa-2)+1\\ \beta &= (1-\omega)(\kappa-2)+1\end{aligned}$$

The ω and κ parameterization is more intuitive for eliciting priors and interpreting the parameters. ω is the inflection point of the CDF and the mode of the probability distribution function (PDF); in the context of the GPM, ω corresponds to the annual point of maximum growth, which in our application is close to the halfway point of annual growth accumulation. In the GPM, κ controls the rate of change of growth and the effective length of the growing season.

We specified an informative prior on ω using a PERT distribution (Malcolm et al. 1959; Vose 2000) with a minimum of 15 May, a most likely value (mode) of 15 July, and maximum of 1 September, which is $\omega \sim PERT(0.37,\ 0.54,\ 0.67)$ on the year fraction scale. To determine a biologically interpretable informative PERT prior on κ, we based it on the time taken to complete 90% of annual growth with a minimum of 21 days, a maximum of six months, and a most likely value (mode) of 2.5 months (corresponding to 30 May – 15 August), while holding ω constant at 0.5. We specified this distribution for the inverse of κ, to ensure a less skewed distribution, which resulted in the prior $\kappa^{-1} \sim PERT(0.0012,\ 0.024,\ 0.101)$. Further explanation of this prior specification is provided in Keevil et al. (2021).

We have abbreviated the GPM component in our notation as function $\mathrm{F}(y.s)$ when applied to a decimal year time value, $y.s$, that potentially includes integer years (Keevil et al. 2021). Function F separates $y.s$ into the fractional component, s, and the remaining integer years, y, applies the GPM to s, and adds it back to y, so:

$$
\begin{aligned}
y.s &= y + s \text{ where } y \in \mathbb{Z} \text{ and } 0 \leq s < 1 \\
y &= \lfloor y.s \rfloor \\
\mathrm{F}(y.s) &= \lfloor y.s \rfloor + \mathrm{betaCDF}'(y.s - \lfloor y.s \rfloor \mid \omega, \kappa) \\
&= y + \mathrm{betaCDF}'(s \mid \omega, \kappa)
\end{aligned}
$$

Note also that:

$$
\mathrm{F}(y.s) = y + \mathrm{F}(s)
$$

where $\lfloor\ \rfloor$ denotes the floor function.

Implementation details

Besides adding a season component, our application of the von Bertalanffy model followed Armstrong and Brooks (2013) except that we have specified a truncated distribution for the individually varying von Bertalanffy asymptote parameter a_i and that we have used a different approach to organize and index the parameters and observation data.

We truncated the distribution of a_i by specifying a lower bound at L', which is the fixed size at maturity [$L' = 24$ cm; Armstrong and Brooks (2013)], using a truncated normal distribution, $a_i \sim \mathcal{N}_{\mathcal{T}}(\mu_a,\ \sigma_a,\ L',\ \infty)$. This prevents proposed values for the asymptotic maximum size from being less than the size at maturity. If $a_i < L'$ then the time of maturity, t', is undefined, which results in an error when an attempt is made to calculate this quantity. Armstrong and Brooks (2013) handled this issue in a slightly different way by using the `max` function within their calculation of t' to avoid taking the logarithm of a negative number so that the term $\ln(1 - L'/a_i)$ became $\ln\big(\max(0.01,\ 1 - L'/a_i)\big)$ in their implementation.

Armstrong and Brooks (2013) used the offset method (Spiegelhalter et al. 2003) to handle indexing for the unbalanced dataset caused by differences in the number of observations per individual, while we formatted the data as ragged 2D arrays along with a vector, **J**, of length *I* equal to the number of individuals. Therefore, for $i = 1, \ldots, I$ where $I = 590$, each individual, i, has observations $j = 1, \ldots, J_i$. In this arrangement, the *j*th length observation of the *i*th individual is represented in the model code as `L[i,j]`. This does not substantively change the model but we believe it makes the code easier to understand and check (Spiegelhalter et al. 2003).

We removed five observations containing obvious transcribing errors and excluded one individual that had been raised in captivity as a juvenile. We fitted the joint model using the Bayesian updating software JAGS version 4.2.0 (Plummer 2003) implemented in R version 4.0.2 (R Development Core Team 2020) using the R2jags package version 0.5-7 (Su and Yajima 2014). We generated 110 000 MCMC draws for each of three chains and applied thinning rate of 50 after discarding 10 000 as burn-in.

R and JAGS code is available at an external repository (Figshare; Keevil et al., 2022).

Growth model summary

Excepting the new GPM parameters ω and κ, we followed the uninformative prior specifications of Armstrong and Brooks (2013). Denoting observed midline carapace length (cm) as $L_{i,j}$ for observation j of individual i occurring at time $y.s_{i,j}$ (decimal calendar years), and the corresponding model-fitted value as $\mu_{L_{i,j}}$, our application of the Armstrong and Brooks (2013) model took the form:

$L_{i,j} \sim \mathcal{N}(\mu_{L_{i,j}},\ \sigma_e)$	Residual error
$k_i \sim \log\mathcal{N}(\mu_k,\ \sigma_k)$	Individual rate parameters
$a_i \sim \mathcal{N}_{\mathcal{T}}(\mu_a,\ \sigma_a,\ L',\ \infty)$	Individual asymptotes (truncated normal distribution)
$sex_i \sim \text{Bernoulli}(0.5)$	For juveniles with unknown sex
β_a	Fixed effect of maturity in females
t_0	Theoretical age when $L = 0$*

For first observations of males and juvenile females ($\mu_{L_{i,1}} < L'$) when year hatched (y_{H_i}) is known ($s_H = 0.706 = 15$ Sep. is the annual timing of hatching and is assumed to be constant):

$$\mu_{L_{i,1}} = a_i\left(1 - \exp\left(-\frac{k_i}{a_i}\right)\Delta t_{i,1}\right) \qquad \text{von Bertalanffy length-at-age equation}^{\dagger}$$

$$\Delta t_{i,1} = \mathrm{F}(y.s_{i,1}) - y_{H\,i} - \mathrm{F}(s_H) - t_0 \qquad \text{Time term; function F applies the GPM}$$

For recaptured males and juvenile females where $\mu_{L_{i,j}} < L'$:

$$\mu_{L_{i,j}} = a_i - \left(a_i - L_{i,j-1}\right)\exp\left(-\frac{k_i}{a_i}\Delta t_{i,j}\right) \qquad \text{von Bertalanffy interval equation}^{\dagger}$$

$$\Delta t_{i,j} = \mathrm{F}(y.s_{i,j}) - \mathrm{F}(y.s_{i,j-1})$$

For first observations of adult females ($\mu_{L_{i,1}} > L'$) when year hatched (y_{H_i}) is known:

$$\mu_{L_{i,1}} = a_i + \beta_a - \left(a_i + \beta_a - L'\right)\exp\left(-\frac{k_i}{a_i + \beta_a}\Delta t_{i,1}\right)$$

$$\Delta t_{i,1} = \mathrm{F}(y.s_{i,1}) - t'_{i,1}$$

$$t'_{i,1} = \ln\left(1 - \frac{L'}{a_i}\right)\left(-\frac{a_i}{k_i}\right) + y_{H\,i} + \mathrm{F}(s_H) + t_0 \qquad \text{Time when size reaches } L'$$

For recaptured adult females where $L_{i,j-1} > L'$:

$$\mu_{L_{i,j}} = a_i + \beta_a - \left(a_i + \beta_a - L_{i,j-1}\right)\exp\left(-\frac{k_i}{a_i + \beta_a}\Delta t_{i,j}\right)$$

$$\Delta t_{i,j} = \mathrm{F}(y.s_{i,j}) - \mathrm{F}(y.s_{i,j-1})$$

For recaptured maturing females where $L_{i,j-1} < L' < \mu_{L_{i,j}}$:

$$\mu_{L_{i,j}} = a_i + \beta_a - \left(a_i + \beta_a - L'\right)\exp\left(-\frac{k_i}{a_i + \beta_a}\Delta t_{i,j}\right)$$

$$\Delta t_{i,j} = \mathrm{F}(y.s_{i,j}) - t'_{i,j}$$

$$t'_{i,j} = \ln\left(\frac{a_i - L'}{a_i - L_{i,j-1}}\right)\left(-\frac{a_i}{k_i}\right) + \mathrm{F}(y.s_{i,j-1}) \qquad \text{Time when size reaches } L'$$

*The von Bertalanffy parameter t_0 is quantified on the seasonal model effective-growth-years scale.

†Following Armstrong and Brooks (2013), k_i is replaced by k_i/a_i in our implementation of the von Bertalanffy model.

Results

There was good convergence of all monitored parameters based on visual inspection of MCMC chains and all $\hat{R} < 1.1$ (Brooks and Gelman 1998). All parameters were estimated with higher precision with the updated data. Compared to Armstrong and Brooks (2013) there were appreciable differences in some of the parameter estimates (Table E.2). Notably, μ_k, the mean of log growth rates, was higher with the updated data and there was less individual variation in growth rate. This resulted in the estimated median age at maturity being about 10 years younger (Figure E.1).

The GPM (seasonal component) based on the beta CDF (Figure E.2) estimated the midpoint of annual growth accumulation at Julian day 181 (30 June in non-leap years) and the length of the 90% growing season (the period during which 90% of annual growth accrues) was estimated as 73 days (Table E.3).

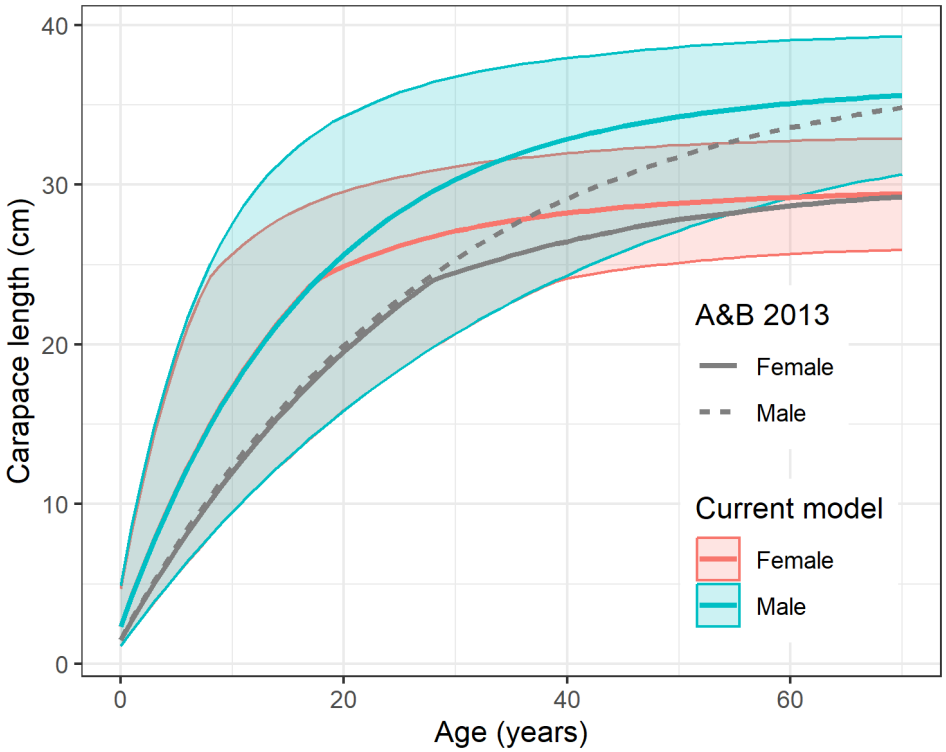

Figure E.1. Median growth curves produced by the hierarchical von Bertalanffy model fit to updated data. Bands show intervals in which 95% of individual growth trajectories are predicted occur. The median growth curves of the same model fit to data up to 2005 by Armstrong and Brooks (2013) are shown in gray. Seasonal variation in growth was included in the current model but is omitted from the plot.

Table E.2. Posterior parameter estimates from the top model of Armstrong and Brooks 2013 and a similar model fitted to updated data (Current model). Parameters μ_a and σ_a are the mean and standard deviation (sd) of the individually varying von Bertalanffy asymptote parameter; μ_k and σ_k are the lognormal mean and sd of the individually varying von Bertalanffy rate parameter. β_a is the fixed effect of sex for females after maturity. The residual error standard deviation is σ_e. The von Bertalanffy parameter t_0 is the theoretical age when size = 0. The seasonal component parameters ω and κ^{-1} apply only to the current model.

Parm.	in code	Current model					Armstrong and Brooks 2013				
		mean	sd	2.5%	50%	97.5%	mean	sd	2.5%	50%	97.5%
μ_a	`Lmax.c`	36.58	0.28	36.03	36.58	37.14	38.19	0.49	37.29	38.17	39.19
σ_a	`sigma.L`	1.80	0.11	1.59	1.80	2.03	1.37	0.20	0.97	1.37	1.78
β_a	`B.lmax`	-6.80	0.30	-7.40	-6.80	-6.21	-7.23	0.48	-8.21	-7.22	-6.32
μ_k	`k.c`	0.74	0.03	0.68	0.74	0.80	0.26	0.07	0.12	0.26	0.39
σ_k	`sigma.k`	0.39	0.03	0.34	0.39	0.44	0.58	0.05	0.49	0.57	0.68
σ_e	`sigma.e`	0.34	0.01	0.33	0.34	0.35	0.29	0.01	0.28	0.29	0.30
t_0	`t0`	-1.14	0.06	-1.26	-1.14	-1.04	-1.18	0.12	-1.42	-1.18	-0.96
ω	`omega`	0.50	0.01	0.48	0.50	0.51					
κ^{-1}	`invkap`	0.015	0.003	0.011	0.015	0.021					

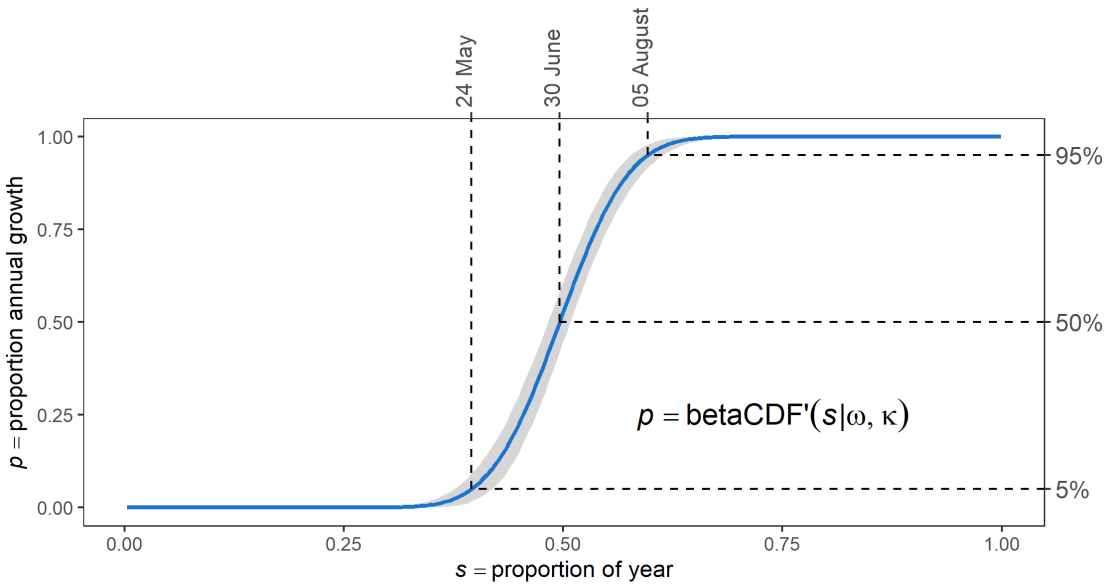

Figure E.2. Beta growth phenology component of the combined hierarchical von Bertalanffy growth model of Snapping Turtles in Algonquin Provincial Park, Ontario. The shaded region indicates the 95% HDI (highest density interval). betaCDF′ denotes the beta cumulative distribution function parameterized in terms of ω (the mode/inflection point) and κ (the concentration, which is a measure of dispersion).

Table E.3. Phenology of Snapping Turtle growth estimated using the fitted beta GPM (growth phenology model) and presented at three scales: s (proportion of year), Julian day-of-year, and date. The model was fitted as proportion of cumulative annual growth $p = \text{betaCDF}'(s|\omega,\kappa)$ and the estimated seasonal timing of a given value of p is given by the inverse: $s = \text{betaQF}'(p|\omega,\kappa)$, where betaQF' is the quantile function of the beta distribution reparameterized in terms of mode and concentration (ω and κ). Values are medians with 95% HDI (highest density intervals)

Cumulative growth	p	s (95% HDI)	Julian day (95% HDI)	Date* (95% HDI)
5%	0.05	0.395 (0.373 – 0.418)	144 (136 – 153)	24 May (16 May – 01 Jun)
50%	0.50	0.496 (0.483 – 0.508)	181 (176 – 186)	30 Jun (25 Jun – 04 Jul)
95%	0.95	0.596 (0.578 – 0.616)	218 (211 – 225)	05 Aug (30 Jul – 12 Aug)
5 to 95%	0.05 to 0.95	0.201 (0.168 – 0.235)†	73 (62 – 86) days	

* In non-leap years

† Duration as a proportion of year

References

Armstrong DP, Brooks RJ (2013) Application of hierarchical biphasic growth models to long-term data for Snapping Turtles. Ecological Modelling 250:119–125. https://doi.org/10.1016/j.ecolmodel.2012.10.022

Brooks SP, Gelman A (1998) General methods for monitoring convergence of iterative simulations. Journal of Computational and Graphical Statistics 7:434–455. https://doi.org/10.1080/10618600.1998.10474787

Keevil MG, Armstrong DP, Brooks RJ, Litzgus JD (2021) A model of seasonal variation in somatic growth rates applied to two temperate turtle species. Ecological Modelling 443:109454. https://doi.org/10.1016/j.ecolmodel.2021.109454

Keevil, M.G., Noble, N., Boyle, S.P., Lesbarrères, D., Brooks, R.J., Litzgus, J.D., (2022). Demographic characteristics of Snapping Turtles (*Chelydra serpentina*) observed on roads in Ontario, Canada. Figshare data repository. https://doi.org/10.6084/m9.figshare.19123163.v1

Kruschke JK (2015) Doing Bayesian Data Analysis: A Tutorial with R, JAGS, and Stan, 2nd edn. Academic Press/Elsevier, Burlington, MA

Malcolm DG, Roseboom JH, Clark CE, Fazar W (1959) Application of a technique for research and development program evaluation. Operations Research 7:646–669. https://doi.org/10.1287/opre.7.5.646

Plummer M (2003) JAGS: a program for analysis of Bayesian graphical models using Gibbs sampling. In: Hornik K, Leisch F, Zeileis A (eds) Proceedings of the 3rd International Workshop on Distributed Statistical Computing (DSC 2003), Vienna, Austria, March 20–22, 2003. Austrian Association for Statistical Computing (AASC); the R Foundation for Statistical Computing, Vienna, Austria, pp 1–10

R Development Core Team (2020) R: A language and environment for statistical computing.

Spiegelhalter DJ, Thomas A, Best N, Lunn DJ (2003) WinBUGS User Manual Version 1.4.1. Imperial College; Medical Research Council, London

Su Y-S, Yajima M (2014) R2jags: A Package for Running JAGS from R.

Vose D (2000) Risk Analysis: A Quantitative Guide. John Wiley & Sons, Chichester, U.K.